Characterization of the Mechanisms of Broad-Spectrum Viral Entry Inhibitors

by

Che Caswell Colpitts

A thesis submitted in partial fulfillment of the requirements for the degree of

Doctor of Philosophy

in Virology

Department of Medical Microbiology and Immunology
University of Alberta

ABSTRACT

Viral entry is an attractive antiviral target. Entry inhibitors prevent infection of healthy cells and inhibit viral replication before viruses establish persistent reservoirs. Two entry steps, the primary attachment to cellular glycans and the lipid rearrangements during fusion, are conserved among many unrelated viruses. Therefore, inhibitors of these entry steps, acting through appropriate mechanisms, are likely to have broad-spectrum antiviral activity.

Using small molecules as probes, I identified and characterized three mechanisms by which it is possible to inhibit the entry of unrelated viruses. The majority of human viruses, including enveloped and nonenveloped viruses, initially bind to cellular glycans. Epigallocatechin gallate (EGCG), a green tea polyphenol, competes for virion binding to heparan sulfate or sialic acid moieties in cellular glycans to inhibit the infectivity of most human viruses. All enveloped viruses rely on lipid rearrangements during entry steps. Rigid amphipathic fusion inhibitors (RAFIs) act through biophysical mechanisms to inhibit the formation of the negative membrane curvature required for the fusion of enveloped viruses. Enveloped viruses constitute a large group of human viruses, including most clinically important pathogens. Curcumin and 25-hydroxycholesterol (25HC) modulate the fluidity and composition of lipid membranes to interfere with the replication of hepatitis C virus (HCV) and other enveloped viruses.

None of these small molecules are ideal candidates for antiviral drugs. More importantly, the identification of these mechanisms opens the possibility for the rational design of small molecule entry inhibitors with broad-spectrum antiviral activities and

appropriate pharmacological properties. Furthermore, the small molecules described in this thesis are useful as probes to characterize viral entry steps.

DEDICATION

This thesis is dedicated to the memory of my grandparents, Edgar and Audrey Caswell, who always appreciated academic accomplishments.

ACKNOWLEDGEMENTS

First and foremost, I would like to thank my supervisor, Dr. Luis Schang, for giving me advice and encouragement when I needed it, for allowing me the independence to develop my own ideas, and for providing me with many opportunities. He showed me how to be a scientist; for this and more, I am deeply grateful.

I thank the other members of the Schang lab, past and present, for experimental assistance and helpful suggestions. I am especially grateful to Abdullah Awadh for his friendship, for his ideas and support in the lab, and for the varied and interesting discussions over numerous lunches. I thank MiYao Hu and Esteban Flores for the conversations and humour that brightened many days in the lab. I am grateful for the contributions of our collaborators, Drs. Alexey Ustinov and Vladimir Korshun (RAFIs) and Drs. Sandra Ciesek and Eike Steinmann (EGCG, curcumin, 25HC), and for the help provided by Dr. Gary Eitzen (fluorometer), Dr. Lorne Tyrrell's group (HCV) and Dr. Maya Shmulevitz's group (equipment).

I am grateful to Dr. Judy Gnarpe, who was an excellent teaching mentor. I appreciate the opportunities she gave me to develop my teaching abilities and the emotional support (and many cups of tea) she provided. I would like to thank the members of my thesis supervisory committee, Dr. David Evans and Dr. Lorne Tyrrell, for their useful insight and guidance during the course of my degree.

Last, but certainly not least, I am grateful to my parents, Jeanne Caswell and Alan Colpitts, and to my partner, Christopher Lohans. Their unwavering support makes all things possible!

TABLE OF CONTENTS

LIST OF TABLES

LIST OF FIGURES

CHAPTER 5: CHARACTERIZATION OF SMALL MOLECULE COMPOUNDS THAT MODULATE VIRAL OR CELLULAR MEMBRANE FLUIDITY TO INHIBIT THE INFECTIVITY OF ENVELOPED VIRUSES

CHAPTER 6: DISCUSSION AND FUTURE DIRECTIONS

LIST OF ABBREVIATIONS

25HC: 25-hydroxycholesterol

AdV: adenovirus
AP2: adaptor protein 2
ATP: adenosine triphosphate
aUY11: 5-(Perylen-3-yl)ethynyl-arabino-uridine
aUY12: 5-(Perylen-3-ylmethyloxymethyl)ethynyl-arabino-uridine

BSA: bovine serum albumin
BVDV: bovine viral diarrhea virus

CAR: coxsackievirus and adenovirus receptor
CCR5: C-C chemokine receptor type 5
CD4: cluster of differentiation 4
CD46: cluster of differentiation 46
CD80: cluster of differentiation 80
CD81: cluster of differentiation 81
CD86: clutser of differentiation 86
CD155: cluster of differentiation 155
CPE: cytopathic effects
CLDN1: claudin 1
CME: clathrin-mediated endocytosis
CMV: cytomegalovirus
CoV: coronavirus
CPM: counts per minute
CV: coxsackievirus
CXCR4: C-X-C chemokine receptor type 4

DAA: direct acting antiviral
DAS181: sialidase from *Actinomyces viscosus*
DENV: dengue virus
DEPE: deilaidoylphosphatidylethanolamine
DMEM: Dulbecco's Modified Eagle Medium
DMSO: dimethyl sulfoxide
DNA: deoxyribonucleic acid
dNTP: deoxyribonucleotide triphosphate
DOPC: 1,2-dioleoyl-L-α-phosphatidylcholine
DPH: 1,6-diphenyl-1,3,5-hexatriene
DSC: differential scanning calorimetry
DTT: dithiothreitol
dUY1: 5-(Estra-1,3,5(10)-triene-17-one-3-yl)ethynyl-2′-deoxyuridine
dUY5: 4-(adamantan-1-yl)phenylethynyl-2'-deoxyuridine
dUY11: 5-(Perylen-3-yl)ethynyl-2'-deoxyuridine

E1: envelope glycoprotein 1
E2: envelope glycoprotein 2
EBV: Epstein-Barr virus
EC: epicatechin
EC_{50}: 50% effective concentration
EC_{90}: 90% effective concentration
EC_{99}: 99% effective concentration
EDTA: ethylenediaminetetraacetic acid
EEA1: early endosome antigen 1
EG: ethyl gallate
EGCG: epigallocatechin gallate
EGFR: epidermal growth factor receptor
EV: extracellular virion
EV70: enterovirus 70
EV71: enterovirus 71

FBS: fetal bovine serum
FFU: focus forming unit

GAG: glycosaminoglycan
gB: glycoprotein B
gC: glycoprotein C
gD: glycoprotein D
GFP: green fluorescent protein
gH: glycoprotein H
gL: glycoprotein L
gp120: glycoprotein 120
gp41: glycoprotein 41
GTP: guanosine triphosphate
GTPase: guanoside triphosphatase

HA: hemagglutinin
HBV: hepatitis B virus
HCV: hepatitis C virus
HCVpp: HCV pseudoparticles
HDL: high-density lipoprotein
HIV: human immunodeficiency virus
HMG: 3-hydroxyl-3-methyl-glutaryl
HNP: human neutrophil peptide
HPIV: human parainfluenza virus
HPV: human papilloma virus
HR: heptad repeat
HRV: human rhinovirus
HS: heparan sulphate
HSV-1: herpes simplex virus 1

HSV-2: herpes simplex virus 2
HVEM: herpesvirus entry mediator
HVR: hypervariable region

IAV: influenza A virus
IBV: influenza B virus
ICV: Influenza C virus
IC_{50}: 50% inhibitory concentration
IE: immediate early
IFITM: interferon-inducible transmembrane protein
IFN: interferon
IgG: immunoglobulin G
ISG: interferon-stimulated gene

JAM-A: junctional adhesion molecule-A
JEV: Japanese encephalitis virus

LAS: Leica application suite
LDL: low-density lipoprotein
LDLR: low-density lipoprotein receptor
LG: lauryl gallate
LPC: lysophosphatidylcholine
LXR: liver X receptor

M2: ion channel
mCMV: murine cytomegalovirus
MERS: Middle Eastern Respiratory Syndrome
MeV: measles virus
MG: methyl gallate
MOI: multiplicity of infection
M-MLV: Moloney Murine Leukemia Virus
MV: mature virion

NA: neuraminidase
NDV: Newcastle disease virus
NNRTI: non-nucleoside reverse transcriptase inhibitor
NRTI: nucleoside reverse transcriptase inhibitor
NS3: nonstructural protein 3
NS4: nonstructural protein 4
NS5: nonstructural protein 5
NSF: N-ethylmaleimide-sensitive factor
NtRTI: nucleotide reverse transcriptase inhibitor

OCLN: occludin
OG: octyl gallate

PBS: phosphate-buffered saline
PCR: polymerase chain reaction
PD: PD 404182
PFU: plaque forming unit
PG: propyl gallate
PGG: pentagalloylglucose
PIPES: piperazine-N,N′-bis(2-ethanesulfonic acid)
PLA2: phospholipase A2
POPC: β-oleoyl-γ-palmitoyl-L-α-phosphatidylcholine
PS: phosphatidylserine
PV: poliovirus
PVR: poliovirus receptor

qRT-PCR: quantitative real time-polymerase chain reaction

R18: octadecyl rhodamine B chloride
RAFI: rigid amphipathic fusion inhibitor
RT: reverse transcriptase

RNA: ribonucleic acid
RNAi: RNA interference
RSV: respiratory syncytial virus
RV: reovirus
RVFV: Rift Valley fever virus

SA: sialic acid
SAR: structure-activity relationship
SARS: severe acute respiratory syndrome
SG: sialoglycan
SINV: Sindbis virus
SNARE: soluble N-ethylmaleimide-sensitive factor attachment protein receptor
SR-BI: scavenger receptor class B type I
SREBP: sterol regulatory element-binding protein

THC: tetrahydrocurcumin
TK: thymidine kinase
TPCK: L-1-tosylamide-2-phenylethyl chloromethyl ketone

VACV: vaccinia virus
VIRIP: virus-inhibitory peptide
VLDL: very low-density lipoprotein
VSV: vesicular stomatitis virus
VZV: varicella zoster virus

WNV: West Nile virus

CHAPTER 1: INTRODUCTION

1.1 VIRAL ENTRY

The first steps in viral infection are generally conserved among most human viruses. Virions first attach to their target cells through non-specific, low-affinity interactions with ubiquitous moieties on cellular surfaces, such as glycans. Primary attachment brings the viral particles into close proximity with the cell surface, facilitating the higher-affinity binding to specific cellular receptors. The higher affinity secondary binding is often critical in determining tropism for particular cell types. High affinity binding may also induce conformational changes in virion proteins, or facilitate trafficking of the viral particle to specific cellular compartments, allowing for subsequent entry steps. After binding, most virions are internalized by different mechanisms into endosomal compartments. Other virions deliver their genomes directly into the cell across the plasma membrane. Following binding and internalization (or not), the entry process differs for enveloped or nonenveloped viruses. Viruses with a lipid envelope fuse their envelope with the host cell membrane, thereby delivering the capsid into the cytoplasm, whereas nonenveloped viruses disrupt the host cell membrane by nonfusogenic mechanisms to enter into the cytoplasm.

After entry, the subsequent replication steps depend on the composition of the viral genome (deoxyribonucleic acid (DNA) or ribonucleic acid (RNA)) and the subcellular replication site (nuclear or cytoplasmic). Viral and cellular enzymes mediate these replication steps, which may share common features but differ mechanistically for each virus group. Antivirals that target replication are typically specific for one particular virus, or closely related group of viruses.

In contrast to later steps in replication, some viral entry steps are broadly conserved for many human viruses. The primary attachment of the vast majority of enveloped and nonenveloped human viruses is to cellular glycans. Many enveloped and nonenveloped viruses enter cells by similar endocytotic pathways. Finally, all enveloped viruses must fuse their envelope with the host cell membranes. Therefore, viral entry is an appealing target for broad spectrum antiviral therapeutics.

1.2 PRIMARY BINDING

1.2.1. Cellular glycans

Most human viruses attach to their target cells by first interacting with cell surface glycans, such as glycosaminoglycans (GAGs) or sialoglycans (SGs). GAGs are long unbranched polysaccharides comprised of a repeating disaccharide unit of an amino sugar (*N*-acetylglucosamine or *N*-acetylgalactosamine) and a uronic sugar (glucuronic acid or iduronic acid) or galactose (Raman *et al.*, 2005). Depending on the composition of the disaccharide unit, GAGs are classified into four groups: heparin/heparan sulfate (HS), chondroitin/dermatan sulfate, keratan sulfate or hyaluronic acid (Esko *et al.*, 2009). GAGs are usually linked to proteins through *O*-linked or *N*-linked glycosylation. The repeating disaccharide unit of GAGs is modified by variable sulfation patterns (David, 1993), resulting in the high diversity and complexity that allows for specific binding with many different GAG-binding proteins. The interactions between GAGs and GAG-binding proteins regulate many biological processes, including cell growth and proliferation pathways, cell adhesion or migration, and tissue hydration (Esko *et al.*, 2009).

GAG-binding proteins have a binding site of positively charged basic amino acids that interact with the negatively charged sulfates and carboxylates in the GAGs. For example, a heparin-binding consensus sequence of XBBXBX or XBBBXXBX (where B is basic lysine or arginine residue and X is any amino acid) is typically found in proteins that bind to HS (Cardin and Weintraub, 1989). The binding affinity depends on the overall shape and conformation of GAGs and is affected by the number and orientation of the sulfate group charges (Raman *et al.*, 2005).

SGs, another group of cellular glycans, are comprised of sialic acid (SA) attached to the termini of *N*-linked and *O*-linked glycans. The carboxylate group at the 1-carbon position of SA is ionized at physiological pH, allowing for interactions with basic residues of saccharide-binding proteins such as lectins (Varki, 1994). However, binding of SGs and proteins is mostly mediated by extensive hydrogen bonding between the functional groups of SA (carboxylate, hydroxyls and an N-acetyl group) and polar amino acid residues.

GAGs and SGs are ubiquitous, and many microbial pathogens have evolved to exploit them for initial attachment to their target cells (Chen *et al.*, 2008). Among the GAGs, HS is the most commonly used as a viral attachment site. The density of cell-surface HS is greater than 10^6 molecules per typical epithelial cell (Bernfield *et al.*, 1992), thus allowing microbes to bind and increase their concentration at the cell surface. Similarly, many viruses recognize and bind SA, which is abundantly expressed in SGs on the cell surface. These interactions with glycans capture virions from extracellular spaces and concentrate them in the vicinity of other receptors and signalling molecules that are used for higher affinity binding and entry into the cell.

1.2.2. Heparan sulfate-binding viruses

Many important human viruses bind to HS proteoglycans by interacting with the negatively charged HS moieties in cellular GAGs (**Figure 1.1**). This group includes hepatitis C virus (HCV) (Barth *et al.*, 2003; Morikawa *et al.*, 2007), hepatitis B virus (HBV (Leistner *et al.*, 2008), human immunodeficiency virus (HIV) (Patel *et al.*, 1993), dengue virus (DENV) (Chen *et al.*, 1997), Sindbis virus (SINV) (Byrnes and Griffin, 1998), respiratory syncytial virus (RSV) (Krusat and Streckert, 1997; Martinez and Melero, 2000; Feldman *et al.*, 2000), Rift Valley fever virus (RVFV) (de Boer *et al.*, 2012), severe acute respiratory syndrome-associated coronavirus (SARS-CoV) (Vicenzi *et al.*, 2004), herpes simplex virus 1 and 2 (HSV-1/-2) (WuDunn and Spear, 1989; Herold *et al.*, 1991; Shieh *et al.*, 1992; Cheshenko and Herold, 2002), human cytomegalovirus (CMV) (Compton *et al.*, 1993), varicella zoster virus (VZV) (Zhu *et al.*, 1995), vaccinia virus (VACV) (Ho *et al.*, 2005), human parainfluenza virus (HPIV) (Bose and Banerjee, 2002), adenovirus (AdV) types 2 and 5 (Dechecchi *et al.*, 2000; Dechecchi *et al.*, 2001), some strains of norovirus (Tamura *et al.*, 2004) and human papillomavirus (HPV) (Giroglou *et al.*, 2001). Other viruses, including the model rhabdovirus vesicular stomatitis virus (VSV), are thought to also require HS for binding (Conti *et al.*, 1991), although the specific details of the interactions remain unclear.

The mechanisms by which virions attach to HS moieties in cellular glycans are generally well conserved. Binding requires interactions between binding pockets of basic amino acids in the virion glycoproteins and negatively charged HS or SA. In HSV-1, glycoprotein B (gB) and glycoprotein C (gC) are responsible for this binding (Shukla and Spear, 2001). gC knockout viruses have a reduced ability to bind to cells (Herold *et al.*,

1991), and absence of both gC and gB eliminates binding to cells altogether (Herold *et al.*, 1994). Both gB- and gC-dependent binding were shown to require cell surface HS. As for other heparin-binding proteins, the interactions between gB/gC and HS rely on electrostatic interactions between basic residues and the negatively charged sulfate esters and carboxylate groups of HS. gB has a basic lysine-rich region (comprised of residues 68 to 76) required for binding to heparin and HS (Laquerre *et al.*, 1998). The gC amino acid residues involved in HS binding are the basic Arg-143, Arg-145 and Arg-147, as well as Thr-150 and Gly 247 (Trybala *et al.*, 1994). gC residues Arg-129, Arg-130, Ile-142, Arg-151, Arg-155 and Arg-160 are also required for binding (Mardberg *et al.*, 2001). The requirement of the non-ionic hydrophobic residues (Thr-150 and Ile-142) indicates that non-ionic binding may also be involved, perhaps to contribute to the binding energy or position the basic residues correctly.

The N-terminal 27-amino-acid hypervariable region (HVR1) of the HCV E2 protein has basic residues conserved at specific positions, as shown by analysis of over 1500 non-redundant HVR1 sequences (Penin *et al.*, 2001). The conserved positively charged residues of the HVR1 were proposed to interact with negatively charged cell surface GAGs. Supporting this model, E2 with a deletion of the basic HVR-1 region showed a decreased ability to bind to heparin (Barth *et al.*, 2003), demonstrating the importance of the basic residues for binding to cellular HS.

Similar heparin-binding domains are found within other virion glycoproteins. HIV gp120 contains four heparin-binding domains of basic amino acids: ^{166}RGKVQK^{171}, ^{304}RRKIR^{308}, ^{500}KAKRR^{504} (Crublet *et al.*, 2008), and a binding pocket of Lys-121, Arg-419, Lys-421 and Lys-432 (Vives *et al.*, 2005). VACV A27 protein binds to HS through

a lysine-rich binding domain (^{21}STKAAKKPEAKR^{32}) (Shih *et al.*, 2009). The RSV G protein has a lysine-rich heparin-binding domain (^{184}AICKRIPNKKPGKKT^{198} or ^{183}KSICKTIPSNKPKKK^{197}, depending on the subgroup) (Feldman *et al.*, 1999). Nonenveloped viruses also bind to HS through similar interactions. A conserved region of basic amino acids in the HPV L1 protein (the consensus sequence from nine HPV types is XBBBBXB, where B is Lys, Arg or His) is involved in binding to heparin (Joyce *et al.*, 1999). For AdV, the ^{91}KKTK^{94} domain of the fiber shaft protein was implicated in heparin binding (Dechecchi *et al.*, 2000). Therefore, binding between most virion glycoproteins and cellular GAGs is mediated by very similar ionic interactions between the same basic amino acids and negatively charged HS moieties. As a result of the conserved binding mechanisms, appropriately shaped and charged molecules that mimic HS disrupt the binding of a broad group of viruses **(discussed in Section 1.7.1)**.

1.2.3. Sialic acid-binding viruses

SA was the first virus receptor identified, in the context of influenza (IAV) infection (Hirst, 1941). Since that discovery, SA was shown to be a receptor for a diverse group of viruses and other pathogens (Matrosovich *et al.*, 2013). This group of viruses includes IAV (Haff and Stewart, 1965), influenza B virus (IBV) (Wang *et al.*, 2007), influenza C virus (ICV) (Rogers *et al.*, 1986), some human coronavirus (CoV) strains (Vlasak *et al.*, 1988), paramyxoviruses such as Sendai virus (Suzuki *et al.*, 1985), some strains of norovirus (Rydell *et al.*, 2009), reovirus (RV) (Gentsch and Pacitti, 1985), enterovirus 70 (EV70) (Nokhbeh *et al.*, 2005), JC polyomavirus (Liu *et al.*, 1998), BK virus (Dugan *et al.*, 2005) and others (reviewed in Lehmann *et al.*, 2006). Additionally, certain strains and isolates of human rhinovirus (HRV), coxsackievirus (CV) and AdV bind to sialic acids

(Uncapher *et al.*, 1991; Nilsson *et al.*, 2008; Arnberg *et al.*, 2000; Arnberg *et al.*, 2002). Similar to HS-binding viruses, attachment of SA-binding viruses requires low-affinity interactions between binding pockets in virion glycoproteins and SA moieties in cellular SGs.

Proteins that bind to SA, including IAV hemagglutinin (HA), do so mainly through a network of hydrogen bonds between polar amino acids and the four functional groups of SA (a carboxylate at C1, a hydroxyl at C2, an N-acetyl group at C5 and a glycerol group at C6) (**Figure 1.1**). The conserved residues in the SA-binding site of IAV HA are Tyr-98, Trp-153, Glu-190, Leu-194 and His-183 (Weis *et al.*, 1988). The pyranose core of SA rests on top of the aromatic residues, Tyr-98 and Trp-153. The carboxylate group of SA forms hydrogen bonds with Ser-136, and to the amide of peptide bond 137. The hydroxyl groups in the glycerol chain of SA hydrogen bond to His-183, Glu-190, and Tyr-98 (Weis *et al.*, 1988). The N-acetyl group of SA also forms hydrogen bonds (to the carbonyl of peptide bond 135). Moreover, van der Waals interactions (such as between the methyl of the N-acetyl group and Trp-153) are also involved in the binding.

Similar hydrogen bonding interactions are described for other viral proteins that bind SA. For example, the hemagglutinin of Newcastle disease virus (NDV), a paramyxovirus, binds to SA by hydrogen bonding mediated by amino acids Glu-401, Arg-416 and Tyr-526 (Connaris *et al.*, 2002). The binding pocket also contains Arg-498, Ser-418, Tyr-317, Glu-258 and Ser-237 (Connaris *et al.*, 2002), all of which can form hydrogen bonds. Reovirus sigma 1 has a binding pocket consisting of Asn-198, Arg-202,

Leu-203, Pro-204 and Gly-205, which interact with sialic acid through a similar network of hydrogen bonds and van der Waals interactions (Reiter *et al.*, 2011).

Molecules that mimic SA compete for receptor binding to inhibit attachment of SA-dependent viruses. However, at least for IAV, the individual interactions between a single binding pocket and sialic acid are weak. Receptor binding is cooperative and depends on multivalent interactions between multiple HA spikes and multiple SA moieties. Consequently, monovalent receptor mimetics are unable to effectively compete with the multivalent interactions of the virions with the cells (Matrosovich, 1989), whereas sialoglycopolymers and other polyvalent sialylmimetics are effective competitors (**discussed in section 1.7.1**).

1.2.4. Other viruses

Only a very small group of human viruses bind to neither HS nor SA moieties on cellular glycans. Poliovirus (PV) binds to the poliovirus receptor (PVR; cluster of differentiation 155, CD155) without previous attachment to either HA or SA (Racaniello, 1996). Most strains of HRV (Uncapher *et al.*, 1991) and some strains of measles virus (MeV) (Terao-Muto *et al.*, 2008) require neither HS nor SA for binding.

Conversely, some viruses appear to require both HS and SA for entry. Merkel cell virus binds to both GAGs and SGs (Schowalter *et al.*, 2011), in a sequential manner. Enterovirus 71 (EV71) also requires both HS and SA for attachment (Tan *et al.*, 2013; Yang *et al.*, 2009; Su *et al.*, 2012). However, the binding sites and specific interactions of these two viruses have not yet been fully elucidated.

1.3 SECONDARY BINDING

A few viruses, such as IAV, bind solely to glycan moieties. Most viruses, in contrast, bind to secondary receptors with higher affinity. The higher affinity binding may be responsible for the tropism of a virus for a particular cell type. For example, the hepatotropic HCV binds to receptors involved in lipid uptake that are expressed mostly on hepatocytes (Pecheur, 2012). The immunotropic HIV binds to the cluster of differentiation 4 (CD4) receptor expressed by immune cells, but tropism for either T-cells or macrophages is determined by binding to the coreceptor, C-X-C chemokine receptor type 4 (CXCR4, T-cells) or C-C chemokine receptor type 5 (CCR5, macrophages) (Coakley *et al.*, 2005). Other cellular factors also affect tropism (such as signalling pathways involved in internalization or the availability of transcription factors for genome replication). In addition to being involved in cellular tropism, binding to secondary receptors can also induce conformational changes in viral glycoproteins that expose regions of the virion glycoprotein involved in fusion or binding to other receptors. Receptor binding can also induce intracellular signalling events to facilitate internalization of the virus particle. Some selected specific examples are discussed in **section 1.6**.

1.4 INTERNALIZATION

There are a limited number of endocytotic pathways available for viruses to use. As a result, many use common internalization pathways. Many viruses are internalized into endosomal compartments through common processes mediated by host cell signalling pathways.

1.4.1 Clathrin-mediated endocytosis

Clathrin-mediated endocytosis (CME), a constitutive process shared among all eukaryotic cells, is the most commonly used endocytotic pathway during viral entry. Clathrin-coated pits are first formed around the selected cargo by cellular proteins such as adaptor protein 2 (AP2). Clathrin-coated pits invaginate inwards from the membrane in a process mediated by Epsin, which recruits clathrin and AP2 complexes (Mousavi *et al.*, 2004). Epsin also binds to phosphatidylinositol-4,5-bisphosphate within the lipid component of the clathrin-coated pit to induce positive membrane curvature (Ford *et al.*, 2002). The invaginated clathrin-coated pits are pinched off from the plasma membrane in a dynamin-dependent manner, forming the clathrin-coated vesicles, which ultimately shed their clathrin and fuse with endosomes (Mousavi *et al.*, 2004). Lipid composition may contribute to the formation of clathrin-coated pits. For example, cholesterol depletion inhibits endocytosis by preventing the endocytotic adaptor proteins from inducing membrane curvature (Subtil *et al.*, 1999).

Many unrelated viruses are internalized by CME, including the nonenveloped AdV (Leopold and Crystal, 2007), HPV type 16 (Day *et al.*, 2003) and RV (Danthi *et al.*, 2010), and the enveloped HCV (Blanchard *et al.*, 2006), SINV (DeTulleo and Kirchhausen, 1998), VSV (Sun *et al.*, 2005) and IAV (Rust *et al.*, 2004). Some viruses even actively induce formation of the clathrin-coated pits (Rust *et al.*, 2004). It is not surprising, therefore, that inhibitors of CME often have broad-spectrum antiviral activity. Many physiological processes also require endocytotic processes and inhibitors of CME are typically associated with toxicity.

1.4.2 Other internalization pathways

Another route of viral internalization is by caveolin-mediated endocytosis. Caveolae are cholesterol-rich lipid microdomains that form invaginations in the plasma membrane through their association with caveolins. Unlike clathrin-mediated endocytosis, caveolae internalization requires triggering (Parton *et al.*, 1994), often by signalling activated when viruses bind to cellular receptors (Pelkmans and Helenius, 2003). Members of the *polyomaviridae* and *picornaviridae* families, as well as HBV, are thought to be internalized by caveolin-mediated endocytosis (Marjomaki *et al.*, 2002; Macovei *et al.*, 2010; Dugan *et al.*, 2006). However, caveolin-mediated endocytosis is not commonly used for viral entry.

Other viruses use clathrin- and caveolin-independent entry pathways. Although the specific mechanisms involved in these pathways are unclear, they require lipid rafts, highly ordered lipid microdomains that are rich in sterols and sphingolipids (Brown and London, 1998; Kirkham and Parton, 2005; Mayor and Pagano, 2007). Viruses in this group include SARS-CoV (Wang *et al.*, 2008b), HPV 16 (Spoden *et al.*, 2008) and IAV (Sieczkarski and Whittaker, 2002).

Another endocytotic pathway exploited by viruses is macropinocytosis, an actin-dependent process that forms membrane extensions to uptake fluid into large vacuoles (Mercer and Helenius, 2009). VACV (Mercer and Helenius, 2008), members of the *herpesviridae* family (Raghu *et al.*, 2009), and filamentous IAV (Rossman *et al.*, 2012), all of which may be too large for other endocytotic routes, can be internalized by macropinocytosis. However, VACV and *herpesviridae* are thought mainly to fuse at the plasma membrane.

It is becoming apparent that many viruses, such as IAV, use multiple internalization pathways, governed by complex and poorly understood regulatory mechanisms. There are some examples of molecules that inhibit viral internalization (described in **section 1.7.3**). However, there appears to be redundancy in the internalization pathways used by viruses. Moreover, internalization is mostly regulated by cellular enzymes and is required for physiological functions. It is difficult to selectively target viral internalization without affecting physiological internalization processes.

1.5 VIRAL FUSION

Entry of enveloped viruses invariably requires fusion of the viral envelope with the host cell membrane. Different classes of viral fusion proteins mediate fusion, but fusion ultimately depends on the lipid core of the viral envelope, a structure conserved among all enveloped viruses. Fusion is thought to occur through the widely accepted hemifusion stalk model (Chernomordik and Kozlov, 2005). According to this model, viral and cellular membranes first come into close apposition, leading to formation of a stalk intermediate (hemifusion) in which the outer leaflets of the membranes are fused, but the inner leaflets are not. Subsequent merging of the inner leaflets forms an early fusion pore, which expands to allow full fusion. The process of fusion is driven by proteins, but depends on the composition and architecture of lipids at the fusion site.

1.5.1 Viral fusion proteins

Viral fusion is facilitated by viral fusion proteins, which are categorized into three classes based on differences in structure and oligomeric state. Class I fusion proteins are mainly

alpha-helical, whereas class II fusion proteins consist primarily of beta-sheets and class III fusion proteins have mixed secondary structures (Harrison, 2008). Regardless of their structures, viral fusion proteins are thought to function by overall similar mechanisms. A specific trigger, such as a pH change or interaction with a cellular receptor activates the fusion protein. The fusion protein then undergoes a conformational change resulting in the exposure of a fusion peptide, which inserts into the target membrane. The fusion proteins then undergo further conformational change to bring transmembrane domains in the viral envelope into close proximity with the viral fusion peptide (Earp *et al.*, 2005). Membrane fusion occurs as a result of close membrane apposition and local membrane disruption mediated by the fusion protein. The activation energy required for viral membrane fusion is derived from binding to the receptor(s) and conformational changes of the viral fusion protein (Blumenthal *et al.*, 2003).

Class I fusion proteins, which are predominantly alpha helical in structure, project outwards from the virion envelope as spikes **(Figure 1.2A)**. They form trimers both before and after fusion. This group includes the fusion proteins of orthomyxoviruses (Skehel and Wiley, 2000), paramyxoviruses (Lamb and Jardetzky, 2007), retroviruses (Chan *et al.*, 1997; Weissenhorn *et al.*, 1997), filoviruses (Weissenhorn *et al.*, 1998a; Weissenhorn *et al.*, 1998b) and coronaviruses (Xu *et al.*, 2004). Class I fusion proteins are comprised of an N-terminal fusion peptide (produced by proteolytic cleavage during virion maturation) and a core of three bundled alpha helices in the pre-fusion state. During fusion, class I fusion proteins refold into a six-helix bundle (Skehel and Wiley, 2000). The proposed mechanism for IAV HA (the prototypical class I fusion protein) involves the folding of an uncleaved protein to a metastable state (Chen *et al.*, 1998a),

which is then activated by proteolytic cleavage (Wiley and Skehel, 1987; Wilson *et al.*, 1981). Low pH triggers an irreversible and major conformational change in the HA, resulting in insertion of the fusion peptide into the target membrane. The fusion protein then folds back on itself into a rod-like trimer of hairpins, pulling its C-terminal transmembrane domain (anchored in the viral envelope) towards the N-terminal fusion peptide (inserted in the cell membrane) (Eckert and Kim, 2001). These structural rearrangements position the two membrane-inserted domains next to each other, bringing the two membranes into close apposition and thereby facilitating fusion of the viral envelope with the cell membrane (Eckert and Kim, 2001). The conformational changes required for fusion of class I proteins can be triggered by low pH, as for IAV HA (Bullough *et al.*, 1994), or by receptor binding at neutral pH, as for HIV gp41 (Moore *et al.*, 1990; Sattentau and Moore, 1991).

Class II fusion proteins have been identified in flaviviruses (Rey *et al.*, 1995; Modis *et al.*, 2004), togaviruses (Lescar *et al.*, 2001; DuBois *et al.*, 2013) and bunyaviruses (Dessau and Modis, 2013) **(Figure 1.2B)**. They differ from class I fusion proteins in several ways. Class II proteins lie flat on the virion surface, consist predominantly of beta sheets, and the fusion peptide is located in internal loops (Kielian and Rey, 2006). Proteolytic cleavage is not required for maturation of class II fusion proteins. Fusion mediated by class II proteins is always triggered by conformational changes induced by low pH, encountered in endosomal compartments. In the pre-fusion state, class II fusion proteins are dimers arranged parallel to the virion surface, but undergo conformational rearrangements to form post-fusion trimers projecting

perpendicularly from the virion envelope (Kielian and Rey, 2006). Unlike class I fusion proteins, however, they do not exhibit coiled coils.

Class III fusion proteins are comprised of mixed alpha helix and beta sheet structure **(Figure 1.2C)**. They have been identified in herpesviruses (Heldwein *et al.*, 2006) and rhabdoviruses (Roche *et al.*, 2006; Roche *et al.*, 2007). Class III fusion proteins have helical bundles (as in class I proteins), but the fusion loop is in internal beta-stranded domains (as in class II proteins) (Roche *et al.*, 2006; Heldwein *et al.*, 2006). Uniquely, some class III proteins undergo a reversible conformational change (unlike class I and II fusion proteins) (Gaudin, 2000a). Extended exposure to low pH inactivates the virions, but the fusion activity is fully recovered when the pH is raised again (Roche and Gaudin, 2002).

HCV E2 was predicted to be a class II fusion protein, like those found in other flaviviridae. This prediction was based on the disulfide bond pattern (Krey *et al.*, 2010). However, HCV E2 was later found to possess a novel globular structure that lacked features common to fusion proteins, such as a hydrophobic fusion motif, a helical core, or a flexible multi-domain structure (Kong *et al.*, 2013; Khan *et al.*, 2014). Similarly, the related pestivirus bovine viral diarrheal virus (BVDV) E2 protein differs in its fold and topology from known viral fusion proteins (Li *et al.*, 2013b; El Omari *et al.*, 2013). As a result of these studies, E1 was proposed instead to be the fusogen for HCV and BVDV, with E2 functioning as a scaffold or chaperone (Li *et al.*, 2013b; El Omari *et al.*, 2013). E1 does not fold correctly without E2 (Patel *et al.*, 2001; Ronecker *et al.*, 2008), and viral particles with disrupted E1-E2 interactions are unable to fuse (Patel *et al.*, 2001). The E1 structure, however, does not resemble any known viral fusion protein, and has been

proposed to belong to a novel class of fusion protein (Li and Modis, 2014). Further studies are needed to elucidate the structure and function of E1-E2, to determine its roles in fusion.

Despite their structural and biochemical differences, viral fusion proteins induce membrane fusion similarly **(Figure 1.3)**. The fusion peptide inserts into the target membrane, locally destabilizing the membrane. Conformational changes in the fusion protein then lead to a hairpin structure, which pulls the two membranes into close proximity to allow for fusion of the apposing membranes. The energy for the unfavourable membrane rearrangements during fusion is generated by the conformational changes of viral fusion proteins (usually from a metastable to stable structure), and their binding to membranes or receptors (Chernomordik and Kozlov, 2005).

1.5.2 Cellular fusion proteins.

Many cellular processes also depend on membrane fusion events. These include exocytosis (e.g. during neurotransmitter release from synapses), endocytosis (e.g. transport of nutrients into the cell or transport of waste products to the lysosome), all vesicular transport, mitosis, meiosis and fusion of sperm and egg cells during fertilization. Cellular fusion events are actively driven by adenosine triphosphate (ATP)-dependent processes. Intracellular vesicle fusions are induced by the activities of the soluble N-ethylmaleimide-sensitive factor (NSF) attachment protein receptor (SNARE) protein superfamily (Sollner *et al.*, 1993; Chen and Scheller, 2001). Vesicle or v-SNAREs are C-terminally anchored in vesicle membranes, whereas target or t-SNAREs are C-terminally anchored in the target membranes (Hay and Scheller, 1997). During fusion, v-SNAREs pair with t-SNAREs to form a complex that originates at the N-

terminal ends of the SNAREs. The SNAREs then zipper together (in a concerted oligomerization and folding reaction) into a stable membrane-bridging complex, which brings the two membranes into close proximity and drives fusion (Fasshauer, 2003). After fusion, NSF disassembles the SNARE complexes in an ATP-dependent manner, restoring the SNAREs for subsequent fusion events (Sollner *et al.*, 1993).

Other proteins are involved in cellular fusions, prior to SNARE complex assembly. Tethering proteins with coiled-coil domains, such as early endosome antigen 1 (EEA1) (Christoforidis *et al.*, 1999) and golgins (Barr and Short, 2003), are involved in the initial contacts of two vesicles. Rab GTPases (in their active, membrane-bound guanosine triphosphate (GTP)-bound form) recruit such tethers to target membranes, promoting attachment between vesicle membranes to allow for SNARE complex formation. Collectively, Rab GTPases, tethers and SNAREs regulate the timing and specificity of eukaryotic membrane fusion events through energy-dependent reactions (i.e., Rab GTP hydrolysis, ATP-dependent assembly and disassembly of SNAREs). Other proteins, such as clathrin, serve as scaffolds to bend membranes to facilitate fusion. Such proteins alter membrane curvature by binding to lipids, helping to drive fusion (Zimmerberg and Kozlov, 2006).

Calcium is also critical for cellular fusions. Ca^{2+} is thought to facilitate vesicle attachment. Ca^{2+} ions dehydrate vesicle surfaces, helping to expose the hydrophobic lipid tails to allow hydrophobic interactions between the lipids of two vesicles, and reduce the repulsion between lipids (Hu *et al.*, 2002). Ca^{2+} may also destabilize the lipid architecture to enhance formation of the hemifusion stalk (Tsai *et al.*, 2013).

1.5.3 Lipids and fusion

Membrane fusion is mediated by fusion proteins, but fusion requires the merging of the lipid bilayers, which occurs as a result of close membrane apposition and local membrane disruption. Therefore, fusion ultimately depends on the lipids themselves. Appropriate lipid architecture is critical for fusion according to the hemifusion stalk model (Teissier and Pecheur, 2007). In this model, the two outer leaflets of the apposing membranes fuse first, resulting in the formation of the intermediate hemifusion stalk structure (Chernomordik and Kozlov, 2005). The inner leaflets subsequently fuse to form a small pore, which then enlarges and allows for content mixing. Formation of the stalk requires rearrangements of lipids from flat (with the hydrophobic head groups bent neither toward nor away from each other) or positive curvature (with the hydrophilic headgroups of the outer leaflet bent away from each other) to negative curvature (with the hydrophilic head groups bent toward each other) **(Figure 1.3)**.

Lipid composition affects the energetics of hemifusion (Chernomordik *et al.*, 1995). Formation of the hemifusion stalk is facilitated by the presence in the outer leaflet of lipids with smaller polar headgroups relative to the hydrophobic tail, such as oleic acid (Chernomordik, 1996). These lipids promote negative curvature. In contrast, stalk formation is hindered by the presence in the outer leaflet of lipids with larger polar headgroups, such as lysophosphatidylcholine (Chernomordik, 1996). Such lipids favour positive curvature, which increases the activation energy necessary for fusion. When in the outer leaflet, such lipids increase the activation energy necessary for fusion and inhibit the fusion of a number of enveloped viruses (Vogel *et al.*, 1993; Gunther-Ausborn *et al.*, 1995; Stiasny and Heinz, 2004; Gaudin, 2000b).

Energy for viral fusion is provided solely by the binding and rearrangements of the virion glycoproteins. Cellular fusion, in contrast, is driven by energy-consuming processes. Unlike viruses, cells actively remodel the lipid composition of membranes to facilitate fusion. ATP-driven lipid translocases, for example, translocate phosphatidylethanolamine and phosphatidylserine from the outer leaflet to the inner leaflet of membranes, which induces membrane bending and stimulates endocytosis (Farge *et al.*, 1999). Lipid acylation of lysophosphatidic acid increases the size of the tail region to favour negative membrane curvature (Schmidt *et al.*, 1999), which facilitates formation of the hemifusion stalk during fusion. Translocation and remodeling of lipids modulates membrane curvature and bending to provide energy for fusion.

Appropriate membrane fluidity is also required for fusion (Howell *et al.*, 1972; Breisblatt and Ohki, 1976). Cellular membrane fluidity depends on protein composition, lipid composition, and the degree of unsaturation in fatty acid chains, which is regulated by lipid desaturases (Aguilar and de Mendoza, 2006). Desaturases introduce double bonds in fatty acid chains, generating kinks that decrease the packing of lipids and thereby increase membrane fluidity (Aguilar and de Mendoza, 2006). Cholesterol content is critical for membrane fluidity and is regulated by sterol regulatory element-binding proteins (SREBPs) (Brown and Goldstein, 1999). Signalling through SREBPs activates transcription of genes encoding enzymes involved in cholesterol and fatty acid biosynthesis. Cholesterol is also internalized from exogenous sources (such as plasma low-density lipoprotein particles) by lipoprotein receptors (Brown and Goldstein, 1986). Therefore, cells actively modulate the composition of cellular membranes, which affects fluidity and curvature.

Factors affecting fusion, such as lipid composition, membrane bending and fluidity, have the potential to impact viral fusions without affecting cellular fusions. As described, cells actively remodel lipid membranes to facilitate fusion. In contrast, viral fusion is driven solely by energy released during binding and rearrangements of virion fusion proteins. Therefore, strategies to selectively inhibit viral fusion with minimal effects on cellular fusions could be designed.

1.6 ENTRY MECHANISMS OF SELECTED VIRUSES

Viral entry steps are generally conserved for many unrelated viruses and offer a broad-spectrum target for antivirals. Representative unrelated viruses (HCV, IAV, VSV and HSV-1) were selected as models for my studies **(Table 1)**. The viruses were chosen to differ in their secondary receptors, internalization pathways and sites of fusion, class of fusion protein, genome composition, and strategies and sites of replication. However, the primary binding of all of them is to saccharide moieties in cellular glycans, and the fusion of all of them requires conserved changes in the lipid core of the virion envelopes. The model viruses and their entry mechanisms are described below.

1.6.1 Hepatitis C virus (HCV)

HCV globally infects an estimated 170 million people, with three to four million people newly infected each year (Sy and Jamal, 2006; Mohd Hanafiah *et al.*, 2013). HCV establishes chronic infections in the majority of infected individuals. Chronically infected patients are at higher risk for liver-related complications, such as cirrhosis and hepatocellular carcinoma (de Oliveria Andrade *et al.*, 2009). HCV is an enveloped cytoplasmic-replicating RNA virus in the *hepacivirus* genus in the *flaviviridae* family.

HCV has a positive sense single-stranded RNA genome, consisting of a 9.6 kilo-base pair single open reading frame. A host-derived membrane containing the E1 and E2 glycoproteins surrounds the nucleocapsid core. HCV particles are heterogeneous in size and density as a result of their association with serum lipoproteins, such as low-density lipoprotein (LDL) and very low-density lipoprotein (VLDL). Virions associated with VLDL, forming so-called lipoviral particles, are the most infectious. Associations with lipoproteins are thought to conceal viral epitopes from the immune system, facilitate maturation and release by hijacking host pathways, or allow interactions with lipoprotein receptors to facilitate attachment and entry (Felmlee *et al.*, 2013).

HCV entry into hepatocytes is a complex, multi-step process that requires many cellular receptors. The primary attachment of HCV virions is by low-affinity interactions with HS-containing GAGs on the cell surface (Barth *et al.*, 2003; Morikawa *et al.*, 2007; Jiang *et al.*, 2012). The cellular low-density lipoprotein receptor (LDLR) is also required for binding (Monazahian *et al.*, 1999; Agnello *et al.*, 1999; Scarselli *et al.*, 2002; Molina *et al.*, 2007) and most likely interacts with the virion-associated apolipoproteins (Owen *et al.*, 2009). However, the roles of LDLR in the entry process remain unclear, and HCV virions that bind to LDLR do not always initiate productive infection (Albecka *et al.*, 2012). Nonetheless, the interactions with cellular GAGs and LDLR serve to concentrate viral particles on the cell surface to facilitate further entry steps.

Following primary attachment, HCV virions interact with secondary receptors and other cellular factors. The human scavenger receptor class B type I (SR-BI), which is highly expressed in the liver, binds to lipoproteins (mostly high-density lipoprotein, HDL) to facilitate the uptake of cholesterol (Acton *et al.*, 1996). SR-BI binds to virion-

associated lipoproteins (Dao Thi *et al.*, 2011) and to HCV E2 protein (Scarselli *et al.*, 2002), contributing to virion attachment. Furthermore, the lipid transfer activities of SR-BI were proposed to remove virion-associated lipoproteins, thereby priming the virus particle for interactions with other cellular factors (Dao Thi *et al.*, 2011; Zeisel *et al.*, 2007). HCV E2 HVR1 binds directly to SR-BI (Scarselli *et al.*, 2002; Bankwitz *et al.*, 2010), which is thought to expose the regions in E2 that bind to the Cluster of Differentiation 81 (CD81).

CD81 is a member of the tetraspanin family, a group of cell-surface proteins that mediate signal transduction events (Levy *et al.*, 1998). CD81 was the first cellular receptor identified to bind HCV, through interaction with the virion E2 protein (Pileri *et al.*, 1998). Later studies with HCVpp and HCVcc confirmed the involvement of CD81 during entry of infectious HCV particles (Bartosch *et al.*, 2003; Zhang *et al.*, 2004; Cormier *et al.*, 2004). Although HCV E2 binds to CD81, time-course studies with CD81-specific antibodies indicated that CD81 also mediates post-attachment events (Bertaux and Dragic, 2006; Farquhar *et al.*, 2012). CD81 engagement by HCV particles was later shown to trigger signaling through the epidermal growth factor receptor (EGFR) (Lupberger *et al*., 2011) and Rho and Ras GTPases (Brazzoli *et al*., 2008; Zona *et al*., 2013). These signaling pathways induce actin remodeling, facilitating the lateral movement of CD81-bound HCV particles along the cell surface to tight junctions. They also promote tetraspanin receptor complex assembly (Zona *et al*., 2013), allowing for the interaction of CD81 with tight junction proteins and HCV internalization via clathrin-mediated endocytosis (Farquhar *et al*., 2012).

A critical role of CD81 during HCV entry is to deliver the viral particle to the tight junctions, which are thought to be the site of HCV internalization. Claudin 1 (CLDN1), a tight junction protein highly expressed in the liver (Furuse *et al.*, 1998), is required for HCV infection (Evans *et al.*, 2007). Occludin (OCLN), another tight junction protein (Furuse *et al.*, 1993), is also required for HCV entry (Benedicto *et al.*, 2009). OCLN is thought to be involved in a post-binding step (Benedicto *et al.*, 2009; Ploss *et al.*, 2009), although its specific functions in HCV entry are not known. CLDN1, on the other hand, interacts with CD81 (bound to HCV particles) (Harris *et al.*, 2010), inducing clathrin-mediated endocytosis of the CLDN1-CD81-HCV complex (Farquhar *et al.*, 2012). Endocytosis of HCV virions is slow. In studies with pseudotyped HCV, only 50% of particles were internalized 53 minutes after the initiation of entry, which suggests the involvement of additional internalization or trafficking mechanisms (Meertens *et al.*, 2006).

Clathrin-mediated endocytosis ultimately delivers the HCV-receptor complex to Rab5-containing (early) endosomal compartments, where the low pH induces the actual fusion between the viral envelope and endosomal membranes (Farquhar *et al.*, 2012). It is thought that the interaction of E2 with CD81 primes the HCV glycoproteins for low pH-triggered fusion (Sharma *et al.*, 2011). Although it has been established that the HCV glycoproteins mediate low pH-dependent fusion (Lavillette *et al.*, 2006), there is still debate regarding the relative contributions of E1 and E2. HCV E2 was initially predicted to be a class II fusion protein (Krey *et al.*, 2010), like other *flaviviridae* E proteins. However, recent x-ray structures for E2 revealed a globular architecture that differs from the typical extended three-domain fold of class II fusion proteins (Kong *et al.*, 2013;

Khan *et al.*, 2014). Furthermore, E2 did not undergo conformational changes or oligomeric rearrangements when exposed to low pH (Khan *et al.*, 2014). Such changes would be expected for a fusion protein that mediates low pH-dependent fusion. More likely, E1 or the E1E2 heterodimer are responsible for fusion. Supporting this model, the interaction between E1 and E2 is critical for HCV entry into cells (Douam *et al.*, 2014).

Entry of HCV requires other cellular factors, although their specific roles are not yet known. The Niemann-Pick C1-like 1 cholesterol adsorption receptor is thought to contribute to virion binding or internalization, perhaps through its interactions with virion-associated cholesterol (Sainz *et al.*, 2012). Transferrin receptor 1 is required for a post-CD81 entry step (Martin and Uprichard, 2013). The cell death-inducing DNA fragmentation factor-like effector b was identified as another HCV entry factor. It was proposed to be involved in a late step of entry, such as membrane fusion (Wu *et al.*, 2014). However, the overall contributions of these receptors during entry are unclear.

Following entry, HCV genomes replicate in the cytoplasm, using membranous webs derived from the endoplasmic reticulum (Egger *et al.*, 2002). Viral assembly requires cellular lipid droplets as a platform (Boulant *et al.*, 2007; Miyanari *et al.*, 2007). Assembled particles bud into the endoplasmic reticulum and traffic through the secretory pathway. During this trafficking, E1 and E2 are post-translationally modified by *N*-linked glycosylation (Goffard *et al.*, 2005). Infectious viral particles are then exported from the cell in conjunction with lipoprotein secretion (Gastaminza *et al.*, 2008).

HCV exemplifies an enveloped, HS-binding RNA virus with complex entry pathways involving many cellular factors. HCV fusion is induced by low pH in the endosome and mediated by a member of the proposed novel class IV fusion proteins.

1.6.2 Herpes simplex virus 1 (HSV-1)

HSV-1 latently infects the majority of the world's population (Smith and Robinson, 2002). Rarely, HSV-1 can cause encephalitis (Whitley, 2006) and causes severe outcomes in immunocompromised individuals. HSV-1 is an enveloped nuclear-replicating DNA virus in the *herpesviridae* family, with a linear double-stranded genome of approximately 150 kilo-base pairs (Kieff *et al*., 1971). The genome is enclosed by the nucleocapsid, which is surrounded by a proteinacious tegument layer (Grunewald *et al*., 2003). The viral particle is enveloped, with several glycoproteins embedded within the envelope.

Entry of HSV-1 into cells involves five surface glycoproteins: gB, gC, gD, gH and gL (Shukla and Spear, 2001). gC and gB are responsible for the primary attachment, through an interaction with HS moieties on cell-surface GAGs (WuDunn and Spear, 1989; Herold *et al*., 1991; Herold *et al*., 1994). Secondary binding is mediated by gD, which binds to one of several entry receptors: 3O-sulfated HS, herpesvirus entry mediator (HVEM) or nectin (O'Donnell *et al.*, 2010; Whitbeck *et al.*, 1997; Di Giovine *et al.*, 2011). Binding of gD to any one of its receptors triggers a conformational change, exposing a C-terminal peptide chain that interacts with gB or the gH/gL complex to activate the fusion process (Cocchi *et al.*, 2004).

HSV-1 fusion itself is less clearly understood. Although gB has now been established to be the fusion protein (Heldwein *et al.*, 2006), the roles of gH/gL are less clear. The structure of gH/gL has no homology to any known fusion protein (Chowdary *et al.*, 2010). However, interactions between gB and gH/gL are required for fusion (Atanasiu *et al.*, 2010), suggesting a model in which gH/gL is required to regulate the

activity of gB during fusion (Jackson and Longnecker, 2010). gL is required for posttranslational processing and surface expression of gH (Hutchinson *et al.*, 1992). Otherwise, the functions of gL/gH remain elusive. The entry pathway of HSV is dependent on cell type. For example, fusion with neurons or Vero cells occurs at the plasma membrane at neutral pH (Wittels and Spear, 1991), whereas fusion with HeLa and Chinese hamster ovary cells involves pH-dependent endocytosis (Nicola *et al.*, 2003). Nonetheless, all known routes of HSV entry require gD, gB and gH/gL.

HSV-1 is an example of an enveloped, nuclear-replicating, HS-binding DNA virus that fuses mostly by pH-independent mechanisms at the plasma membrane. Entry of HSV-1 requires four glycoproteins to mediate binding and fusion. Fusion itself is mediated by gB, a class III viral fusion protein.

1.6.3 Vesicular stomatitis virus (VSV)

VSV is an arbovirus that is transmitted by insects between mammalian hosts, typically infecting livestock but occasionally causing a flu-like illness in humans (Reis Jr *et al.*, 2009). VSV is an enveloped cytoplasmic-replicating RNA virus in the *rhabdoviridae* family, and as such is often used as a model for rabies virus. VSV has a non-segmented negative sense single-stranded RNA genome of approximately 11 kilo-base pairs. VSV virions have a bullet-shaped morphology and encode an envelope glycoprotein (G), the matrix protein (M), the nucleocapsid protein (N), the phosphoprotein (P) and the RNA-dependent RNA polymerase (L). VSV has a broad tropism in cell culture and infects a wide range of cell types.

The VSV G protein is the only glycoprotein embedded in the lipid envelope of VSV virions. VSV G is necessary for the binding, internalization and fusion of viral

particles (Harrison, 2008; Sun *et al*., 2005). Despite the wide tropism of VSV, its receptors have not been identified with certainty. The primary attachment of VSV is thought to involve low affinity interactions with glycans, such as HS (Conti *et al*., 1991) or SA (Superti *et al*., 1986). However, subsequent binding steps have not been clearly defined. VSV binding was unaffected by proteolytic digestion of cell surface proteins (Schloemer and Wagner, 1975). This observation led to a proposed model in which the receptor is not a membrane protein, but rather an integral component of the plasma membrane, such as phosphatidylserine (PS) (Schlegel *et al*., 1983; Yamada and Ohnishi, 1986). However, the model was later refuted based on the argument that most PS localizes to the inner leaflet of the plasma membrane, where it would be inaccessible to the virions (Coil and Miller, 2004). More recently, LDLR was proposed as the receptor for VSV (Finkelshtein *et al*., 2013), based on several lines of evidence. Soluble LDLR inhibits VSV infectivity, and antibodies against LDLR inhibited VSV binding to some extent (Finkelshtein *et al*., 2013). VSV bound to cells inhibits the binding of LDL, the physiological LDLR ligand. The endoplasmic reticulum chaperone gp96 was also shown to be involved in VSV binding (Bloor *et al*., 2010), perhaps by assisting with the proper folding and glycosylation of LDLR (Finkelshtein *et al*., 2013). However, multiple genome-wide RNAi screens did not identify LDLR among the host genes essential for VSV replication (Panda *et al*., 2011; Lee *et al*., 2014), and further studies are much needed to clarify the roles of the proteins implicated in VSV entry.

Following binding, VSV undergoes clathrin-mediated endocytosis (Sun *et al*., 2005), but not by classical physiological mechanisms. As a result of their much larger size compared to cellular cargo, VSV virions are internalized in vesicles that are only

partially coated with clathrin in a process that requires actin (Cureton *et al*., 2009). Once internalized into acidic endosomes, VSV G induces fusion by low pH-dependent mechanisms (Blumenthal *et al*., 1987) that involve structural rearrangements of the G protein (Carneiro *et al*., 2001). Fusion and nucleocapsid release into the cytoplasm are sequential processes, suggesting a two-step process in which VSV first fuses to internal vesicles within early endosomes at pH 6 (Le Blanc *et al*., 2005; Blumenthal *et al*., 1987). Internal vesicles containing VSV nucleocapsids subsequently "back-fuse" to the outermost endosomal membrane, releasing the nucleocapsids into the cytoplasm (Le Blanc *et al*., 2005).

VSV G is a class III fusion protein of mixed alpha helical and beta sheet structure (Roche *et al*., 2006). It triggers fusion following low pH-induced structural rearrangements that lead to the post-fusion hairpin conformation commonly found in viral fusion proteins (Roche *et al*., 2006; Roche *et al*., 2007). Interestingly, whereas other fusion proteins are inactivated following low pH-induced structural changes, the conformational changes of VSV G are reversed when exposed to neutral pH (Gaudin, 2000a). The biological relevance of this reversibility is not clear.

Following fusion, the nucleocapsid is released into the cytoplasm together with the polymerase. The viral RNA remains sequestered in the nucleocapsid for all steps of the replication cycle, including the RNA synthesis steps of transcription and replication (Luo, 2012). Following RNA synthesis and protein synthesis, the nucleocapsid is assembled simultaneously with replication of the viral RNA genome (Patton *et al*., 1984). The newly formed nucleocapsids then bud through the plasma membrane, acquiring M and G proteins at the membrane.

In summary, VSV is an enveloped HS- or SA-binding RNA virus that fuses by pH-dependent mechanisms in early endosomes. Furthermore, binding and fusion are mediated by only one class III fusion protein, VSV G. The cellular factors involved in VSV entry are not clearly defined.

1.6.4 Influenza A virus (IAV)

IAV causes seasonal epidemics and less frequent pandemics as a result of antigenic drift and shift (Taubenberger and Kash, 2010). IAV is an enveloped nuclear-replicating RNA virus classified in the *orthomyxoviridae* family. IAV has a segmented, negative sense single-stranded genome. Virions are comprised of eight gene segments bound to the RNA polymerase and nucleocapsid protein, surrounded by matrix protein (M) lining the inner leaflet of a host-derived lipid envelope. The HA, neuraminidase (NA) and M2 ion channel are embedded within the envelope. Influenza virions can have spherical or filamentous morphology, depending on genetic determinants (Smirnov *et al*., 1991) and host cell type (Roberts and Compans, 1998). The morphology of IAV virions influences the entry pathway.

IAV entry is perhaps the most studied viral entry pathway. Human IAV strains bind to α(2,6)-linked SA, which is abundant on epithelial cells in human upper respiratory tracts. Attached virions are then internalized by endocytosis, although the route of endocytosis may vary. The predominant internalization route is clathrin-dependent endocytosis involving classical cellular proteins (Zhang and Whittaker, 2014; Matlin *et al*., 1981; Chen and Zhuang, 2008; Roy *et al*., 2000). However, clathrin-independent pathways have also been observed (Nunes-Correia *et al*., 2004; Rust *et al*., 2004; Sieczkarski and Whittaker, 2002; de Vries *et al*., 2011; Rossman *et al*., 2012).

Regardless of the particular internalization pathway, the low pH (5.0) of late endosomes triggers fusion (Guinea and Carrasco, 1994a). The low pH induces conformational changes in HA, projecting the fusion peptide into the target endosomal membrane, which may induce membrane perturbation to facilitate lipid exchange during fusion. Prior to fusion, however, the fusion peptide diffuses through the lipid bilayer to become self-associated, which is a critical event for fusion (Chernomordik *et al*., 1998). Ultimately, the fusion protein folds back on itself, pulling the target membrane and the viral envelope into close proximity (Eckert and Kim, 2001). Fusion is widely understood to occur according to the hemifusion stalk model.

In the endosomal compartments, the virion interior is acidified through the action of the M2 ion channel (Pinto and Lamb, 2006). Virion acidification dissociates the envelope protein M1 from the nucleocapsid (Bui *et al*., 1996), which allows cellular transport machinery to translocate the nucleocapsid and viral RNA segments into the nucleus (O'Neill *et al*., 1995). Uniquely for an RNA virus, transcription and replication of the viral genome occurs within the host cell nucleus (Herz *et al*., 1981). Newly assembled virions bud from the plasma membrane, but remain attached to the cell surface until viral NA cleaves sialic acids, releasing the viral particles from the plasma membrane (Palese *et al*., 1974).

In summary, IAV is an enveloped, nuclear-replicating, SA-binding RNA virus that fuses by pH-dependent mechanisms within acidified endosomal compartments. Binding and fusion of IAV is mediated by HA, a class I viral fusion protein.

1.6.5 Other viruses used as models

Other viruses share a number of features with those described for HCV, VSV, HSV-1 and

IAV, in terms of their entry pathways.

Vaccinia virus (VACV), a large enveloped DNA virus classified in the *poxviridae* family, uniquely has two different enveloped forms (Smith *et al.*, 2002). Both forms contain the same nucleocapsid core, but differ in the number of envelopes. The mature virion (MV) form is wrapped in a single lipid envelope (Smith *et al.*, 2002) and is released from cells by lysis. The extracellular virion (EV) form is wrapped in an additional envelope containing four viral proteins that are not found in the MV (Smith *et al.*, 2002). MV membrane proteins (D8, A27 and H3) bind to cell surface glycosaminoglycans (Hsiao *et al.*, 1998; Hsiao *et al.*, 1999; Chung *et al.*, 1998; Lin *et al.*, 2000). EVs are thought to attach to cells by different mechanisms (Vanderplasschen *et al.*, 1998), although the viral proteins and cellular receptors involved are unknown. It is thought that the additional envelope of EVs is shed, by nonfusogenic dissolution, prior to fusion (Law *et al.*, 2006). Viral fusion occurs by pH independent mechanisms at the plasma membrane, or by pH dependent mechanisms after endocytosis (Townsley *et al.*, 2006). However, the specific fusion mechanisms and the proteins involved are unknown.

Sindbis virus (SINV) is an enveloped RNA virus classified in the *togaviridae* family. The E2 protein mediates primary attachment of SINV to HS-containing glycosaminoglycans on the cell surface (Byrnes and Griffin, 1998), and the higher affinity secondary binding partners have been suggested to include the high-affinity laminin receptor (Wang *et al.*, 1992). Attached virions are internalized into endosomal compartments (DeTulleo and Kirchhausen, 1998), where fusion is induced by exposure to low pH (Smit *et al.*, 1999). Endosomal acidification dissociates the E1/E2 heterodimer, leading to the trimerization of E1 subunits and exposing the fusion peptide (Kielian *et al.*,

2010). E1 is a class II fusion protein.

Reovirus (RV) is a nonenveloped segmented double-stranded RNA virus classified in the *orthoreoviridae* family. The low-affinity primary attachment of RV is to α-linked sialic acid on the cell surface (Gentsch and Pacitti, 1985; Paul *et al.*, 1989; Reiter *et al.*, 2011), followed by higher-affinity interactions with the junctional adhesion molecule-A (JAM-A) (Barton *et al.*, 2001). These interactions are mediated by RV sigma 1 protein (Lee *et al.*, 1981). Activation of β1 integrins is subsequently required for the internalization of RV virions (Maginnis *et al.*, 2006), through clathrin-mediated endocytosis or other endocytotic routes (Schulz *et al.*, 2012). Within endosomal vesicles, proteolysis removes the outermost capsid protein, exposing a membrane penetration protein μ1 (Sturzenbecker *et al.*, 1987). μ1 undergoes structural rearrangements that result in the insertion of a hydrophobic peptide into the membrane, mediating membrane disruption (Chandran *et al.*, 2002). Replication of viral RNA then occurs in the cytoplasm.

Adenovirus (AdV) is a nonenveloped double-stranded DNA virus classified in the *adenoviridae* family. Fifty-one serotypes of AdV have been identified and are further classified into six groups (A to F) (Zhang and Bergelson, 2005). In addition to other properties, viruses within each group display a specific tissue tropism, which may reflect their receptor usage. Group B, C and E viruses tend to cause respiratory infections, whereas group F viruses cause gastroenteritis and group D viruses cause keratoconjunctivitis. All AdV types are comprised of a nucleocapsid from which the fiber proteins project. The distal end of the fiber proteins attaches to cellular receptors. AdV types 2 and 5 (group C) bind initially to HS-containing proteoglycans (Dechecchi *et al.*,

2000; Dechecchi *et al.*, 2001). Many AdV types bind with higher affinity to the coxsackievirus and adenovirus receptor (CAR) (Zhang and Bergelson, 2005). Group B AdV is thought to bind to Cluster of Differentiation 46 (CD46) (Gaggar *et al.*, 2003), whereas other types appear to bind to CD80 and CD86 (Short *et al.*, 2004). Group D viruses bind to α(2,3)-linked SA (Arnberg *et al.*, 2000). Cellular integrins are also important receptors for many AdV types. Engagement of integrins induces signalling pathways (Li *et al.*, 1998a; Li *et al.*, 1998b) that are important for virion internalization (Wickham *et al.*, 1993). AdV is internalized by clathrin-mediated endocytosis (Greber *et al.*, 1993; Wang *et al.*, 1998) but may also use other pathways, such as macropinocytosis (Meier *et al.*, 2002). Endosomal acidification triggers changes in the AdV capsid that lead to lysis of the endosomal membrane and entry of the viral capsid into the cytosol (Leopold and Crystal, 2007). Cellular integrins are thought to promote AdV-mediated membrane permeabilization (Wickham *et al.*, 1994). Replication and transcription of the AdV genomes occurs in the host cell nucleus (Pombo *et al.*, 1994).

1.6.6 Emerging viruses

Emerging viruses are newly discovered or zoonotic viruses increasing in incidence in human populations. Usually, the increased incidence is accompanied by changes in pathogenicity (Howard and Fletcher, 2012). Two novel coronaviruses, SARS-CoV and Middle Eastern Respiratory Syndrome (MERS)-CoV, have emerged within the last decade (Graham *et al.*, 2013; Kupferschmidt, 2014). SARS-CoV and MERS-CoV likely emerged from bats and camels, respectively (Ge *et al.*, 2013; Azhar *et al.*, 2014; Alagaili *et al.*, 2014). Filoviruses (Ebola virus and Marburg virus) and some orthomyxoviruses (avian H5N1 and H7N2 IAV strains) are also considered emerging viruses (Morens and

Fauci, 2013). Although many details about their proteins and replication steps are unknown, they are understood to enter cells following similar mechanisms as other viruses. Filoviruses bind to HS moieties in cellular GAGs (Salvador *et al.*, 2013), and are internalized into endosomal compartments (Nanbo *et al.*, 2010) where fusion occurs, mediated by a class I fusion protein (Lee *et al.*, 2008). Some coronaviruses bind to HS or SA moieties (Vlasak *et al.*, 1988; Vicenzi *et al.*, 2004; Lang *et al.*, 2011), and then are internalized (Wang *et al.*, 2008b; Qian *et al.*, 2013). Fusion is mediated by the S protein, a class I fusion protein, and can occur within endosomes or at the plasma membrane, depending on cleavage of the S protein (Bosch *et al.*, 2003; Lu *et al.*, 2014). Avian IAV strains that adapt to spread well in humans bind to α(2,6)-linked SA *(Shelton 2011)* and fuse within endosomal compartments as a result of low pH activation of HA, a class I fusion protein. The similarities in entry steps for these emerging viruses highlight the potential uses of inhibitors targeting these steps in pandemic or epidemic situations.

1.7 VIRAL ENTRY AS AN ANTIVIRAL TARGET

Viral entry is an attractive target for therapeutic intervention. Entry inhibitors prevent infection, thereby inhibiting virus replication before persistent reservoirs can be established through genome integration (for retroviruses such as HIV) or covalently closed circular DNA (for HBV). Entry inhibitors block the activation of potentially harmful cell-mediated immune responses, such as the cytokine storm induced by IAV, which strongly affects the outcome and pathogenesis of IAV infections (Oldstone *et al.*, 2013). Furthermore, compounds targeting certain steps of viral entry may have broad-

spectrum activity, as the basic principles of primary attachment and fusion are conserved for many unrelated human viruses.

1.7.1 Inhibitors of primary attachment

The conserved mechanisms involved in binding to HS allow for the binding of many viruses to be disrupted with appropriately shaped and charged molecules. Soluble heparin, HS mimetics, and other similarly charged (and shaped) polyanions inhibit the infectivity of this group of viruses. Sulfated polysaccharide derivatives, and sulfated polymers in general, mimic HS and compete for the binding of virion glycoproteins. Dextran sulfate, pentosan polysulfate and other sulfated polysaccharides all inhibit the infectivity of HSV-1/-2, CMV, VSV, SINV, HIV and some flaviviruses (Baba *et al.*, 1988; Lee *et al.*, 2006a), which all bind to HS. Similarly, many polysulfonates and sulfonic acid polymers inhibit the infectivity of the HS-binding HIV (Cardin and Weintraub, 1989; Clanton *et al.*, 1992; Mohan *et al.*, 1992) and the polysulfonate suramin inhibits adsorption of the HS-binding HSV-1 (Aguilar *et al.*, 1999). Sulfated homologues of heparin also inhibit HCV entry (Basu *et al.*, 2007). Collectively, these compounds block the binding of positively charged amino acids residues in the viral gp120 to the cell surface heparan sulfate (Moulard *et al.*, 2000). Polycarboxylates such as aurintricarboxylic acid (Schols *et al.*, 1989), as well as polyhydroxycarboxylates derived from phenolic compounds (Schols *et al.*, 1991; Meerbach *et al.*, 2001), also have inhibitory activity against HS-binding viruses, including HIV, HSV-1, CMV and VACV (Neyts *et al.*, 1992). It is likely that the polycarboxylates, which compete with heparin for binding (Neyts *et al.*, 1992), also disrupt the interaction between basic regions of virion

glycoproteins and cellular heparan sulfate. The acidic carboxylic groups of the phenolic compounds are necessary for antiviral activity (Helbig *et al.*, 1997). Other natural products act through similar mechanisms. Sulfated polysaccharides from various species of algae (Witvrouw and De Clercq, 1997; Harden *et al.*, 2009), and natural products fucoidan and carrageenan (Baba *et al.*, 1988) inhibit the infectivity of various HS-binding enveloped viruses. Recently, two tannins (chebulagic acid and punicalagin) isolated from the deciduous *Terminalia chebula* tree were shown to block attachment of a diverse group of viruses that utilize GAGs for binding (Lin *et al.*, 2013). In the case of HSV-1, chebulagic acid and punicalagin prevented HSV-1 glycoproteins from interacting with cell-surface GAGs (Lin *et al.*, 2011). Although all of these compounds are notable for their broad-spectrum activity, they do not inhibit the binding of another important group of human viruses, those that bind to SA.

SA derivatives and sialyl mimetics are active against SA-binding viruses. They have been tested mainly against IAV. As for virion attachment to cells, binding of HA to soluble sialyl mimetics requires multiple HA-sialic acid contacts (Matrosovich and Klenk, 2003) and depends on the spatial orientation, size and flexibility of the inhibitor. Polyvalent inhibitors are far more potent than monovalent ones. For example, equine α-macroglobulin (with multiple SA residues in appropriate orientations) has a million-fold higher potency against IAV than free N-linked oligosaccharides (Pritchett and Paulson, 1989). Optimized synthetic sialylglycopolymers on a poly[N-(acryoyloxysuccinimide], polyacrylic acid or polyacrylamide backbone, with variable arrangement and number of sialyl residues, were even more potent against IAV binding, with EC_{50} in the nanomolar range (Mammen *et al.*, 1995; Choi *et al.*, 1997; Lees *et al.*, 1994). Similarly, sialic acid-

conjugated dendritic polymers and glycopolymers are more effective than monomeric SA at inhibiting IAV binding (Reuter *et al.*, 1999; Hidari *et al.*, 2008). Monovalent sialyl mimetics cannot effectively compete with multivalent interactions with cellular glycans (Matrosovich, 1989). Sialyl mimetics ideally should selectively interact with HA and not with the viral neuraminidase (NA) (Sparks *et al.*, 1993; Itoh *et al.*, 1995). Otherwise, the effectiveness of the HA inhibitor will be reduced as a result of cleavage by NA. However, it may be possible to inhibit both HA and NA with a single molecule (Guo *et al.*, 2002).

Glycopeptides that interfere with IAV binding have also been described. A star-like trivalent glycopeptide mimetic, comprised of three sialyl moieties linked by peptide regions, was designed to bind the receptor sites in each monomer of the HA homotrimer (Waldmann *et al.*, 2014). The glycopeptide had high binding affinity for HA, although its anti-IAV activities were not tested. Pharmacological delivery of such a large molecule would be difficult.

Another means of inhibiting primary attachment is to remove the glycan receptors from the cell surface. DAS181, a sialidase from *Actinomyces viscosus* is in phase II clinical development (Moss *et al.*, 2012). The sialidase is fused to an epidermal growth factor-like domain that targets the sialidase to respiratory epithelial cells (Malakhov *et al.*, 2006). DAS181 prevents attachment of respiratory viruses that utilize SA as a receptor (Nicholls *et al.*, 2013).

Overall, the search for primary attachment inhibitors has proved difficult, and despite more than 30 years of research, no small-molecule inhibitor with therapeutic application has yet been found. HS mimetics suffer from drawbacks that limit their use in

vivo. Polysulfates, for example, are poorly absorbed after oral administration (Lorentsen *et al.*, 1989), and cause thrombocytopenia when administered intravenously (Flexner *et al.*, 1991). Most sulfated polymers have strong anticoagulant activity (Rosenberg, 1978), arguing against their clinical use for antiviral therapy. It was possible, however, to dissociate the antiviral effects of sulfated polysaccharides from their antithrombin activity (Baba *et al.*, 1990; Barzu *et al.*, 1993). The number, distribution and spatial configuration of the sulphate groups were proposed to differentially influence the antiviral and antithrombin activities. Therefore, appropriate chemical modifications or novel compound scaffolds could help to overcome the limitations of HS mimetic antivirals.

Many natural products of different scaffolds are biologically active. Green tea polyphenols such as epigallocatechin gallate (EGCG) have a number of interesting biological activities, including antiviral effects against many unrelated enveloped and nonenveloped viruses (Steinmann *et al.*, 2013). EGCG interferes with the primary attachment of unrelated viruses that bind to HS or to SA. The specific activities and mechanisms of EGCG are described in **Chapter 3** of this thesis.

1.7.2 Inhibitors of higher affinity binding

Another group of entry inhibitors target the higher affinity secondary binding, providing more specific but also more limited spectrum activity. Such inhibitors have been best described for HIV therapy. One such inhibitor, maraviroc, was approved in 2007 for clinical use against HIV-1 (Lieberman-Blum *et al.*, 2008). Maraviroc is an antagonist of the HIV-1 co-receptor CCR5 (Dragic *et al.*, 1996), a G protein-coupled receptor. CCR5 was established as an attractive target based on a population of individuals with a natural genetic absence of surface-expressed CCR5. These individuals are resistant to HIV-1

(Liu *et al.*, 1996). Epidemiological studies highlighted the importance of CCR5 in HIV-1 infection, and also suggested that antagonists of CCR5 would have minimal off-target effects. Maraviroc was then identified by a high-throughput screen. It demonstrated high selectivity as a CCR5 antagonist with minimal cytotoxicity (Dorr *et al.*, 2005). Maraviroc acts through allosteric mechanisms, altering the conformation of CCR5 extracellular loops to prevent the binding of HIV-1 gp120 (Tsamis *et al.*, 2003). Without binding of gp120 to CCR5, subsequent entry steps are blocked (Dorr *et al.*, 2005). However, maraviroc is not active against T-cell-tropic HIV strains, which use CXC-receptor 4 as a co-receptor (Bleul *et al.*, 1996). Other HIV entry inhibitors in clinical development have broader activity against HIV, by blocking interactions between HIV gp120 and its main receptor, CD4. BMS-378806, an azaindole derivative, interacts directly with gp120 to prevent its binding to CD4 (Lin *et al.*, 2003; Guo *et al.*, 2003). BMS-626529 similarly blocks the interactions between gp120 and the CD4 receptor (Nowicka-Sans *et al.*, 2012).

Other pre-clinical strategies to inhibit viral binding have been identified. Proteins that bind to viral glycoproteins also interfere with virion binding. Lectins, saccharide-binding proteins, bind to glycans on viral glycoproteins to disrupt entry functions, including binding to secondary receptors. The algal griffithsin binds to HIV-1 gp120 to inhibit its interactions with CD4 (Mori *et al.*, 2005), to glycans on HCV envelope proteins to prevent binding to CD81 (Meuleman *et al.*, 2011), and to the SARS-CoV glycoprotein (O'Keefe *et al.*, 2010). Cyanovirin-N, a lectin isolated from cyanobacterial species, binds to contain N-linked high mannose oligosaccharides (Bolmstedt *et al.*, 2001) on HIV-1 gp120 (Boyd *et al.*, 1997), HCV E2 (Helle *et al.*, 2006), Ebola virus glycoprotein (Barrientos *et al.*, 2003) and IAV HA (O'Keefe *et al.*, 2003). Cyanovirin-N

blocks recognition of the cellular receptors, preventing binding and subsequent entry steps.

1.7.3 Inhibitors of internalization

Inhibitors of endocytosis often have broad-spectrum activity, as a diverse group of viruses enter cells by endocytosis. Acidification of endosomes, which is driven by the vacuolar H(+)-ATPase, is necessary for entry of many viruses. Inhibitors of the vacuolar H(+)-ATPase, such as bafilomycin A (Perez and Carrasco, 1994; Ochiai *et al.*, 1995), concanamycin A (Guinea and Carrasco, 1994b) have broad antiviral activities. Dynasore, a dynamin GTPase inhibitor, prevents scission of endocytotic vesicles with concomitant antiviral activity (Abban *et al.*, 2008; de la Vega *et al.*, 2011; Edinger *et al.*, 2014). Although these inhibitors are often used in research, they are cytotoxic and not suitable for clinical use. Milder perturbations of endocytotic pathways may be able to disrupt virion entry with minimal effects on cellular functions.

Silymarin is an extract from milk thistle with antiviral properties, mostly described in the context of HCV. Silymarin is a mixture of seven flavanolignans (silibinin A, silibinin B, isosilybin A, isosilybin B, isosilychristin, silychristin and silydianin) and one flavonoid (taxifolin) (Kroll *et al.*, 2007) **(Figure 1.4A)**. The silymarin mixture has many effects on the HCV replication cycle (Wagoner *et al.*, 2010), and silibinin itself was recently described as an inhibitor of HCV clathrin-mediated endocytosis (Blaising *et al.*, 2013a). Silibinin also showed some activity against IAV, VSV and RV, which depend at least partially on clathrin-mediated endocytosis for infection (Blaising *et al.*, 2013a). The specific mechanisms were not identified, but silibinin appeared to induce the accumulation of clathrin-coated structures in the cytosol. It was proposed that silibinin

decreases the rate of clathrin-coated pit formation at the plasma membrane. HCV virions may perhaps be directed to a non-productive path of infection as a result.

Arbidol **(Figure 1.4B)** is a synthetic indole-based antiviral that has been approved in Russia and China against IAV, although its mechanism of action remains unclear. Arbidol has broad activity against several unrelated viruses (Blaising *et al.*, 2014), mostly through direct effects on viral entry. Arbidol interacts with both lipids (through intercalation in a layer above the glycerol backbone of phospholipids) and proteins (through aromatic stacking interactions) (Teissier *et al.*, 2011b). Recently, arbidol was shown to interfere with several steps in clathrin-mediated endyctosis. Arbidol inhibited dynamin-induced membrane scission, therefore preventing the release of clathrin-coated vesicles from the inner surface of the plasma membrane (Blaising *et al.*, 2013b). Virions trapped in these vesicles were not properly trafficked to the Rab5-containing endosomal compartments where fusion occurs (Blaising *et al.*, 2013b). However, inhibition of endosomal trafficking does not account for all the activities of arbidol (Teissier *et al.*, 2011b; Boriskin *et al.*, 2008), and additional mechanisms are likely involved.

1.7.4 Inhibitors of fusion

Peptides that mimic domains of fusion proteins inhibit fusion by preventing formation of helical bundles. They were first described in the context of paramyxoviridae fusion (Richardson *et al.*, 1980). One such peptide, enfuvirtide (Fuzeon, T-20), was the first approved entry inhibitor for use against HIV. Enfuvirtide is a 36-residue biomimetic peptide based on the C-terminal domain (heptad repeat (HR)-2) of the HIV-1 fusion protein, gp41 (Wild *et al.*, 1994). Enfuvirtide binds to the HR-1 region of gp41, preventing it from interacting with HR-2 and therefore inhibiting formation of the

fusogenic six-helix bundle (Greenberg and Cammack, 2004). Similar peptide-based fusion inhibitors against other viruses are in pre-clinical development. Inhibitory peptides derived from other class I fusion proteins were identified for paramyxoviruses (Rapaport *et al.*, 1995; Lambert *et al.*, 1996) and coronaviruses (Sainz *et al.*, 2006; Lu *et al.*, 2014). Peptides derived from flavivirus envelope (E) proteins inhibit infectivity of DENV, WNV and HCV (Hrobowski *et al.*, 2005; Liu *et al.*, 2010). The E-derived peptide blocked the conformational changes required for fusion of DENV (Schmidt *et al.*, 2010). Peptides based on HSV-1 gB sequences were also inhibitory to HSV-1 (Akkarawongsa *et al.*, 2009). Therefore, peptide-based inhibitors of fusion are effective for all classes of viral fusion proteins.

Small molecule inhibitors of fusion, with more conventional drug-like properties, have also been tested in pre-clinical studies. A high-throughput screen identified small molecules that bind to the HIV-1 gp41 inner core and inhibit fusion by preventing gp41 structural rearrangements (Frey *et al.*, 2006). Small molecule inhibitors of RSV, such as VP-14637, were also shown to inhibit fusion by disrupting the activity of the fusion protein (Douglas *et al.*, 2003). Small molecules can also inhibit fusion triggered by low pH. Compound 1662G07 and analogs bind to the prefusion DENV E protein dimer. They then inhibit endosome-induced fusion by preventing fusogenic rearrangements of the E protein (Schmidt *et al.*, 2012). Several small molecules inhibit IAV HA-mediated fusion (Luo *et al.*, 1997; Plotch *et al.*, 1999; Vanderlinden *et al.*, 2010; Basu *et al.*, 2014), but act only on particular subtypes of IAV. These inhibitors bind directly to HA and block conformational changes required for fusion, for example by stabilizing the neutral pH structure of HA (Russell *et al.*, 2008).

The fusion inhibitors described so far are designed to bind directly and specifically to viral fusion proteins, resulting in a narrow spectrum of activity. This approach requires detailed knowledge of each fusion protein and the molecular mechanisms underlying the fusion process. For newly emerging viruses, the molecular details are not available. Furthermore, inhibition of virally encoded proteins readily selects for resistance (discussed further in **section 1.7.6**). Novel strategies, such as targeting non-virally encoded factors, may help to overcome these limitations.

One such strategy is to target lipids, which play a crucial role in the fusion process. Unlike viral proteins, lipids are not encoded by viral genomes and the structure of the lipid core of the virion envelope is conserved among enveloped viruses (although it differs in the specific lipid composition). Phospholipids with larger polar headgroups relative to their hydrophobic tails disfavour the curvature changes in membranes required for fusion (Chernomordik, 1996) and inhibit the fusion of several enveloped viruses (Vogel *et al.*, 1993; Gunther-Ausborn *et al.*, 1995; Stiasny and Heinz, 2004; Gaudin, 2000b). Although phospholipids are not pharmacologically useful, other molecules of appropriate shape and polarity could be designed to inhibit fusion by similar mechanisms. The rigid amphipathic fusion inhibitors (RAFIs) and other compounds that may act through these mechanisms are described in **Chapter 4** of this thesis.

Other compounds apparently inhibit fusion through interactions with lipid membranes. Silymarin and arbidol, described in **section 1.7.3** as inhibitors of clathrin-mediated endocytosis, also inhibit fusion. Silymarin did not affect the binding of HCV cell culture-derived virions, but did inhibit the fusion of pseudotyped HCV (HCVpp), and other pseudotyped enveloped viruses, with liposomes (Wagoner *et al.*, 2010; Blaising *et*

al., 2013a). The hydrophobic flavanolignan components of silymarin may incorporate into the lipid membranes to affect fusion. A possible explanation for its effects on both fusion and endosomal trafficking is that silibinin inhibits fusion between vesicles (transporting HCV virions) and endosomes (Blaising *et al.*, 2013a). Arbidol similarly inhibited the fusion of HCVpp of different genotypes (Pecheur *et al.*, 2007; Teissier *et al.*, 2011b). Arbidol was shown to interact with lipid membranes (binding to the polar head-groups of phospholipids) and also with tryptophan residues (Teissier *et al.*, 2011b). Arbidol was proposed to increase the affinity of viral glycoproteins for the membrane, inhibiting the conformational rearrangements required for fusion.

Fusion also depends on appropriate membrane fluidity (Harada *et al.*, 2005). Compounds that modulate membrane fluidity therefore affect fusion. Glycyrrhizin (**Figure 1.4C**), a natural product from licorice roots, inhibited HIV-1 fusion by decreasing the membrane fluidity, similar to cholesterol (Harada, 2005). Glycyrrhizin has long been known as a broad antiviral, with activity against VACV, HSV-1, VSV (Pompei *et al.*, 1979), VZV (Baba and Shigeta, 1987), MV (Hosoya *et al.*, 1989) and SARS (Cinatl *et al.*, 2003), in addition to HIV-1 (Harada, 2005). It may well be that glycyrrhizin inhibits the infectivity of these enveloped viruses by decreasing the fluidity of the virion envelopes. Interestingly, increasing membrane fluidity also inhibits infectivity. Phenothiazines that inhibit HCV entry were recently shown to increase the fluidity of the cholesterol-rich domains that HCV requires for entry (Chamoun-Emanuelli *et al.*, 2013). Phenothiazines or similar compounds may be active against other viruses that require cholesterol-rich membrane domains for entry. Another modulator of membrane fluidity, curcumin, is described in **Chapter 5** of this thesis.

LJ001 is a membrane-targeting compound active against all enveloped viruses tested, although its mechanisms remained elusive (Wolf *et al.*, 2010). LJ001 was proposed to act as a photosensitizer and induce modifications to the virion envelopes resulting from light-dependent lipid oxidation (Vigant *et al.*, 2013). Such oxidation, it was suggested, would affect the biophysical properties of viral envelopes (such as curvature and fluidity) to impair fusion. Cells, which use active mechanisms to repair membrane damage, are less susceptible (Vigant *et al.*, 2013). LJ001 and its derivatives will be discussed further in **Chapter 4** of this thesis.

An inhibitor of fusion, docosanol (Abreva), was approved for the treatment of herpes simplex infections (Katz *et al.*, 1991). Docosanol also inhibits the infectivity of other enveloped viruses (Katz *et al.*, 1991). Docosanol inhibits fusion of the HSV-1 envelope with the cellular membrane (Pope *et al.*, 1998), although the mechanisms are not clear. Docosanol did not act directly on virions (Pope *et al.*, 1998). Instead, the incorporation of docosanol into cellular membranes was proposed to alter the biophysical properties of the membrane to inhibit fusion.

1.7.5 Virucidal agents

Disrupting the viral envelope altogether is another method to block the entry of enveloped viruses. One inhibitor of HCV and HIV infectivity, PD404,182, lyses virion envelopes through unclear mechanisms that may involve the non-lipidic components of virion envelopes (Chamoun *et al.*, 2012). C5A, an amphipathic peptide derived from HCV NS5A, destabilizes viral membranes to inhibit entry of several enveloped viruses, including HCV and HIV (Cheng *et al.*, 2008; Bobardt *et al.*, 2008). C5A appears to selectively target viral membranes, in contrast to earlier membrane-disrupting agents that

were tested. Nonoxynol-9 was tested in the context of microbicide development to prevent HIV infection (Malkovsky *et al.*, 1988). Although it showed promising *in vitro* activity, nonoxynol-9 treatment actually increased HIV seroincidence in clinical trials, perhaps through detrimental effects on cellular membranes such as the vaginal epithelium (Van Damme *et al.*, 2002).

1.7.6 Other approved antivirals

Most current antivirals approved for clinical use target enzymes involved in viral replication, such as polymerases and proteases. These antivirals are limited to date to a handful of viruses: HIV, HCV, IAV, HBV and herpesviruses. All antivirals currently approved for clinical use, including the entry inhibitors previously discussed, are listed in **Tables 2 and 3**.

1.7.6.1 ***Antivirals against HIV.*** Anti-HIV drugs constitute the largest group of approved antivirals **(Table 2, Figure 1.5)**. Many of these target the viral reverse transcriptase (RT) **(Figure 1.5A)**, although by different mechanisms. The nucleoside reverse transcriptase inhibitors (NRTIs) include zidovudine, didanosine, zalcitabine, stavudine, abacivir, lamivudine and emtricitabine (De Clercq, 2004). As analogs of natural deoxynucleotides, NRTIs compete for incorporation into viral DNA. NRTIs lack a 3′-hydroxyl group and therefore cannot form the necessary phosphodiester bond to add additional nucleotides to extend the DNA chain. Such molecules are chain terminators. Tenofovir disoproxil, a nucleotide reverse transcriptase inhibitor (NtRTI), acts by similar chain termination mechanisms (Suo and Johnson, 1998). Non-nucleoside reverse transcriptase inhibitors (NNRTIs), including nevirapine, delavirdine, efavirenz, entravirine and rilpivirine, act through allosteric mechanisms, binding to a site distinct from the RT active site (de

Bethune, 2010). The binding induces conformational changes that affect the catalytic activity of the RT (Sluis-Cremer and Tachedjian, 2008).

Several HIV protease inhibitors have also been approved **(Figure 1.5B)**. The HIV protease cleaves HIV polyproteins to generate mature HIV progeny virions (Kohl *et al.*, 1988). Protease inhibitors include saquinavir, ritonavir, indinavir, nelfinavir, amprenavir, lopinavir, atazanavir, fosamprenavir, darunavir and tipranavir (De Clercq, 2010). With the exception of tipranavir, these are competitive peptidomimetics that mimic the transition state of the natural protease substrate and bind to the active site (De Clercq, 2004). They have a hydroxyethylene core that cannot be cleaved by the protease (Wensing *et al.*, 2010). Tipranavir is the only non-peptidomimetic inhibitor of the HIV protease (Turner *et al.*, 1998).

Other HIV inhibitors target different replication steps. The entry inhibitors maraviroc and enfuvirtide **(Figure 1.5C)** inhibit binding and fusion, respectively. Their activities are described in **sections 1.7.2** and **1.7.4** of this thesis. HIV integrase, which catalyzes the integration of the viral DNA into the host genome is the target of another group of antivirals **(Figure 1.5D)**. Raltegravir, elvitegravir and dolutegravir (De Clercq, 2010; Wills and Vega, 2012; Temesgen *et al.*, 2014) bind to the active site of the integrase to inhibit the strand transfer reaction required for integration of proviral DNA (McColl and Chen, 2010).

Any of these antivirals used alone quickly selects for resistant variants, due to the high mutation rate during HIV replication and the existence of HIV quasispecies (discussed further in **section 1.7.6**). Therefore, combination therapy, consisting of three or four different antivirals, is essential for the management of HIV infections (Shafer and

Vuitton, 1999). When a mutation conferring resistance to one drug arises, the other drugs suppress replication of that mutant. Several such combinations are approved for use.

1.7.6.2 Antivirals against HCV. For many years, ribavirin and pegylated interferon **(Table 2, Figure 1.6A)** were the only options for treatment of HCV. Treatment was lengthy, had many negative side effects, mostly associated with interferon, and was effective in only ~50% of patients infected with genotype 1 (the most common in North America) (Ghany *et al.*, 2009). The first direct-acting antivirals (DAA) for HCV were approved, for treatment of genotype 1, in 2011 **(Table 2, Figure 1.6B)**. The first drugs were two NS3-4A protease inhibitors, telaprevir and boceprevir. Both are peptidomimetic compounds that bind in the protease catalytic site. They must be used in combination with ribavirin and pegylated interferon to avoid selection of drug-resistant variants (Liang and Ghany, 2013). Simeprevir, another NS3-4A protease inhibitor, was approved in 2013 and is active against genotypes 1, 2 and 4 (Rosenquist *et al.*, 2014). However, it also presents a low barrier to selection of resistance.

The first member of a new class of anti-HCV drugs was approved in 2014. Sofosbuvir is a nucleotide analog that inhibits HCV NS5B (RNA-dependent RNA polymerase) by chain termination (Sofia *et al.*, 2010). Sofosbuvir is active against all HCV genotypes and has a high barrier to resistance (Pawlotsky, 2014). Resistant variants are not fit enough to replicate at high levels. Sofosbuvir is effective in combination with ribavirin without interferon (Gane *et al.*, 2013), meeting the goal of interferon-free therapy. Many other DAA are in late stages of clinical development, including other NS5B polymerase inhibitors (Chow *et al.*, 2010; Haudecoeur *et al.*, 2013), second-generation protease inhibitors (Summa *et al.*, 2012), NS5A inhibitors (Pawlotsky, 2013)

and host-targeting antivirals, such as cyclophilin inhibitors (Coelmont *et al.*, 2009) and a miRNA-122 antagonist (Janssen *et al.*, 2013).

As for HIV, HCV monotherapy readily selects for resistant variants. Combination therapy will be important for treating HCV infections (Pawlotsky, 2014).

1.7.6.3 Antivirals against IAV. The antivirals targeting IAV can be divided into two groups, those that target the M2 ion channel and those that target the NA **(Table 2, Figure 1.7)**. The first group is comprised of two adamantanes: amantadine and rimantadine (Davies *et al.*, 1964). These small molecules block the M2 ion channel, preventing the passage of H^+ ions and subsequent acidification of the virion core that is essential for the uncoating process (Pinto *et al.*, 1992). M2 inhibitors target only IAV, not other influenza types. However, there is currently widespread resistance among IAV strains (Ison, 2011), and the M2 inhibitors are not recommended for clinical use.

The neuraminidase (NA) inhibitors are *N*-acetylneuramic acid (SA) analogues that inhibit the viral NA, thereby preventing the release of progeny virions from the cell surface (Meindl *et al.*, 1974; von Itzstein *et al.*, 1993). Zanamivir and oseltamivir bind to the active site of the NA in an energetically favourable interaction, thereby inhibiting NA activity. Resistance to the current NA inhibitors is readily selected for (Ison, 2011). Other NA inhibitors, peramivir and laninamivir, are approved for use in Japan but are still undergoing Phase III trials in the USA (Shetty and Peek, 2012; Ikematsu and Kawai, 2011).

1.7.6.4 Antivirals against HBV. Some HIV drugs are also active against HBV, which also requires a reverse transcription step during replication (Summers and Mason, 1982) **(Table 3, Figure 1.8)**. Lamivudine, a cytosine nucleoside analog that was the first

approved anti-HBV drug, inhibits HBV replication (Suzuki *et al.*, 1988) by acting as a chain terminator for the HBV RT (Severini *et al.*, 1995). Adefovir dipivoxil, an acyclic phosphonate analog of adenosine, also targets the HBV RT and acts as a chain terminator (Marcellin *et al.*, 2003). Entecavir, a guanosine nucleoside analog, inhibits reverse transcription, DNA replication and transcription (Seifer *et al.*, 1998). Finally, telbivudine, a thymidine nucleoside analog, inhibits the HBV DNA polymerase through chain termination mechanisms (Ruiz-Sancho *et al.*, 2007).

As for HCV, interferon and pegylated interferon **(Figure 1.6A)** are approved for the treatment of HBV. They act by inducing an antiviral state (Asselah *et al.*, 2007), but are associated with adverse effects.

1.7.6.5 Antivirals against herpesviruses. The antivirals targeting herpesviruses are the second largest group of antivirals **(Table 3, Figure 1.9)**. Most are chain terminators that target the viral DNA polymerase after activation by intracellular phosphorylations, the first of which is catalyzed by virally encoded thymidine kinase (TK). The acyclic nucleoside analogs include acyclovir and its prodrug valaciclover, penciclovir and its prodrug famciclovir, and finally ganciclover and its prodrug vanganciclovir (De Clercq, 2004). Cidofovir does not depend on viral TK for activation. Following phosphorylation by intracellular kinases, cidofovir is incorporated into viral DNA, where it acts as a chain terminator (De Clercq and Holy, 1991).

Other anti-herpesvirus drugs target viral DNA synthesis by other mechanisms. Brivudin is phosphorylated by TK and cellular kinases and then acts as a competitive inhibitor of the viral DNA polymerase. It is also incorporated into viral DNA (Allaudeen *et al.*, 1981). Idoxuridine, a thymidine analog, was the first commercial antiviral drug

(Prusoff, 1959). Idoxuridine is phosphorylated and then incorporated into replicating viral DNA, which leads to abnormal transcription and translation (Kaplan and Ben-Porat, 1966), thereby inhibiting the production of infectious progeny virions. Trifluridine, another thymidine analog, is phosphorylated intracellularly and incorporated into viral DNA, like idoxuridine (Prusoff *et al.*, 1984). Trifluridine also inhibits thymidylate synthetase (Prusoff *et al.*, 1984). Foscarnet is a pyrophosphate analog that interferes with exchange of pyrophosphate from deoxynucleoside triphosphate during viral DNA synthesis (Oberg, 1982; Crumpacker, 1992).

Fomivirsen **(Figure 1.9)**, an antisense oligodeoxynucleotide, is used in the treatment of CMV. It binds to complementary sequences on the viral immediate early (IE) 2 mRNA, preventing expression of IE2 (Azad *et al.*, 1993). Fomivirsen, like other oligonucleotides at higher concentrations, has additional sequence-independent inhibitory effects on the attachment of virions to cells (Azad *et al.*, 1993). Oligonucleotides are known to induce interferon expression, which may also contribute to the antiviral effects of fomivirsen.

Docosanol (Abreva) **(Figure 1.9)**, described in **section 1.7.4**, inhibits entry of HSV-1 by interfering with viral fusion (Pope *et al.*, 1998).

1.7.7 Limitations of current antiviral therapies

Most current antivirals specifically target viral proteins or enzymes. This approach requires detailed molecular knowledge of the structure and function of the targeted viral protein, which takes time and much research. In the case of emerging viruses, it may not be possible to acquire such knowledge. Some viruses encode few “druggable” proteins, so there are a limited number of targets. Most RNA viruses have small genomes, as do

several DNA viruses, such as papillomaviruses. Most clinical antivirals act on polymerases or proteases (De Clercq, 2004; De Clercq, 2010). Although they are specific for virally infected cells, many are specific against only one virus, or even one strain or genotype.

Host-targeting antivirals, which target a host cell protein instead of a viral enzymatic process, overcome some of these limitations. Viruses with few proteins require many cellular factors to replicate, and many unrelated viruses may interact with conserved cellular proteins. As cellular targets are not encoded by highly mutable viral genomes, there is a higher barrier to selection for resistance. However, targeting host factors still requires knowledge of virus-host interactions for each particular virus.

A major limitation of antiviral therapy is the prompt selection for resistance. Viral polymerases (particularly RNA polymerases) lack proofreading activity and have high error rates, resulting in the distribution of quasispecies within a virus population. Antiviral therapy selects for drug resistant variants pre-existing within the quasispecies population (Lauring and Andino, 2010). Alternatively, mutations could arise during exposure to the drug during therapy (Kimberlin and Whitley, 1996). All approved antiviral agents have been demonstrated to select for resistance. Often a single non-lethal nucleotide mutation results in an amino acid substitution that confers resistance (Kimberlin and Whitley, 1996), as was observed for the first NNRTIs (Tambuyzer *et al.*, 2009). A mutation of Y181C in the HIV RT inhibitor binding site reduces the binding affinity of NNRTIs, which depends in part on hydrophobic stacking with the tyrosine (Tambuyzer *et al.*, 2009). Likewise, the M184V/I mutation confers resistance to the NRTI lamivudine by altering the active site architecture of the HIV RT to prevent

lamivudine binding (Diallo *et al.*, 2003). In the case of IAV antivirals, resistance to the adamantanes requires only a single amino acid substitution in the transmembrane domain of the M2 ion channel (Belshe *et al.*, 1988). HSV-1 resistance to acyclovir is conferred by mutations in the viral TK or in the viral DNA polymerase (Coen and Schaffer, 1980). Antivirals such as these have a low barrier to resistance.

Mutations that confer resistance may concomitantly decrease the replicative fitness of the virus, requiring compensatory mutations to allow replication at rates comparable to those of wild type virus. In this case, multiple mutations are required to confer resistance, resulting in a higher barrier to resistance. Resistance to enfuvirtide, for example, arises from primary mutations at the site of inhibitor binding in the heptad repeat (HR)-1 of gp41 (Greenberg and Cammack, 2004). However, these mutations impair the kinetics of fusion, requiring compensatory mutations with the HR-2 domain to restore fusion rates (Ray *et al.*, 2009). Similarly, resistance to protease inhibitors is first conferred by a substitution in the substrate-binding site of the protease. These mutations decrease the binding of both the inhibitor and the natural substrate, decreasing the replicative fitness (Croteau *et al.*, 1997). Compensatory mutations in the substrate-binding site (Nijhuis *et al.*, 1999) or in the substrate itself (the viral polyprotein cleavage site) (Mammano *et al.*, 1998) increase the replication kinetics to wild type levels. Genetic barriers to the development of resistance have been identified (Gotte, 2012). Mutational biases of viral polymerases affect the barrier to the development of resistance. For example, transitions are more common than transversions (Gotte, 2012).

Host-targeting antivirals have a higher barrier to resistance, but still select for resistance. Some HIV variants resistant to maraviroc (the CCR5 receptor-targeting

antiviral) bind to the CCR5 receptor-inhibitor complex (Westby *et al.*, 2007). Alternatively, maraviroc treatment selects for variants that bind to the CXCR4 receptor (Westby *et al.*, 2006) or with altered binding to the CD4 receptor (Ratcliff *et al.*, 2013). Even immunomodulatory approaches can select for resistance. Interferon (IFN), used in the treatment of HBV and HCV, stimulates the expression of IFN-stimulated genes, generating an antiviral state. However, HCV can become resistant to IFN by downregulating IFN signalling pathways (Datta *et al.*, 2011).

Antivirals with intracellular targets are subject to metabolic steps within the cell. Nucleoside analogs must be phosphorylated within the cell to produce the active inhibitor. Compounds are also metabolized to inactive forms by cellular enzymes. For example, many HCV antivirals are metabolized by cytochrome P450 enzymes (Kiser *et al.*, 2013). Intracellular-targeted antivirals also require delivery across membranes, by passive mechanisms or active transport (i.e. nucleoside transporters). As many antivirals are hydrophilic, they are poorly able to cross lipid membranes to reach effective intracellular concentrations.

1.7.8 Benefits of entry inhibitors

Entry inhibitors circumvent several of the limitations discussed in the previous section. They avoid both the need for intracellular drug delivery and problems associated with intracellular drug metabolism, as their targets are extracellular. Entry inhibitors offer other therapeutic advantages, by preventing spread of infection to healthy cells and graft re-infection (as in the case of liver transplant following HCV infection). They also inhibit virus replication before viruses can establish persistent reservoirs, or could be used prophylactically to prevent infection altogether. The initial binding of virions to glycans

and the lipid membrane rearrangements required during fusion are conserved entry steps among unrelated viruses and are therefore potential targets for broad-spectrum antivirals. Entry is also an interesting target for emerging viruses, since entry steps are generally conserved and require no detailed molecular knowledge of the viral proteins involved.

1.8 INNATE IMMUNE APPROACHES TO TARGET VIRAL ENTRY

Highlighting the effectiveness of antiviral approaches targeting entry, evolution has selected for several such approaches. Many secondary metabolites produced by microbial or plant species have antibacterial, antifungal or antiviral activities. Eukaryotic immune mechanisms have also evolved to inhibit the entry of pathogens.

1.8.1 Innate antiviral molecules

Antimicrobial peptides are one of the first lines of defense against infection. Defensins are small (29-42 amino acids) cationic and amphipathic peptides with activity against a wide range of microorganisms, including viruses (Klotman and Chang, 2006). Based on their disulphide bond organization, defensins are classified into α–, β– and θ–defensins. Humans lack functional versions of the latter (Wilson *et al.*, 2013). One α-defensin, human neutrophil peptide (HNP)-1, directly inhibits the infectivity of enveloped viruses (HSV-1/2, VSV and IAV) (Daher *et al.*, 1986). HNP-1 and other defensins also directly inactivate HIV particles (Mackewicz *et al.*, 2003). Although nonenveloped viruses were not initially found to be direct targets of defensins (Daher *et al.*, 1986), later studies demonstrated that HNP-1 inhibits escape of nonenveloped HPV and AdV virions from endosomes (Buck *et al.*, 2006; Smith and Nemerow, 2008). The mechanisms involved in the inactivation of enveloped virions are unclear, but may involve disruption of viral

envelopes (Kota *et al.*, 2008) or binding to glycans on virion glycoproteins involved in attachment and entry (Yasin *et al.*, 2004). Some defensins bind to cellular HS to block virion attachment (Hazrati *et al.*, 2006).

Retrocyclins are cyclic θ-defensins produced by some nonhuman primates. In humans, retrocyclins are not expressed because they are encoded by a truncated pseudogene (Venkataraman *et al.*, 2009). Retrocyclins have interesting inhibitory activities against viral entry. In the case of IAV, retrocyclin-2 inhibits HA-mediated fusion by binding to glycans and crosslinking virion glycoproteins (Leikina *et al.*, 2005). Similar effects were reported for other enveloped viruses (Leikina *et al.*, 2005). Retrocylin-1 inhibits HIV-1 fusion by mechanisms strikingly similar to those of the approved fusion inhibitor enfuvirtide. Retrocyclin-1 interacts with the gp41 C-terminal heptad repeat to prevent formation of the 6-helix bundle (Gallo *et al.*, 2006). HNP-1, an α-defensin produced by humans, also inhibits HIV-1 fusion by apparently disrupting formation of the gp41 6-helix bundle (Demirkhanyan *et al.*, 2012). Similarly, an oligopeptide isolated from blood plasma (virus-inhibitory peptide, VIRIP) targets gp41 to inhibit HIV-1 fusion (Munch *et al.*, 2007). Clearly, understanding the mechanisms of innate immune effectors could facilitate the design of small-molecule inhibitors with broad-spectrum antiviral activity.

Lactoferrin is another immune factor with antiviral, antibacterial and antifungal properties. Lactoferrin was first isolated from bovine milk but is highly homologous to lactoferrin from human milk (Berlutti *et al.*, 2011). Found in mucosal secretions, lactoferrin is an 80-kDa glycosylated protein of net positive charge (van der Strate *et al.*, 2001). Through its high net positive charge, lactoferrin interacts with negatively charged

GAGs (Wu *et al.*, 1995; El Yazidi-Belkoura *et al.*, 2001). This binding is thought to be responsible for most of its antimicrobial activities. Lactoferrin inhibits the infectivity of HS-binding enveloped viruses (including HSV-1/-2, CMV, HBV and HCV) and nonenveloped viruses (including rotavirus and AdV) (Marchetti *et al.*, 1996; Andersen *et al.*, 2003; Harmsen *et al.*, 1995; Hara *et al.*, 2002; Ikeda *et al.*, 2000; Arnold *et al.*, 2002). Lactoferrin was also report to inhibit the infectivity of a non-HS-binding virus, PV, but only at concentrations 100-fold higher than those sufficient to inhibit the infectivity of HS-binding viruses (Marchetti *et al.*, 1999). The antiviral activities of lactoferrin may also be the result of interactions with viral particles (Berlutti *et al.*, 2011).

1.8.2 Interferon-inducible transmembrane proteins (IFITMs)

IFN signaling induces a broad antiviral response. Type I IFNs (including IFNα and IFNβ) are cytokines that signal through the IFNα/β receptor, ultimately inducing the expression of interferon-stimulated genes (ISGs). ISGs encode proteins that target multiple stages of virus replication: entry, replication, translation, assembly and spread (Diamond and Farzan, 2013). Included in this group are the IFN-induced transmembrane (IFITM) proteins, which block the entry of unrelated viruses, including orthomyxoviruses (IAV), filoviruses (Ebola virus and Marburg virus), coronaviruses (SARS), rhabdoviruses (VSV), flaviviruses (HCV, DV, WNV), retroviruses (HIV), a nonenveloped virus (RV) (Brass *et al.*, 2009) (Huang *et al.*, 2011) (Weidner *et al.*, 2010) (Wilkins *et al.*, 2013) (Lu *et al.*, 2011) (Anafu *et al.*, 2013), and others (Smith *et al.*, 2014). IFITM3 in particular was shown to be critical for the control of IAV infections in mice and humans (Everitt *et al.*, 2012). IFITM1, 2 and 3 did not inhibit HPV, AdV or CMV infections (Warren *et al.*, 2014).

With the exception of HIV, the viruses affected by IFITMs (whether enveloped or not) are internalized by endocytosis, suggesting that IFITMs target processes that occur within endosomes (Feeley *et al*., 2011). IFITM3 localizes primarily to endosomal organelles, whereas IFITM1 localizes to the plasma membrane and IFITM2 to yet-unidentified intracellular compartments (Jia *et al*., 2014). IFITM1 may restrict viruses that fuse at the plasma membrane (such as HIV) while IFITM3 restricts viruses entering from endosomal pathways. Consistently, IFITM2 and IFITM3 but not IFITM1, inhibited the entry of Rift Valley Fever virus, which fuses within the endosome (Mudhasani *et al*., 2013).

The specific antiviral mechanisms of IFITM proteins remain unclear. Initially, IFITMs were shown to inhibit fusion by affecting membrane curvature and fluidity (Li *et al.*, 2013a). IFITM3 overexpression increases endosomal cholesterol levels by disrupting proteins that regulate cholesterol content (Amini-Bavil-Olyaee *et al.*, 2013), thereby providing a mechanism for effects on fluidity. However, accumulation of cholesterol in endosomes induced by other mechanisms did not affect fusion (Desai *et al.*, 2014). IFITM3 expression did not block lipid mixing during hemifusion, but did prevent the formation of fusion pores during IAV entry (Desai *et al.*, 2014). The mechanisms involved remain unclear.

1.8.3 Other interferon-inducible antiviral activities

Most ISGs remain uncharacterized. Among them, the cholesterol-25-hydroxylase gene, encoding an ER-associated enzyme that oxidizes cholesterol to 25-hydroxycholesterol (25HC), is important to this thesis. 25HC decreases cellular cholesterol levels through downregulation of LDLR and inhibition of 3-hydroxyl-3-methyl-glutaryl (HMG)-CoA

reductase **(Figure 1.10)** (Pezacki *et al.*, 2009). It also has important roles in immunity (Liu *et al.*, 2013). 25HC broadly inhibits viral entry through unclear mechanisms (Liu *et al.*, 2013). It will be discussed further in **Chapter 5**.

1.9 RATIONALE

Targeting viral entry is an antiviral approach with many advantages. Entry inhibitors prevent infection of uninfected cells, protecting healthy cells and inhibiting virus replication before viruses establish persistent reservoirs. The targets of most entry inhibitors are extracellular. Most entry inhibitors, therefore, avoid the need for intracellular drug delivery and limiting cell toxicity. Finally, primary attachment to cellular glycans and lipid rearrangements during fusion are conserved and required processes in the entry of many unrelated viruses. My overarching model is that inhibitors of these entry steps, acting through appropriate mechanisms, have broad-spectrum antiviral activity. The goal of this research is to identify antiviral mechanisms that allow broad inhibition of viral infectivity.

Several small molecule compounds generated synthetically or identified from nature and the innate immune system are known to possess broad antiviral activity. In the first group are the rigid amphipathic fusion inhibitors, which inhibit the infectivity of unrelated enveloped viruses (St Vincent *et al.*, 2010). Some natural products, such as EGCG and curcumin, have broad antiviral activity against unrelated viruses (Steinmann *et al.*, 2013). The sterol regulator 25HC is a recent example of an innate immunity-induced small molecule with broad effects on viral entry (Liu *et al.*, 2013). These molecules are useful probes for viral entry steps. They can also be used to identify and

characterize the mechanisms responsible for broad-spectrum antiviral activities. The identification of these antiviral mechanisms opens the possibility for the rational design of small molecule entry inhibitors with broad-spectrum activities and appropriate pharmacological properties.

Table 1.1. Model viruses used in this research. *Proposed; **in particular cell types.

Virus	Enveloped/ Nonenveloped	Binding (HS or SA)	Entry site	Fusion protein	Genome composition	Replication site
HCV	Enveloped	HS	Endosome	Class IV*	RNA	Cytoplasm
IAV	Enveloped	SA	Endosome	Class I	RNA	Nucleus
VSV	Enveloped	HS/SA (?)	Endosome	Class III	RNA	Cytoplasm
SINV	Enveloped	HS	Endosome	Class II	RNA	Cytoplasm
HSV-1	Enveloped	HS	Plasma membrane Endosome**	Class III	DNA	Nucleus
VACV	Enveloped	HS/SA (?)	Plasma membrane Endosome**	?	DNA	Cytoplasm
RV	Nonenveloped	SA	Endosome	N/A	RNA	Cytoplasm
AdV	Nonenveloped	HS/SA	Endosome	N/A	DNA	Nucleus
PV	Nonenveloped	Neither	Endosome	N/A	RNA	Cytoplasm

Table 1.2. Clinically approved antiviral drugs for RNA viruses

Anti-HIV compounds	**Target**
Nucleoside Reverse Transcriptase Inhibitors	
Zidovudine, Didanosine, Zalcitabine, Stavudine, Abacivir	Viral reverse transcriptase (HIV)
Lamivudine, Emtricitabine	Viral reverse transcriptase (HIV, HBV)
Nucleotide Reverse Transcriptase Inhibitors	
Tenofovir disoproxil	Viral reverse transcriptase (HIV, HBV)
Non-nucleoside Reverse Transcriptase Inhibitors	
Nevirapine, Delavirdine, Efavirenz, Entravirine	Viral reverse transcriptase (HIV-1)
Protease Inhibitors	
Saquinavir, Ritonavir, Indinavir, Nelfinavir, Amprenavir, Lopinavir, Atazanavir, Fosempranivir, Darunavir, Tipranivir	Viral protease (HIV)
Entry Inhibitors	
Enfuvirtide	Viral fusion protein gp41 (HIV)
Maraviroc	Cellular CCR5 receptor for gp120 (HIV)
Integrase Inhibitors	
Raltegravir	Viral integrase (HIV)

Anti-HCV Compounds	
Non-specific Inhibitors	
Ribavirin	Viral RNA synthesis
Pegylated interferon alpha-2a	Immunomodulatory
Protease Inhibitors	
Telaprevir, Boceprevir, Simeprevir	Viral NS3/4A protease (HCV)
Nucleotide Analog Inhibitors	
Sofosbuvir	Viral NS5B RNA polymerase (HCV)

Anti-IAV Compounds	
M2 Ion Channel Inhibitors	
Amantadine, Rimantadine	Viral M2 ion channel (IAV)
Neuraminidase Inhibitors	
Zanimivir, Oseltamivir, Peramivir, Laninamivir	Viral NA (IAV)

Table 1.3. Clinically approved antiviral drugs for DNA viruses

Anti-HBV Compounds	**Target**
Lamivudine, Adefovir dipivoxil, Emtricitabine, Tenofovir disoproxil, Entecavir	Viral reverse transcriptase (HBV, HIV)
Telbivudine	Viral DNA polymerase (HBV)
Anti-herpesvirus Compounds	
Polymerase Inhibitors	
Acyclovir, Valaciclovir, Penciclovir, Famciclovir	Viral DNA polymerase (HSV-1/2, VZV)
Ioxuridine	Viral DNA polymerase (HSV)
Trifluridine	Viral DNA polymerase (HSV, VZV)
Brivudin	Viral DNA polymerase (HSV-1, VZV)
Ganciclovir	Viral DNA polymerase (HSV-1/2, CMV)
Valganciclovir	Viral DNA polymerase (CMV)
Foscarnet	Viral DNA polymerase (HSV-1/2, VZV, CMV)
Cidofovir	Viral DNA polymerase (CMV)
Expression Inhibitors	
Fomiversen	Viral IE2 mRNA (CMV)

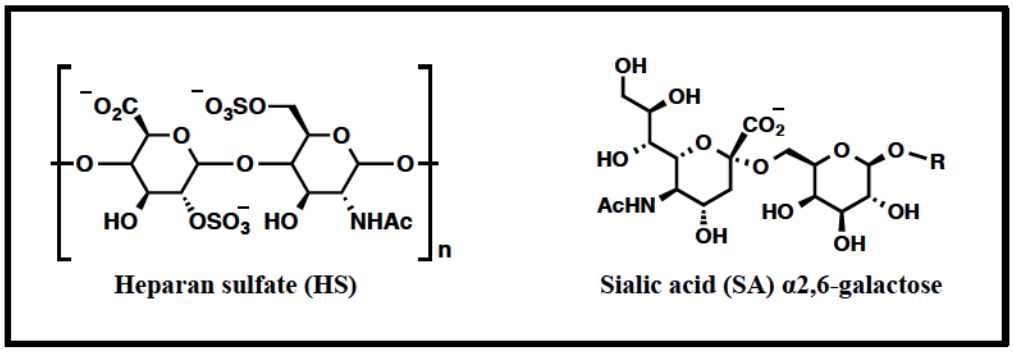

Figure 1.1. Structures of glycan moieties involved in virion attachment. The heparan sulfate and sialic acid moieties in cellular glycans used by most human viruses for primary attachment.

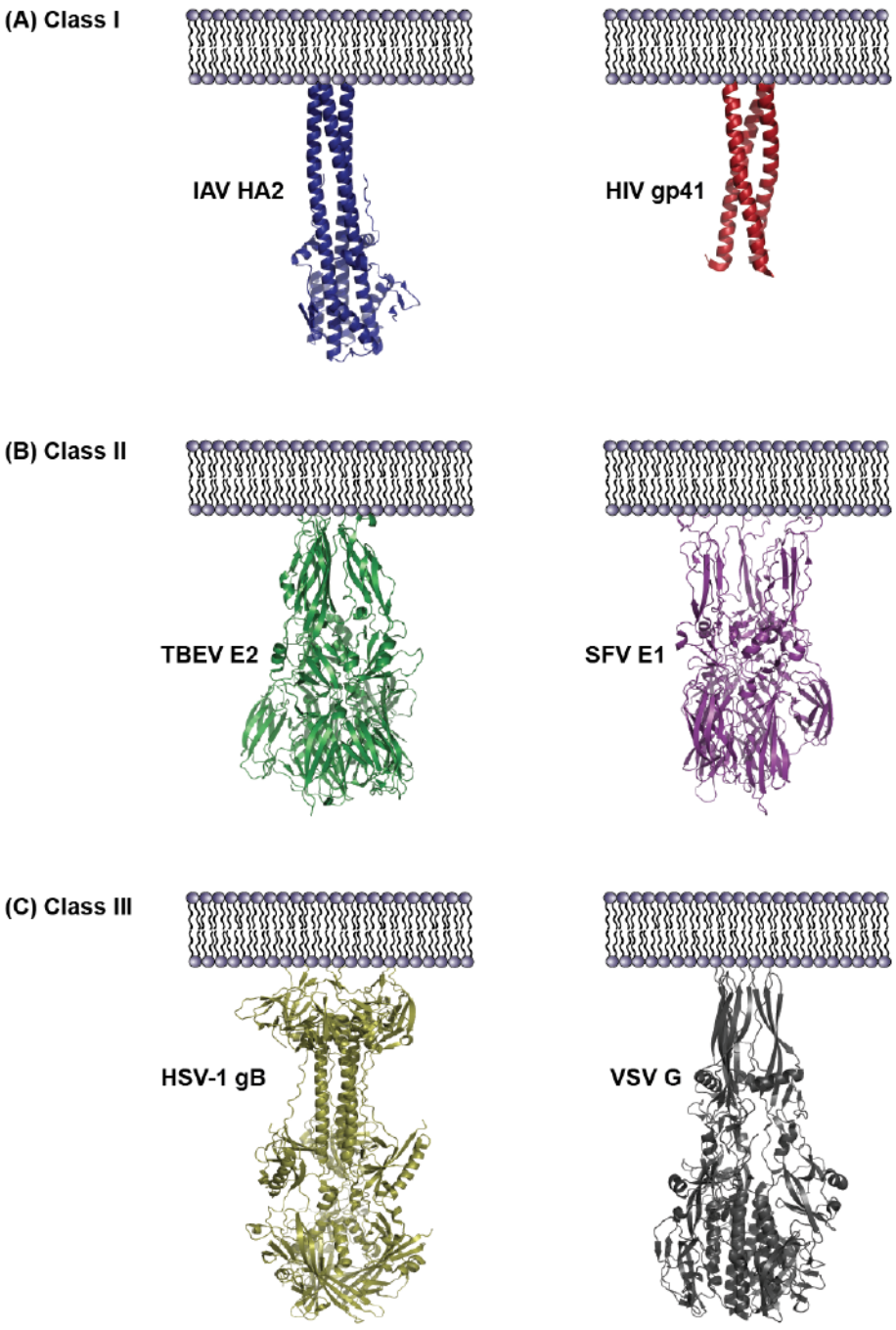

Figure 1.2. Classes of viral fusion proteins in their post-fusion conformations. Class I **(A)**: IAV, influenza A virus hemagglutinin; HIV gp41, human immunodeficiency virus glycoprotein 41. Class II **(B)**: TBEV E2, tick-borne encephalitis envelope 2 protein; SFV E1, Semliki-forest virus envelope 1 protein. Class III **(C)**: HSV-1 gB, herpes simplex virus 1 glycoprotein B; VSV G, vesicular stomatitis G protein.

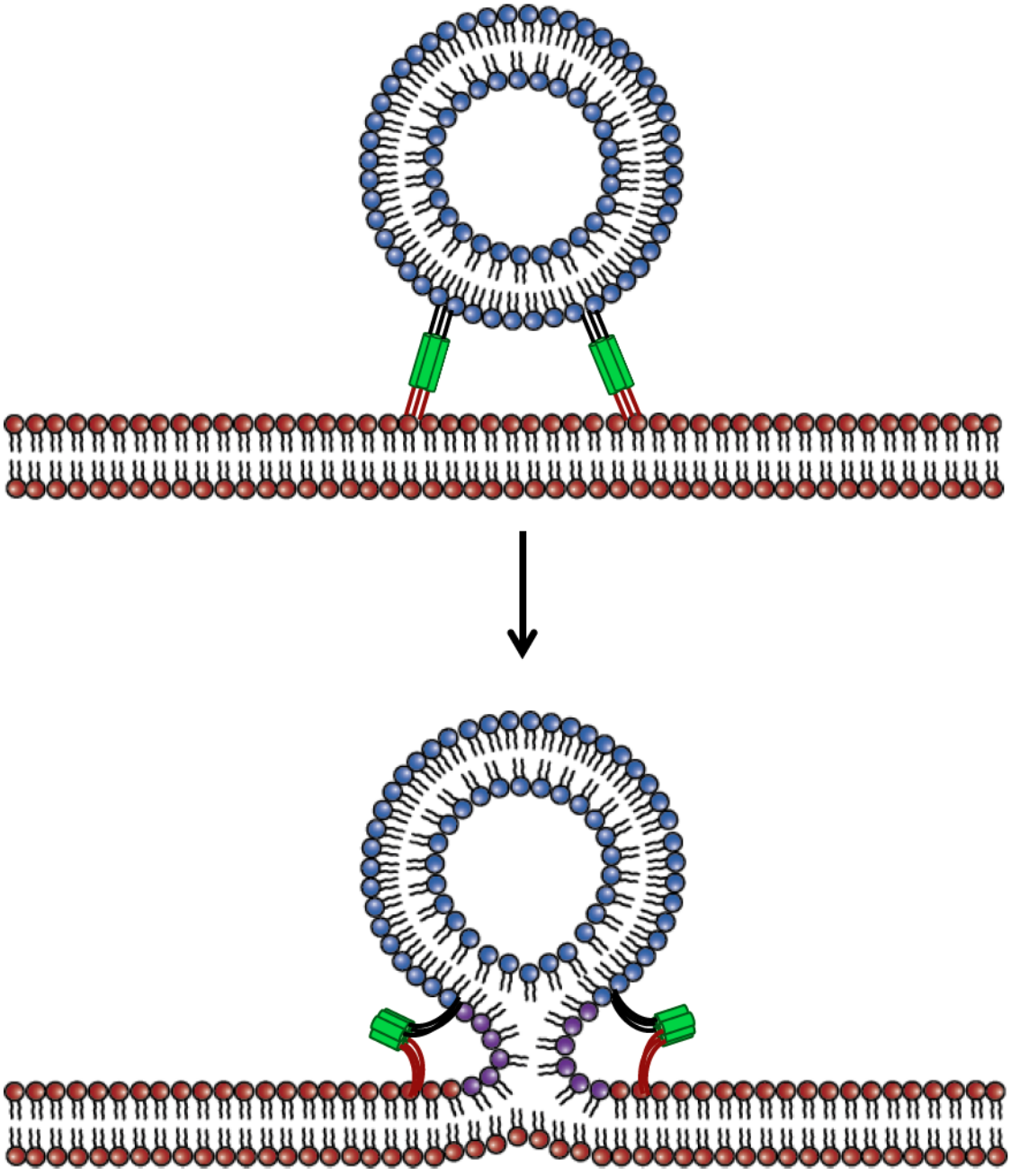

Figure 1.3. Schematic of viral membrane fusion. Shown is a class I fusion protein mediating fusion according to the hemifusion stalk model. All classes of viral fusion proteins induce fusion similarly. The fusion peptide inserts into the target membrane. The fusion protein undergoes conformational changes, resulting in the formation of a hairpin structure, which pulls the membranes into close proximity to allow for fusion.

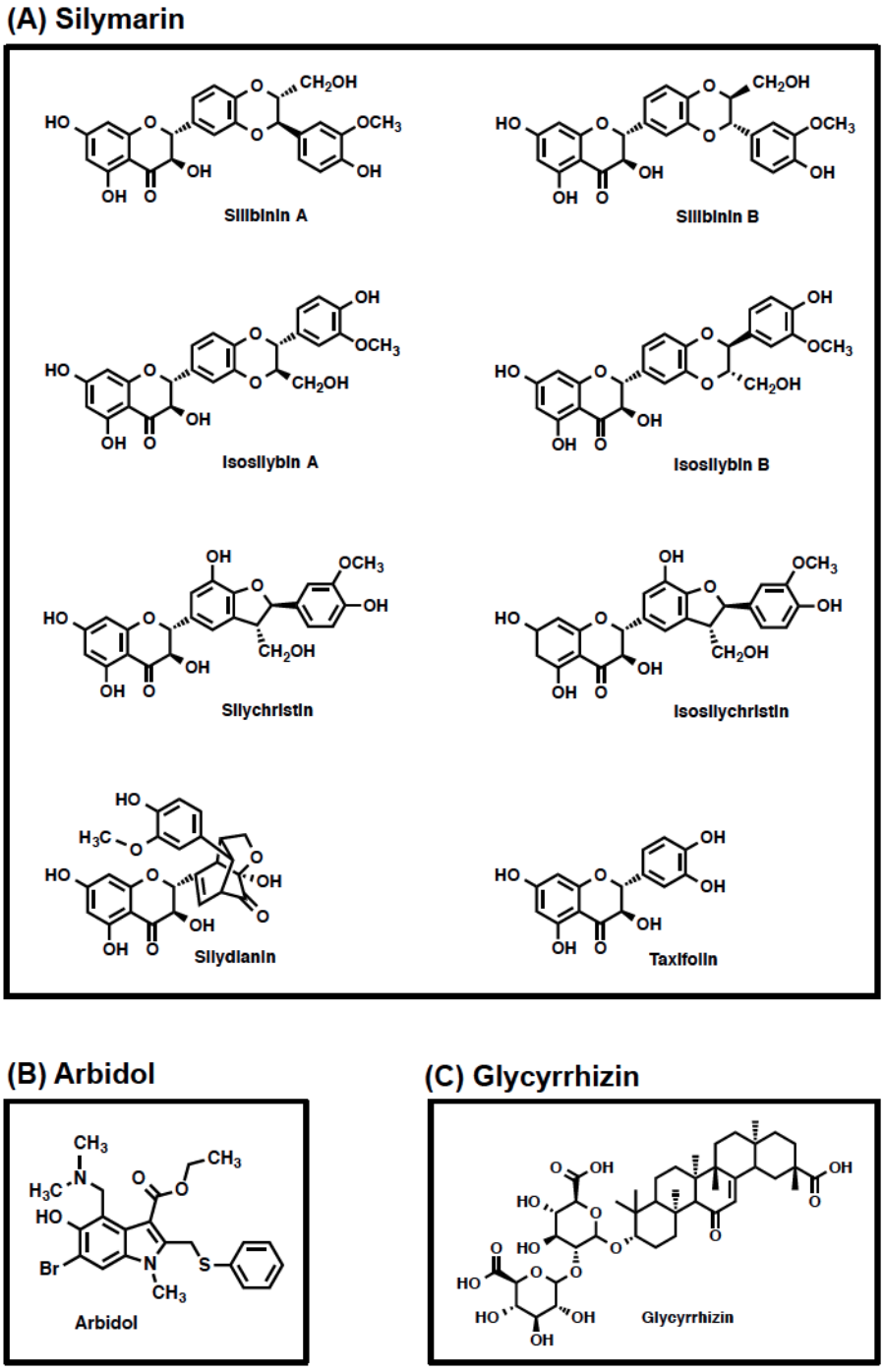

Figure 1.4. Structures of silymarin components (A), arbidol (B) and glycyrrhizin (C). Silymarin is a mixture of seven flavanolignans (silibinin A, silibinin B, isosilybin A, isosilybin B, silychristin, isosilychristin and silydianin) and one flavonoid (taxifolin).

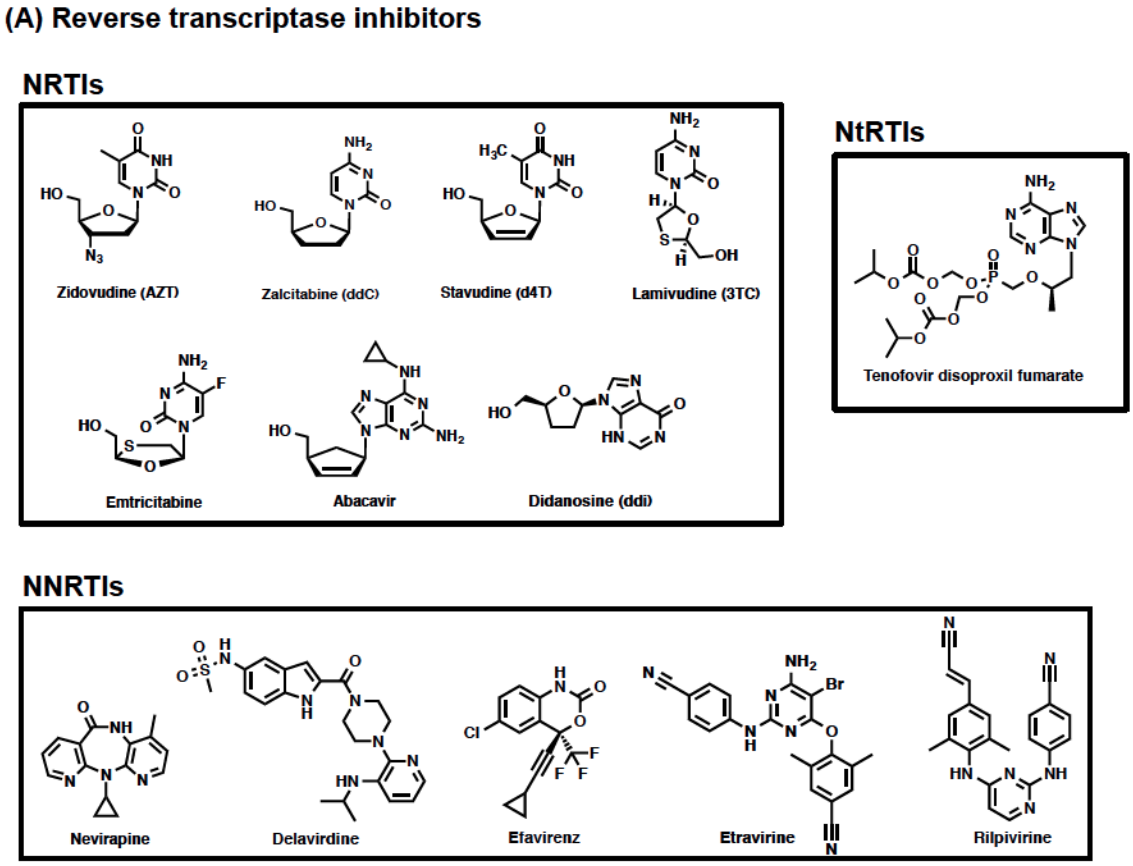

Figure 1.5. Antivirals approved to treat HIV infections. There are reverse transcriptase inhibitors **(A)**, protease inhibitors **(B)**, entry inhibitors **(C)** and integrase inhibitors **(D)**. NRTIs, nucleoside reverse transcriptase inhibitors; NtRTIs, nucleotide reverse transcriptase inhibitors; NNRTIs, non-nucleotide reverse transcriptase inhibitors.

(B) Protease inhibitors

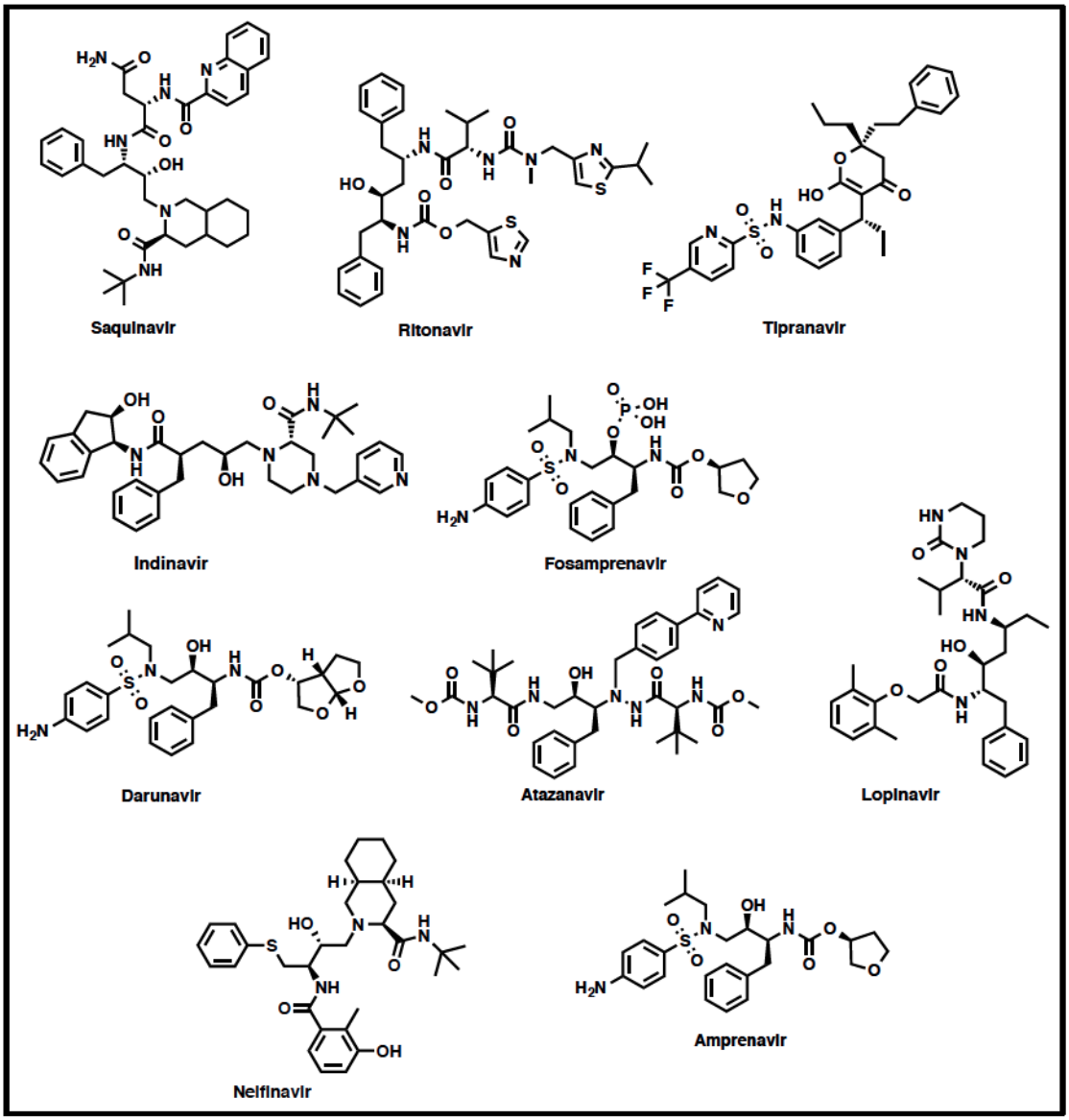

Figure 1.5. Antivirals approved to treat HIV infections. There are reverse transcriptase inhibitors **(A)**, protease inhibitors **(B)**, entry inhibitors **(C)** and integrase inhibitors **(D)**. NRTIs, nucleoside reverse transcriptase inhibitors; NtRTIs, nucleotide reverse transcriptase inhibitors; NNRTIs, non-nucleotide reverse transcriptase inhibitors.

(C) Entry inhibitors

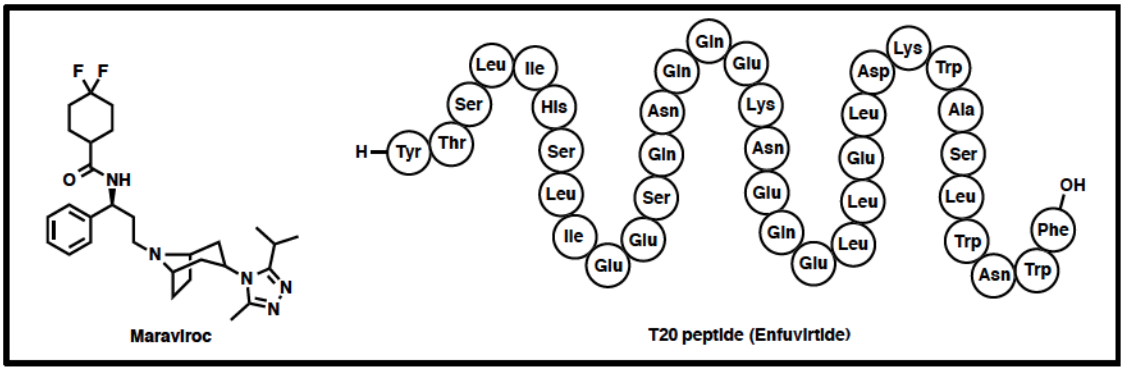

(D) Integrase inhibitors

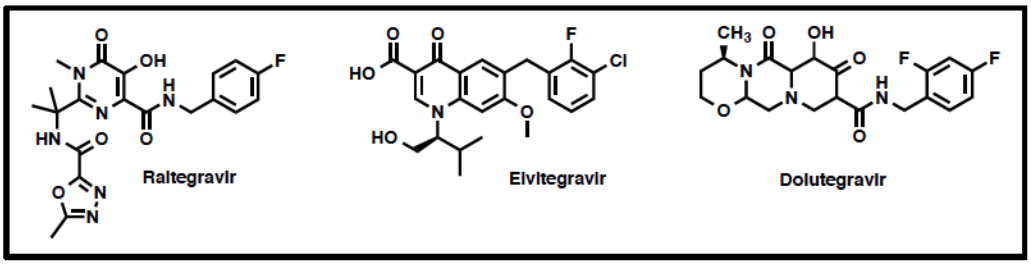

Figure 1.5. Antivirals approved to treat HIV infections. There are reverse transcriptase inhibitors **(A)**, protease inhibitors **(B)**, entry inhibitors **(C)** and integrase inhibitors **(D)**. NRTIs, nucleoside reverse transcriptase inhibitors; NtRTIs, nucleotide reverse transcriptase inhibitors; NNRTIs, non-nucleotide reverse transcriptase inhibitors.

(A) Non-specific antivirals

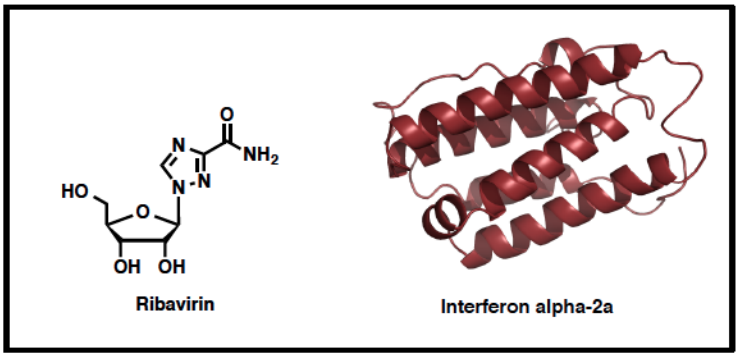

(B) Direct-acting antivirals

Protease inhibitors

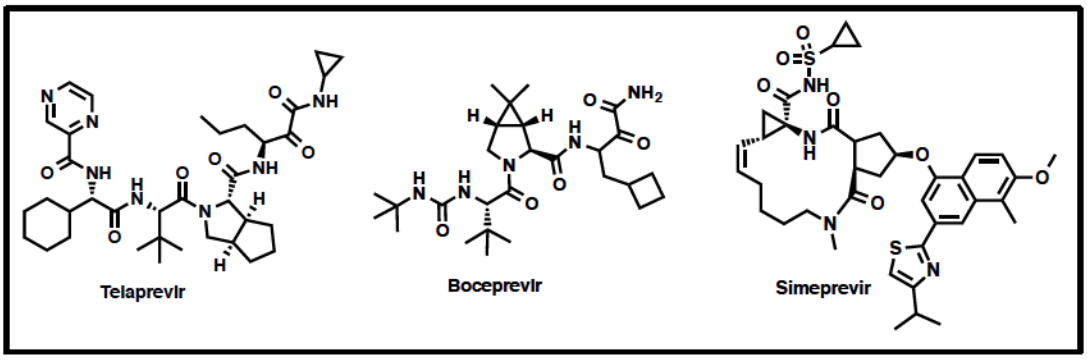

Polymerase inhibitor

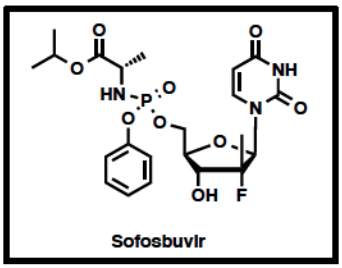

Figure 1.6. Antivirals approved to treat HCV infections. The non-specific antivirals **(A)** are ribavirin and pegylated interferon alpha-2a. The direct-acting antivirals **(B)** are NS3/4A protease inhibitors telaprevir, boceprevir and simeprevir, and the NS5A polymerase inhibitor sofosbuvir.

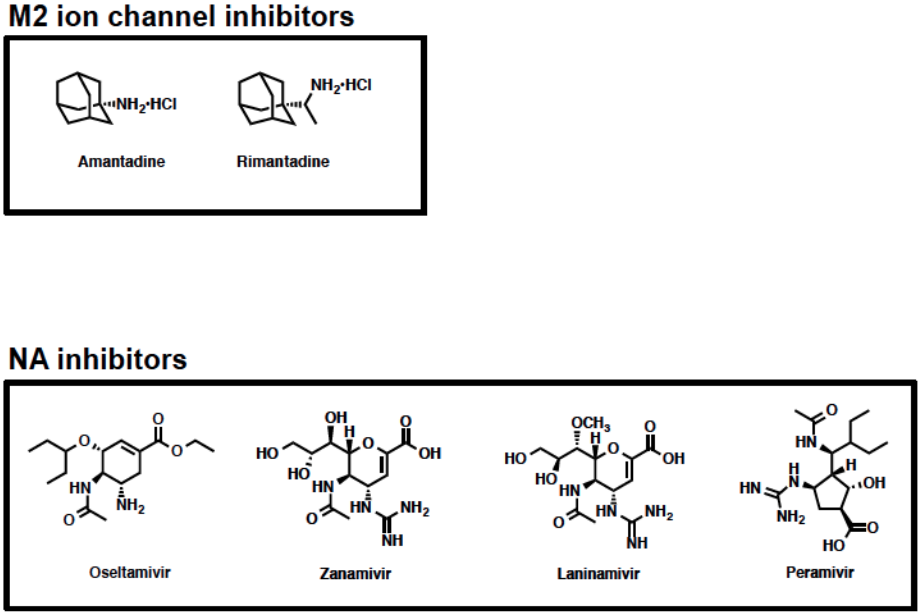

Figure 1.7. Antivirals approved to treat IAV infections. They are comprised of M2 ion channel inhibitors and neuraminidase (NA) inhibitors.

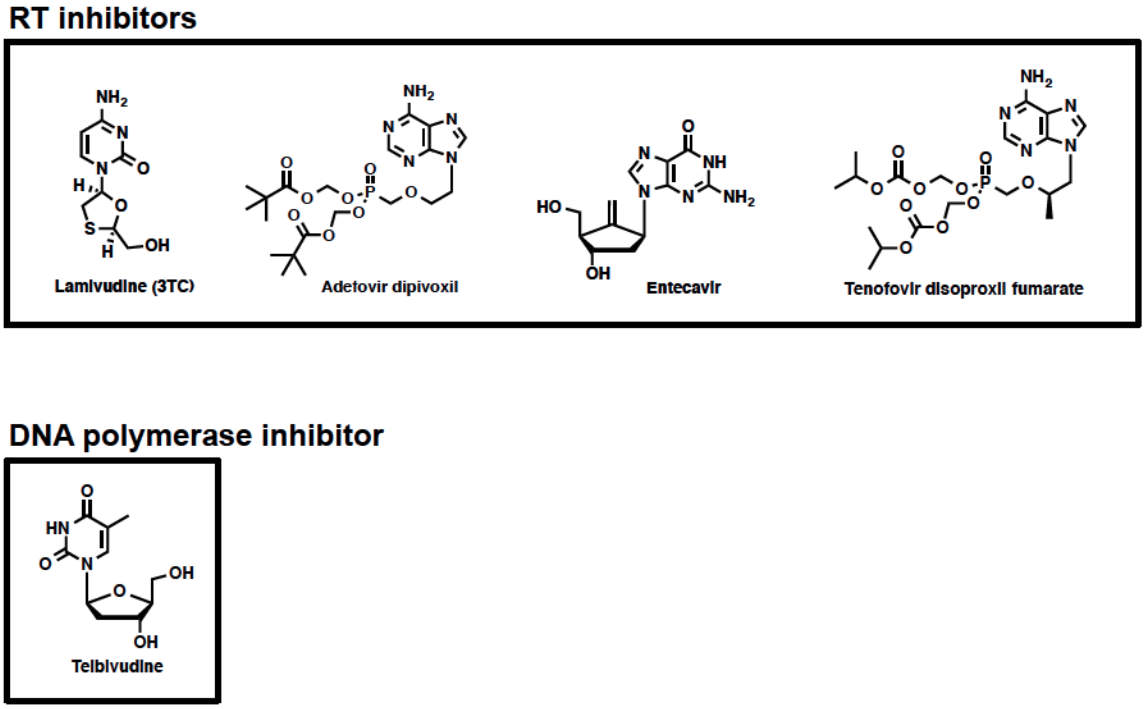

Figure 1.8. Antivirals approved to treat HBV infections. They are comprised of reverse transcriptase inhibitors and DNA polymerase inhibitors.

DNA polymerase inhibitors

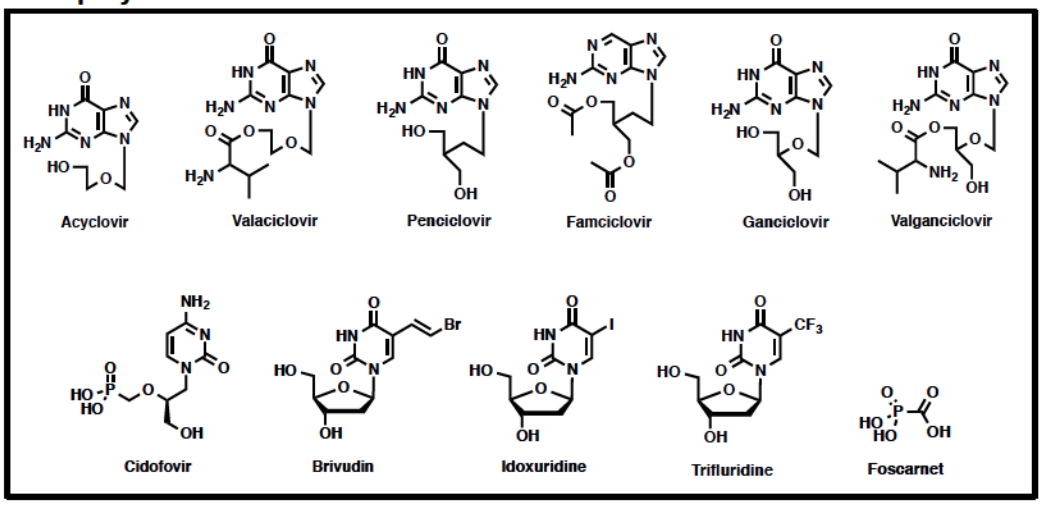

Phosphothiorate oligonucleotide

5′-GCG TTT GCT CTT CTT CTT GCG-3′

Entry inhibitors

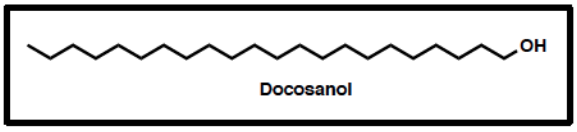

Figure 1.9. Antivirals approved to treat herpesvirus infections. They are comprised of DNA polymerase inhibitors and a gene expression inhibitor.

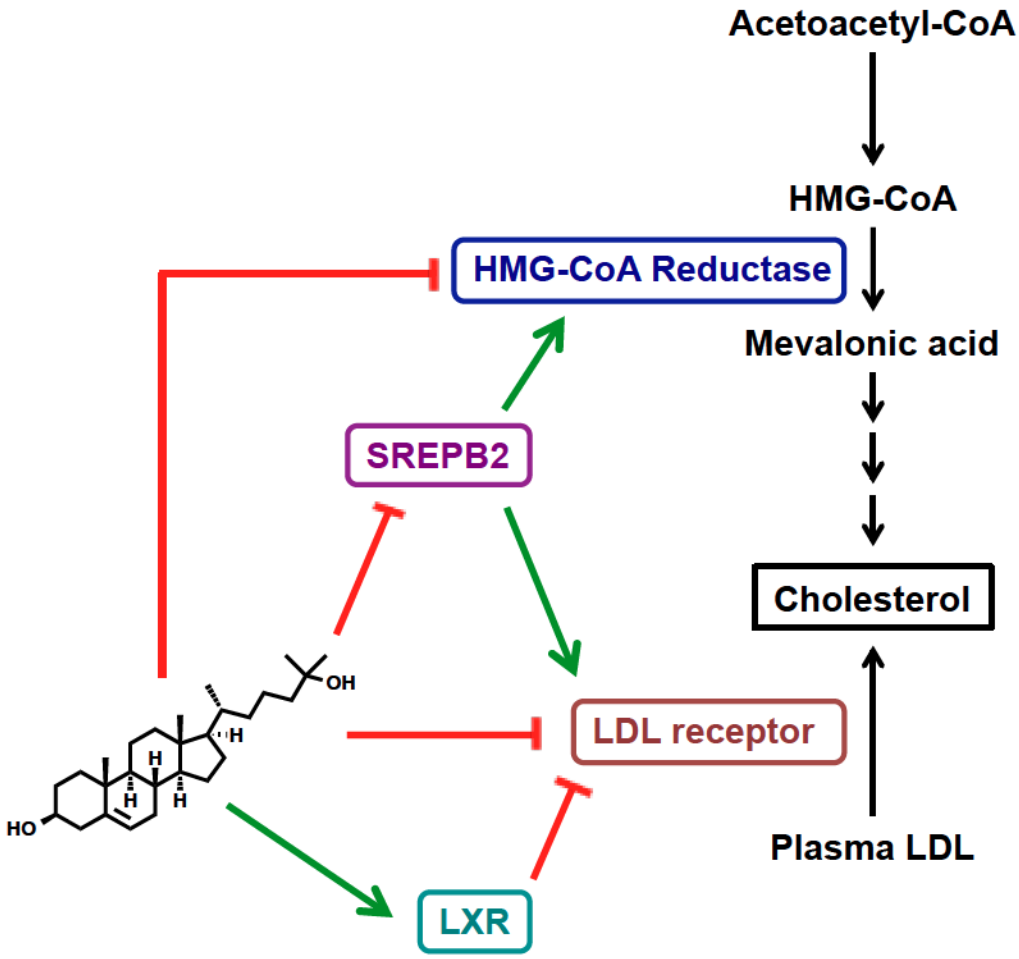

Figure 1.10. Effects of 25HC on cholesterol homeostasis. 25HC decreases cellular cholesterol levels through several mecahnisms involving inhibition or downregulation of HMG-CoA reductase (Brown and Goldstein, 1997), SREBP2 (Brown and Goldstein, 1999) and the LDL receptor (Pezacki *et al.*, 2009), or activation of the liver X receptor (Ma *et al.*, 2008).

CHAPTER 2: MATERIALS AND METHODS

2.1 ANTIVIRAL COMPOUNDS

The rigid amphipathic fusion inhibitors (RAFIs; dUY11, dUY1, dUY5, aUY11 and aUY12) were synthesized by Drs. Alexey Ustinov and Vladimir Korshun (Russian Academy of Sciences, Moscow, Russia). Epigallocatechin gallate (EGCG), epicatechin (EC), curcumin, tetrahydrocurcumin (THC), and 25-hydroxycholesterol (25HC) were initially provided by Dr. Eike Steinmann (Twincore, Hannover, Germany) and later purchased from Sigma-Aldrich (Oakville, ON, Canada) as necessary. With the exception of 25HC, the compounds were dissolved in dimethyl sulfoxide (DMSO) as 20 mM (curcumin, THC), 30 mM (aUY11) or 100 mM (EGCG, dUY11) stocks, aliquoted and stored at -20°C. Compounds were diluted in DMSO vehicle as necessary and resuspended just before use to the indicated concentrations in warmed Dulbecco's Modified Eagle Medium (DMEM), such that the concentration of vehicle never exceeded 0.2%. 25HC was dissolved in ethanol as a 10 mM stock and stored under the same conditions. Equivalent concentrations of the appropriate vehicle were used in the controls. All antiviral compounds used in this study are listed in **table 2.1**.

2.2 CHEMICALS AND REAGENTS

2.2.1 Chemicals. Octadecyl rhodamine B chloride (R18) was obtained from Molecular Probes (Invitrogen, Grand Island, NY, USA). DMSO, 1,6-diphenyl-1,3,5-hexatriene (DPH), heparin and N-acetylneuraminic acid (sialic acid) were obtained from Sigma-Aldrich. L-^{35}S-methinione was purchased from PerkinElmer (Boston, MA, USA). Cholesterol, β-oleoyl-γ-palmitoyl-L-α-phosphatidylcholine (POPC), and 1,2-dioleoyl-L-

α-phosphatidylcholine (DOPC) were purchased from Sigma-Aldrich and used for liposome preparation. Catalog numbers for all chemicals are listed in **table 2.2**.

2.2.2 Cell Culture Reagents. Cells were cultured in Dulbecco's Modified Eagle Medium (DMEM) (Invitrogen, Life Technologies Inc., Burlington, ON, Canada) supplemented with fetal bovine serum (FBS; PAA Laboratories, now GE Healthcare, Westborough, MA, USA) and penicillin/streptomycin (10,000 U/mL stock; Invitrogen), used at the indicated concentrations. Some experiments required phenol red-free DMEM or methionine-free DMEM (Invitrogen). Trypsin-EDTA (0.5% stock; Invitrogen) was diluted tenfold in phosphate-buffered saline (PBS) prior to use. L-1-tosylamide-2-phenylethyl chloromethyl ketone (TPCK)-treated trypsin was purchased from Sigma-Aldrich. To overlay and visualise viral plaques, agarose or low melting point agarose (Invitrogen), methylcellulose (Sigma-Aldrich) and crystal violet (Sigma-Aldrich) were used. PBS was comprised of 1 mM KH_2PO_4, 150 mM NaCl, 3 mM Na_2HPO_4 adjusted to pH 7.4. Catalog numbers for all reagents are listed in **table 2.3**.

2.2.3 Antibodies and Immunostaining Reagents. The following antibodies were used: mouse IgG anti-HCV core (Thermo Scientific, Rockland, IL, USA or Enzo Life Sciences, Farmingdale, NY, USA), mouse IgG anti-CD81 (JS81 clone, BD Biosciences, Mississauga, ON, Canada), biotinylated horse anti-mouse IgG (Vector Laboratories, Burlingame, CA, USA), and goat anti-mouse IgG Alexa Fluor 488 antibody (Molecular Probes). For blocking steps, normal goat serum (Sigma-Aldrich), normal horse serum (Vector Laboratories), or bovine serum albumin (BSA; Albumin Fraction V, USA Biochemical Corp., Cleveland, OH, USA) were used at the indicated concentrations. Immunocytochemistry was performed using reagents provided in the VectaStain ABC kit

and the ImmPACT SG peroxidase substrate (Vector Laboratories). Catalog numbers for all reagents can be found in **table 2.4**.

2.2.4 Molecular Biology Reagents. RNA was isolated using the High Pure Viral RNA Kit (Roche, Laval, QC, Canada) or TRIzol (Ambion, Life Technologies Inc., Burlington, ON, Canada). Moloney Murine Leukemia Virus Reverse Transcriptase (M-MLV RT) or Superscript III RT (Invitrogen) were used to synthesize cDNA. For quantitative real-time polymerase chain reactions (qRT-PCR), the TaqMan universal PCR master mix (Applied Biosystems, Life Technologies Inc., Burlington, ON, Canada) was used along with appropriate primers and probes. For PCR for sequencing, *Pfx50* high fidelity DNA polymerase (Invitrogen) was used. Deoxynucleotide triphosphates (dNTPs; mixture set, 100 mM), first-strand buffer (FSB; 50 mM Tris-HCl (pH 8.3), 75 mM KCl, 3 mM $MgCl_2$), dithiothreitol (DTT; 100 mM) and RNaseOUT (5000 U) were purchased from Invitrogen and used at the indicated concentrations. DNA was extracted from agarose gels using the MinElute Gel Extraction Kit (Qiagen, Mississauga, ON, Canada). Catalog numbers for kits and reagents are listed in **table 2.5**.

2.3 CELLS

African green monkey Vero fibroblasts (Vero; catalog number CCL-81) and Madin-Darby canine kidney (MDCK; catalog number CCL-34) cells were obtained from the American Type Culture Collection (Manasses, VA, USA). Human hepatoma Huh7.5 cells were obtained from Dr. Charles Rice (Rockefeller University, NY) through Dr. Lorne Tyrrell (University of Alberta, Edmonton, Canada). NIH/3T3 fibroblasts, human embryonic kidney (HEK) 293T and L929 murine fibroblasts were obtained from Drs.

Denise Hemmings, Rob Ingham and Maya Shmulevitz (University of Alberta, Edmonton, Canada), respectively.

Vero, MDCK and 3T3 cells were cultured in DMEM supplemented with 5% FBS, 50 U/mL penicillin and 50 μg/mL streptomycin (complete DMEM) at 37°C in 5% CO_2. Huh7.5, 393T and L929 cells were cultured in DMEM-10% FBS, 50 U/mL penicillin and 50 μg/mL streptomycin at 37°C in 5% CO_2. For passaging and plating, cells were washed once with PBS and detached by incubation in trypsin-EDTA (0.05%) at 37°C for approximately 5 minutes. Detached cells were resuspended in complete DMEM and seeded into flasks or plates at the indicated densities for each experiment.

2.4 VIRUSES

Herpes simplex virus 1 strain KOS (HSV-1 KOS) and herpes simplex virus 2 strain 186 (HSV-2 186) were obtained from the late Dr. Priscilla Schaffer (Harvard Medical School, Boston, MA). Murine cytomegalovirus (mCMV) strain RM427$^+$ (containing a *lacZ* insertion in the nonessential immediate-early 2 gene) was originally acquired from Edward Mocarski (Emory University, Atlanta, GA) through Denise Hemmings (University of Alberta, Edmonton, Canada). Vaccinia virus (VACV) strains Western Reserve (WR) and International Health Department-white (IHD-W) were provided by Dr. David Evans (University of Alberta, Edmonton, Canada). Adenovirus type 5 (AdV) expressing green fluorescent protein (GFP) was obtained from Dr. Dennis Vance (University of Alberta, Edmonton, Canada).

HCV strain JFH-1 was originally obtained from Dr. Takaji Wakita (Tokyo Metropolitan Institute for Neuroscience, Tokyo, Japan) through Dr. Lorne Tyrrell

(University of Alberta, Edmonton, Canada). Influenza A virus (IAV) H1N1 strains A/Puerto Rico/8/1934 (PR8) and A/USSR/90/77 (USSR), and H3N2 strains A/Aichi/2/68 (Aichi) and A/Port Chalmers/1/73 (PC) were obtained from Veronika von Messling (INRS-Institut Armand-Frappier Research Centre, Quebec, Canada). Sindbis virus (SINV), vesicular stomatitis virus (VSV), poliovirus (PV) and mammalian orthoreovirus type 3 (RV) were provided by Drs. Tom Hobman, Paul Melancon, Michael James and Maya Shmulevitz, respectively (University of Alberta, Edmonton, Canada).

2.5 PREPARATION OF VIRAL STOCKS

Vero cell monolayers at approximately 70% confluency were infected with HSV-1, HSV-2 or VACV at a multiplicity of infection (MOI) of 0.05 plaque forming unit (pfu)/cell for 1 hour at 37°C in 5% CO_2, rocking and rotating the flasks every 10 minutes to prevent cell drying. The inoculum was removed, and cells were washed twice with DMEM and then overlaid with DMEM-5% FBS. Infected cells were incubated at 33°C in 5% CO_2 until cytopathic effects (CPE) were observed (cell rounding with minimal detachment) at approximately 48 hours post infection (hpi). The cells were harvested by scraping with sterile disposable lifters. The resulting cell suspensions were collected in 50-mL conical tubes and centrifuged at 3,200 × *g* for 30 minutes at 4°C in an Eppendorf 5810R centrifuge equipped with the swinging bucket rotor A-4-62 (Eppendorf Canada, Mississauga, ON, Canada). The resulting supernatants were collected and virions were pelleted by centrifuging at 10,000 × *g* for 2 hours at 4°C in a Beckman Coulter J-series centrifuge equipped with a JA-14 rotor (Beckman Coulter Inc., Mississauga, ON, Canada). Meanwhile, the cell pellets were resuspended in DMEM and lysed by 3 freeze-

thaw cycles in an ethanol-dry ice bath and 37°C water bath. The cell lysates were then placed in an ice-water bath and sonicated using an Ultrasonic Processor XL 2020 (Mandel Scientific Company, Guelph, ON, Canada) at a power setting of 3 for 30 second intervals, repeated thrice with 15-second rest periods in between. Cellular debris was then pelleted by centrifugation at 3,200 × *g* for 30 minutes at 4°C (Eppendorf 5810R centrifuge, A-4-62 rotor), and the resulting supernatant was used to resuspend the viral pellet obtained from the initial supernatant. The viral stocks were then aliquoted into glass vials and stored at -80°C.

Near-confluent Vero cell monolayers were infected with VSV, PV or SINV at an MOI of 0.02 pfu/cell for 1 hour at 37°C in 5% CO_2. Flasks were rocked and rotated every ~10 minutes to prevent cell drying. The inoculum was removed, and the infected cells were overlaid with DMEM-5% FBS. Culture supernatants were collected when full CPE was observed at ~48 hpi and centrifuged at 3,200 × *g* for 30 minutes at 4°C (Eppendorf 5810R centrifuge, A-4-62 rotor) to pellet cell debris. The supernatant was centrifuged at 10,000 × *g* for 2 hours at 4°C (Beckman Coulter J-series centrifuge, JA-14 rotor), and the resulting virion pellet was resuspended in serum-free DMEM, aliquoted into glass vials, and stored at -80°C.

NIH 3T3 cells were infected with mCMV at 0.01 pfu/cell for 1 hour at 37°C in 5% CO_2. Infected cells were overlaid with DMEM-10% FBS and were incubated at 33°C in 5% CO_2 for approximately 4 days, until CPE were observed. Two days after 90% of the cells displayed CPE, virions were harvested as described for HSV-1 and HSV-2.

Huh7.5 cells were infected with 0.003 focus-forming units (ffu)/cell of HCV JFH-1 for 4 hours at 37°C. Inocula were removed, and cells were overlaid with DMEM-10%

FBS and passaged as necessary. After 6-7 days, culture medium was collected and centrifuged at 800 × *g* for 10 minutes at 4°C (Eppendorf 5810R centrifuge, A-4-62 rotor) to pellet cellular debris. The supernatant was filtered through a 0.22-μm filter and concentrated using Amicon 100 kDa cutoff centrifugal filter units (Millipore, Billerica, MA, USA). For some experiments, the cell monolayers were immediately overlaid with DMEM supplemented with 0.2% bovine serum albumin (BSA). At 8 days post-infection, "serum-free" virions were harvested as described. When needed, the concentrated supernatant was purified by ultracentrifugation at 108,000 × *g* through a 20% sucrose cushion, using a Beckman-Coulter OptimaMax ultracentrifuge equipped with a TLA120.2 rotor. In all cases, resulting virus stocks were titrated by focus-forming assay (**section 2.6**) and stored at -80°C.

Near-confluent MDCK cell monolayers were infected with 0.01 PFU/cell of IAV for 1 hour at 37°C. The infected cells were then incubated in DMEM supplemented with 0.2% BSA and 2 μg/ml TPCK trypsin in 5% CO_2 at 33°C for approximately 2 days, until at least 90% of the cells displayed CPE. Virions were harvested as described for VSV.

Adenovirus type 5 (AdV) expressing green fluorescent protein (GFP) was obtained from Dr. Dennis Vance (University of Alberta, Edmonton, Alberta, Canada) and was titrated in HEK293T cells maintained with DMEM-10% FBS. Mammalian orthoreovirus type 3 was kindly provided by Dr. Maya Shmulevitz (University of Alberta, Edmonton, Alberta, Canada) and was titrated in L929 cells maintained in DMEM-10% FBS.

2.6 VIRUS TITRATIONS

HSV-1/2, VSV, VACV, SIN and PV were titrated in Vero cells. Aliquots of viral stocks were thawed rapidly at 37°C and immediately placed on ice. Ten-fold serial dilutions were prepared in serum-free DMEM and each dilution was mixed by gentle vortexing. Near-confluent Vero cell monolayers (5×10^5 or 2.5×10^5 cells/well in 6-well or 12-well plates, respectively) were then infected with 200 μL (6-well plates) or 100 μL (12-well plates) of serially diluted virions. After 1 hour, inocula were removed and the cells were washed twice with 1 mL/well of cold serum-free DMEM. Infected cells were then overlaid with 2% methylcellulose (Sigma-Aldrich) containing 5% FBS and incubated at 37°C in 5% CO_2 until well-defined plaques developed (typically, 2-3 days post-infection). The infected cells were then fixed and stained with crystal violet (Sigma-Aldrich) in methanol (0.5% or 1% [w/v] crystal violet, 17% [v/v] methanol in H_2O).

HCV was titrated by focus-forming assay in Huh7.5 cells. As for the other viruses, ten-fold serial dilutions were prepared in DMEM. Huh7.5 cells (9×10^4 cells/well in 24-well plates) were then infected with 150 μL of the appropriate dilution. The inocula were removed 4 hours later, and the monolayers were washed and overlaid with DMEM-10% FBS. At 72 or 96 hours post-infection, the infected cells were fixed with methanol-acetone (1:1) for 20 minutes at -20°C. Fixed cells were blocked with normal horse serum for 20 minutes at room temperature and then incubated with primary mouse IgG anti-HCV core antibody diluted 1:1000 in PBS-0.1% BSA for 2 hours at room temperature. Cells were then washed three times with PBS. Secondary biotinylated horse anti-mouse IgG antibody was then added for 30 minutes at room temperature. After three washes with PBS, the avidin-biotin-peroxidase complex (Vectastain ABC kit) was

added for 30 minutes at room temperature. Finally, the ImmPact SG peroxidase substrate was added for 12 minutes at room temperature. Cells were then washed with PBS and foci of infected cells were counted under a microscope. Alternatively, fixed cells were blocked with 2% normal goat serum (Sigma-Aldrich) in PBS, incubated with the same primary antibody, and then incubated with secondary goat anti-mouse IgG Alexa Fluor 488 antibody for immunofluorescence analysis using a fluorescence microscope with a UV light source (Leica DM IRB, Itzlar, Germany).

For IAV and RV, near-confluent MDCK or L929 cells (~5×10^5 or 2.5×10^5 cells/well in 6-well or 12-well plates, respectively) were infected with 200 μL (6-well plate) or 100 μL (12-well plate) of serially diluted IAV or RV virions. The inocula were removed after 1 hour, and the monolayers were washed twice with DMEM and overlaid with 0.8% agarose (containing 0.1 μg/mL TPCK-trypsin, for IAV only) in DMEM (IAV) or DMEM-10% FBS (RV). When the plaques were visible and clearly defined (~48-72 hpi), they were visualized by crystal violet staining (1% [w/v] crystal violet, 17% [v/v] methanol in H_2O).

For mCMV, NIH 3T3 cells (3×10^5 cells/well in 12-well plates) were infected with 150 μL of serially diluted mCMV virions. The inocula were removed after 1 hour, and the monolayers were washed and overlaid with DMEM-10% FBS. Foci of infected cells were detected after 24 hours using a LacZ cell detection kit (InvivoGen, San Diego, CA), according to the manufacturer's instructions. Briefly, infected cells were rinsed once with 0.5 mL of PBS, and then fixed with 0.5 mL of the provided fixative solution for 10 minutes at room temperature. The fixed cells were rinsed twice with PBS and stained with 0.5 mL per well of the provided staining solution (4 mM potassium

ferricyanide, 4 mM potassium ferrocyanide, 2 mM $MgCl_2$, 2 mg/mL X-gal solution in PBS). After 1-2 hours at 37°C, the cells were examined under a basic microscope for the development of blue colour (indicating infected cells).

For AdV, serially diluted virions were used to infect HEK293 cell monolayers (2.5 x 10^5 cells/well in 12-well plates). The inocula were removed after 30 minutes to 1 hour, and the monolayers were washed and overlaid with fresh DMEM-10% FBS. Infected cells expressing GFP were visualized and counted after 24 hours using a fluorescence microscope with a UV light source.

2.7 INFECTIVITY ASSAYS

Semi-logarithmic dilutions of the compounds were prepared in serum-free DMEM from the 10, 20, 30 or 100 mM stocks and incubated at 37°C. Approximately 200 pfu of HSV-1/-2, VSV, SINV, PV, VACV, RV or IAV in a volume of 100 μL were then mixed with 100 μL of the diluted compound or equivalent volume of vehicle and incubated for 10 minutes at 37°C, in serum-free DMEM at pH 7.2. For IAV infections, MDCK cells were washed twice with DMEM prior to infection. Vero (HSV-1/2, VSV, SINV, PV and VACV), L929 (RV) or MDCK (IAV) cell monolayers (5×10^5 cells/well in 6-well plates or 2.5×10^5 cells/well in 12-well plates) were then infected with the 200 μL or 100 μL inoculum. The plates were rocked and rotated every ~10 minutes to prevent cell drying. After 1 hour, the inocula were removed and cells were washed twice with cold DMEM. Infected cells were then overlaid with appropriate semi-solid medium and incubated until plaques developed, as described for standard viral titrations in **section 2.6**.

For HCV, 75 μL containing 100 ffu were mixed with 75 μL of the diluted compound or equivalent volume of vehicle (in DMEM) and incubated for 10 minutes at 37°C. Huh7.5 cell monolayers (9×10^4 cells/well in 24-well plates) were then infected with 150 μL of the inoculum. The plates were rocked and rotated every 1 hour, and after 4 hours, the inocula were removed and cells were washed twice with DMEM. Infected cells were overlaid with DMEM-10% FBS. At 72 or 96 hours post-infection, cells were evaluated for HCV infection by immunocytochemistry, as described in **section 2.6**.

For mCMV, NIH 3T3 cells (3×10^5 cells/well in 12-well plates) were infected with a 150 μL inoculum containing approximately 200 ffu of mCMV RM427$^+$ pre-exposed for 10 minutes at 37°C to compound or vehicle. The cells were infected for 1 hour at 37°C, with rocking and rotating every 10 minutes. Inocula were removed and cells were washed twice with DMEM, and then overlaid with DMEM-5% FBS. Foci of infected cells were detected after 24 hours using a LacZ cell detection kit (**section 2.6**).

For AdV, virions were exposed to compound or vehicle for 10 minutes at 37°C prior to infecting HEK293 cell monolayers (2.5×10^5 cells/well in 12-well plates). The cells were infected for 30-60 minutes (depending on potential cell detachment), with rocking and rotating of the plates every 10 minutes. After the infection, the inocula were removed and cells were overlaid with DMEM-10% FBS. Infected cells expressing GFP were visualized 24 hours later as described in **section 2.6**.

To determine EC_{50}, plaques or foci were counted and expressed as a percentage relative to the plaques produced by the vehicle-treated controls. EC_{50} were then calculated by nonlinear regression analysis (unrestrained fit) using GraphPad Prism (Version 5.0, GraphPad Software, Inc., USA).

2.8 TIME-OF-ADDITION ASSAYS

For cell pre-treatment experiments, MDCK, Huh7.5, or Vero cells were treated with compound or vehicle for 1 hour at 37°C. The cells were then washed three times with DMEM warmed to 37°C and infected with IAV PR8, HCV JFH-1, or HSV-1 KOS, respectively, in the absence of any drug. Infectivity was assessed by plaque or focus formation as described in **section 2.6**.

To test whether the compounds were effective when added to already-infected cells, MDCK, Huh7.5, or Vero cells were infected with 5, 3 or 0.5 pfu/cell (depending on the experiment) of IAV PR8, HCV JFH-1, or HSV-1 KOS. The inocula were removed after 1 h of adsorption. The infected cells were washed and then overlaid with DMEM-10% FBS (HCV) or DMEM-5% FBS (IAV and HSV-1) supplemented with the compound or vehicle for 24-48 hours (IAV and HSV-1) or 48-72 hours (HCV). The supernatants and cell lysates were then harvested as described in **section 2.5**. IAV and HSV-1 virions were pelleted by centrifugation at 10,000 × *g* for 2 hours at 4°C (Beckman Coulter J-series centrifuge, JA-14 rotor) and resuspended in drug-free DMEM. HCV virions were concentrated using Amicon centrifugal filters with a 100-kDa molecular-mass cutoff, or pelleted by ultracentrifugation through a 20% sucrose cushion at 108,000 × *g* for 4 hours at 4°C (Beckman-Coulter OptimaMax ultracentrifuge, TLA120.2 rotor). Standard titrations were performed using logarithmic dilutions of the viruses in DMEM, and MDCK, Vero, or Huh7.5 cells as described in **section 2.6**.

2.9 SELECTION FOR RESISTANCE

IAV PR8, IAV Aichi and HSV-1 KOS were serially passaged in the presence of increasing concentration of compound or vehicle. MDCK or Vero cells were seeded into 60 cm^2 round dishes (2.5×10^6 cells/dish) and incubated for approximately 16 hours. For aUY11 selection, cells were first infected with 0.01 pfu/cell (or, if the viral titer was too low, 0.001 pfu/cell) for 1 hour at 37°C. Inocula were removed, and the infected cells were overlaid with DMEM-5% FBS containing aUY11. Virions were harvested (as described in **section 2.5**) when cells exhibited 80-90% CPE, typically at ~24 hpi for IAV and ~48 hpi for HSV-1 (although more time was usually required for EGCG-treated virions to produce 80-90% CPE). For EGCG selection, virions were pre-treated with EGCG for 10 minutes at 37°C. Treated virions were then used to infect cell monolayers for 1 hour. The inocula were removed, and infected cells were washed twice with DMEM and overlaid with DMEM-5% FBS containing no drug. Virions were harvested (as described in **section 2.5**) when cells exhibited 80-90% CPE, typically at ~24 hpi for IAV and ~48 hpi for HSV-1. Titers were determined by standard plaquing assays.

Resistant variants were plaque-purified. EGCG-resistant virions and control virions (from passage 6 for IAV PR8 and Aichi) were used to infect MDCK cells. Five plaques from each group were then selected for plaque purification. Isolated plaques were scraped with a P200 pipette tip, resuspended in 200 μL of DMEM, and used to infect near-confluent MDCK cell monolayers (5×10^5 cells in 6-well plates). Virions were harvested (as described in **section 2.5**) when cells exhibited 90% CPE, at ~24 hpi. The virion pellets were resuspended in 50 μL of DMEM. To confirm resistance, the isolates were treated with EGCG for 10 minutes at 37°C and used to infect MDCK cell

monolayers (as described for infectivity assays in **section 2.7**). To identify mutations conferring resistance, viral RNA was isolated and reverse-transcribed to cDNA (described in **section 2.23**). The hemagglutinin gene was then PCR-amplified and sequenced (described in **section 2.23**).

2.10 ^{35}S-METHIONINE LABELLING OF HSV-1, VSV, HCV, ADV, RV AND PV

Vero, HEK293T, L929 or Huh7.5 cells were seeded in 60 cm^2 round dishes (2.5×10^6 cells/dish) and incubated at 37°C in 5% CO_2 for approximately 16 hours. Vero cells were infected with HSV-1 (2.5 pfu/cell), VSV (5 pfu/cell) or PV (5 pfu/cell). HEK293T or L929 cells were infected with AdV (5 pfu/cell) or RV (5 pfu/cell). Huh7.5 cells were infected with HCV JFH-1 (MOI 0.1 ffu/cell). A mock-infected sample was also included for each cell type. For HSV-1, VSV, PV and RV, the plates were rocked and rotated every 10 minutes and inocula were removed after 1 hour at 37°C. For AdV, the plates were rocked and rotated every 10 minutes and the inoculum was removed after 30 minutes at 37°C. For HCV, the plates were rocked and rotated every hour and the inoculum was removed after 4 hours. The infected cells were then washed twice with cold (4°C) DMEM and overlaid with DMEM-5% FBS (HSV-1, VSV, PV) or DMEM-10% FBS (HCV, AdV, RV). Infected cells were methionine-starved at 3 hpi (HSV-1, VSV, PV, AdV and RV) or 7 hpi (HCV) by replacing the media with methionine-free DMEM-5% FBS. After 2 hours, the cells were washed twice with warmed DMEM and overlaid with 4 mL (HSV-1, VSV, HCV) or 5 mL (AdV, PV, RV) of methionine-free DMEM-5% FBS supplemented with 42 μCi/mL L-^{35}S-methinione (PerkinElmer, Boston, MA, USA). Supernatants were recovered when full cytopathic effects were observed,

ranging from 6 to 48 hpi. The supernatants were centrifuged at 3,200 × *g* at 4°C for 30 minutes (Eppendorf 5810R centrifuge, A-4-62 rotor) to remove cell debris. The resulting supernatants were collected and centrifuged at 10,000 × *g* for 2 h at 4°C (Beckman Coulter J-series centrifuge, JA-14 rotor). The viral pellets were resuspended in 100 μL of serum-free methionine-free DMEM. For HCV, supernatants were centrifuged at 800 × *g* for 10 minutes (Eppendorf 5810R centrifuge, A-4-62 rotor) to remove cellular debris. The supernatant was filtered through a 0.22 μm filter and concentrated using Amicon 100K centrifugal filters.

Titers of ^{35}S-labelled viruses were determined by standard plaquing or focus-forming assays (**section 2.6**). To test incorporation of ^{35}S, 1 μL of the labelled virions or mock preparation were fixed in 100 μL of 100% ethanol and added to scintillation vials containing 4 mL of aqueous scintillant. ^{35}S radioactivity was then determined using a Beckman Coulter LS 6500 scintillation counter. Virions were labeled to approximately 0.02 cpm/pfu (HSV-1 and VSV), 1 cpm/pfu (PV), 14 cpm/pfu (RV), 7 cpm/pfu (AdV) or 199 cpm/ffu (HCV).

2.11. R18 LABELLING OF VSV, HCV, IAV, HSV-1 AND VACV

Virions were labelled with 0.59 μM (VSV and HCV), 1.8 μM (IAV, HSV-1) or 2.7 μM (VACV) R18. VSV, IAV, HSV-1 (10^8 pfu), HCV JFH-1 (10^6 ffu) or VACV (10^6 pfu) virions were mixed with 1.97 μL (VSV, HCV), 5.91 μL (IAV, HSV-1) or 9.1 μL (VACV) of 300 μM R18 (dissolved in ethanol) in 1 mL of freshly prepared 180 mM Na_2HPO_4, 10 mM citric acid (pH 7.4) (fusion buffer) for 1 hour at room temperature on a rotary shaker in the dark. The labelled virions were purified through a column containing

4 mL of Sephadex G-100 resin (GE Healthcare). The column was pre-equilibrated with two washes each of approximately 12 mL of fusion buffer. Labelled virions (1 mL) were then added to the column and eluted with fusion buffer. Fractions of approximately 500 μL were collected every minute for 15 minutes. The viral protein concentration in each fraction was determined using a Bradford assay (Bio-Rad, Hercules, CA, United States).

Fractions containing the most viral protein were pooled and concentrated using Amicon 100K centrifugal filters. Labelled virions were then titrated on Vero, Huh7.5, or MDCK cells (**section 2.5**). Finally, the pooled fractions were tested for R18 incorporation by R18 dequenching after addition of Triton X-100 to a final concentration of 0.1% (VSV, IAV, HSV-1, VACV) or 0.01% (HCV), using a QuantaMaster 40 scanning spectrofluorometer (Photon Technology International, Birmingham, NJ, United States) with a 75-W xenon lamp. R18 fluorescence was excited at 560 nm and detected at 590 nm using a model 814 switchable photon-counting/analog photomultiplier detection unit with an R1527 photomultiplier tube. Data were collected using FeliX32 software (Photon Technology International).

2.12. LIPOSOME PREPARATION

Cholesterol, β-oleoyl-γ-palmitoyl-L-α-phosphatidylcholine (POPC) and 1,2-dioleoyl-L-α-phosphatidylcholine (DOPC) were obtained from Sigma-Aldrich. POPC liposomes were prepared by hydrating 2 μmol dry lipid with 1 mL of 180 mM Na_2HPO_4, 10 mM citric acid (pH 7.4), followed by vortexing. DOPC-cholesterol (1.7:1 molar ratio) liposomes were prepared by the hydration method. DOPC and cholesterol were dissolved and mixed in 500 μL chloroform, which was then evaporated; 1 mL of 180 mM Na_2HPO_4, 10 mM

citric acid (pH 7.4) was added to the resulting lipid film, and the mixture was vortexed to form large multilamellar liposomes. R18 was added (to a final concentration of 5 mol%) as required by first mixing R18 and lipids as ethanol and chloroform solutions, respectively.

Large multilamellar liposomes were extruded to a diameter of 200 nm as required, using an Avanti liposome mini-extruder (Avanti Polar Lipids Inc., Alabaster, AL, USA) and according to the manufacturer instructions. Briefly, the liposome preparation was loaded into a glass gas-tight syringe and placed in one side of the mini-extruder. An empty gas-tight glass syringe was placed in the other side of the mini-extruder. The liposome mixture was transferred from one syringe to the other, through a polycarbonate membrane with pore diameter of 0.2 μm. The process was repeated such that the liposome mixture was passed through the membrane ten times.

2.13. BINDING ASSAYS

2.13.1 Radioactive binding assays. ^{35}S-Methionine labeled HSV-1, VSV, HCV, PV or RV virions (~1×10^4 infectious particles) were exposed to EGCG, DMSO vehicle or 100 μg/mL heparin for 10 minutes at 37°C. Next, the pre-exposed virions were adsorbed onto Vero (HSV-1, VSV, PV), Huh7.5 (HCV) or L929 (RV) cells for 1 hour at 4°C before washing three times with ice-cold PBS. Radioactivity still attached to cells was measured using a Beckman Coulter LS 6500 scintillation counter. Binding was calculated as cpm bound to cells divided by total cpm, expressed as percentage and adjusted by background. Percent binding was expressed relative to binding of virions exposed to vehicle control.

For AdV, ^{35}S-methionine labeled virions were exposed to compound or vehicle for 10 minutes at 37°C, then chilled on ice and mixed with 293T cells (1×10^6 cells) in suspension. The suspensions were incubated in Eppendorf tubes on ice for 1 hour, and were mixed by gentle pipetting every 10 minutes. AdV virion-cell complexes were washed three times by centrifugation at 300 × *g* for 5 minutes at 4°C. Radioactivity still attached to cells was measured using a Beckman Coulter LS 6500 scintillation counter. Binding was calculated as cpm bound to cells divided by total cpm (in the input, washes and cells), expressed as percentage and adjusted by the background radioactivity of the mock sample. Percent binding was then expressed relative to binding of virions exposed to vehicle control.

2.13.2. Fluorescence binding assays. R18-labeled HSV-1, VACV, VSV, HCV or IAV virions (1×10^4 infectious particles) were exposed for 10 minutes at 37°C to EGCG, DMSO vehicle or 100 μg/mL heparin. The exposed virions were then chilled at 4°C for 15 minutes prior to being adsorbed onto pre-chilled Vero (HSV-1, VACV, VSV), Huh7.5 (HCV) or MDCK (IAV) cells for 1 hour at 4°C. After three washes with cold phenol red-free DMEM, the cells and attached virions were lysed with 0.1% Triton-X 100 to dequench R18. Fluorescence was excited at 560 nm using a QuantaMaster 40 spectrofluorometer, and detected at 590 nm. Fluorescence still attached to cells after the washes was normalized to the fluorescence of the input virions. Binding was calculated as fluorescence bound to cells divided by total fluorescence. Percent binding was then expressed relative to binding of virions treated with vehicle control.

2.14. FUSION ASSAYS

2.14.1 Virus-cell fusion. Vero, MDCK, or Huh7.5 cells were cultured in DMEM-5% FBS (Vero and MDCK) or DMEM-10% FBS (Huh7.5) as described previously. The cells were washed with phosphate-buffered saline (PBS) and incubated for less than 5 minutes at 37°C in 3 ml of 1X trypsin in PBS to generate cell suspensions. The cell suspensions were then washed twice by centrifugation in fusion buffer at 800 x g for 5 minutes at 4°C (Eppendorf 5810R centrifuge, A-4-62 rotor).

R18-labelled VSV (0.60 μg viral protein containing 1×10^4 pfu) was exposed to compound or vehicle for 10 minutes at 39°C, and then incubated on ice for 3 minutes. R18-VSV was then mixed with 1×10^6 Vero cells in fusion buffer and incubated on ice for 30 min to allow VSV binding but not fusion. Virion-cell complexes were then washed with fusion buffer by centrifugation at 300 × *g* for 5 minutes at 4°C (Eppendorf 5810R centrifuge, FA45-30-11 rotor). Virion-cell pellets were resuspended in 2.5 mL of the same buffer. The R18-VSV-Vero cell suspension was warmed at 37°C for 5 minutes, and then added to a polymethacrylate cuvette (Sigma-Aldrich) pre-warmed to 37°C. Fluorescence was excited at 560 nm and detected at 590 nm, using a QuantaMaster 40 scanning spectrofluorometer equipped with a 75-W xenon lamp. Emitted light was detected using a model 814 switchable photon-counting/analog photomultiplier detection unit with an R1527 photomultiplier tube, and data was collected using FeliX32 software. After 10 minutes, the pH of a duplicate sample was adjusted to 5.5 by adding 0.31 mL of 500 mM citric acid, while the other duplicate was kept at pH 7.4 by adding 0.31 mL of 180 mM Na_2HPO_4, 10 mM citric acid (pH 7.4) buffer.

Percent fusion was calculated from changes in fluorescence according to:

$$\% \text{ fusion} = (((F_{5.5} - F_0)/(F_{max} - F_0)) - ((F_{7.4} - F_0)/(F_{max} - F_0))) \times 100$$

where $F_{5.5}$ is the fluorescence at pH 5.5 at each time point, $F_{7.4}$ is the fluorescence at pH 7.4 at each time point, F_0 is the fluorescence of the complex after incubation for 10 minutes at pH 7.4, and F_{max} is the total fluorescence measured by disrupting the cells with Triton X-100 (to a final concentration of 0.1%).

R18-labelled IAV, HCV or occasionally VSV (1 x 10^4 infectious particles) were exposed to compound or vehicle in a volume of 100 μL for 10 minutes at 37°C and then incubated on ice for 3 minutes. The virions were then diluted 3.5-fold by mixing with 1 x 10^6 pre-chilled MDCK (IAV), Huh7.5 (HCV) or Vero (VSV) cells in 250 μL of phenol red-free DMEM and incubated on ice for 30 minutes (IAV) or 60 minutes (HCV, VSV) to allow binding but not fusion. Alternatively, virions were first adsorbed onto cells for 1 hour at 4°C, and then exposed to the compound or DMSO vehicle for 10 minutes at 37°C. The virus-cell complexes were then washed twice with phenol red-free DMEM by centrifugation at 300 × *g* for 5 minutes at 4°C (Eppendorf 5810R centrifuge, FA45-30-11 rotor). The virus-cell pellets were resuspended in 2.38 mL of fusion buffer pre-chilled to 4°C. Fusion was triggered by increasing the temperature to 37°C and lowering the pH to 5 (IAV) or 5.5 (HCV, VSV) by adding 500 mM citric acid. For HCV fusion, pH 4, 4.5, 5, and 6 were also tested. An identical sample was kept at pH 7.4 by adding fusion buffer, and an additional non-fusion control was maintained at 4°C (pH 7.4). Equivalent aliquots were removed at discrete time points, fixed with 10% formalin, and transferred to polymethacrylate cuvettes. Fluorescence was excited at 560 nm and detected at 590 nm, using a QuantaMaster 40 scanning spectrofluorometer and FeliX32 software. Percent fusion was calculated from changes in fluorescence according to the following equation:

percent fusion = $((F_{5.5}/F_{max})/(F_{initial}/F_{max})) \times 100$, where $F_{5.5}$ is the fluorescence at pH 5.5 at each time point, $F_{initial}$ is the initial fluorescence of the complex, and F_{max} is the total fluorescence after Triton X-100 lysis to a final concentration of 0.01% (HCV) or 0.1% (VSV, IAV). $F_{7.4}$, the fluorescence at pH 7.4 for each time point, is also shown on the graphs.

2.14.2 Virus-liposome fusion. VSV virions (10^7 pfu) were labeled with 20 μM of the membrane fluidity probe DPH by incubating the virion-DPH mixture for 10 minutes at 37°C. DPH-labeled virions were then treated with compound or vehicle for 10 minutes at 37°C in a total volume of 100 μL. DOPC/cholesterol liposomes (200 nm diameter; 0.3 μmol) were then added to a final volume of 200 μL. Fusion was triggered by increasing the temperature to 37°C and lowering the pH to 5. The polarization of DPH fluorescence was then tested, as a measure of fusion. DPH polarization is increased in membranes with higher rigidity/lower fluidity (such as the virion envelope) and decreased in membranes with lower rigidity/higher fluidity (such as the liposome membrane).

2.14.3. Liposome-cell fusion. R18-labeled DOPC-cholesterol liposomes (2 nmol) were exposed to 0.1% DMSO or 2 μM aUY11 in a minimal volume for 10 minutes at 37°C and then incubated on ice for 3 minutes. The exposed liposomes were then mixed with 1 × 10^6 pre-chilled Vero cells in fusion buffer and incubated on ice for 10 min. The liposome-cell mixtures were then diluted to 2.38 mL in fusion buffer and warmed to 37°C prior to transfer to polymethacrylate cuvettes. Fusion was triggered by increasing the temperature to 37°C and lowering the pH to 5.5 by addition of 500 mM citric acid. An identical sample was kept at pH 7.4 by adding fusion buffer. Fluorescence was excited at 560 nm and detected at 590 nm, using a QuantaMaster 40 scanning

spectrofluorometer and FeliX32 software. Percent fusion of liposomes was calculated from changes in fluorescence according to the following equation: percent fusion = (($F_{5.5}$ - $F_{initial}$)/(F_{max} - $F_{initial}$) / ($F_{7.4}$ - $F_{initial}$)/(F_{max} - $F_{initial}$)) × 100, where $F_{5.5}$ is the fluorescence at pH 5.5 at each time point, $F_{7.4}$ is the fluorescence at pH 7.4 at each time point, $F_{initial}$ is the fluorescence of the complex after incubation for 10 min at pH 7.4 at 37°C, and F_{max} is the total fluorescence after lysis with Triton X-100 (at a final concentration of 0.1%).

2.15. FLUIDITY ASSAYS

DPH was dissolved in tetrahydrofuran and then added to DOPC-cholesterol liposomes (20 nmol) or HCV virions (10^5 ffu) to a final concentration of 2 μM. To allow insertion of DPH into the hydrophobic core of the lipid membrane, the liposome-DPH mixture was incubated for 10 minutes at 37°C. The DPH-labeled liposomes were then incubated with compound, vehicle or cholesterol (as a control) for 10 minutes at 37°C and transferred to cuvettes pre-warmed to 37°C. DPH fluorescence was excited at 350 nm, and emission was measured at 450 nm using a QuantaMaster 40 scanning spectrofluorometer and FeliX32 soft-ware. Fluorescence polarization (P) was calculated according to the following equation: $P = (I_{VV} - GI_{VH})/(I_{VV} + 2GI_{VH})$, where I_{VV} and I_{VH} are the intensities obtained with polarizers aligned parallel and perpendicular to the polarized excitation beam, respectively. G is the instrument grating correction factor, which is the intensity ratio of the vertical to horizontal emitted fluorescence ($G = I_{HV}/I_{HH}$) obtained when the sample is excited with horizontally polarized light.

2.16. DIFFERENTIAL SCANNING CALORIMETRY

DSC experiments were performed by Drs. Richard and Raquel Epand (McMaster University, Hamilton, Canada). Mixtures of dielaidoylphosphatidylethanolamine (DEPE) (Avanti Polar Lipids, Alabaster, AL) and aUY11 were made by dissolving the components in chloroform-methanol (2:1). The solvent was then evaporated under nitrogen gas and placed in a vacuum desiccator for 3 hours. The dried films were hydrated with 0.8 mL of 20 mM PIPES, 0.14 M NaCl, 1 mM EDTA, pH 7.4, by vortexing; degassed; and placed in the sample cell of a Nano II calorimeter (Calorimeter Sciences Corp., Linden, UT, USA), and buffer was placed in the reference cell. The lamellar-to-inverted-hexagonal phase transition temperature was evaluated at a heating scan rate of 1°C/minute. The cell volume was 0.34 mL, and the total lipid concentration was 2.5 mg/mL. The results were plotted in ORIGIN 7.0 and analyzed with DA-2 (Microcal, Inc., Northampton, MA, USA).

2.17. FLUORESCENCE SPECTRA

Emission spectra of aUY11 or dUY11 were collected using the QuantaMaster 40 spectrofluorometer. aUY11 or dUY11 was added to 2.5 mL of fusion buffer, or to 2.5 mL of 1-octanol (Sigma-Aldrich), to a final concentration of 48 nM or 0.48 nM, respectively, in a polymethacrylate cuvette pre-warmed to 37°C. Alternately, aUY11 or dUY11 was added to 10^7 PFU of VSV, HSV-1 or -2, or IAV; 10^6 FFU of HCV; or 2 nmol POPC liposomes in 2.5 mL of fusion buffer at 37°C to a final concentration of 48 nM. For other experiments, approximately 10^4 IAV, HCV, or HSV-1 virions produced by cells treated with vehicle, or equivalent volumes from cells treated with aUY11, were diluted to 2.5

mL in fusion buffer. Emission spectra were obtained at the maximum excitation wavelength, 455 nm, and examined from 475 to 575 nm. Spectra were normalized to the highest fluorescence signal intensity obtained for all conditions.

2.18. TRYPTOPHAN FLUORESCENCE QUENCHING

HSV-1, VSV, RV or AdV virions (10^6 pfu) were exposed to 250 μM EGCG or DMSO vehicle in a volume of 100 μL for 10 minutes at 37°C, in serum-free DMEM at pH 7.2. Treated virions were then diluted 25-fold to 2.5 mL and added to polymethacrylate cuvettes. Tryptophan fluorescence was excited at 280 nm using the QuantaMaster 40 spectrofluorometer. Emission spectra were obtained from 300 nm to 450 nm. Spectra were normalized to the highest fluorescence signal intensity within each each sample.

2.19. CONFOCAL MICROSCOPY

Near-confluent Vero cells were seeded onto 22 × 22 mm coverslips (Fisher) placed in 6-well plates and incubated for ~16 h at 37°C. The cells were first incubated with 250 nM PKH26-GL fluorescent dye (Sigma-Aldrich) for 10 minutes at 37°C and were then washed twice with 2 mL/well of room temperature DMEM. The washed cells were exposed to 2 μM aUY11 or dUY11 for 1, 5, 15, 40, or 120 min at 37°C. The RAFIs were removed, and the cells were washed twice with 2 mL/well of DMEM at room temperature. The cells were then fixed with 10% formalin for 30 minutes at room temperature, washed once with 1X PBS at room temperature, and mounted onto glass slides using Mowiol mounting medium (10% Mowiol (Sigma-Aldrich) in 25% glycerol in 0.2 M phosphate buffer, pH 7.4).

Confocal microscopy was performed using a Leica SP5 laser scanning confocal microscope with a 100X oil immersion (numerical aperture, 1.44) lens. Images were obtained using a 5-mW argon laser (458 nm) to excite the RAFIs fluorescence and a 1-mW HeNe laser (543 nm) to excite PKH26 fluorescence. Emitted fluorescence was detected with band-pass filters of 470 to 535 nm (RAFIs) and 560 to 650 nm (PKH26). The pinhole aperture was set to 1.0 Airy unit for each channel. The images were collected as 8-bit images using Leica Application Suite (LAS) microscope software and adjusted for contrast and brightness in Microsoft PowerPoint. Scale bars were added using LAS or Fiji ImageJ (NIH, Bethesda, MD, USA) software.

2.20. HEPARIN COLUMN CHROMATOGRAPHY

R18-labelled HSV-1 virions (10^5 pfu) were loaded onto a 1 mL HiTrap heparin sepharose column (GE Healthcare Life Sciences, Westborough, MA, USA) in 10 mM sodium phosphate (pH 7.4) containing 0.3 M NaCl (loading buffer). The column was then washed with 10 mL of loading buffer to remove unbound virions. The heparin-bound virions were then eluted with soluble heparin or equivalent concentrations of EGCG, EC or sialic acid in loading buffer. Virions that were still bound after the elution were eluted with 2 M NaCl in 10 mM sodium phosphate (pH 7.4). The flow rate was 1 mL/minute for washes and elution. Eluted virions were detected by R18 fluorescence after lysis by 0.1% Triton X-100.

HCV virions (10^5 ffu) were loaded onto the heparin column in 10 mM sodium phosphate (pH 7.4). The column was washed with 10 mL of the same buffer, and eluted with heparin, EGCG, EC or sialic acid in the same buffer. Virions still bound to the

column were then eluted with 2 M NaCl in 10 mM sodium phosphate (pH 7.4). Fractions were concentrated using Amicon 100K ultrafiltration tubes, and analyzed for HCV RNA (**section 2.23**). Results are expressed as the percentage of the bound virions that were eluted by the compounds.

2.21. HEMAGGLUTINATION ASSAY

IAV virions (PR8, USSR, Aichi and PC strains) were exposed to 100 μM EGCG or EC, 50 μg/mL heparin, 50 μg/mL sialic acid or equivalent volume of DMSO in DMEM for 15 minutes at 37°C. The virions were then serially diluted 2-fold in DMEM in 96-well round-bottom plates. 50 μL of a 0.5% suspension of chicken erythrocytes was added to each well and mixed by pipetting up and down. The plates were incubated for 1-2 hours at room temperature before scanning.

2.22. HEMOLYSIS ASSAY

Rabbit erythrocytes were originally obtained from Hemostat Laboratories (Dickson, CA, USA) and provided by Christopher Lohans (Dr. John Vederas, University of Alberta, Edmonton, AB, Canada). Defibrinated rabbit erythrocytes (1 mL) were diluted to 20 mL in PBS and washed three times by centrifugation at 1,000 × *g* for 5 minutes (Eppendorf 5810R centrifuge, A-4-62 rotor). 100 μL of the 5% suspension of erythrocytes was added to each of twelve wells in a 96-well plate and mixed with EGCG or vehicle control (50 μL). The plate was incubated at 37°C for 90 minutes. At 0 min, 30 min, 60 min and 90 min, 20 μL aliquots were removed. To each aliquot, 200 μL of fresh PBS was added and the erythrocytes were pelleted by centrifugation at 1,000 × *g* for 5 minutes (Eppendorf

5810R centrifuge, A-4-62 rotor). The supernatant was transferred to a new well in a 96-well plate and the absorbance of the haemoglobin was measured at 415 nm. As a control for lysis, 50 μL of Triton X-100 (0.1%) was added to one of the wells.

2.23. RNA ISOLATION, cDNA SYNTHESIS AND PCR AMPLIFICATION

2.23.1 RNA isolation. IAV RNA segments from EGCG-resistant or vehicle-treated plaques were isolated using the High Pure Viral RNA Kit (Roche), according to the manufacturer instructions. Briefly, 40 μL of IAV was diluted to 200 μL in DMEM and mixed with 400 μL of binding buffer (2.5 M guanidine-HCl, 5 mM Tris-HCl, 30% (w/v) Triton X-100, pH 6.6) supplemented with 50 μg of PolyA carrier RNA. The mixture was incubated at room temperature for 10 minutes, then transferred to a filter tube assembly and centrifuged at 8,000 × *g* for 30 seconds (Eppendorf 5810R centrifuge, FA45-30-11 rotor). The filter-bound RNA was then washed with inhibitor removal buffer (5 M guanidine-HCl, 20 mM Tris-HCl, 38% (v/v) ethanol, pH 6.6) by centrifugation at 8,000 × *g* for 1 minute (Beckman Coulter Microfuge 18, F241.5P rotor). The RNA was then washed twice with wash buffer (20 mM NaCl, 2 mM Tris-HCl, 80% (v/v) ethanol, pH 7.5) by centrifugation at 8000 × *g* for 1 minute. Residual ethanol was removed by centrifugation at 13,000 × *g* for 15 seconds. RNA was then eluted in nuclease-free water by centrifugation at 8,000 × *g* for 1 minute.

HCV RNA from virus preparations or heparin column elutions was isolated using the Roche High Pure Viral RNA Kit, as described above. Cell-associated HCV RNA was harvested using TRIzol, following the manufacturer's instructions. The cell media was removed, and 1 mL/10 cm^2 of TRIzol reagent was added. Cells were lysed by pipetting

up and down several times, and samples were incubated for 5 minutes at room temperature. Next, 0.2 mL of chloroform (per 1 mL TRIzol) was added and the tubes were shaken vigorously for 15 minutes. The samples were then centrifuged at 12,000 × *g* for 15 minutes at 4°C (Eppendorf 5810R centrifuge, FA45-30-11 rotor). The upper aqueous layer (containing RNA) was removed by careful pipetting. RNase-free glycogen (5 μg) was added as a carrier, and then 0.5 mL of 100% isopropanol (per 1 mL TRIzol) was added. The samples were incubated for 10 minutes at room temperature, and then centrifuged at 12,000 × *g* for 10 minutes at 4°C (Eppendorf 5810R centrifuge, FA45-30-11 rotor). The resulting RNA pellet was washed with 1 mL of 75% ethanol (per 1 mL TRIzol) and centrifuged at 7,500 × *g* for 5 minutes at 4°C (Eppendorf 5810R centrifuge, FA45-30-11 rotor). The RNA pellets were air-dried for 5-10 minutes, resuspended in 50 μL of RNase-free water, and incubated at 55-60°C for 15 minutes before storage at -80°C.

2.23.2 cDNA synthesis. The IAV RNA segments were transcribed to cDNA using M-MLV RT and an IAV universal primer (UniFlu, 5′-AGCRAAAGCAGG-3′), which is complementary to the 3′ end of all IAV H1N1 and H3N2 RNA segments (Chan *et al.*, 2006). The RNA, dNTPs (10 mM) and UniFlu primer (2 μM) were mixed together and incubated at 65°C for 5 minutes, then chilled on ice. Next, first-strand buffer (50 mM Tris-HCl (pH 8.3), 75 mM KCl, 3 mM $MgCl_2$), DTT (0.1 M), RNaseOUT (40 U) and M-MLV RT (200 U) were added. Using a T100 thermocycler (Bio-Rad), the reaction was incubated for 50 minutes at 37°C, and terminated by heating at 75°C for 15 minutes.

HCV RNA was transcribed to cDNA using Superscript III reverse transcriptase and an HCV-specific primer (5′-GTG TTT CTT TTG GTT TTT CTT TGA GGT TTA

GG-3′) (Santer *et al.*, 2013). cDNA was synthesized as described for IAV RNA, except Superscript III RT (200 U) was used instead of M-MLV RT and the reaction was incubated for 50 minutes at 55°C instead of 37°C.

2.23.3 PCR of IAV hemagglutinin. To PCR-amplify the IAV hemagglutinin (HA) gene, primers corresponding to the 5′ and 3′ ends of IAV PR8 HA (PR8HAfwd, 5′-GCA GGG GAA AAT AAA AAC AAC-3′ and PR8HArev, 5′-GGG TGT TTT TCC TCA TAT TTC-3′) and Aichi HA (AichiHAfwd, 5′-CAA AAG CAG GGG ATA ATT CTA-3′ and AichiHArev, 5′-ACA AGG GTG TTT TTA ATT ACT-3′) sequences were used. 10X *Pfx50* PCR mix (supplied with the polymerase), dNTPs (10 mM each), each primer (10 μM each), template DNA (2 μL of the cDNA) and *Pfx50* DNA polymerase (5 U/μL) were mixed together for a final concentration of 1X PCR mix, dNTPs (0.3 mM each), primers (0.3 μM each) and *Pfx50* DNA polymerase (5 U). The following amplification conditions were used in a T100 thermocycler (Bio-Rad): 2 minutes at 94°C, 20 cycles of (20 seconds at 94°C, 30 seconds at 47°C, 5 minutes at 68°C) and a final extension of 68°C for 5 minutes. Primers and PCR conditions are listed in **table 2.6** and **table 2.7**, respectively.

2.23.4 Agarose gel electrophoresis. When necessary, PCR products were resolved by agarose gel electrophoresis, using a 1.2% agarose gel. Briefly, 1.2 g of agarose was dissolved in 100 mL of Tris-Acetate-EDTA (40 mM Tris-acetate, 1 mM EDTA) by heating in a microwave. The agarose was allowed to cool to approximately 50°C prior to addition of ethidium bromide (0.5 μg/mL), and then the solution was poured into a casting tray. DNA samples were resuspended in 6X orange DNA loading dye (Thermo Scientific) and loaded into the wells along with GeneRuler 1 kb DNA ladder (Fermentas).

The gel was electrophoresed at 85 V for 60 minutes, using a Bio-Rad Wide Mini-Sub Cell GT Cell horizontal gel apparatus. Ethidium bromide staining was visualized using a Gel-Doc XR$^+$ Imager (Bio-Rad).

2.23.5 Purification of PCR products for sequencing. PCR product for sequencing was separated by agarose gel electrophoresis as described in **section 2.23.4**, except with low melting point agarose. Bands of the desired size (1770 base pairs for IAV HA) were then excised from the gel, and DNA was eluted from each gel piece using the Qiagen MinElute Gel Extraction Kit (Qiagen, Mississauga, ON, Canada). Briefly, 3 volumes of the provided buffer QC (containing guanidine hydrochloride) were added to 1 volume of gel (assuming that 100 mg gel is equivalent to 100 mL). The gel slice was dissolved at 50°C for 10 minutes. Once dissolved, 1 volume of isopropanol was added. The samples were applied to a MinElute column and centrifuged at 18,000 × *g* (Eppendorf 5810R centrifuge, FA45-30-11 rotor) at room temperature for 1 minute. DNA bound to the column was washed once with 500 μL of buffer QC and centrifuged at 18,000 × *g* for 1 minute. Next, 750 μL of Buffer PE was added to the column and incubated at room temperature for 5 minutes prior to centrifugation at 18,000 × *g* for 1 minute. The flowthrough was discarded, and the tubes centrifuged again at 18,000 × *g* for 1 minute to remove residual ethanol. DNA was then eluted in 10 μL of elution buffer (10 mM Tris-Cl, pH 8.5) by centrifugation at 18,000 × *g* for 1 minute. DNA concentrations were determined using a BioDrop DUO UV/vis spectrophotometer (Isogen Life Science).

2.23.6 Quantitative real-time PCR (qRT-PCR). qRT-PCR was performed with a 7900HT Fast Real-Time PCR system (Applied Biosystems) or a CFX96 Real-Time system (Bio-Rad) and the TaqMan universal PCR master mix, using primers amplifying

the conserved 5′-untranslated region of the HCV genome (HCVfwd, 5′-TCT GCG GAA CCG GTG AGT A-3′ and HCVrev, 5′-GTG TTT CTT TTG GTT TTT CTT TGA GGT TTA GG-3′). The HCV-specific detection probe was 5′-6-FAM-CAC GGT CTA CGA GAC CTC CCG GGG CAC-TAMRA-3′ (HCVprobe). Ten-fold dilutions from 10^1 to 10^6 copies of a linearized plasmid containing the sequence of HCV JFH-1 kindly provided by Justin Shields (University of Alberta, Edmonton, AB, Canada) were used to generate a standard curve for quantitation.

2.24. CHOLESTEROL ASSAY

Cholesterol amounts were determined using the Amplex Red Cholesterol Assay (catalog number A12216, Molecular Probes). Amplex Red reagent (20 mM), Reaction Buffer (1X; 0.1 M potassium phosphate, 0.1 M NaCl, 5 mM cholic acid, 0.1% Triton X-100, pH 7.4), horseradish peroxidase (200 U/mL), cholesterol oxidase (200 U/mL) and cholesterol esterase (200 U/mL) were prepared in sterile, deionized H_2O according to the manufacturer instructions. Cholesterol standards (ranging from 0.2 μM to 20 μM) and samples were diluted in 50 μL in 1X Reaction Buffer and each dilution was mixed with 50 μL of 300 μM Amplex Red reagent containing 2 U/mL horseradish peroxidase, 2 U/mL cholesterol oxidase and 0.2 U/mL cholesterol esterase. The reactions were incubated for 30 minutes at 37°C. Cholesterol is oxidized by cholesterol oxidase to yield H_2O_2, which reacts with Amplex Red reagent to form the fluorescent resorufin. Resorufin fluorescence was detected using a fluorescence microplate reader (550 nm excitation and 590 nm emission).

Table 2.1. Antiviral compounds

Reagent name	Source	Catalog number
4-(adamantan-1-yl)phenylethynyl-2'-deoxyuridine **(dUY5)**	Drs. Alexey Ustinov and Vladimir Korshun (Russian Academy of Sciences, Moscow, Russia)	N/A
5-(Estra-1,3,5(10)-triene-17-one-3-yl)ethynyl-2′-deoxyuridine **(dUY1)**	Drs. Alexey Ustinov and Vladimir Korshun	N/A
5-(Perylen-3-yl)ethynyl-arabino-uridine **(aUY11)**	Drs. Alexey Ustinov and Vladimir Korshun	N/A
5-(Perylen-3-ylmethyloxymethyl)ethynyl-arabino-uridine **(aUY12)**	Drs. Alexey Ustinov and Vladimir Korshun	N/A
5-(Perylen-3-yl)ethynyl-2'-deoxyuridine **(dUY11)**	Drs. Alexey Ustinov and Vladimir Korshun	N/A
Epicatechin **(EC)**	Dr. Eike Steinmann (Twincore, Hannover, Germany)	N/A
Epigallocatechin gallate **(EGCG)**	Sigma-Aldrich (Oakville, ON, Canada)	E4143
Curcumin	Dr. Eike Steinmann	N/A
25-hydroxycholesterol **(25HC)**	Sigma-Aldrich	H1015
Tetrahydrocurcumin **(THC)**	Dr. Eike Steinmann	N/A

Table 2.2. Chemicals

Reagent name	Supplier	Catalog number
Cholesterol	Sigma-Aldrich (Oakville, ON, Canada)	C3045
1,2-dioleoyl-L-α-phosphatidylcholine (DOPC)	Sigma-Aldrich	P6354
Dimethyl sulfoxide (DMSO)	Sigma-Aldrich	D4540
1,6-diphenyl-1,3,5-hexatriene (DPH)	Sigma-Aldrich	D208000
Heparin	Sigma-Aldrich	H3393
L-^{35}S-Methionine	Perkin Elmer (Boston, MA, USA)	NEG009T005MC
N-acetylneuraminic acid (sialic acid)	Sigma-Aldrich	A0812
Octadecyl rhodamine B chloride (R18)	Molecular Probes (Life Technologies Inc., Burlington, ON, Canada)	O-246
β-oleoyl-γ-palmitoyl-L-α-phosphatidylcholine (POPC)	Sigma-Aldrich	P3017

Table 2.3. Cell culture reagents

Reagent name	Supplier	Catalog number
Crystal Violet	Sigma-Aldrich	C3886
Dulbecco's Minimal Eagle Medium (DMEM)	Invitrogen (Life Technologies Inc., Burlington, ON, Canada)	11885
DMEM (phenol red-free)	Invitrogen	11054-001
DMEM (Methionine-free)	Invitrogen	21013-024
Fetal Bovine Serum (FBS)	PAA Laboratories (GE Healthcare, Westborough, MA, USA)	A15-70
Methylcellulose	Sigma-Aldrich	M0387
Penicillin/Streptomycin (10000 U/mL)	Invitrogen	15140-122
Trypsin/EDTA (0.5%)	Invitrogen	15400-054
TPCK-treated trypsin	Sigma-Aldrich	T1426
UltraPure Agarose	Invitrogen	16500-500
UltraPure Low Melting Point Agarose	Invitrogen	16520-050

Table 2.4. Antibodies and immunostaining reagents

Reagent name	Supplier	Catalog number
Mouse IgG anti-HCV core	Thermo Scientific (Rockland, IL, USA)	MA1-080
Mouse IgG anti-HCV core	Enzo Life Sciences (Farmingdale, NY, USA)	ALX-804-277-C100
Mouse IgG anti-CD81	BD Biosciences (Mississauga, ON, Canada)	555675
Biotinylated horse anti-mouse IgG	Vector Laboratories (Burlingame, CA, USA)	BA-2000 (included with PK-4002)
Goat anti-mouse IgG Alexa Fluor 488	Molecular Probes	A-11001
Normal goat serum	Sigma-Aldrich	G9023
Normal horse serum	Vector Laboratories	S-2000 (included with PK-4002)
Bovine serum albumin (BSA)	USA Biochemical Corp. (Cleveland, OH, USA)	70195
VectaStain ABC kit	Vector Laboratories	PK-4002
ImmPACT SG peroxidase substrate	Vector Laboratories	SK-4705

Table 2.5. Molecular biology reagents

Reagent name	Supplier	Catalog number
First-strand buffer	Invitrogen	Included with 28025-013
High pure viral RNA kit	Roche (Laval, QC, Canada)	11858874001
TRIzol	Ambion (Life Technologies Inc., Burlington, ON, Canada)	15596-026
DTT (100 mM)	Invitrogen	Included with 28025-013
dNTP mixture set (100 mM)	Invitrogen	10297-018
RNase out (5000 U)	Invitrogen	10777-019
MinElute gel extraction kit	Qiagen (Qiagen, Mississauga, ON, Canada)	28604
M-MLV RT (40000 U)	Invitrogen	28025-013
Superscript III RT (10000 U)	Invitrogen	18080-044
TaqMan universal PCR master mix	Applied Biosystems (Life Technologies Inc., Burlington, ON, Canada)	4304437
Pfx50 DNA polymerase	Invitrogen	12355-012

Table 2.6. Primers used for PCR

Primer name	Sequence
UniFlu	5′-AGC RAA AGC AGG-3′
PR8HAfwd	5′-GCA GGG GAA AAT AAA AAC AAC-3′
PR8HArev	5′-GGG TGT TTT TCC TCA TAT TTC-3′
AichiHAfwd	5′-CAA AAG CAG GGG ATA ATT CTA-3′
AichiHArev	5′-ACA AGG GTG TTT TTA ATT ACT-3′
HCVfwd	5′-TCT GCG GAA CCG GTG AGT A-3′
HCVrev	5′-GTG TTT CTT TTG GTT TTT CTT TGA GGT TTA GG-3′
HCVprobe	5′-6-FAM-CAC GGT CTA CGA GAC CTC CCG GGG CAC-TAMRA-3′

Table 2.7. PCR amplification conditions

PCR	Cycle number	Thermal conditions
Flu PR8 HA	1	94°C (2 min)
	20	94°C (20 sec), 47°C (30 sec), 68°C (5 min)
	1	68°C (5 min)
	1	4°C (∞)
Flu Aichi HA	1	94°C (2 min)
	20	94°C (20 sec), 45°C (30 sec), 68°C (5 min)
	1	68°C (5 min)
	1	4°C (∞)
HCV qRT-PCR	1	50°C (2 min)
	1	95°C (10 min)
	45	95°C (15 sec), 60°C (1 min)

CHAPTER 3: CHARACTERIZATION OF A SMALL MOLECULE INHIBITOR OF VIRION ATTACHMENT TO HEPARAN SULFATE- OR SIALIC ACID-CONTAINING GLYCANS

Data in this chapter were published in the *Journal of Virology* and in *Hepatology*:

Colpitts, C.C. and Schang, L.M. **(2014)** A small molecule inhibits virion attachment to heparan sulfate- or sialic acid-containing glycans. ***J. Virol.*** doi: 10.1128/JVI.00896-14

Ciesek, S., von Hahn, T., **Colpitts, C.C.**, Schang, L.M., Friesland, M., Steinmann, J., Manns, M.P., Ott, M., Wedermeyer, H., Meuleman, P., Pietschmann, T. and Steinmann, E. **(2011)** The green tea polyphenol epigallocatechin-3-gallate (EGCG) inhibits hepatitis C virus (HCV) entry. ***Hepatology*** *54(6):* 1947-55

I performed all of the experiments described in this chapter. I wrote the J. Virol. manuscript, with editorial contributions from Dr. Schang, and wrote the sections of the Hepatology paper corresponding to my experiments.

3.1 INTRODUCTION

The primary attachment of most human viruses depends on conserved low-affinity interactions between basic binding pockets in the virion glycoproteins and negatively charged heparan sulfate (HS) moieties in cellular glycosaminoglycans (GAGs) (Compton *et al.*, 1993; Conti *et al.*, 1991; Dechecchi *et al.*, 2001; Germi *et al.*, 2002; Leistner *et al.*, 2008; WuDunn and Spear, 1989; Morikawa *et al.*, 2007; Patel *et al.*, 1993; Zhu *et al.*, 1995; Bengali *et al.*, 2009; Byrnes and Griffin, 1998). Attachment of another group of viruses requires similar low-affinity interactions with sialic acid (SA)-containing sialoglycans (SGs) (Gentsch and Pacitti, 1985; Neu *et al.*, 2011; Weis *et al.*, 1988; Nilsson *et al.*, 2008; Reiter *et al.*, 2011). Only a very small group of human viruses binds to neither HS nor SA moieties. The primary low-affinity attachment step most often serves to concentrate virions on the cell surface to facilitate the higher affinity interactions with secondary receptors. For a small group of human viruses, the glycan

moieties are the only known receptors.

Attachment to glycan moieties is therefore conserved among many unrelated viruses. Molecules that interfere with these low-affinity interactions often have antiviral activities. Many such compounds act as receptor mimetics, competing for virion binding to cellular HS or SA moieties (Baba *et al.*, 1988; Aguilar *et al.*, 1999; Lin *et al.*, 2013; Fazli *et al.*, 2001; Matsubara *et al.*, 2010). However, such competitors are restricted to viruses that bind to either HS or SA. No compound has yet been identified that inhibits the attachment of both groups of viruses, precluding the development of truly broad-spectrum small molecule inhibitors of attachment.

Polyphenolic compounds from green tea possess many beneficial properties, including anti-cancer, anti-obesity, anti-atherosclerotic, anti-inflammatory, anti-diabetic, antibacterial and broad antiviral effects (Cabrera *et al.*, 2006). The most abundant of these polyphenols are the green tea catechins, which are predominantly comprised of epicatechin (EC), epigallocatechin (EGC), epicatechin gallate (ECG) and epigallocatechin gallate (EGCG). EGCG is responsible for many of the activities of green tea. For example, EGCG inhibits the attachment of cancer cells to components of the endothelial basement membrane, thereby preventing cancer cell metastasis (Sazuka *et al.*, 1995). EGCG also induces the apoptosis of cancer cells (Chen *et al.*, 1998b) and arrests cell growth by targeting cell regulatory proteins, caspases, transcription factors such as NFκB and many signal transduction pathways (Gupta *et al.*, 2004; Berger *et al.*, 2001). Modulation of these signalling pathways, and inhibition of the activity or expression of lipogenic enzymes, contributes to the anti-adipogenic effects of EGCG (Moon *et al.*,

2007). The effects of EGCG on glucose and lipid metabolism also have anti-diabetic benefits (Wolfram *et al.*, 2006).

Green tea catechins, in particular the gallate derivatives ECG and EGCG, also have antiviral activities. EGCG is the most active of them, with activities against a wide spectrum of viruses, including human immunodeficiency virus (HIV), influenza A (IAV), enterovirus 71 (EV71), adenovirus (AdV), hepatitis B virus (HBV) and clinical isolates of herpes simplex virus type 1 and 2 (HSV-1/-2), among others (Steinmann *et al.*, 2013; Nance *et al.*, 2009; Yamaguchi *et al.*, 2002; Weber *et al.*, 2003; Song *et al.*, 2005; Xu *et al.*, 2008; He *et al.*, 2011; Isaacs *et al.*, 2008; Isaacs *et al.*, 2011; Kim *et al.*, 2013). It may be active against HPV as well, since external genital warts, which are caused by human papillomavirus (HPV), are treatable with a mixture of green tea catechins (Polyphenon E) (Tatti *et al.*, 2010). EGCG has been shown to inhibit the infectivity of a broad range of unrelated enveloped and nonenveloped viruses, including those that bind to HS and to SA. However, the specific antiviral mechanisms of EGCG remain unclear, as do the bases for its broad antiviral spectrum.

EGCG binds to a range of proteins, including virion glycoproteins (Kawai *et al.*, 2003; Isaacs *et al.*, 2008). This binding likely contributes to its ability to inhibit viral entry. EGCG was proposed to interact with the hemagglutinin (HA) envelope glycoprotein of IAV (Nakayama *et al.*, 1993; Song *et al.*, 2005). HA binds to SA terminally linked to a galactose in cell-surface glycans. Modelling studies support the binding of EGCG (and related galloyl analogs) to the SA-binding domain of HA, through hydrogen bonding and σ-π stacking interactions (Ge *et al.*, 2014). EGCG treatment induces aggregation of HSV-1 gB (Isaacs *et al.*, 2008), suggesting an interaction between

EGCG and gB, which binds to HS residues on cellular glycans (Laquerre *et al.*, 1998). Similarly, EGCG treatment aggregates HSV-1 gD, which binds to 3O-sulfated HS (and to herpesvirus entry mediator (HVEM) and nectin) (Isaacs *et al.*, 2008; O'Donnell *et al.*, 2010; Whitbeck *et al.*, 1997; Di Giovine *et al.*, 2011). EGCG inhibits binding of the HIV envelope glycoprotein gp120 to CD4 on cells (Kawai *et al.*, 2003). My hypothesis is that the interactions of EGCG with viral glycoproteins interfere with virion attachment to both HS and SA.

My objectives were to characterize the antiviral mechanisms of EGCG, in order to identify the basis for its broad-spectrum activity. I selected hepatitis C virus (HCV), vesicular stomatitis virus (VSV), Sindbis virus (SINV), vaccinia virus (VACV), HSV-1, adenovirus (AdV), IAV, reovirus (RV) and poliovirus (PV) as model unrelated RNA or DNA viruses. HCV, SIN, VACV, HSV-1 and AdV bind to HS moieties in cellular GAGs (Barth *et al.*, 2003; WuDunn and Spear, 1989), but otherwise differ in their entry pathways, genome composition and genome replication. HCV and SINV are enveloped RNA viruses that fuse within endosomal compartments, whereas VACV and HSV-1 are enveloped DNA viruses that fuse mainly at the plasma membrane. AdV is a nonenveloped DNA virus that is internalized by endocytosis. IAV and RV, on the other hand, bind to a terminal SA linked to galactose on cellular glycans. Both are RNA viruses internalized by endocytotic pathways, but IAV is enveloped and RV is not. Primary attachment of VSV requires electrostatic interactions that likely involve HS or SA, although the specific details are not well characterized (Conti *et al.*, 1991). PV requires neither HS nor SA for entry (Racaniello, 1996). With the exception of PV, all these viruses initially attach to glycan moieties, but otherwise differ in the presence or absence

of an envelope, their secondary receptors, the membranes they fuse to and the fusion mechanisms, their genome compositions (RNA or DNA), replication sites (cytoplasmic or nuclear), replication strategies, and other characteristics. Their collective inhibition by EGCG suggests an antiviral mechanism targeting their common feature of glycan binding during primary attachment.

3.2 RESULTS

3.2.1 EGCG inhibits the infectivity of unrelated viruses that bind HS or SA. I first tested the effects of EGCG **(Figure 3.1)** on the infectivity of enveloped or non-enveloped RNA or DNA viruses (**Figure 3.2**). HCV, SIN, VSV, IAV, RV, PV, HSV-1/-2, VACV, mCMV or AdV virions (~200 pfu) were exposed to EGCG or DMSO vehicle in DMEM (pH 7.2) for 10 minutes at 37°C prior to infecting monolayers of susceptible cells. Inocula were removed 1 hour later and the monolayers were overlaid with appropriate semi-solid or liquid medium. Infected cells were incubated at 37°C in 5% CO_2 until well-defined plaques developed (VSV, SIN, RV, PV, IAV, HSV-1/-2 and VACV). Alternatively, foci of infected cells were identified by immunocytochemistry after 72 hours (HCV), or LacZ or GFP expression after 24 hours (for mCMV or AdV, respectively).

EGCG inhibited the infectivity of HCV, SIN, VSV, four IAV strains (H1N1 or H3N2), RV, HSV-1, HSV-2, mCMV, two VACV strains (WR and IHD-W) and AdV at low micromolar concentrations (EC_{50}, 1.7, 8.1, 1.8, 3.9-20.3, 3.8, 0.3, 1.0, 1.7, 2.7-4.1 and 9.3 μM, respectively) (**Figure 3.2A and 3.2B**). In contrast, EGCG did not inhibit the infectivity of PV, which does not bind to HS or SA, even at 200 μM (**Figure 3.2C**). EGCG inhibited the infectivity of all the HS- or SA-binding viruses that were tested, at similar low micromolar concentrations.

We next tested epicatechin (EC) (**Figure 3.1**), a catechin chemically related to EGCG but lacking the gallate moiety, against selected unrelated enveloped RNA and DNA viruses. In contrast to EGCG, EC did not inhibit the infectivity of HCV, VSV, HSV-1, mCMV or IAV (PR8) at concentrations up to 200 μM **(Figure 3.2D)**. These

findings highlight the importance of the gallate moiety or its hydroxyl groups for the antiviral effects of EGCG.

3.2.2 EGCG acts directly on virions. Based on previous literature, the inhibitory effect of EGCG could result from effects on the target cells, rather than direct effects on the virions. To test this model, time-of-addition assays were performed using VSV and HSV-1. Cells were treated with EGCG or DMSO vehicle prior to infecting them with VSV or HSV-1 virions. Alternatively, cells were first infected with VSV or HSV-1 virions, and then exposed to EGCG or DMSO vehicle for either 4 hours or 48 hours. EGCG did not inhibit VSV or HSV-1 plaquing under any of these conditions (**Figure 3.3A and 3.3B**). To test for the possibility that EGCG may act on cellular factors exposed only when virions are added, a dilution assay was used. VSV or HSV-1 virions were treated with EGCG and then diluted 10-fold prior to infecting cells, such that the cells were exposed to 10-fold lower concentrations of EGCG than the virions. This dilution did not affect the inhibitory activity of EGCG, further supporting the conclusion that EGCG acts directly on the virions (**Figure 3.3C**).

3.2.3 EGCG does not disrupt membranes. EGCG inhibited the infectivity of all enveloped viruses we tested (as well as the non-enveloped adenovirus and reovirus). EGCG can undergo chemical changes such as oxidation and dimerization in solution *(Sang 2005)*. One possibility, therefore, is that EGCG or its reaction products could disrupt the integrity of virion envelopes. To test for envelope lysis, VSV, HCV or IAV virions labeled at self-quenching concentrations with R18 were exposed for 10 minutes at 37°C to EGCG or DMSO vehicle in DMEM (pH 7.2). EGCG did not induce the increase in R18 fluorescence that would result from dequenching if the envelopes were disrupted.

In contrast, and as expected, 0.1% Triton X-100 (which lyses the envelopes) did increase the R18 fluorescence (**Figure 3.4A**).

EGCG did not disrupt cellular membranes at relevant antiviral concentrations, either. Defibrinated rabbit erythrocytes were exposed to EGCG or vehicle and incubated for 90 minutes. At 0, 30, 60 and 90 minutes, aliquots were removed and the absorbance of haemoglobin in the supernatant was measured. Only the highest concentration of EGCG (500 μM) for longer than 30 minutes induced the increase in haemoglobin absorbance that results from leakage through disrupted erythrocyte membranes **(Figure 3.4B)**.

3.2.4 EGCG does not affect membrane fluidity. Another possibility was that EGCG might modulate the fluidity of virion envelopes, which is critical for virion infectivity (Harada, 2005). The DPH fluorescence polarization assay was used to test envelope fluidity (Anggakusuma *et al.*, 2013; Shinitzky and Inbar, 1976). In this assay, decreases in membrane fluidity increase the polarization of DPH fluorescence. DPH-labelled liposomes or HCV virions were treated with EGCG or cholesterol for 10 minutes at 37°C. In contrast to cholesterol, which decreases membrane fluidity and was therefore used as a control, EGCG did not induce any increase in DPH polarization. Therefore, EGCG has no major effects on membrane fluidity (**Figure 3.5**).

3.2.5 EGCG interacts with VSV, HSV-1, RV and AdV surface proteins. I next tested whether EGCG interacted with the surface proteins of VSV, HSV-1, RV or AdV. I obtained the fluorescence spectra of virions in the absence and presence of EGCG, using a wavelength of 280 nm to excite the tryptophan residues (including those in the virion surface proteins). The fluorescence intensity of the virions was quenched upon addition

of EGCG (**Figure 3.6**), indicating an interaction between EGCG and tryptophan residues in virion surface proteins.

3.2.6 EGCG inhibits attachment of HCV, HSV-1, VACV, VSV and IAV to cells. One of the critical functions of virion surface proteins is attachment to cellular receptors. We therefore tested whether the interaction of EGCG with the virion surface proteins interfered with the primary attachment of virions to cells. To test this model, R18-labeled VSV, IAV, HCV, HSV-1 or VACV virions pre-exposed to EGCG or DMSO vehicle in DMEM at pH 7.2 were adsorbed onto Vero (VSV, HSV-1, VACV), MDCK (IAV) or Huh7.5 (HCV) cell monolayers at 4°C, to allow binding but not fusion. EGCG inhibited the attachment of HS-binding viruses HCV, VSV, HSV-1 and VACV to their target cells (EC_{50}, 44.1 μM, 17.6 μM, 5.7 μM and 28.8 μM, respectively) (**Figure 3.7A**). EGCG also inhibited the attachment of SA-binding IAV (EC_{50}, 78.4 μM) **(Figure 3.7B)**.

R18 attachment assays had not been used before. We therefore validated these assays by testing the effects of EGCG on binding using conventional attachment assays with ^{35}S-methionine labeled virions. ^{35}S-methionine-labeled VSV and HSV-1 virions pre-exposed to EGCG or DMSO were adsorbed onto Vero cells at 4°C. EGCG inhibited binding of ^{35}S-labelled HCV, VSV and HSV-1 to cells to a similar extent as the heparin control (EC_{50}, 29.7 μM, 29.6 μM and 10.2 μM, respectively) (**Figure 3.7C**). We also used the ^{35}S-methionine binding assay to test nonenveloped viruses. EGCG inhibited the attachment of HS-binding AdV and SA-binding RV (EC_{50}, 10.1 μM and 331.4 μM, respectively) (**Figure 3.7A and 3.7B**). In contrast, EGCG actually enhanced PV binding (~110% compared to the vehicle control) at concentrations up to 200 μM (**Figure 3.7D**).

Only at the highest concentration was PV binding inhibited, and then by only 25% (**Figure 3.7D**).

Most unexpectedly, therefore, EGCG inhibited the attachment of virions that bind to either HS (HSV-1, HCV, VSV, VACV, AdV) or SA (IAV, RV). EGCG is thus the first example of a small molecule that inhibits attachment of HS- and SA-binding viruses.

3.2.7 EGCG does not directly inhibit HCV, IAV or VSV fusion. If EGCG inhibits attachment, then it should also inhibit fusion, which occurs after attachment. I first tested fusion of IAV and VSV, which are triggered by low pH to fuse to endosomal membranes after clathrin-mediated endocytosis. These three viruses represent different classes of fusion proteins. Virions labelled with self-quenching concentrations of R18 were exposed to EGCG or DMSO vehicle in phenol red-free DMEM at pH 7.2 prior to mixing with MDCK (IAV) or Vero (VSV) cells. Fluorescence was dequenched by approximately 10% for virions treated with DMSO vehicle, but dequenching was inhibited to background levels when virions were treated with EGCG prior to adding them to cells (**Figure 3.8**). These results could indicate that EGCG inhibits fusion as well as attachment. Therefore, we next tested whether EGCG directly inhibited fusion itself, independently of its effects on virion attachment. Virions were first allowed to attach to cells at 4°C prior to treatment with EGCG. Under these conditions, EGCG did not inhibit fusion (**Figure 3.8**), in contrast to compounds that inhibit fusion directly (**Chapter 4***,* Colpitts *et al.*, 2013). The effects of EGCG on entry, therefore, are at a step prior to fusion, such as binding.

I developed a fluorescence dequenching assays to test fusion between HCV JFH-1 virions and Huh7.5 cells. I first tested whether the requirements for HCV fusion matched the requirements for HCV infectivity. HCV JFH-1 virions labeled at self-quenching

concentrations of R18 were mixed with Huh7.5 cells. Fusion was triggered by low pH, with optimal fusion expectedly occurring at pH 5 (**Figure 3.9A**). Furthermore, HCV fused to Huh7.5 cells but not to Vero cells (**Figure 3.9B**). Finally, I tested whether fusion required CD81, one of the known receptors for HCV. Huh7.5 cells were either pre-treated with an anti-CD81 monoclonal antibody, or treated with the antibody after HCV virion attachment. Fusion was inhibited only when cells were treated with the CD81 antibody after attachment **(Figure 3.9C)**, which is consistent with the involvement of CD81 in post-binding entry steps (Bertaux and Dragic, 2006; Farquhar *et al.*, 2012). Therefore, the requirements for fusion in our assay match the known requirements for HCV infectivity, which validates its use to test HCV fusion. I used the assay to test whether EGCG inhibited the fusion of HCV. R18-labelled HCV JFH-1 virions were exposed to EGCG or DMSO vehicle prior to mixing with Huh7.5 cells. Fluorescence was dequenched by approximately 18% for HCV virions treated with DMSO vehicle, but by less than 5% for HCV virions treated with EGCG (**Figure 3.9D**).

3.2.8 EGCG competes with heparin for virion binding. The primary, low-affinity attachment of many viruses, including all those we found to be inhibited by EGCG, is to HS or SA moieties in cellular glycans. We proposed as a model that EGCG might, most unexpectedly, compete with both HS and SA moieties for virion binding. To test this model, we first used heparin affinity chromatography. R18-labelled HSV-1 (10^5 pfu) or unlabeled HCV (10^5 ffu) was loaded onto a heparin column. The column was then washed to remove unbound virions. Bound virions were eluted with equivalent concentrations of soluble heparin, SA, EGCG or EC. The eluted virions were detected by R18 fluorescence (HSV-1) or RNA (HCV). EGCG eluted the HSV-1 virions from the

heparin column very much like the heparin control. Approximately 75% of bound virions were eluted by 0.5 mg/mL EGCG or heparin, and 50% by 0.05 mg/mL (**Figure 3.10A**). In contrast, neither sialic acid nor the inactive catechin EC (at 0.5 mg/mL) eluted the HSV-1 virions (**Figure 3.10A**). EGCG (0.5 mg/mL) also eluted HCV virions bound to the heparin column, as did heparin (**Figure 3.10B**), whereas neither sialic acid nor EC did (**Figure 3.10B**).

3.2.9 EGCG competes with sialic acid to inhibit hemagglutination. The binding of IAV hemagglutinin to sialic acid agglutinates red blood cells. If EGCG inhibits IAV binding to sialic acid moieties in cellular glycans, then it should inhibit hemagglutination. We exposed IAV virions (H1N1 and H3N2 strains) to 100 μM (50 μg/mL) EGCG or EC, 50 μg/mL heparin or equivalent volume of DMSO in DMEM for 15 minutes at 37°C. The treated virions were then tested for their ability to hemagglutinate chicken erythrocytes. Treatment with EGCG inhibited hemagglutination by all four IAV strains by four-fold (**Table 3.1, Figure 3.11**). As expected, treatment with heparin or EC had no effects on hemagglutation (**Table 3.1, Figure 3.11**). Treatment with monomeric sialic acid only partially inhibited hemagglutination, as expected (Fazli *et al.*, 2001; Matrosovich and Klenk, 2003; Sun, 2007; Matsubara *et al.*, 2010; Reuter *et al.*, 1999), and not to the same extent as EGCG (**Figure 3.11**).

3.2.10 EGCG treatment selects for resistant IAV variants with mutations in HA. IAV PR8 (H1N1) and Aichi (H3N2) were serially passaged in the presence of increasing concentrations of EGCG. For both strains, viral titers recovered fully (to vehicle-treated control levels) after 5 passages **(Tables 3.2 and 3.3, Figure 3.12)**. Resistant variants from passage 6 were plaque-purified. To identify mutations conferring resistance, the HA

gene was PCR-amplified and sequenced. For IAV PR8, the T434I substitution was conserved in all EGCG-resistant sequences **(Figure 3.13A)**. For IAV Aichi, the R453G substitution was conserved in all EGCG-resistant sequences **(Figure 3.13B)**. Interestingly, these are both non-conservative mutations from polar or charged amino acids to hydrophobic amino acids. Examination of HA crystal structures (PR8, protein data bank 1RU7; Aichi, protein data bank 3VUN) in the pre-fusion neutral pH conformation (Gamblin *et al.*, 2004), showed that both of these mutations map to the HA2 stalk domain of HA **(Figure 3.14A and 3.14B)**.

3.2.11 Other galloylated esters inhibit viral infectivity by similar mechanisms. Based on our observations that the gallate moiety is necessary for antiviral activity, I next tested four alkyl gallates and a pentahydroxy gallate compound. Alkyl gallate derivatives ethyl gallate (EG), propyl gallate (PG), octyl gallate (OG) and lauryl gallate (LG) **(Figure 3.1)** inhibited the infectivity of HCV, VSV, HSV-1 and IAV, when virions were pre-exposed for 10 minutes at 37°C. Potency depended on alkyl chain length. For HCV, the EC_{50} were 2.6, 50.5, 12.3, 0.8 and 0.8 μM for EGCG, EG, PG, OG and LG, respectively. For VSV, the EC_{50} were 3.3, 132.6, 121.8, 6.8 and 2.8 μM for EGCG, EG, PG, OG and LG, respectively. For HSV-1, EC_{50} were 0.1, 119.4, 146.8, 1.0 and 0.9 μM for EGCG, EG, PG, OG and LG, respectively. For IAV, the EC_{50} were 9.0, 20.5, 41.5, 0.8 and 4.1 μM for EGCG, EG, PG, OG and LG, respectively **(Table 3.4, Figure 3.15A)**. Pentagalloyl glucose (PGG), the pentahydroxy gallic acid ester of glucose **(Figure 3.1)**, inhibited the infectivity of HCV (EC_{50}, 0.05 μM) at ~30-fold lower concentrations than EGCG (EC_{50}, 1.7 μM), greater than any of the alkyl gallate derivatives **(Table 3.4, Figure 3.15B)**.

The alkyl gallates inhibited HCV binding, with IC_{50} of 570 (EG), 550 (PG), 1.2 (OG) and 1.2 (LG) μM, compared to 41.7 μM for EGCG **(Figure 3.16A)**. The pentagalloylated PGG inhibited binding most potently, with an EC_{50} of 0.1 μM **(Figure 3.16B)**. PGG inhibits HCV fusion when virions are pre-treated **(Figure 3.16C)**, which is consistent with our findings for EGCG **(Figure 3.8A)**.

3.3 DISCUSSION

EGCG was already known to inhibit the infectivity of many unrelated viruses, including important human pathogens (Yamaguchi *et al.*, 2002; Weber *et al.*, 2003; Nance *et al.*, 2009; Song *et al.*, 2005; Xu *et al.*, 2008; Isaacs *et al.*, 2008; Calland *et al.*, 2012; Chang *et al.*, 2003; He *et al.*, 2011; Ho *et al.*, 2009; Kim *et al.*, 2013) **(Table 3.4)**. I tested additional viruses, including HCV and VACV. I also showed that EGCG acts directly on the virions to inhibit their entry into cells (Ciesek *et al.*, 2011; Colpitts and Schang, 2014). EGCG has no obvious effects on membrane integrity or fluidity. It does, however, interact with virion surface proteins to inhibit virion attachment, but not post-binding steps such as fusion. EGCG inhibited the attachment of several unrelated enveloped or nonenveloped DNA or RNA viruses that bind to either HS or SA (HCV, VSV, HSV-1, VACV, AdV, IAV and RV). Although these viruses differ in their secondary receptors, internalization pathways, sites and mechanisms of fusion, genome composition, replication strategies and replication sites, they do have in common their primary attachment to modified saccharide moieties in cellular glycans.

The primary attachment of many unrelated viruses (including HCV, HSV-1 and others we tested) is to HS moieties in cellular glycans. Another group of viruses, including IAV, RV, rotavirus, enteroviruses and Sendai virus, depend on binding to SA-containing glycans (Weis *et al.*, 1988; Nilsson *et al.*, 2008; Nokhbeh *et al.*, 2005; Isa *et al.*, 2006; Gentsch and Pacitti, 1985; Reiter *et al.*, 2011; Villar and Barroso, 2006; Scott *et al.*, 2005). Treatment with heparin or related molecules inhibits the attachment of viruses that bind to HS moieties, such as HCV and HSV-1 (Lin *et al.*, 2013; Barth *et al.*, 2003; WuDunn and Spear, 1989). Treatment with sialylmimetics inhibits the attachment

of viruses that bind to SA moieties, such as IAV (Matrosovich and Klenk, 2003). Many such receptor mimetics with antiviral properties have been described. For example, heparin and other sulfated polysaccharides and polysulfonated compounds inhibit the adsorption of viruses that bind to HS moieties (Baba *et al.*, 1988; Aguilar *et al.*, 1999; Lin *et al.*, 2013). Sialylmimetics inhibit the adsorption of IAV and other viruses that bind SA (Fazli *et al.*, 2001; Matrosovich and Klenk, 2003; Sun, 2007; Matsubara *et al.*, 2010; Reuter *et al.*, 1999). Such compounds act as receptor mimics, competing with cellular HS or SA moieties for virion binding. However, the different binding specificities of the two groups of viruses has so far precluded the development of broad-spectrum primary attachment inhibitors active against viruses that bind to HS and those that bind to SA.

EGCG, however, uniquely inhibits the primary attachment of both types of viruses. EGCG (but not SA) competed with heparin for HSV-1 and HCV virion binding, as shown by heparin column chromatography. EGCG (but not heparin) inhibited IAV hemagglutination, which requires interaction of IAV HA with SA residues on erythrocytes (Haff and Stewart, 1965). In contrast, EGCG did not inhibit the infectivity of PV, which does not require binding to HS or SA moieties (Racaniello, 1996). These findings support our model that EGCG unexpectedly competes with both HS and SA moieties for virion binding. EGCG is the first example of a small molecule that similarly inhibits the attachment of viruses that bind to HS and to SA.

EGCG has been reported to inhibit the infectivity of many unrelated viruses, including the HS-binding HIV, AdV, HBV, HSV-1/-2 and HCV, and the SA-binding IAV and enterovirus 71. The specific antiviral mechanisms of EGCG have been unclear, and different mechanisms have even been proposed for different viruses (reviewed by

Steinmann, 2013*)*. Most of the previously reported activities of EGCG, however, are consistent with the mechanism proposed here. EGCG was shown to be a strong inhibitor of HIV replication (Fassina *et al.*, 2002; Vives *et al.*, 2005), although the mechanisms were not identified. EGCG was later shown to inhibit recombinant gp120 binding to $CD4^+$ T cells (Kawai *et al.*, 2003). Yamaguchi *et al* (2002) also observed that EGCG inhibited HIV-1 binding to cells, although at 100 μM or higher concentrations (Yamaguchi *et al.*, 2002). Specific effects of EGCG on HIV-1 gp120 binding to cellular HS were not tested. EGCG was shown to interact with the HSV-1 glycoproteins gB and gD to inhibit viral infectivity (Isaacs *et al.*, 2008). Interestingly, gB interacts with HS and gD with 3O-sulfated HS (Herold *et al.*, 1991; O'Donnell *et al.*, 2010). The effects of EGCG on gC, which also binds to HS (Herold *et al.*, 1991), were not investigated.

The activity of EGCG against IAV, a SA-binding virus, has been described in several publications. EGCG inhibited the infectivity of influenza A and B viruses to MDCK cells (Nakayama *et al.*, 1993). EGCG prevented influenza virions from adsorbing to MDCK cells and inhibited haemagglutination (Nakayama *et al.*, 1993; Song *et al.*, 2005), as we confirmed. EGCG was shown to directly inhibit neuraminidase and viral RNA synthesis (Song *et al.*, 2005), as well as to agglutinate virions (Nakayama *et al.*, 1993), but only at millimolar concentrations, far higher than the concentrations required to inhibit virion binding. Recently, EGCG was proposed to interfere with IAV fusion, but not adsorption or hemagglutination, by affecting the integrity of the viral envelope (Kim *et al.*, 2013). In these experiments, IAV virions were not pre-treated with EGCG, which is necessary for inhibition of binding and hemagglutination *(our data,* Song *et al.*, 2005). Moreover, in contrast to Kim *et al*, we did not observe any major effects of EGCG on

IAV fusion (when virions were treated after attachment) or IAV envelope integrity at the concentrations required to inhibit infectivity and binding (**Figure 3.4**).

EGCG was also active against nonenveloped viruses, through apparently similar mechanisms. EGCG inhibited AdV infection by targeting multiple steps of the viral replication cycle. A direct inhibition of the virion particles, by unknown mechanisms, was observed (Weber *et al.*, 2003). It may well be that EGCG interacts with AdV fiber protein to inhibit its binding to cellular GAGs (Dechecchi *et al.*, 2000). EGCG also inhibited the infectivity of rotavirus and enteroviruses, which was attributed to interference with virion adsorption to cells (Mukoyama *et al.*, 1991). Rotavirus and enteroviruses bind to SA-containing glycans, although the specific mechanisms were not tested. These activities are consistent with our proposed mechanism for EGCG, although of course other mechanisms are also possible for other viruses.

Isaacs et al. (2011) tested EGCG (mostly as a control for several oxidative dimerization products of EGCG) against a panel of enveloped and nonenveloped viruses (Isaacs *et al.*, 2011). EGCG was active against the HS-binding respiratory syncytial virus and Semliki Forest virus, but not against PV (which does not bind heparan sulfate or sialic acid), consistent with our results. In those experiments, EGCG failed to inhibit infectivity of measles virus, coxsackie A9 virus, coxsackie B4 virus and echovirus 6 (Isaacs *et al.*, 2011). Although many of these viruses are thought to bind to HS, this binding is actually strain dependent. Some strains of these viruses require HS for binding and some do not (Goodfellow *et al.*, 2001; McLeish *et al.*, 2012; Feldman *et al.*, 2000; Terao-Muto *et al.*, 2008). Isaacs et al. did not specify which strains were tested. Surprisingly, Isaacs et al reported that EGCG was not active against VSV at pH 7.4

(Isaacs *et al.*, 2011). In contrast, we found that EGCG inhibits VSV infectivity (**Figure 3.2**; EC_{50}, 3.3 μM) and attachment (**Figure 3.6A and 3.6B**; EC_{50}, 3.0 μM and 19.6 μM, respectively), and prevents fusion (**Figure 3.7C**). Differences in experimental conditions (buffer, time of incubation) may explain these apparent discrepancies. The experiments described by Isaacs et al. were performed in phosphate-buffered saline at pH 8.0 (Isaacs *et al.*, 2011), whereas we used DMEM at pH ~7.2. The pH may well affect the ionization of the hydroxyl groups in EGCG and affect its activity, and the different cations can help form or disrupt polar interactions.

There are several possible mechanisms whereby EGCG may inhibit the attachment of viruses that bind to either HS or SA. A moiety of EGCG may resemble HS, whereas another may resemble SA-linked galactose. However, this simple mechanism appears unlikely. The catechins EC and epigallocatechin (EGC), which together contain two of the three moieties of EGCG, did not inhibit the infectivity of either HS- or SA-binding virions (our data; Song *et al.*, 2005; Ciesek *et al.*, 2011; Isaacs *et al.*, 2008). On the other hand, epicatechin gallate (ECG) has a similar overall shape and polarity distribution as EGCG, and has similar activity to EGCG against many viruses (Isaacs *et al.*, 2008; Song *et al.*, 2005). Another possibility is that EGCG may be able to interact with basic or polar residues in the binding pockets of both HS- and SA-binding virion glycoproteins. Consistently, modelling studies demonstrated that EGCG fits into the SA-binding pocket of IAV HA, through similar interactions as SA itself (Ge *et al.*, 2014).

IAV PR8 (H1N1) and Aichi (H3N2) variants that were resistant to EGCG had mutations in the stalk domain of HA2. The mutations were non-conservative; T434I in the case of PR8, and R453G in the case of Aichi. The amino acids differ in their polarity,

charge and size. These mutations could destabilize or disrupt intra- and inter-subunit contacts by preventing hydrogen bonding or salt bridge interactions, thereby altering the overall HA structure. The mutation of Thr-434 to Ile-434 in the stalk could disrupt the alignment of the helix, causing subtle rearrangements in the receptor binding domains of HA. Arg-453 is close enough to form salt bridges with either Glu or Asp from the neighbouring monomer, thereby helping to hold the monomers together. Mutation of Arg-453 to Gly-453 would prevent formation of the salt bridges and could weaken the overall interaction between monomers, which may disrupt the HA trimer formation and alter the alignment of receptor binding domains. Alternatively, Thr-434 and Arg-453 (but not Ile or Gly) would be able to directly interact with EGCG by hydrogen bonding, suggesting that EGCG could bind to the HA2 region, possibly to induce structural rearrangements that disrupt binding. This possibility, however, is unlikely given that neither amino acid is surface-exposed.

Notably, EGCG and epicatechin gallate (ECG) have a similar spectrum of antiviral activity, whereas epicatechin (EC) and epigallocatechin (EGC) are inactive. Furthermore, alkyl gallate derivatives have been shown to inhibit the absorption of unrelated viruses (Yamasaki *et al.*, 2007; Uozaki *et al.*, 2007; Kratz *et al.*, 2008a; Kratz *et al.*, 2008b; Hurtado *et al.*, 2008). Even methyl gallate (MG) showed some activity against HSV-1. Structure-activity studies showed that the three hydroxyl groups on the galloyl moiety were required for the antiviral activity, and the size of the alkyl ester was also important for activity (Kane *et al.*, 1988). It was proposed that MG interacted with virion proteins to interfere with viral adsorption (Kane *et al.*, 1988). Gallic acid and pentyl gallate inhibited the infectivity of HSV-1/-2 and, to some extent, HIV (Kratz *et al.*,

2008a; Kratz *et al.*, 2008b). Octyl gallate and lauryl gallate were active against DNA and RNA viruses, although the mechanisms were not characterized (Yamasaki *et al.*, 2007; Uozaki *et al.*, 2007).

I therefore tested four alkyl gallate derivatives against HCV, IAV, VSV and HSV-1: ethyl gallate, propyl gallate, octyl gallate and lauryl gallate. EGCG and the longer chain derivatives were the most potent. These results suggest a model in which the gallate moiety is necessary for activity but the adjoining moiety is also important for potency. Consistent with this model, a pentahydroxy gallic acid ester (pentagalloylglucose, PGG) was the most potent of the gallate derivatives that I have tested to date. Similarly to EGCG, the alkyl gallate derivatives and PGG inhibited the binding of HCV to cells.

The activities of PGG against IAV and HBV were previously reported (Liu *et al.*, 2011; Lee *et al.*, 2006b). In the case of HBV, the mechanisms of PGG were not identified. However, PGG inhibited IAV infection by interacting with HA, likely to prevent virion binding (Liu *et al.*, 2011). PGG, EGCG and other analogs that differ in their galloyl substituents also inhibited IAV-mediated hemagglutination, IAV infectivity, and IAV entry into cells (Ge *et al.*, 2014), consistent with our findings. Interestingly, analogs with four or more galloyl substituents were most potent. Modelling studies suggested that PGG and its analogs (including EGCG) bind to the receptor-binding globular domain of IAV HA (Ge *et al.*, 2014). The ability to bind and link multiple HA monomers was important for the activity of the galloyl analogs (Ge *et al.*, 2014).

EGCG has been chemically modified to enhance its pharmacological and antiviral properties. EGCG modified with fatty acids, for example, could be formulated in lipophilic preparations. Such modifications may also improve its antiviral potency.

Palmitoyl-EGCG inhibited HSV-1 infectivity more potently than unmodified EGCG, and also blocked virion attachment to cells (de Oliveira *et al.*, 2013). Fatty acid monoester derivatives of EGCG inhibited IAV infectivity with 24-fold increased potency (for EGCG-monopalmitate) (Mori *et al.*, 2008). However, the specific antiviral mechanisms of lipid-modified EGCG derivatives were not tested.

Digallate and monogallate EGCG dimers also showed increased antiviral activity, with the digallate derivatives being most potent (Isaacs *et al.*, 2011). The EGCG dimers inhibited the infectivity of a broad panel of enveloped and nonenveloped viruses that bind to HS or SA, although their specific effects on binding were not evaluated. Interestingly, theaflavin (a monogallate EGCG dimer) and its derivatives inhibited HIV entry by targeting gp41 (Liu *et al.*, 2005). Theaflavin may interfere with the binding of gp41 to HS moieties (Cladera *et al.*, 2001), consistent with our proposed model for the mechanism of EGCG.

EGCG, like other green tea polyphenols, is unstable in aqueous solutions, poorly absorbed, and undergoes metabolic alterations such as oxidation (Smith, 2011). The serum concentration obtained after oral ingestion of pure EGCG (2 mg/kg in 100 mL of water, which is approximately the equivalent of two cups of green tea) was 0.17 μM (Lee *et al.*, 2002), below the antiviral EC_{50} for most viruses. Although EGCG itself is therefore not likely to become a clinical antiviral drug, our findings show that it is indeed possible for a single small molecule to have broad-spectrum activity against virion attachment. Furthermore, other gallate derivatives had similar activities as EGCG. Other molecules with appropriate shape and polarity distribution (but improved pharmacological

properties) may be designed to inhibit the attachment of unrelated viruses that bind to either HS or SA moieties.

In conclusion, EGCG and other gallate derivatives inhibit the infectivity of many unrelated viruses, including important human pathogens. EGCG block the primary low-affinity attachment of unrelated virions to cells, including those that bind to HS and those that bind to terminal SA in glycans. Our results show that EGCG competes with HS or SA moieties in cellular glycans for virion binding. In summary, we provide the first proof-of-principle that a single small molecule can inhibit binding of both types of viruses. This most unexpected finding opens the possibility for the development of small molecule compounds with broad-spectrum activity against viral attachment.

Table 3.1. EGCG inhibits hemagglutination by IAV. Hemagglutination titers for IAV virions (PR8, USSR, Aichi and PC) exposed to 50 μg/mL (~100 μM) EGCG or EC, 50 μg/mL heparin or equivalent volume of DMSO for 15 minutes at 37°C.

	A/PR8		**A/USSR**		**A/Aichi**		**A/PC**	
	Titer	Ratio*	Titer	Ratio*	Titer	Ratio*	Titer	Ratio*
DMSO	6400	1	3200	1	16000	1	16	1
EGCG	1600	1/4	800	1/4	4000	1/4	4	1/4
EC	6400	1	3200	1	16000	1	16	1
Heparin	6400	1	3200	1	16000	1	16	1
Sialic acid	3200	1/2	3200	1	16000	1	8	1/2

*$\text{Titer}_{(\text{compound})}/\text{titer}_{(\text{DMSO})}$

Table 3.2. IAV PR8 [H1N1] titers recovered under EGCG selection. Influenza PR8 was passaged in the presence of DMSO vehicle (**A**) or EGCG (**B**) and harvested at full cytopathic effect. Viral titers were evaluated by plaque assay.

(A)

Passage number	MOI (pfu/cell)	[Cpd] (µM)	[DMSO] (%, vol/vol)	Viral titer (PFU/10^6 cells)	Ratio of titer (DMSO/DMSO)
1	0.01	-	0.12	2.09×10^7	1
2	0.01	-	0.12	2.39×10^7	1
3	0.01	-	0.12	5.21×10^6	1
4	0.01	-	0.12	1.38×10^6	1
5	0.01	-	0.12	7.42×10^6	1
6	0.01	-	0.12	2.50×10^7	1

(B)

Passage number	MOI (pfu/cell)	[EGCG] (µM)	[DMSO] (%, vol/vol)	Viral titer (PFU/10^6 cells)	Ratio of titer (EGCG/DMSO)
1	0.1	3	0.12	2.84×10^6	1.4×10^{-1}
2	0.1	13.5	0.12	7.83×10^5	3.3×10^{-2}
3	0.1	40	0.12	8.50×10^3	1.6×10^{-3}
4	0.001	40	0.12	1.31×10^6	9.5×10^{-1}
5	0.1	120	0.12	2.13×10^7	2.9×10^0
6	0.1	120	0.12	1.25×10^7	1.6×10^0

Table 3.3. IAV Aichi [H3N2] titers recovered under EGCG selection. Influenza Aichi was passaged in the presence of DMSO vehicle (**A**) or EGCG (**B**) and harvested at full cytopathic effect. Viral titers were evaluated by plaque assay.

(A)

Passage number	MOI (pfu/cell)	[Cpd] (µM)	[DMSO] (%, vol/vol)	Viral titer (PFU/10^6 cells)	Ratio of titer (DMSO/DMSO)
1	0.01	-	0.12	1.15×10^6	1
2	0.01	-	0.12	1.30×10^7	1
3	0.001	-	0.12	4.00×10^7	1
4	0.001	-	0.12	8.89×10^7	1
5	0.01	-	0.12	6.83×10^7	1
6	0.1	-	0.12	2.08×10^8	1

(B)

Passage number	MOI (pfu/cell)	[EGCG] (µM)	[DMSO] (%, vol/vol)	Viral titer (PFU/10^6 cells)	Ratio of titer (EGCG/DMSO)
1	0.01	40	0.12	1.38×10^6	1.2×10^0
2	0.01	80	0.12	6.09×10^7	4.7×10^0
3	0.001	600	0.12	5.67×10^2	1.4×10^{-5}
4	0.001	80	0.12	4.44×10^5	5.0×10^{-3}
5	0.01	80	0.12	8.17×10^7	1.2×10^0
6	0.1	120	0.12	1.63×10^8	7.8×10^{-1}

Table 3.4. EC_{50} of EGCG and other galloylated esters against unrelated viruses. Numbers that are italicized and bolded were published elsewhere. EGCG: HBV (Xu *et al.*, 2008; He *et al.*, 2011), HIV-1 (Yamaguchi *et al.*, 2002; Nance *et al.*, 2009), EV71 (Ho *et al.*, 2009); PGG: HBV (Lee *et al.*, 2006b), IAV (Liu *et al.*, 2011).

	EC_{50}, μM					
Virus	**EGCG**	**PGG**	**EG**	**PG**	**OG**	**LG**
HCV	1.7	0.05	50.5	12.3	0.8	0.8
SIN	8.1					
VSV	1.8		133	122	6.8	2.8
HSV-1	0.3		119	147	1.0	0.9
HSV-2	1.0					
mCMV	1.7					
VACV (WR)	4.1					
VACV (IHDw)	2.7					
AdV	9.3					
HBV	***25-50***	***1.1***				
HIV-1	***10-100***					
IAV (PR8)	9.6	***0.4***	20.5	41.5	0.8	4.1
IAV (USSR)	3.9					
IAV (Aichi)	5.3					
IAV (PC)	20.3					
RV	3.8					
EV71	***10***					
PV	> 200					

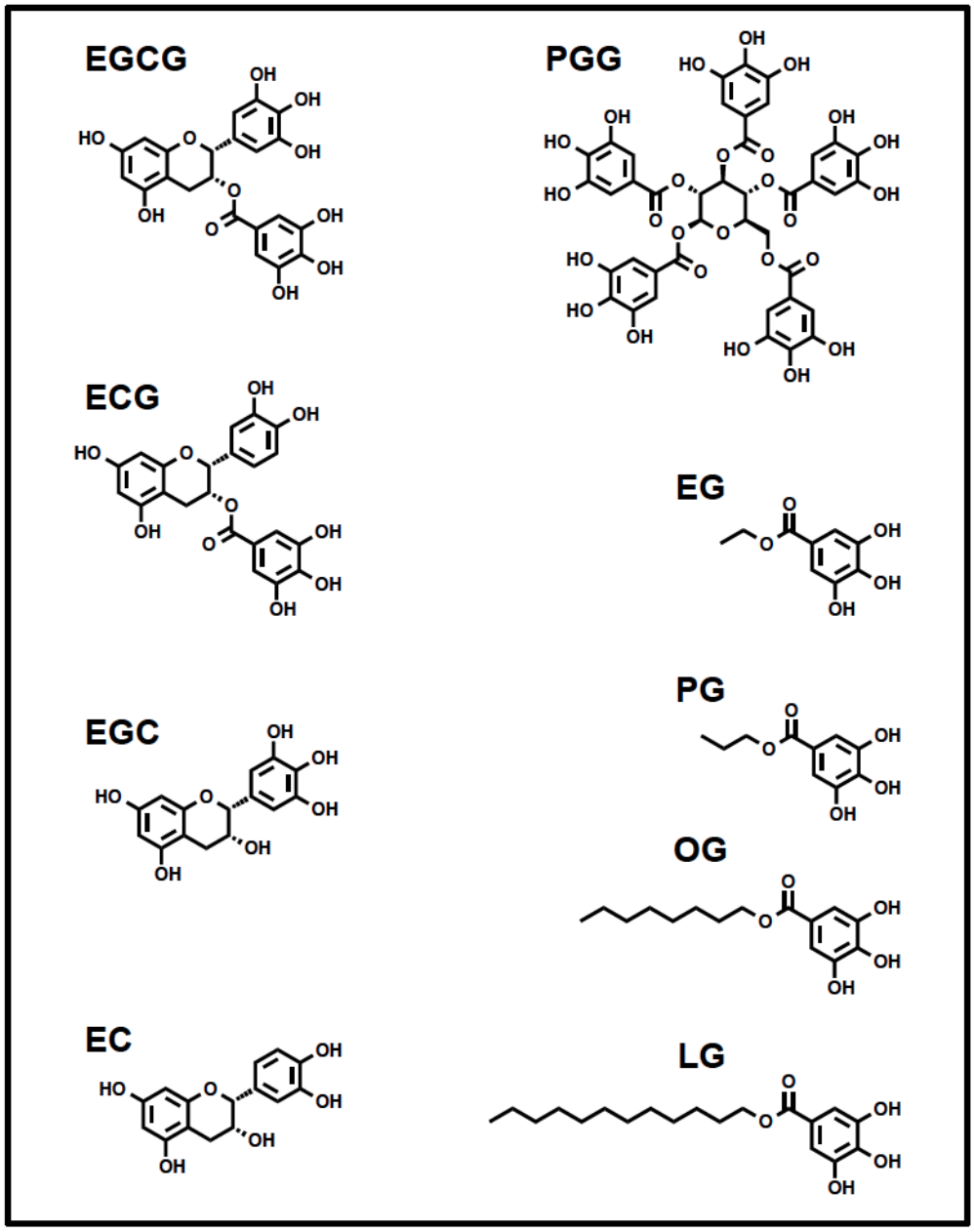

Figure 3.1. Structures of gallate derivates. The green tea catechins include epigallocatechin gallate **(EGCG)**, epicatechin **(EC)**, epicatechin gallate **(ECG)** and epigallocatechin **(EGC)**. Pentagalloylglucose **(PGG)** is another natural product. Alkyl gallate derivatives include ethyl gallate **(EG)**, propyl gallate **(PG)**, octyl gallate **(OG)** and lauryl gallate **(LG)**.

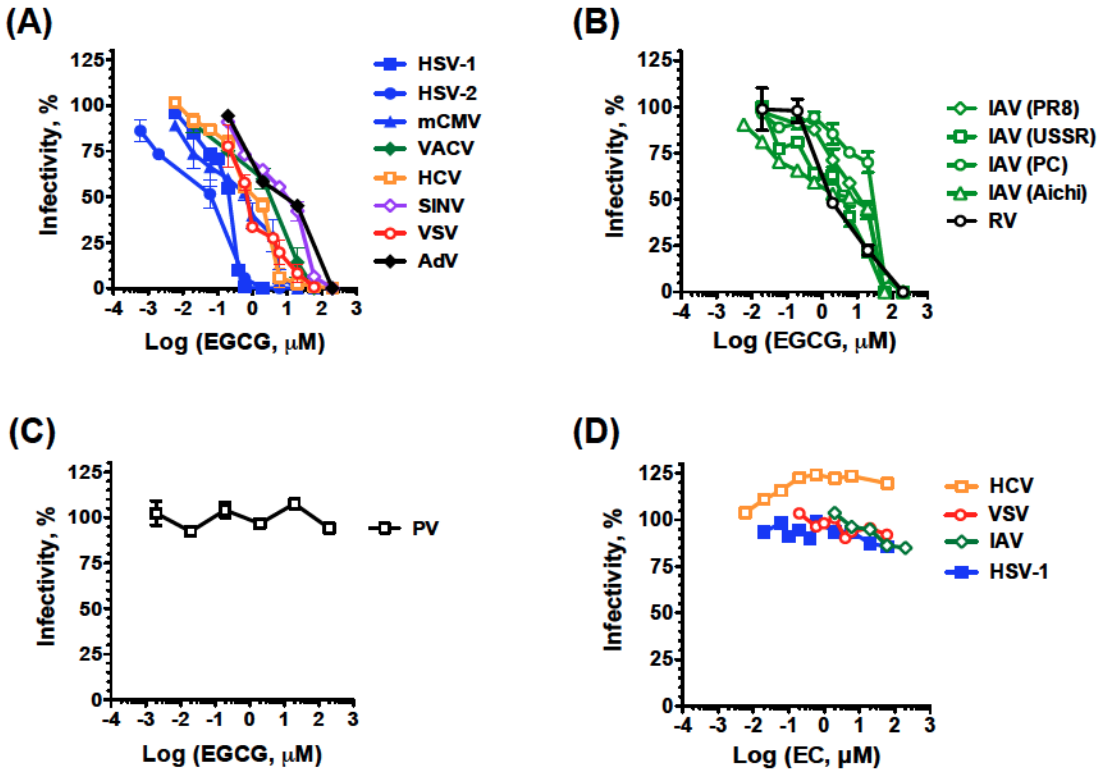

Figure 3.2. EGCG, but not its analog EC, inhibits the infectivity of unrelated viruses. Cell monolayers were infected with HS-binding **(A)**, SA-binding **(B)**, or neither HS- nor SA-binding **(C)** virions pre-exposed to EGCG **(A, B, C)** or EC **(D)** for 10 minutes at 37°C. Infectivity was assessed by plaquing or focus forming efficiency and is expressed as percentage relative to DMSO-treated control. (Dose response curves, average ± S.D.; n = 3).

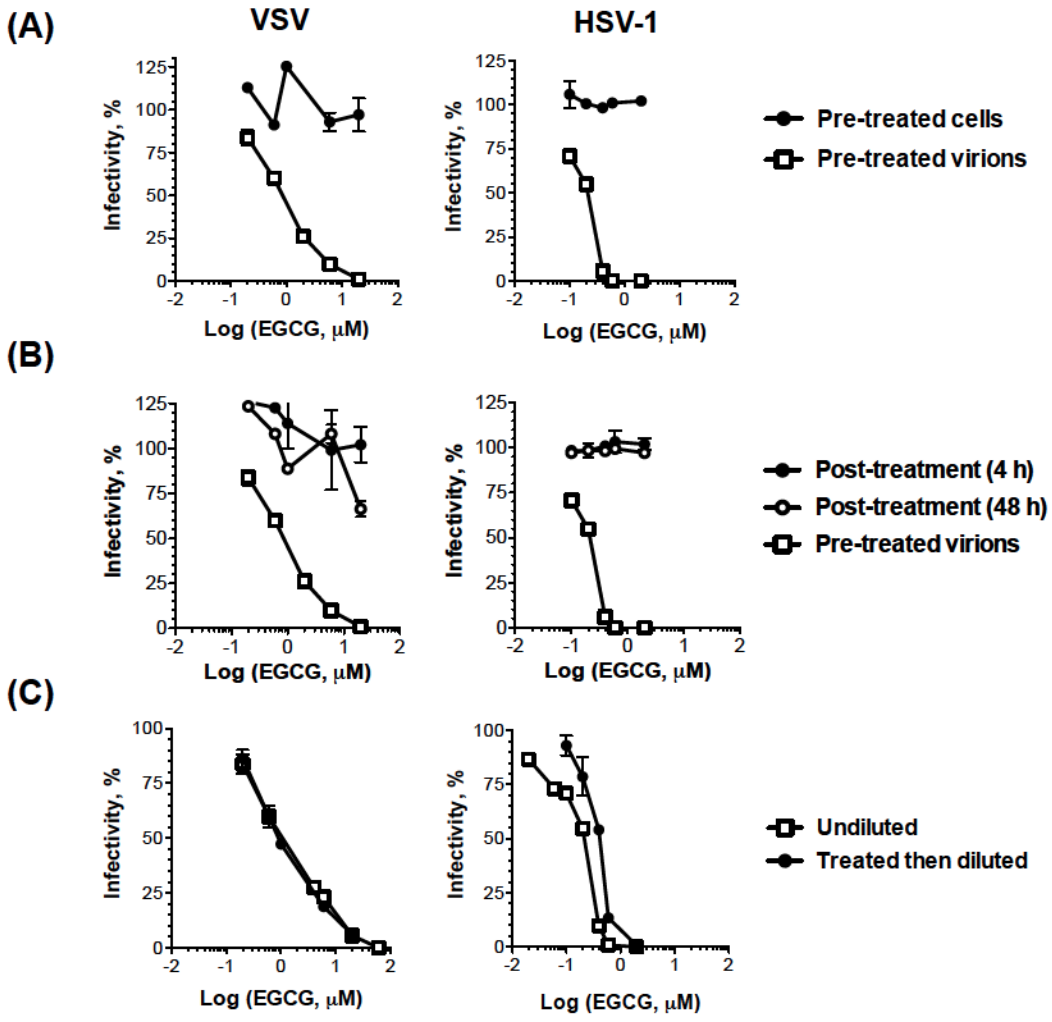

Figure 3.3. EGCG does not inhibit infectivity by acting on cellular factors. Vero cell monolayers were infected with ~200 pfu of HSV-1 or VSV, pre-exposed to EGCG or DMSO vehicle for 10 min at 37°C **(A)**. Alternatively, cells were treated with EGCG or DMSO for 1 hour at 37°C prior to infection or for 4 or 48 hours after infection **(B)**, or virions were treated with EGCG and then diluted 10-fold prior to infecting cells **(C)**. Dose response curves (average ± range; n = 2).

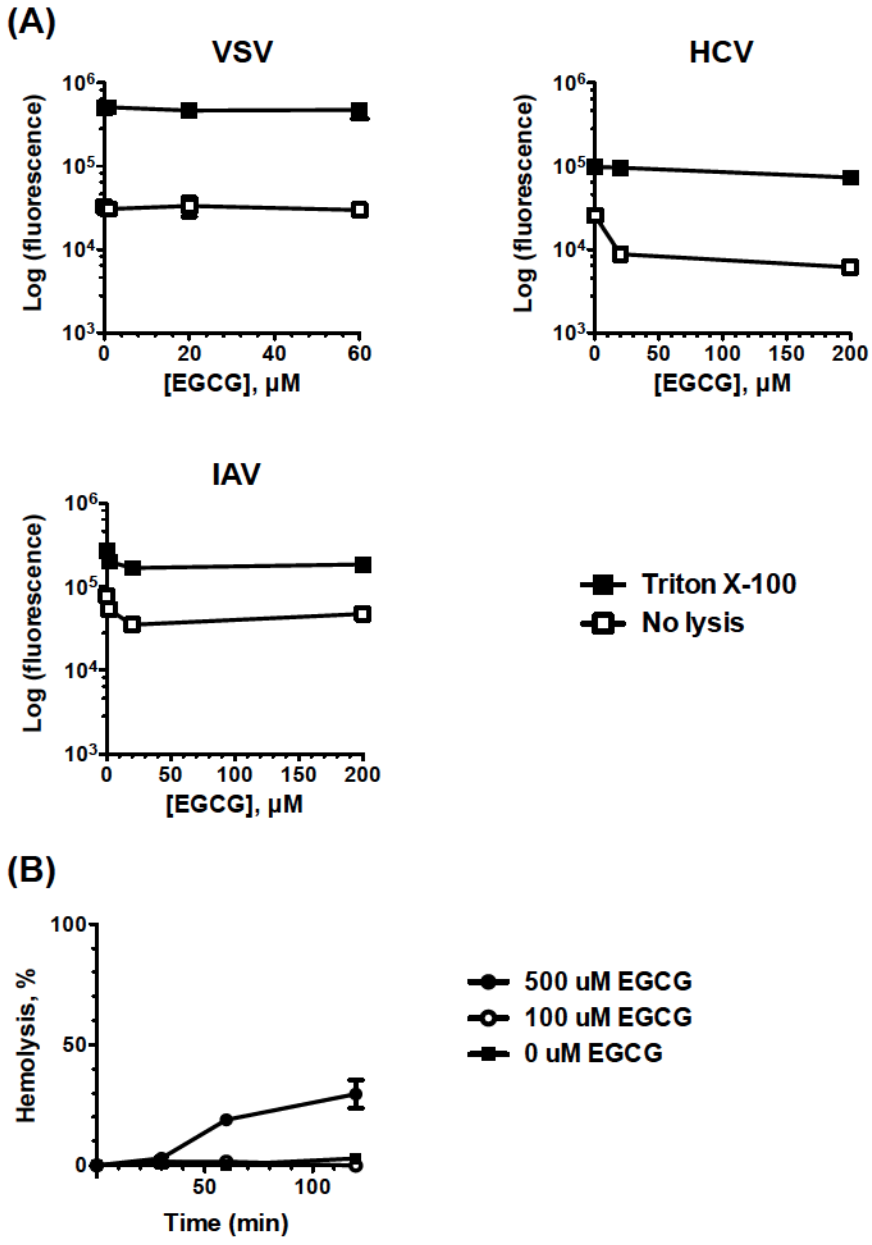

Figure 3.4. EGCG does not disrupt the integrity of virion envelopes or cellular membranes at relevant concentrations. (A) Self-quenched R18-labeled VSV, HCV or IAV virions were exposed for 10 min at 37°C to EGCG or DMSO vehicle. R18 fluorescence was then measured. As a lysis control, 0.1% Triton X-100 was then added. EGCG did not induce the increase in R18 fluorescence that would result from the release of self-quenched R18 if the envelopes were disrupted. **(B)** Haemaglobin release from rabbit erythrocytes exposed to EGCG. Data are expressed as a percentage relative to the lysis induced by addition of 0.1% Triton X-100.

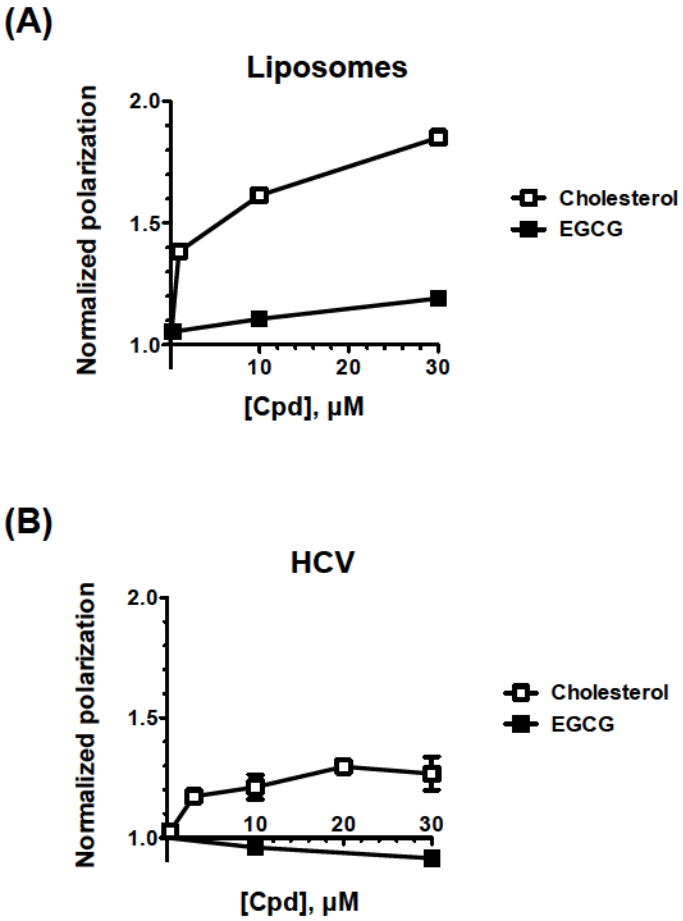

Figure 3.5. EGCG does not disrupt the fluidity of liposomes or virion envelopes. DPH-labelled liposomes **(A)** or HCV virions **(B)** were treated with EGCG for 10 min at 37°C. DPH fluorescence polarization was measured. An increase in polarization indicates a decrease in membrane fluidity. Graphs represent the average ± range, n = 2 (some error bars are too small to be seen at this scale).

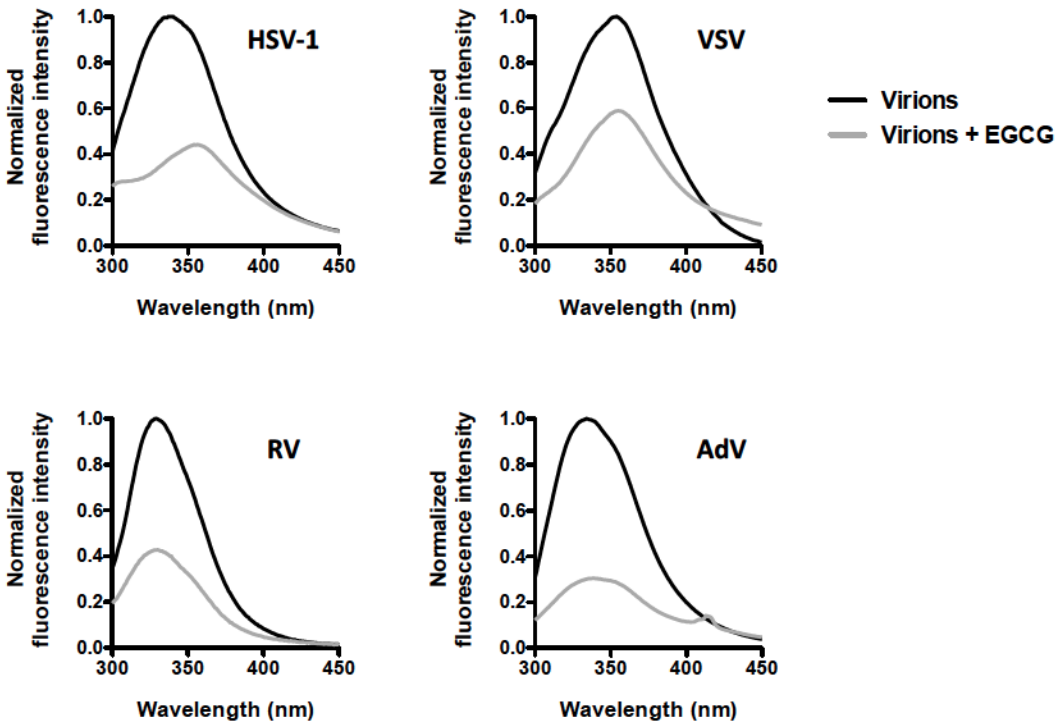

Figure 3.6. EGCG interacts with HSV-1, VSV, RV and AdV surface proteins. Fluorescence emission spectra of HSV-1, VSV, RV or AdV virions in the absence or presence of EGCG. Excitation wavelength, 280 nm (to excite the tryptophan residues). EGCG quenched the emitted fluorescence of the tryptophan residues.

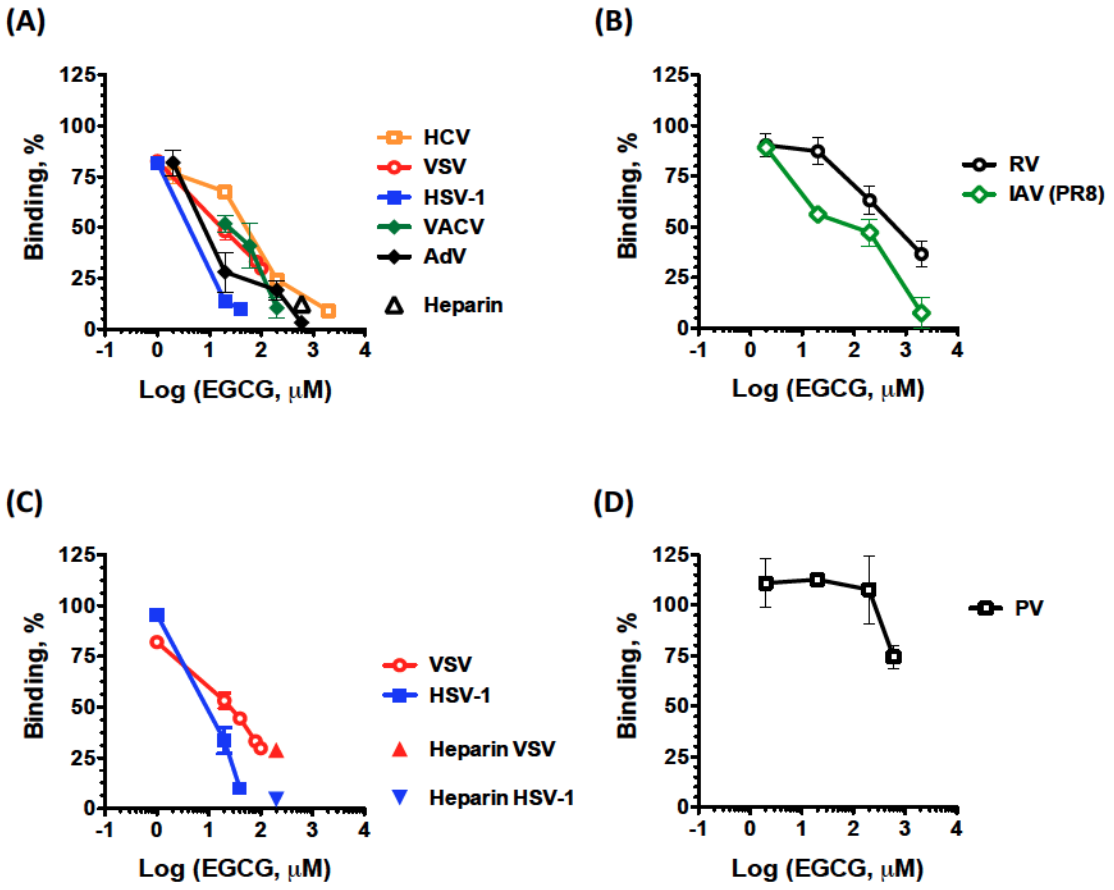

Figure 3.7. EGCG inhibits the attachment of enveloped and nonenveloped viruses. EGCG inhibits the binding of HS-binding HCV, VSV, HSV-1 and VACV **(A).** EGCG also inhibits attachment of SA-binding IAV and RV **(B)**. HCV, HSV, HSV-1, VACV and IAV were labeled with fluorescent R18 **(A, B)**, while AdV, RV **(A, B)**, HSV-1 and VSV **(C)** were labeled with ^{35}S-methionine. EGCG did not affect the binding of ^{35}S-methionine-labelled PV at the active concentrations for the other viruses **(D)**. Virions pre-exposed to EGCG were adsorbed onto target cells for 1 hour at 4°C. The radioactivity or fluorescence attached to the cells was then measured, normalized to total input, and is presented as a percentage relative to attachment of DMSO vehicle-treated control virions (average ± range; n = 2). Several error bars are too small to be seen at this scale.

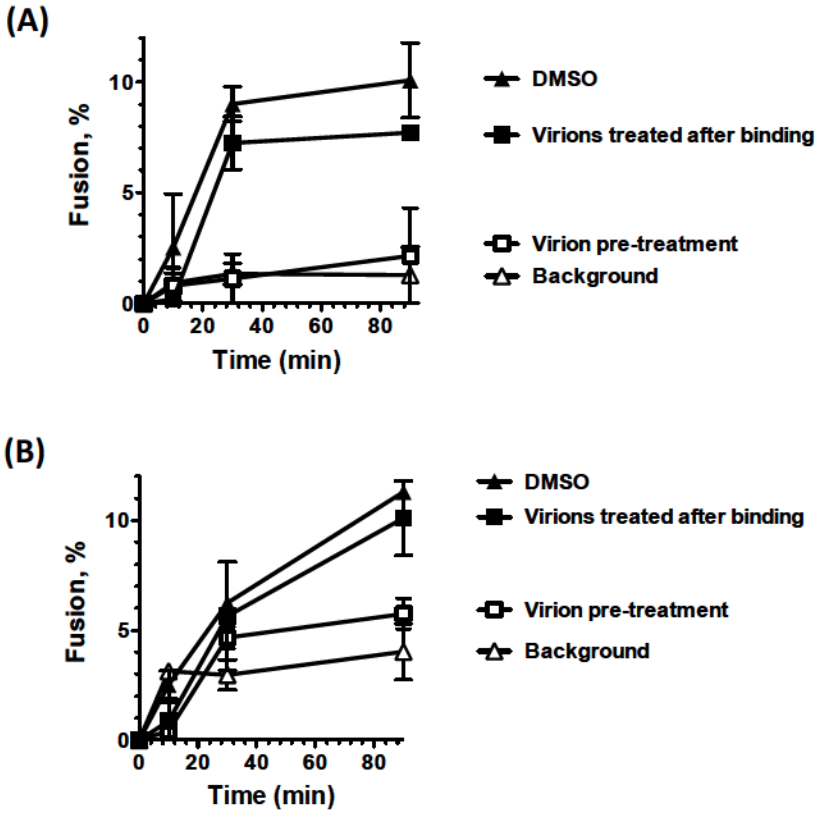

Figure 3.8. EGCG inhibits IAV and VSV fusion only if virions are treated prior to attachment. R18-labelled IAV **(A)** or VSV **(B)** virions pre-exposed to EGCG were adsorbed onto target cells for 1 hour at 4°C. Alternatively, virions were first adsorbed onto target cells for 1 hour at 4°C, and then virion-cell complexes were treated with EGCG. Fusion was triggered by increasing the temperature to 37°C and lowering the pH to 5. Fusion was evaluated by fluorescence dequenching of R18.

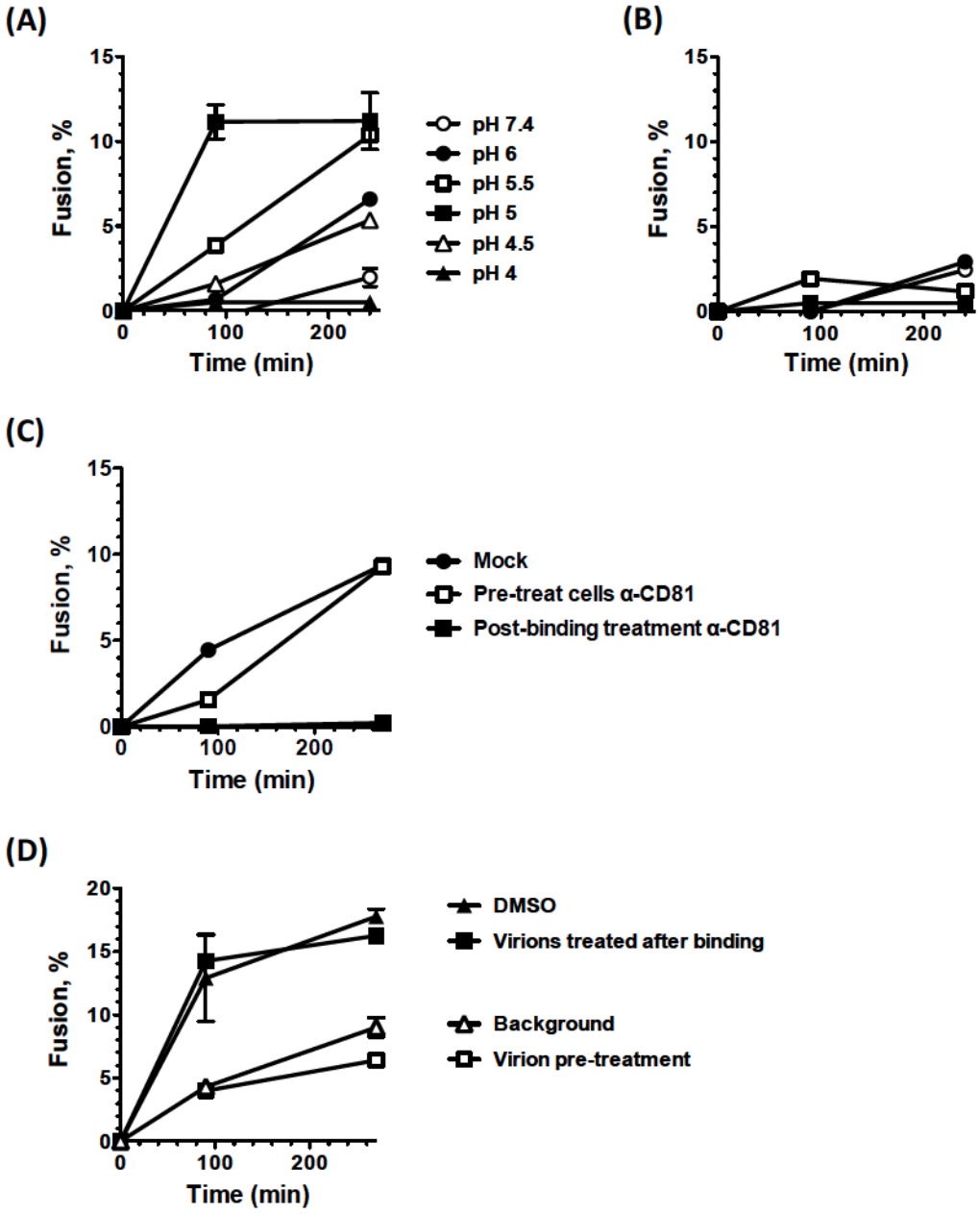

Figure 3.9. EGCG inhibits HCV fusion if virions are treated prior to attachment, in a novel HCV fusion assay. HCV fuses selectively to Huh7.5 cells by low pH dependent mechanisms in a novel HCV fluorescence dequenching fusion assay that requires post-binding activity of the CD81 receptor. **(A)** Fusion of HCV to Huh7.5 cells was tested at several pHs. The pH requirements in our fusion assay match those for HCV infectivity. **(B)** HCV fused to Huh7.5 cells but, as expected, not to Vero cells, which is consistent with the ability of HCV to infect the former but not the latter. **(C)** Fusion of HCV required CD81 at a post-binding step. **(D)** EGCG inhibited fusion of HCV to Huh7.5 cells when virions were pre-treated, but not if added after virion attachment.

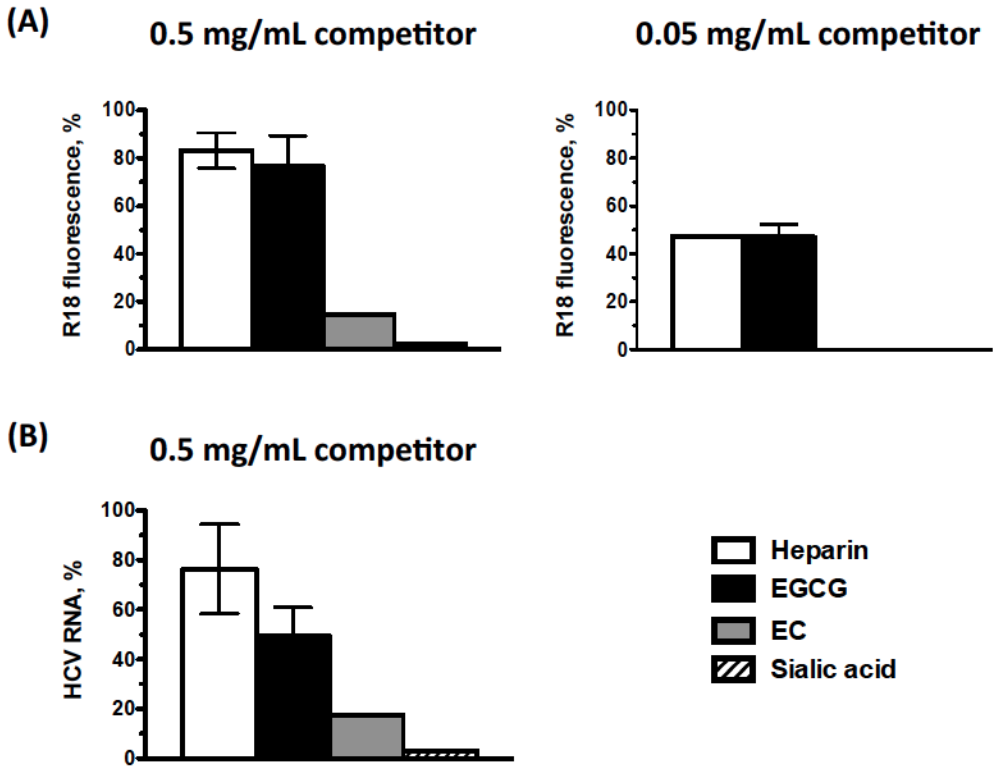

Figure 3.10. EGCG elutes HSV-1 and HCV virions bound to a heparin column with approximately equal efficiency as heparin. (A) R18-HSV-1 (10^5 pfu) or **(B)** HCV (10^5 ffu) virions were loaded onto a heparin column. Bound virions were eluted with soluble heparin (as a positive control) or equivalent concentrations of EGCG, EC and sialic acid. Eluted virions were detected by R18 fluorescence (average ± range; n = 2) **(A)** or viral RNA (average ± S.D.; n = 3) **(B)**.

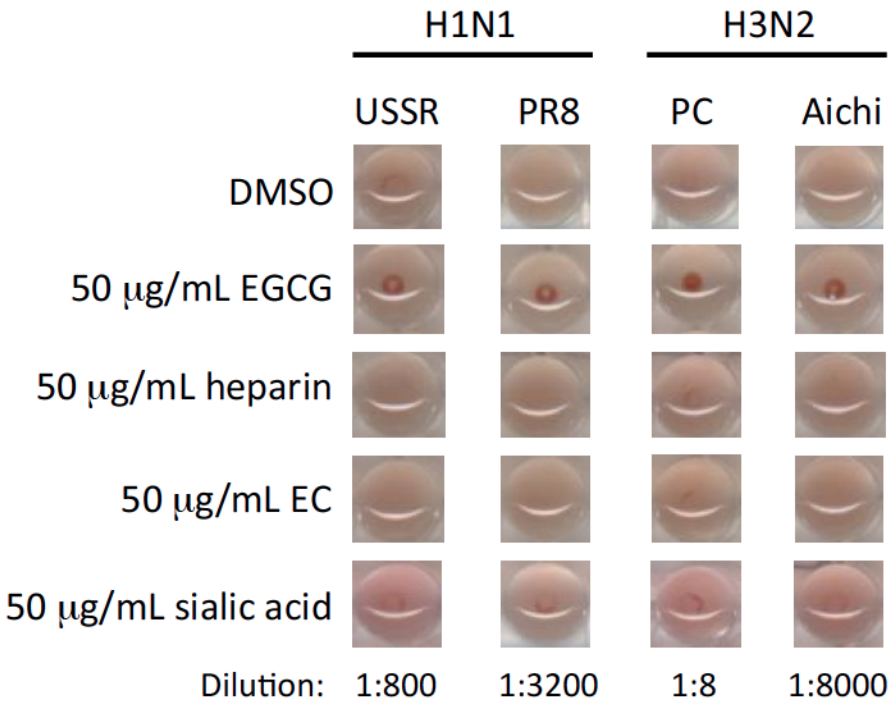

Figure 3.11. EGCG inhibits hemagglutination of erythrocytes by IAV. IAV virions (PR8, USSR, Aichi and PC) were exposed to 50 μg/mL (~100 μM) EGCG, EC, heparin, sialic acid, or equivalent volume of DMSO for 15 minutes at 37°C. The treated virions were then added to chicken erythrocytes.

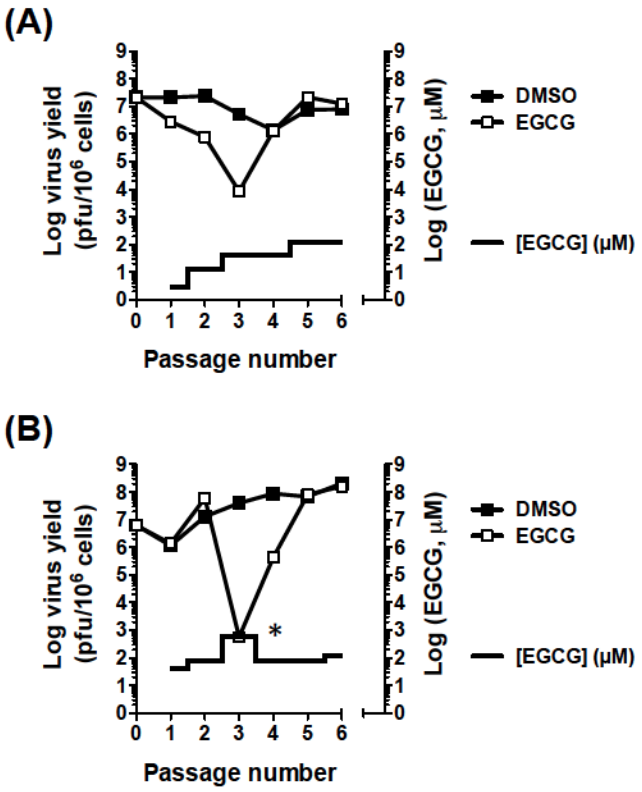

Figure 3.12. Viral titers under EGCG selection pressure. IAV PR8 (**A**) and IAV Aichi (**B**) were passaged in the presence of DMSO vehicle or EGCG and harvested at full cytopathic effect. Viral titers were evaluated by plaque assay.
*concentration marginally toxic to MDCK cells

(A) IAV/PR/8/34 [H1N1]

```
PR8      MENLNKKVDDGFLDIWTYNAELLVLLENERTLDFHDSNVKNLYEKVKSQLKNNAKEIGNG 463

DMSO_1   MENLNKKVDDGFLDIWTYNAELLVLLENERTLDFHDSNVKNLYEKVKSQLKNNAKEIGNR 463
DMSO_2   MENLNKKVDDGFLDIWTYNAELLVLLENERTLGFHDSNVKNLYEKVKSQLKNNAKEIGNG 463
DMSO_3   MENLNKKVDDGFLDIWTYNAELLVLLENERTLDFHDSNVKNLYEKVKSQLKNNAKEIGNR 463
DMSO_4   MENLNKKVDDGFLDIWTYNAELLVLLENERTLDFHDSNVKNLYEKVKSQLKNNAKEIGNR 463
DMSO_5   MENLNKKVDDGFLDIWTYNAELLVLLENERTLDFHDSNVKNLYEKVKSQLKNNAKEIGNR 463

EGCG_1   MENLNKKVDDGFLDIWTYNAELLVLLENERILDFHDSNVKNLYEKVKSQLKNNAKEIGNG 463
EGCG_2   MENLNKKVDDGFLDIWTYNAELLVLLENERILDFHDSNVKNLYEKVKSQLKNNAKEIGNG 463
EGCG_3   MENLNKKVDDGFLDIWTYNAELLVLLENERILDFHDSNVKNLYEKVKSQLKNNAKEIGNG 463
EGCG_4   MENLNKKVDDGFLDIWTYNAELLVLLENERILDFHDSNVKNLYEKVKSQLKNNAKEIGNG 463
EGCG_5   MENLNKKVDDGFLDIWTYNAELLVLLENERILDFHDSNVKNLYEKVKSQLKNNAKEIGNG 463
         ****************************** *.*************************
```

(B) IAV/Aichi/2/68 [H3N2]

```
Aichi    RIQDLEKYVEDTKIDLWSYNAELLVALENQHTIDLTDSEMNKLFEKTRRQLRENAEDMGN 464

DMSO_1   RIQDLEKYVEDTKIDLWSYNAELLVALENQHTIDLTESEMNKLFEKTRRQLRENAEDMGN 464
DMSO_2   RIQDLEKYVEDTKIDLWSYNAELLVALENQHTIDLTDSEMNKLFEKTRRQLRENAEDMGN 464
DMSO_3   RIQDLEKYVEDTKIDLWSYNAELLVALENQHTIDLTDSEMNKLFEKTRRQLRENAEDMGN 464
DMSO_4   RIQDLEKYVEDTKIDLWSYNAELLVALENQHTIDLTESEMNKLFEKTRRQLRENAEDMGN 464
DMSO_5   RIQDLEKYVEDTKIDLWSYNAELLVALENQHTIDLTDSEMNKLFEKTRRQLRENAEDMGN 464

EGCG_1   RIQDLEKYVEDTKIDLWSYNAELLVALENQHTIDLTDSEMNKLFEKTRGQLRENAEDMGN 464
EGCG_2   RIQDLEKYVEDTKIDLWSYNAELLVALENQHTIDLTDSEMNKLFEKTRGQLRENAEDMGN 464
EGCG_3   RIQDLEKYVEDTKIDLWSYNAELLVGVENQHTIDLTDSEMNKLFEKTRGQLRENAEDMGN 464
EGCG_4   RIQDLEKYVEDTKIDLWSYNAELLVALENQHTIDLTDSEMNKLFEKTRGQLRENAEDMGN 464
EGCG_5   RIQDLEKYVEDTKIDLWSYNAELLVALENQHTIDLTDSEMNKLFEKTRGQLRENAEDMGN 464
         ************************.:*********:********** ***********
```

Figure 3.13. EGCG-resistant IAV PR8 and Aichi variants have mutations in the HA2 region of HA. Partial sequence alignment of PR8 **(A)** and Aichi **(B)** HA sequences.

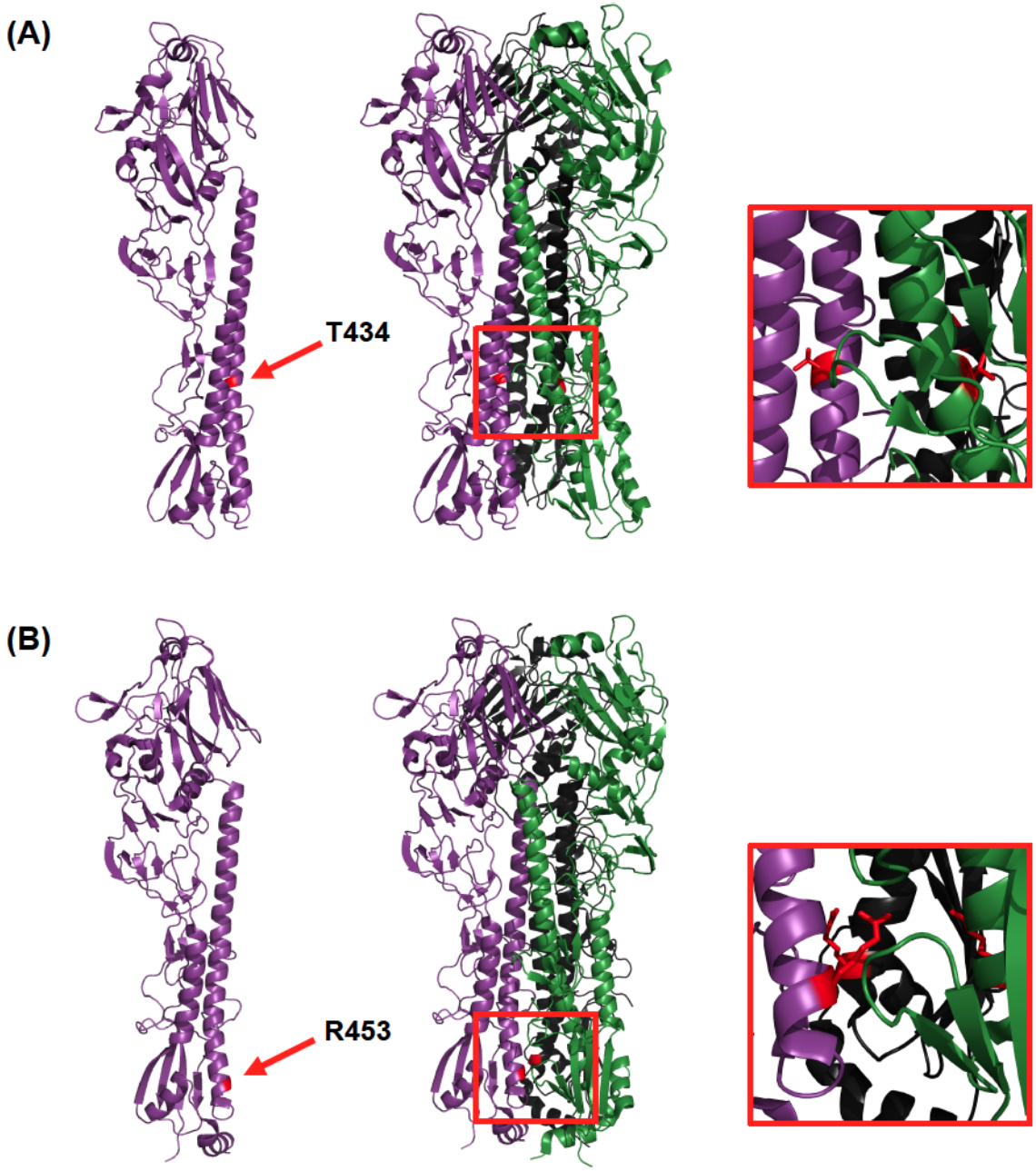

Figure 3.14. EGCG-resistant IAV PR8 and Aichi variants have single amino acid substitutions in the stalk region of the HA2 domain of HA. The wild-type crystal structure of IAV PR8 (H1N1) HA **(A)** as a monomer and trimer (Protein Data Bank 1RU7). Thr-451 is indicated in red and is replaced by Ile in the EGCG-resistant HA sequence. IAV Aichi (H3N2) HA **(B)** is also shown as a monomer and trimer (Protein Data Bank 3VUN). Arg-468 is indicated in red and is replaced by Gly in the EGCG-resistant HA sequence.

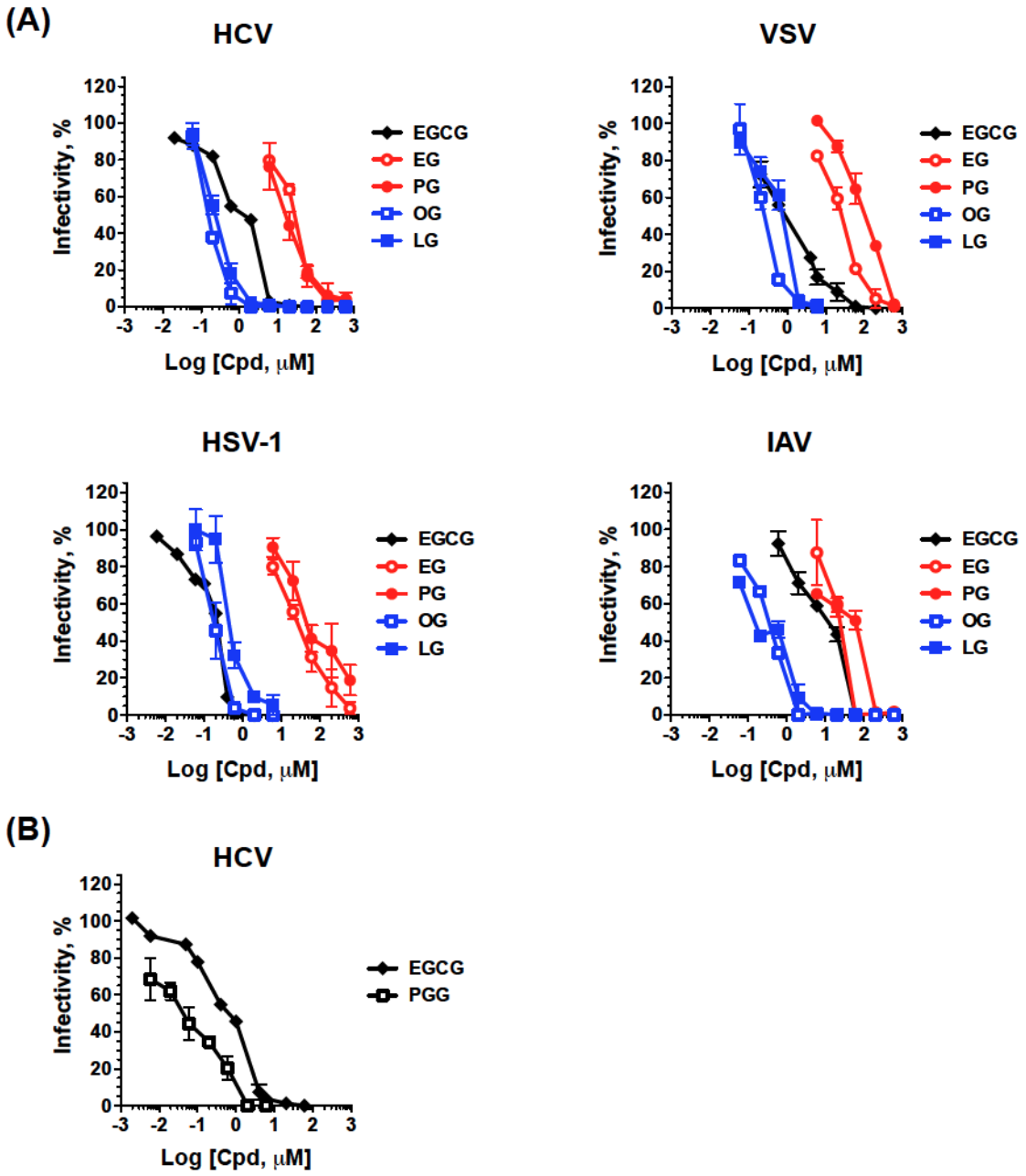

Figure 3.15. Galloylated esters inhibit the infectivity of several unrelated viruses. Cell monolayers were infected with HCV, VSV, HSV-1 or IAV virions pre-exposed to EGCG (black filled diamonds), **(A)** alkyl gallate derivatives ethyl gallate (EG, red open circles), propyl gallate (PG, red filled circles), octyl gallate (OG, blue open squares) and lauryl gallate (LG, blue filled squares) or **(B)** a pentahydroxy gallic acid ester, pentagalloylglucose (PGG, black open squares). Infectivity was assessed by plaquing or focus forming efficiency and is expressed as percentage relative to DMSO-treated control. Dose response curves; n = 2, average ± range.

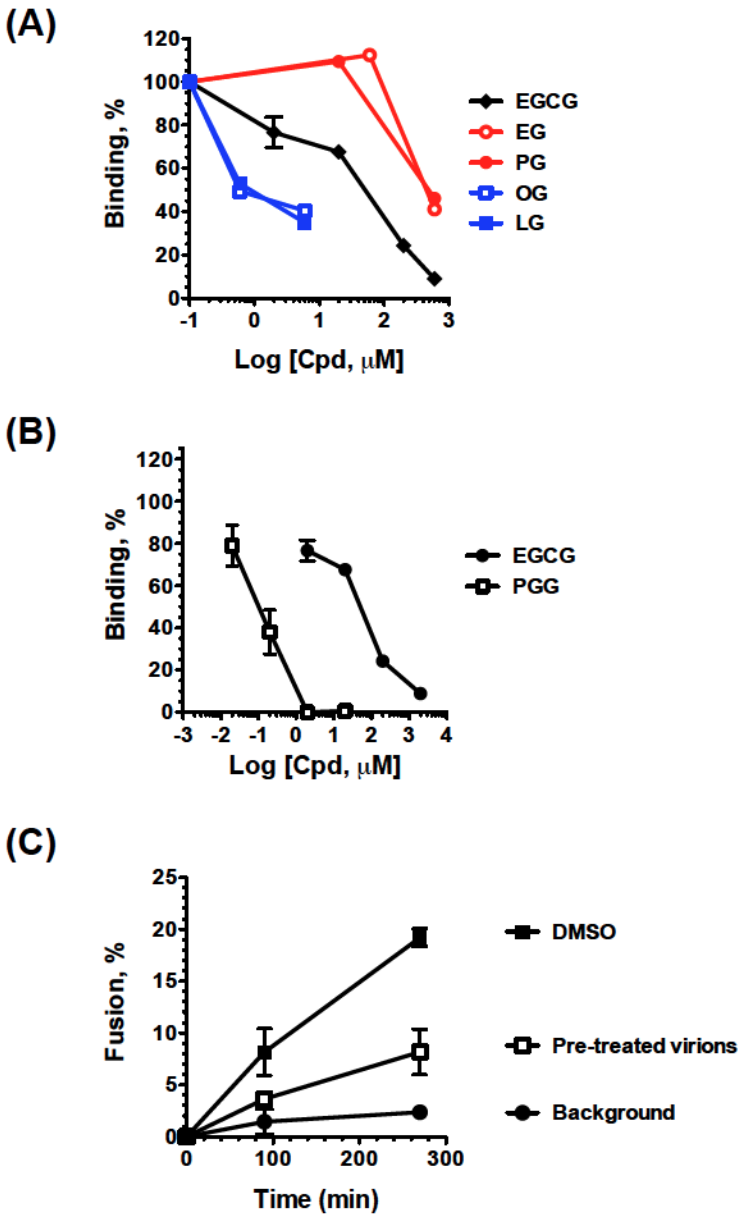

Figure 3.16. Galloylated esters inhibit the binding and fusion of pre-treated HCV virions to cells. Fluorescently labeled HCV virions pre-exposed to EGCG, alkyl gallates **(A)** or PGG **(B)** were adsorbed onto target cells for 1 hour at 4°C. The fluorescence attached to the cells was then measured, normalized to total input, and is presented as a percentage relative to attachment of DMSO vehicle-treated control virions (average ± range; n = 2). Alkyl gallates and PGG inhibited the attachment of HCV virions. **(C)** PGG inhibits HCV fusion when virions are treated prior to attachment. Dose response curves; n = 2, average ± range.

CHAPTER 4: CHARACTERIZATION OF SMALL MOLECULE COMPOUNDS THAT MODULATE MEMBRANE CURVATURE TO INHIBIT FUSION OF ENVELOPED VIRUSES

Data in this chapter were published in the *Journal of Virology* and in *PNAS*:

Colpitts, C.C., Ustinov, A.V., Epand, R.F., Epand, R.M., Korshun, V.A. and Schang, L.M. **(2013)** 5-(Perylen-3-yl)ethynyl-arabino-uridine (aUY11), an arabino-based rigid amphipathic fusion inhibitor, targets virion envelope lipids to inhibit fusion of influenza, hepatitis C and other enveloped viruses. ***J. Virol.*** *87(7):* 3640-54

St.Vincent, M.R., **Colpitts, C.C.**, Ustinov, A.V., Muqadas, M., Joyce, M.A., Barsby, N.L., Epand, R.F., Epand, R.M., Khramyshev, S.A., Valueva, O.A., Korshun, V.A., Tyrrell, D.L.J., Schang, L.M. (**2010**) Rigid amphipathic fusion inhibitors, small molecule antiviral compounds against enveloped viruses. ***PNAS*** *107(40):* 17339-44

I performed all of the experiments described in this chapter, except for the differential scanning calorimetry experiments, which were done by Drs. Richard and Raquel Epand (McMaster University, Hamilton, Canada). I wrote the J. Virol manuscript (with editorial contributions from Dr. Schang) and the sections of the PNAS manuscript corresponding to my experiments.

4.1 INTRODUCTION

All enveloped viruses require the fusion of the viral and cellular membranes to enter the cell. The energy required for this process is provided by the attachment, binding and conformational changes of viral fusion proteins, which undergo major structural rearrangements from the pre- to the post-fusion states during fusion. The viral fusion proteins are classified according to structural differences (Earp *et al.*, 2005; Li and Modis, 2014), but they all nonetheless mediate fusion in an overall similar manner. Generally, the insertion of the viral fusion peptides disrupts the target membranes and results in the formation of the hemifusion stalk. This stalk is an intermediate structure in which only the outer leaflets of the two membranes are fused (Chernomordik and Kozlov, 2005). The inner leaflets subsequently fuse, forming a small pore that then enlarges to

allow for full fusion.

Formation of the hemifusion stalk requires curvature changes in the lipid bilayer, an energetically demanding rearrangement of lipids from flat (with the hydrophobic head groups bent neither toward nor away from each other) or positive curvature (with the hydrophilic headgroups of the outer leaflet bent away from each other) to negative curvature (with the hydrophilic head groups are bent toward each other) **(Figure 4.1)**. The molecular shape of lipids affects this process. Fusion is promoted by enrichment in the outer leaflet of lipids that induce negative curvature, such as oleic acid *(Chernomordik and Kozlov 2003)*. Conversely, enrichment in the outer leaflet of lipids that favour positive curvature, specifically those with larger hydrophilic headgroups than their hydrophobic tails (such as lysophosphatidylcholine, LPC), impairs fusion (Chernomordik *et al.*, 1995). These phospholipids prevent the fusion of enveloped viruses, including influenza A virus (IAV) (Chernomordik *et al.*, 1997; Gunther-Ausborn *et al.*, 1995), rabies virus (Gaudin, 2000b) and Sendai virus (Yeagle *et al.*, 1994). However, such phospholipids also tend to be disruptive to all membranes (including cellular ones), have signalling activities, be toxic, and be too rapidly metabolized to be useful as drugs.

My hypothesis is that synthetic compounds with the same overall shape and amphipathicity as these lipids could act by the same biophysical mechanisms to inhibit viral fusion. Previous studies in our laboratory had identified a family of small molecules called rigid amphipathic fusion inhibitors (RAFIs), which inhibited the infectivity of enveloped but otherwise unrelated viruses. Much of this work focused on one particular RAFI, 5-(perylen-3-yl)ethynyl-2′-deoxyuridine (dUY11), a nucleoside derivative that

does not act by classical nucleosidic mechanisms (St Vincent *et al.*, 2010). dUY11 inhibited the infectivity of several enveloped viruses at nanomolar concentrations, but did not inhibit the infectivity of non-enveloped viruses. dUY11 inhibited HSV-1 entry without affecting binding. Furthermore, dUY11 inhibited the formation of negative curvature (required to form the hemifusion stalk during fusion of enveloped viruses) in model lipid bilayers. However, the specific effects of dUY11 (and other RAFIs) on fusion had not been tested, and the mechanisms of dUY11 (and other RAFIs) against other clinically relevant viruses had not been characterized. The RAFI dUY11 is not cytotoxic, but is slightly cytostatic (St Vincent *et al.*, 2010).

According to my hypothesis, chemically distinct molecules of the same overall shape and amphipathicity should also target virion envelope lipids to prevent fusion of viral and cellular membranes. If the model is correct, all of these compounds should act by the same mechanisms against all enveloped viruses, including important human pathogens. Earlier work had shown that a panel of similarly configured RAFIs, including an arabino-derived nucleoside, 5-(perylen-3-yl)ethynyl-arabino-uridine (aUY11), also inhibited the infectivity of HSV-1 (St Vincent *et al.*, 2010). aUY11 differs from the deoxy-derived dUY11 in that it has a 2′ hydroxyl group in the nucleoside moiety. Furthermore, aUY11 is neither cytotoxic nor cytostatic (St Vincent *et al.*, 2010). If the compounds acted by traditional biochemical or nucleosidic mechanisms, then this modification should result in different biological activities. If these compounds act by biophysical mechanisms, however, then the arabino-configured aUY11 and the deoxyuridine-configured dUY11 should act by the same mechanisms. Moreover, the antiviral mechanisms should be the same against several enveloped viruses, regardless of

their particular fusion proteins.

My objectives were to evaluate the antiviral activities of two chemically distinct RAFIs (aUY11 and dUY11) against a broad panel of viruses, to test their specific effects on viral fusion, and to characterize their mechanisms against two other clinically important human viruses, IAV and HCV.

4.2 RESULTS

4.2.1 The RAFIs aUY11 and dUY11 inhibit the infectivity of otherwise unrelated enveloped viruses. I first tested the effects of the arabino-derived aUY11 and deoxyuridine-derived dUY11 (**Figure 4.2**) on the infectivity of unrelated DNA or RNA enveloped viruses, including important human pathogens (IAV, HCV, HSV-1, HSV-2 and SINV) and model viruses (mCMV and VSV). These viruses are internalized by different mechanisms, fuse to different cell membranes and have fusion proteins representing all classes. However, they all require the formation of negative membrane curvature for the fusion of their envelopes with the cellular membranes.

IAV, HSV-1, HSV-2, VSV or SINV virions (~200 pfu) were exposed to aUY11, dUY11 or DMSO vehicle control at 37°C in DMEM for 10 minutes prior to infecting Vero (HSV-1, HSV-2, VSV, SINV) or MDCK (IAV) cell monolayers. For HCV and mCMV infections, JFH-1 or $RM427^{+}$ virions (~200 ffu) were similarly exposed to RAFIs or DMSO vehicle prior to infecting Huh7.5 cell (HCV) or NIH 3T3 cell (mCMV) monolayers. Foci of infected cells were detected by immunocytochemistry (HCV) or by LacZ expression (mCMV) and counted under the microscope. Infectivity was evaluated by plaquing or focus forming efficiency and is expressed as a percentage of the infectivity of virions treated with vehicle control.

aUY11 inhibited the infectivity of enveloped DNA and RNA viruses, including HSV-1 (EC_{50}, 0.259 μM), HSV-2 (EC_{50}, 0.203 μM) and mCMV (EC_{50}, 0.106 μM) **(Figure 4.3A),** and IAV (H1N1 and H3N2 strains; EC_{50}, 0.035 to 0.221 μM), HCV JFH-1 (EC_{50}, 0.236 μM), SINV (EC_{50}, 0.009 μM) and VSV (EC_{50}, 0.015 μM) (**Figure 4.3B**). Similarly, dUY11 inhibited the infectivity of HSV-1 (EC_{50}, 0.100 μM), HSV-2 (EC_{50},

0.071 μM) and mCMV (EC_{50}, 0.013 μM) **(Figure 4.3C)**, and IAV (H1N1 and H3N2 strains; EC_{50}, 0.076 to 0.146 μM), HCV JFH-1 (EC_{50}, 0.107 μM) and VSV (EC_{50}, 0.013 μM) (**Figure 4.3D**). The EC_{50} against each virus were similar for aUY11 and dUY11 **(Table 1)**. aUY11 less potently inhibited the infectivity of VACV, another enveloped DNA virus (EC_{50}, 24.6 μM) **(Figure 4.3A)**.

aUY11 and dUY11 inhibited the infectivity of unrelated enveloped viruses, including important human pathogens, at the nanomolar range (**Table 4.1**). In contrast, and consistently with the proposed mechanism of action, aUY11 did not inhibit the infectivity of three non-enveloped DNA or RNA viruses, AdV, PV or RV (**Figure 4.3A and 4.3B**). Taken together, our results suggest that aUY11 targets a feature conserved among enveloped viruses, such as the virion envelope.

4.2.2 The RAFIs aUY11 and dUY11 localize to virion envelope lipids. To test the localization of aUY11 and dUY11 in virions, I took advantage of their intrinsic fluorescence and analyzed their fluorescence spectra in different environments. Fluorescence spectra are dependent on the polarity of the fluorochrome environment. aUY11 or dUY11 was added to 2.5 mL of aqueous fusion buffer or to 2.5 mL of 1-octanol, to a final concentration of 48 nM or 0.48 nM, respectively, in a polymethacrylate cuvette pre-warmed to 37°C. Alternatively, aUY11 or dUY11 was added to 10^7 pfu of VSV, 10^7 pfu of HSV-1, 10^6 pfu of IAV, 10^6 ffu of HCV, or 2 nmol protein-free POPC liposomes in the same aqueous buffer, to a final concentration of 48 nM. The emission spectra were obtained at the maximum excitation wavelength, 455 nm, and were normalized to the highest fluorescence signal intensity obtained for all conditions (set as 1).

The fluorescence spectra of aUY11 and dUY11 in virions were consistent with their localization to a hydrophobic environment. The spectra of aUY11 and dUY11 were very similar in the presence of HSV-1, HSV-2, IAV, HCV or VSV virions, or protein-free liposomes (**Figure 4.4A and 4.4B**). These viruses have different glycoproteins and different glycoprotein content in their envelopes, but share a common hydrophobic environment in the lipid core of the envelope. These spectra were most similar to the spectra of aUY11 or dUY11 in octanol (which closely mimics the hydrophobic lipid core of the membrane) and clearly distinct from their spectra in aqueous buffer without virions or liposomes. Therefore, aUY11 and dUY11 were in similar hydrophobic environments in virions or protein-free liposomes, consistent with their proposed localization to the hydrophobic lipid core of the virion envelope. Furthermore, aUY11 and dUY11 localized to similar hydrophobic environments in clinically important viruses, such as IAV, HCV and herpesviruses.

4.2.3 The RAFIs aUY11 and dUY11 localize to cellular membranes. I further took advantage of the intrinsic fluorescence of aUY11 and dUY11 to evaluate their potential localization to cellular lipid membranes. Near-confluent Vero, Huh7.5 or MDCK cell monolayers seeded onto cover slips were treated with 0.25 μM PKH26-GL fluorescent cell dye (a general membrane dye) for 10 minutes at 37°C, and then exposed to 2 μM aUY11 or dUY11 for 1 through 120 minutes, also at 37°C. Cells were washed, fixed with 10% formalin, and mounted onto glass slides. aUY11 and dUY11 localized similarly to plasma and intracellular membranes of Vero **(Figure 4.5A)**, Huh7.5 **(Figure 4.5B)** and MDCK **(Figure 4.5C)** cells. As early as 1 minute after exposure, RAFIs accumulated in intracellular membranes, such as the endoplasmic reticulum **(Figure 4.5A)**. In summary,

the RAFIs aUY11 and dUY11 localize to cellular lipid membranes, where they may interfere with viral fusion, or become incorporated into the envelopes of progeny virions.

4.2.4 The RAFIs aUY11 and dUY11 protect cells from infection with IAV, HCV and HSV-1. Since aUY11 and dUY11 localize to cellular membranes, I tested their effects when cells were treated prior to infection. Cells were exposed to aUY11 or dUY11 for 1 hour at 37°C. Following three washes, the cells were infected with IAV, HCV or HSV-1 and evaluated for plaque or foci formation. Infectivity was expressed as a percentage of the infectivity in cells pre-treated with vehicle control. Under these conditions, aUY11 and dUY11 protected MDCK cells from infection by IAV (EC_{50}, 0.446 μM and 0.124 μM, respectively) **(Figure 4.6A)**. The EC_{50} for aUY11 and dUY11 were 0.266 μM and 0.097 μM, respectively, when virions were pre-treated **(Figure 4.6A)**. The EC_{50} were only ~1.5-fold higher when cells were pre-treated than when virions were pre-exposed. aUY11 and dUY11 also protected Huh7.5 cells from infection with HCV (EC_{50}, 0.496 μM and 2.93 μM, respectively), but inhibited infectivity most potently when virions were pre-exposed (EC_{50}, 0.249 μM and 0.121 μM, respectively) **(Figure 4.6B)**. Finally, aUY11 and dUY11 protected Vero cells from HSV-1 infection (EC_{50}, 4.44 μM and 3.23 μM, respectively) but were most potent when virions were pre-treated (EC_{50}, 0.127 μM and 0.100 μM, respectively) **(Figure 4.6C)**. Therefore, aUY11 and dUY11 do protect cells from infection by IAV, HCV and HSV-1, and were most potent against viruses that are internalized prior to fusion (consistent with the accumulation of RAFIs in intracellular compartments observed in Figure 4).

aUY11 and dUY11 most potently protected MDCK cells from infection, at similar concentrations as they inhibit the infectivity of IAV virions. Given the efficacy

against IAV, I next tested how long aUY11 would protect cells from infection. MDCK cells were treated with aUY11 for one hour, and were then washed three times and overlaid with DMEM-5% FBS. Treated cells were then infected with IAV immediately (1 hour), or after 24, 48 or 72 hours. Infectivity was assessed by plaquing efficiency. aUY11 protected cells from infection even after 1, 24, 48 or 72 hours (EC_{50}, 0.166 μM, 0.943 μM, 1.49 μM or 16.5 μM, respectively) **(Figure 4.7A)**. The EC_{50} increased proportionally as cell division occurred, which increases the amount of membrane and concomitantly dilute the concentration of aUY11. When corrected for cell division and corresponding dilution, aUY11 protected cells from infection similarly after 1, 24 and 48 hours (EC_{50}, 0.166 μM, 0.198 μM and 0.148 μM, respectively), with decreased activity after 72 hours (EC_{50}, 1.03 μM) **(Figure 4.7B)**.

4.2.5 The RAFIs aUY11 and dUY11 inhibit the infectivity of IAV, HCV and HSV-1 virions produced by treated cells. Viruses acquire their envelopes from the membranes of infected cells, and aUY11 and dUY11 localize to cellular membranes **(Figure 4.5)**. Therefore, we tested the effects of aUY11 on the infectivity of virions produced by already infected cells. MDCK, Huh7.5 or Vero cells were first infected with 5 or 0.5 pfu/cell of IAV, HCV or HSV-1. After 1 hour, inocula were removed and cells were washed and overlaid with media containing aUY11 for 24 or 48 hours (for IAV and HSV-1 or HCV, respectively). Supernatants and cell lysates were harvested and titrated. Almost no infectious virus could be recovered from already infected cells treated with 6 μM aUY11 **(Figure 4.8)**. The concentrations at which aUY11 inhibited the production of infectious virus from cells treated after infection were very similar to the concentrations at which it inhibited the infectivity of exposed virions. In cells infected at an MOI of 5,

the IC_{50} for IAV, HCV or HSV-1 was 0.2, 0.4 or 0.35 μM, respectively. In cells infected at an MOI of 0.5, the IC_{50} for IAV, HCV or HSV-1 was 0.06, 0.14 or 0.28 μM, respectively. Previous work in our laboratory by Dr. Mireille St.Vincent showed that dUY11 does not affect viral replication in previously infected cells, and has no apparent effects on virion assembly or integrity, only minimal ones on virion budding, and no cytotoxic effects (St Vincent *et al.*, 2010). My results show that aUY11 and dUY11 localize to the membranes of treated cells **(Figure 4.5)**. Therefore, the effects on the virions produced by cells treated after infection are most likely a result of inhibition of the infectivity of the progeny virions, which acquire their envelopes by budding from the cell membranes to which aUY11 localizes.

In this model, aUY11 would become incorporated into the virion envelopes (derived from cellular membranes) during budding. To test the model, I examined the fluorescence spectra of aUY11 in 10^4 IAV, HCV or HSV-1 virions produced by cells treated with DMSO vehicle, or equivalent volumes from cells treated with aUY11. The characteristic emission spectrum of aUY11 was detected, in decreasing intensity, for samples treated with 6, 2 or 0.6 μM aUY11, for IAV **(Figure 4.8A)**, HCV **(Figure 4.8B)** and HSV-1 **(Figure 4.8C)**. As expected, aUY11 fluorescence was not detected in samples from the untreated cells. Therefore, aUY11 added to already-infected cells becomes incorporated into the membranes of virions produced by the treated cells, resulting in the production of non-infectious virions.

4.2.6 The RAFI aUY11 does not affect HCV attachment. Compounds that inhibit infectivity may interfere with the first step of entry, attachment. Previous studies in our laboratory showed that dUY11 did not affect the binding of an enveloped DNA virus,

HSV-1 (St Vincent *et al.*, 2010). I now tested the effects of aUY11 on the binding of an unrelated enveloped virus, HCV. Fluorescently labeled HCV virions were exposed to aUY11 for 10 minutes at 37°C, and then added to pre-chilled Huh7.5 cell monolayers. After 1 hour, the inoculum was removed and cells were washed four times with cold DMEM. Fluorescence attached to cells was then measured, and binding is expressed as percentage fluorescence relative to the vehicle-treated control. aUY11 only minimally inhibited HCV binding by ~10% at the highest concentration tested, 20 μM (~100-fold above the EC_{50}) **(Figure 4.9A)**.

4.2.7 The RAFI aUY11 does not perturb membrane fluidity. Viral entry steps (including binding and fusion) require appropriate membrane fluidity. Compounds that target membranes can modulate their fluidity, which in turn affects the infectivity of enveloped virions (Harada, 2005). For example, cholesterol increases the ordering of phospholipid acyl chain packing (Lande *et al.*, 1995). Decreases in membrane fluidity reduce the infectivity of enveloped virions such as HIV (Harada *et al.*, 2005). We therefore tested the effects of aUY11 on membrane fluidity, using the DPH fluorescence polarization method (Shinitzky and Inbar, 1976). As membrane fluidity decreases (such as by addition of cholesterol), the polarization of DPH increases. The addition of aUY11 up to 20 μM (approximately 100-fold above the antiviral EC_{50}) to DOPC liposomes only minimally increased the DPH polarization **(Figure 4.9B)**, indicating that aUY11 does not affect membrane fluidity.

4.2.8 The RAFIs inhibit the formation of negative curvature in model lipid membranes without affecting membrane integrity. In collaboration with Drs. Richard Epand and Raquel Epand (McMaster University, Hamilton, Canada), we used differential

scanning calorimetry (DSC) to test whether aUY11 and other RAFIs inhibited the formation of lipid structures with negative curvature. Dielaidoylphosphatidylethanolamine (DEPE) lamellar phases were reconstituted with increasing concentrations of the RAFIs aUY11, ddUY11 or dUY1. The transition from the flat morphology of the lamellar phase to the negative curvature of the inverted hexagonal phase **(Figure 4.10A)** was evaluated by DSC. Less than 3% aUY11 in DEPE increased the transition temperature between the lamellar and inverted hexagonal phases by ~1°C **(Figure 4.10B)**. Less than 3% ddUY11 or dUY1 in DEPE increased the T_H transition temperature by ~2°C **(Figures 4.10C and 4.10D)**. Earlier work had shown that 2% dUY11 in DEPE increased T_H by ~3°C **(Figure 4.10E)** (St Vincent *et al.*, 2010). These effects on the transition temperature required for the formation of negative monolayer curvature indicate that RAFIs disfavour the formation of negative membrane monolayer curvature.

The cooling scans, which evaluate the reciprocal inverted hexagonal to lamellar phase transition, exhibit a characteristic hysteresis caused by kinetic factors. They also show that aUY11, ddUY11 and dUY1 raise the hexagonal to bilayer transition temperature, as observed in the heating scans **(Figure 4.10B-D)**. The fact that a characteristic transition due to hysteresis is recovered on each cooling scan, and that the cooling regression is similar to that obtained in the heating scans, demonstrates that the RAFIs did not affect the integrity of the multilamellar membranes. The membranes were not disrupted or lysed by aUY11, either, based on the constancy of the main transition, which appears at 37°C on reheating. The hysteresis of DSC transitions of phosphatidylethanolamines has been previously noted (Epand and Epand, 1988).

Taken together, aUY11 and other RAFIs raise the transition temperature necessary to form inverted hexagonal phases, without disrupting the membranes or affecting their fluidity **(Figure 4.9)**. This activity is consistent with inhibitors of fusion that prevent formation of negative monolayer curvature (Epand, 1986).

4.2.9 The RAFIs aUY11 and dUY11 inhibit the fusion of viral and cellular membranes. Since aUY11 and dUY11 inhibit the formation of negative curvature in model membranes **(Figure 4.10)**, I next tested whether aUY11 inhibited virion-envelope-to-cell-membrane fusion, which similarly requires the formation of negative curvature. Using fluorescence dequenching fusion assays, which analyze lipid mixing between the outer leaflets of virions and target cells, I tested the fusion of VSV, IAV and HCV (representing the different classes of fusion proteins).

VSV virions labeled with self-quenching concentrations of R18 were exposed to aUY11 or dUY11 prior to mixing with Vero cells. Fusion was triggered by lowering the pH, and analyzed by the dequenching of R18 fluorescence. Fluorescence was dequenched by ~15% when VSV virions exposed to DMSO vehicle were induced to fuse to target cells, but by only 5% when VSV virions exposed to aUY11 were induced to fuse under the same conditions (**Figure 4.11A**). Similarly, fluorescence was dequenched by only 3% when VSV virions were pre-exposed to dUY11 **(Figure 4.11A)**.

I next tested the effects of aUY11 and dUY11 on fusion of IAV (PR8, an H1N1 strain) and HCV JFH-1. IAV virions labeled at self-quenching concentrations of R18 were exposed to aUY11 or dUY11 prior to mixing with MDCK (IAV) or Huh7.5 (HCV) cells. Fusion was triggered by increasing the temperature and decreasing the pH to 5. Under these conditions, fluorescence was dequenched by approximately 8% for IAV

virions treated with DMSO vehicle, but by less than 1% (background levels) for IAV virions treated with 600 nM dUY11 or aUY11, even after 2.5 hours (IAV fuses in less than 10 minutes). The background dequenching at neutral pH was ~2% after 2.5 hours (**Figure 4.11B**). For HCV, fluorescence was dequenched by approximately 12% for HCV virions treated with DMSO vehicle, but by less than 5% for HCV virions treated with 600 nM dUY11 or aUY11 (EC_{99} in infectivity assays), in the range of the background dequenching at neutral pH in these assays (~3%) (**Figure 4.11C**).

4.2.10 The RAFI aUY11 inhibits fusion by acting on lipids, not proteins. To determine if the effects of RAFIs on fusion involved cellular factors, I tested their effects on cell-free virus-liposome fusion, using VSV and DOPC/cholesterol liposomes. VSV virions were labeled with diphenylhexatriene (DPH; a membrane fluidity probe), and then exposed to aUY11 or DMSO vehicle. Treated virions were mixed with liposomes, and triggered to fuse. DPH fluorescence polarization was tested as a measure of fusion. DPH polarization is increased in membranes with lower fluidity (such as the virion envelope) and decreased in membranes with higher fluidity (such as the liposome membrane). DPH polarization was decreased by ~10% when VSV virions exposed to DMSO vehicle were induced to fuse to liposomes, but by only 4% when VSV virions exposed to aUY11 were induced to fuse under the same conditions (**Figure 4.12A**).

IAV has a class I fusion protein, whereas VSV has a class III fusion protein and HCV has a putative class IV fusion protein. Although these proteins differ structurally and mechanistically, they mediate fusions that require conserved curvature changes in the lipid envelopes. Therefore, RAFIs likely inhibit fusion by acting on the lipid membranes (to prevent formation of negative curvature), and not by interacting with any viral

protein. To test this model, I analyzed the effects of aUY11 on fusion of protein-free liposomes to cells, which is induced by acidic conditions (Connor *et al.*, 1984). I first exposed R18-labeled protein-free DOPC liposomes to aUY11, and then added the exposed liposomes to cells. Fusion was triggered by decreasing the pH to 5.5 and monitored by fluorescence dequenching of R18 from liposomal membranes into cellular membranes. Under these conditions, fluorescence was dequenched by approximately 45% for liposomes treated with DMSO vehicle, but by only approximately 20% for liposomes first exposed to 2 μM aUY11 (**Figure 4.12B**). Therefore, aUY11 partially inhibits fusion that is not mediated by any viral protein.

4.2.11 The RAFIs inhibit infectivity and fusion at similar concentrations. If RAFIs inhibited infectivity mainly by inhibiting fusion, then the concentrations required to inhibit infectivity or fusion should be similar. To test such potential correlation, I tested different concentrations of aUY11 and dUY11 in plaquing efficiency and fusion assays. The respective dose-responses were then analyzed. Both aUY11 and dUY11 inhibited fusion and plaquing at similar concentrations (**Figure 4.13A and 4.13B**). Their EC_{50} in fusion consequently closely corresponded with their EC_{50} in plaquing efficiency.

Structure-activity relationship studies had previously shown that amphipathicity, a larger hydrophilic head group than the hydrophobic group, and rigidity and planarity of the hydrophobic moiety were all necessary for inhibition of HSV-1 plaquing (St Vincent *et al.*, 2010). Modifications that disrupt the amphipathicity and rigidity of RAFIs therefore disrupt their ability to inhibit infectivity. I tested the effects of these modifications on fusion. dUY1 has a polar group in the hydrophobic moiety (and is less amphipathic than aUY11 or dUY11), whereas dUY5 has a non-planar hydrophobic group

(of similar size to the hydrophilic moiety in aUY11 and dUY11) and aUY12 has a flexible and polar linker between the hydrophobic and hydrophilic groups (**Figure 4.2**). Several concentrations of dUY1, dUY5 and aUY12 were tested in VSV fusion and plaquing efficiency assays. Although these RAFIs vary in their potency by over 100-fold, each inhibited fusion and plaquing at similar concentrations (**Figures 4.13C, 4.13D and 4.13E**). Consequently, their EC_{50} in fusion closely corresponded with their EC_{50} in plaquing efficiency.

4.2.12 The RAFI aUY11 does not readily select for resistant variants. Influenza A/PR8 [H1N1] was serially passaged in the presence of increasing concentrations of aUY11. However, after 10 passages in the presence of aUY11, the viral titers did not recover **(Figure 4.14A, Table 4.2)**. I also passaged HSV-1 KOS in the presence of aUY11. As of passage 4, there has been no selection for resistance **(Figure 4.14B, Table 4.3)**.

4.3 DISCUSSION

The results presented in this chapter show that the two lead RAFIs, aUY11 and dUY11, inhibit the infectivity of enveloped but otherwise unrelated viruses. These include clinically important viruses with DNA or RNA genomes, which replicate in the nucleus or in the cytoplasm, and which use different cellular receptors and enter cells by different mechanisms. aUY11 was active only at micromolar concentrations against VACV, which is enveloped but differs from other enveloped viruses in that some VACV have a second envelope (Law *et al.*, 2006). The second envelope is shed by nonfusogenic mechanisms prior to fusion. aUY11 and dUY11 failed to inhibit the infectivity of nonenveloped viruses, suggesting that their targets are conserved among enveloped viruses but absent in nonenveloped viruses. All enveloped viruses share phospholipid-based bilayer envelopes, which must fuse with cellular membranes during entry into the cell. Therefore, we proposed that aUY11 most likely targets the conserved lipid core of the virion envelopes.

Consistently with this model, both aUY11 and dUY11 localize to the hydrophobic core of the lipid membrane of protein-free liposomes or virion envelopes. Furthermore, aUY11 and dUY11 inhibit lipid mixing in fluorescence dequenching fusion assays for IAV, HCV and VSV (which represent three different classes of viral fusion proteins), and inhibit the acid-induced fusion of liposomes to cells, in the absence of any viral protein. aUY11 did not affect membrane fluidity, but aUY11 and other RAFIs did inhibit the transition of model lipid bilayers from lamellar to hexagonal phases, a transition which requires the formation of negative curvature. Such activities are consistent with the inhibition of the negative curvature necessary for virion envelopes to fuse to cell membranes as the main antiviral mechanism of 5-perylene-ethynyl deoxyuridine- or

arabino-derived RAFIs. aUY11 and dUY11 likely act by the same biophysical mechanisms targeting the virion envelope lipids to prevent the formation of the negative curvature necessary for fusion, therefore inhibiting the infectivity of enveloped viruses.

RAFIs inhibit the fusion of the three different viruses that I tested (IAV, HCV and VSV) which represent different classes of viral fusion proteins. IAV hemagglutinin (HA), like other class I fusion proteins, is predominantly composed of alpha helices containing an N-terminal hydrophobic fusion peptide (Wilson *et al.*, 1981). Class I fusion proteins are trimers both before and after fusion. The proposed mechanism for HA suggests the folding of an uncleaved protein to a metastable state (Chen *et al.*, 1998a), which is then activated by cleavage (Wiley and Skehel, 1987) (Wilson *et al.*, 1981). Fusion is triggered by low pH, resulting in irreversible conformational changes leading to a more stable post-fusion conformation (Bullough *et al.*, 1994). HCV E2 protein was initially proposed to be a class II fusion protein, like those in other flaviviridae (Krey *et al.*, 2010), but this was recently disputed when the crystal structures of E2 revealed a globular architecture distinct from any class II fusion protein (Kong *et al.*, 2013; Khan *et al.*, 2014). The properties of E2 (such as low pH-induced conformational changes) are also inconsistent with its proposed role as a class II fusion protein (Khan *et al.*, 2014). It is currently thought that E1 or the E1E2 heterodimer may belong to a novel class of fusion protein (Li and Modis, 2014). Finally, VSV G protein is a class III fusion protein, consisting of mixed alpha helix and beta sheet structure (Roche *et al.*, 2007). Class III fusion proteins can uniquely undergo a reversible conformational change (unlike class I and II fusion proteins). Extended exposure to low pH inactivates the virions, but the fusion activity is fully recovered when the pH is raised again (Gaudin, 2000a).

The fusion proteins of IAV, HCV and VSV represent different classes, with different structures and fusion mechanisms. However, aUY11 and dUY11 inhibited fusion of all three viruses at similar concentrations. The targets of aUY11 and dUY11 are therefore not likely the fusion proteins themselves. The actual target must be even more conserved among enveloped viruses. aUY11 also inhibited acid-induced fusion of protein-free liposomes to cells (in the absence of any viral protein), supporting a model in which RAFIs inhibit infectivity by acting on lipids. The lipids in the envelope of all enveloped viruses (or vesicles) must form a hemifusion stalk structure when fusing to target cell membranes (Harrison, 2008). This process requires the formation of negative curvature by the outer leaflet of the envelope. DSC experiments showed that aUY11 and other RAFIs inhibit the transition from the lamellar phase (exhibiting flat curvature) to the hexagonal phase (exhibiting negative curvature), indicating that they inhibit the formation of negative curvature required for fusion. These results support our model that RAFIs target virion envelope lipids to prevent fusion of viral and cellular membranes by biophysical mechanisms (*i.e.,* inhibiting the formation of negative curvature in virion envelopes).

Virion fusion is affected by the lipid composition of the virion envelope (Teissier *et al.*, 2011a). The molecular shape of lipids affects the formation of the negative curvature of the hemifusion stalk fusion intermediate. Lipids with polar headgroups of larger diameter than their hydrophobic tails in the outer leaflet favour positive curvature and therefore increase the activation energy required for formation of the hemifusion stalk (Chernomordik *et al.*, 1995). Not unexpectedly, addition of exogenous lipids of the appropriate shape and polarity (such as LPC) prevents the fusion of a number of

enveloped viruses (Chernomordik *et al.*, 1997; Gunther-Ausborn *et al.*, 1995). Phospholipids, however, are rapidly metabolized and disruptive to membranes, and as such are not pharmacologically useful.

Unlike LPC and related phosopholipids, RAFIs are small synthetic compounds of appropriate shape and polarity to inhibit formation of the negative curvature necessary for the formation of the hemifusion stalk, but they do not disrupt membranes or inhibit physiological fusions. aUY11 and dUY11 had no apparent effects on cellular fusion events, such as those required for endocytosis. For example, aUY11 did not inhibit the infectivity of the nonenveloped polio- and reovirus, which are internalized by endocytosis and require fusion of endocytotic vesicles for entry. Furthermore, aUY11 had no apparent effects on exocytosis (Dr. Gary Eitzen, University of Alberta, Edmonton, Canada; unpublished data) or mitosis (St Vincent *et al.*, 2010). We speculate that the lack of effects on cellular fusions is due to the activity of cellular proteins, which actively modulate the lipid composition and curvature of cellular membranes. Such activities are not possible for metabolically inert virions. Consistently, neither aUY11 nor dUY11 was cytotoxic to cells (selectivity index > 3000) (St Vincent *et al.*, 2010).

Other membranotropic inhibitors of viral entry have been described in the past few years. C5A inhibited the entry of several enveloped viruses, including HCV and HIV (Cheng *et al.*, 2008; Bobardt *et al.*, 2008), by virucidal mechanisms. Another inhibitor of HCV and HIV infectivity, PD 404182 (PD), was recently identified (Chamoun *et al.*, 2012; Chamoun-Emanuelli *et al.*, 2014). PD was proposed to disrupt virion envelopes, perhaps by interfering with membrane fluidity or curvature (Chamoun *et al.*, 2012). One possibility is that PD acts as a weak RAFI to prevent the curvature changes in the virion

envelopes necessary for fusion, although this remains to be tested. Other compounds that target virion envelopes act by non-virucidal mechanisms (Teissier *et al.*, 2011b). Arbidol interacts with lipid membranes (Pecheur *et al.*, 2007; Villalain, 2010), and inhibited the fusion of enveloped viruses such as IAV and HCV (Boriskin *et al.*, 2008; Teissier *et al.*, 2011b). It was proposed that arbidol might also interact with tryptophan residues of viral proteins to prevent fusion (Teissier *et al.*, 2011b).

LJ-001 is another small molecule that targets virion envelopes to inhibit the infectivity of enveloped viruses. LJ-001 and other thiazolidine and oxazolidine derivatives are type II photosensitizers that are thought to inactivate virions by damaging the membranes through generation of reactive oxygen species after exposure to ambient light (Wolf *et al.*, 2010; Vigant *et al.*, 2013). Enveloped virions exposed to LJ-001 had increased amounts of some oxidized forms of unsaturated phospholipids (Vigant *et al.*, 2013). The authors proposed that LJ-001-generated singlet oxygen species oxidize unsaturated fatty acid chains within the viral membrane. Such oxidation would introduce a polar group in the hydrophobic core of the lipid bilayer and cause a *cis*-to-*trans* isomerization of a double bond in the unsaturated fatty acid chain (Vigant *et al.*, 2013). Both of these modifications would likely result in clustering of the oxidized lipids, thereby affecting biophysical properties of the envelope, such as membrane fluidity. It was postulated that such oxidative damage could be repaired by metabolically active cells, but not by inert virions, thus explaining the selectivity of these compounds.

The hydrophobic moiety of aUY11 and dUY11 is perylene, a known photosensitizer. Indeed, dUY11 did generate singlet oxygen species (Vigant *et al.*, 2014), which Vigant *et al.* proposed to be necessary for its antiviral activity. Vigant *et al.* found

that the antiviral activity of dUY11 was abrogated in the absence of light, or in the presence of singlet oxygen quenchers, suggesting that its photosensitizing properties are involved in its antiviral activity. Vigant *et al*. proposed that the antiviral activity of dUY11 is a result of reduction in virion envelope fluidity induced by clustering of oxidized phospholipids. However, changes in membrane fluidity were only observed at millimolar concentrations of dUY11 (Vigant *et al.*, 2014), far higher than the relevant antiviral concentrations, and I found that aUY11 only very minimally affected liposome membrane fluidity at concentrations up to 20 μM, ~100-fold higher than the antiviral EC_{50} **(Figure 4.9)**. Our preliminary findings show that aUY11 is still active against HSV-1 in the absence of light, albeit at low micromolar concentrations instead of nanomolar concentrations in the presence of light. Furthermore, other RAFIs with similar shapes and amphipathicities, but lacking photosensitizing moieties such as perylene, inhibited the infectivity of HSV-1 at low micromolar concentrations (St Vincent *et al.*, 2010). Although the photosensitizing properties of perylene-containing RAFIs may contribute to their antiviral activities and potencies, RAFIs as a group most likely inhibit viral fusion by biophysical mechanisms as a result of their shapes and amphipathicities.

Virion envelopes can be targeted by many different approaches, either through disruption of virion envelopes (*e.g.,* PD 404182) (Chamoun *et al.*, 2012), inhibition of fusion by as yet understood mechanisms (*e.g.,* arbidol) (Boriskin *et al.*, 2008), oxidative damage to the virion lipid envelopes (*e.g.,* LJ-001) (Wolf *et al.*, 2010) or by modulating membrane curvature (*e.g.,* RAFIs) (St Vincent *et al.*, 2010; Colpitts *et al.*, 2013). Regardless of the particular mechanisms, inhibitors that target highly conserved structural elements of virions, such as the lipid core of the virion envelope, have broad-spectrum

activity against otherwise unrelated enveloped viruses. The entry inhibitors in clinical use target viral glycoproteins, cellular receptors, or the interactions between them. Such molecules have very specific activities, often against only one virus. Interactions between viral proteins and their receptors can be disrupted, for example by small molecules such as the anti-HIV drug maraviroc (Dorr *et al.*, 2005). Biomimetic peptides such as enfuvirtide, another anti-HIV drug, interfere with the structural rearrangements of viral fusion proteins that are necessary for fusion (Kilby *et al.*, 1998; Dwyer *et al.*, 2007; Schmidt *et al.*, 2010; Liu *et al.*, 2010). Antibodies have also been explored as inhibitors of infectivity, mostly in the context of RSV infection (Huang *et al.*, 2010). Unfortunately, peptides and antibodies have poor oral bioavailability or stability (Vlieghe *et al.*, 2010). Furthermore, these approaches suffer from the limitations of targeting any viral protein, such as narrow specificity and selection for resistance (Wei *et al.*, 2002; Baba *et al.*, 2007). Selection for resistance is particularly problematic for antivirals that target viral surface proteins, since they commonly undergo rapid mutation to avoid immune responses (Iannello *et al.*, 2006). In contrast, RAFIs target viral envelope lipids, which are not encoded by the viral genome and are a necessary structural component of all enveloped viruses. Therefore, the RAFIs are expected to have a higher barrier to selection for resistance. Consistently with this expectation, we have not yet been able to select for dUY11-resistant HSV-1 mutants (after 10 serial passages conducted by Dr. Mireille St.Vincent) or aUY11-resistant HSV-1 or IAV mutants **(Tables 4.2 and 4.3)**.

In addition to inhibiting viral infectivity, RAFIs also protected cells from infection. aUY11 and dUY11 were particularly effective at preventing infection of cells by IAV and HCV, which are internalized by endocytosis before fusion is triggered by the

low pH in the endosome (Chen and Zhuang, 2008; Farquhar *et al.*, 2012). In contrast, pre-treatment of cells was less effective at inhibiting the infectivity of HSV-1, which fuses to most cell types at the plasma membrane (Wittels and Spear, 1991). These differences likely reflect the different entry mechanisms of the viruses. aUY11 may be internalized by cells and accumulate in cellular endosomes, resulting in a reservoir to which virions internalized by endocytosis are exposed.

aUY11 is also effective when used to treat cells already infected with IAV, HCV or HSV-1. Although it does not protect the cells from the virus-induced cytopathic effects, as expected from its mechanisms of action, the virions produced from the infected cells are not infectious. This effect is likely due to the incorporation of aUY11 in progeny virion envelopes **(Figure 4.8)**, which are acquired during budding from the cellular membranes to which aUY11 localizes **(Figure 4.5)**. Therefore, treatment with aUY11 not only protects uninfected cells from infection, but also renders virions produced by infected cells noninfectious.

These studies demonstrate that chemically distinct compounds with the same overall three-dimensional shape and amphipathicity inhibit viral infectivity by inhibiting fusion of viral and cellular membranes. The two RAFIs, aUY11 and dUY11, inhibit viral fusion due to their shapes and amphipathicities, acting through biophysical and not biochemical mechanisms. Specifically, they inhibit the formation of the negative curvature necessary to generate the hemifusion stalk intermediate, a critical step in the fusion of enveloped viruses. aUY11 and dUY11 act by the same mechanisms against several enveloped but otherwise unrelated viruses, including important human pathogens such as IAV, HCV and HSV-1/-2. Therefore, RAFIs are a novel family of antiviral

compounds, which act by biophysical mechanisms to prevent fusion of viral and cellular membranes.

Table 4.1. EC_{50} of aUY11 and dUY11 against unrelated viruses. Numbers that are italicized and bolded are from experiments conducted by Dr. Mireille St.Vincent (St Vincent *et al.*, 2010). N.D., no data.

		EC_{50}, µM	
Virus family	**Virus**	**aUY11**	**dUY11**
Herpesviridae	HSV-1	0.26	0.10
	HSV-2	0.20	0.071
	mCMV	0.11	0.013
Poxviridae	VACV	25	N/D
Orthomyxoviridae	IAV (PR8) [H1N1]	0.22	0.10
	IAV (USSR) [H1N1]	0.035	0.076
	IAV (Aichi) [H3N2]	0.067	0.15
	IAV (PC) [H3N2]	0.053	0.083
Flaviviridae	HCV	0.24	0.11
Rhabdoviridae	VSV	0.015	0.013
Togaviridae	SINV	0.010	***0.011****
Adenoviridae	AdV	> 20	***> 20****
Picornaviridae	RV	> 200	***> 200****
Reoviridae	PV	> 200	N/D

Table 4.2. IAV PR8 [H1N1] titers under aUY11 selection pressure. Influenza PR8 was passaged in the presence of DMSO vehicle **(A)** or aUY11 **(B)** and harvested at full cytopathic effect. Viral titers were evaluated by plaque assay.

(A)

Passage number	MOI (pfu/cell)	[Cpd] (μM)	[DMSO] (%, vol/vol)	Viral titer (PFU/10^6 cells)	Ratio of titer (DMSO/DMSO)
1	0.01	-	0.12	2.09×10^7	1
2	0.01	-	0.12	2.39×10^7	1
3	0.01	-	0.12	5.21×10^6	1
4	0.01	-	0.12	1.38×10^6	1
5	0.01	-	0.12	7.42×10^6	1
6	0.01	-	0.12	2.50×10^7	1
7	0.01	-	0.12	2.00×10^7	1
8	0.001	-	0.12	5.67×10^7	1
9	0.001	-	0.12	6.11×10^7	1
10	0.01	-	0.12	5.00×10^7	1

(B)

Passage number	MOI (pfu/cell)	[aUY11] (μM)	[DMSO] (%, vol/vol)	Viral titer (PFU/10^6 cells)	Ratio of titer (aUY11/DMSO)
1	0.01	0.05	0.12	1.47×10^7	7.0×10^{-1}
2	0.01	0.2	0.12	1.00×10^7	4.2×10^{-1}
3	0.01	2	0.12	9.60×10^4	1.8×10^{-2}
4	0.01	2	0.12	5.68×10^3	4.3×10^{-3}
5	0.01	2	0.12	2.19×10^5	3.0×10^{-2}
6	0.01	4	0.12	2.50×10^5	1.0×10^{-2}
7	0.01	4	0.12	2.26×10^4	1.1×10^{-3}
8	0.001	4	0.12	5.00×10^3	8.8×10^{-5}
9	0.001	0.2	0.12	4.17×10^5	6.8×10^{-3}
10	0.01	0.2	0.12	6.83×10^5	1.4×10^{-2}

Table 4.3. HSV-1 KOS titers under aUY11 selection pressure. HSV-1 KOS was passaged in the presence of DMSO vehicle **(A)** or aUY11 **(B)** and harvested at full cytopathic effect. Viral titers were evaluated by plaque assay.

(A)

Passage number	MOI (pfu/cell)	[Cpd] (µM)	[DMSO] (%, vol/vol)	Viral titer (PFU/10^6 cells)	Ratio of titer (DMSO/DMSO)
1	0.01	-	0.12	5.52×10^7	1
2	0.01	-	0.12	4.21×10^7	1
3	0.01	-	0.12	2.32×10^7	1
4	0.01	-	0.12	1.78×10^8	1

(B)

Passage number	MOI (pfu/cell)	[aUY11] (µM)	[DMSO] (%, vol/vol)	Viral titer (PFU/10^6 cells)	Ratio of titer (aUY11/DMSO)
1	0.01	0.15	0.12	2.59×10^7	4.7×10^{-1}
2	0.01	2	0.12	2.81×10^6	6.7×10^{-2}
3	0.01	4	0.12	3.08×10^6	1.3×10^{-1}
4	0.01	4	0.12	7.40×10^3	4.2×10^{-4}

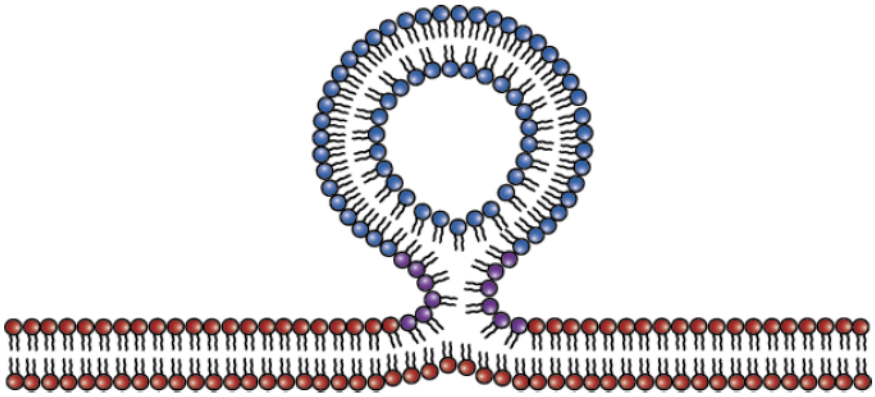

Figure 4.1. The hemifusion stalk intermediate requires the formation of local membrane negative curvature. The outer leaflet of the virion lipid envelope (blue) demonstrates positive curvature, whereas the cell lipid membrane (red) has comparatively flat curvature. The merging of the outer leaftets of the virion envelope and the cell membrane forms the hemifusion stalk intermediate (purple), which has negative curvature.

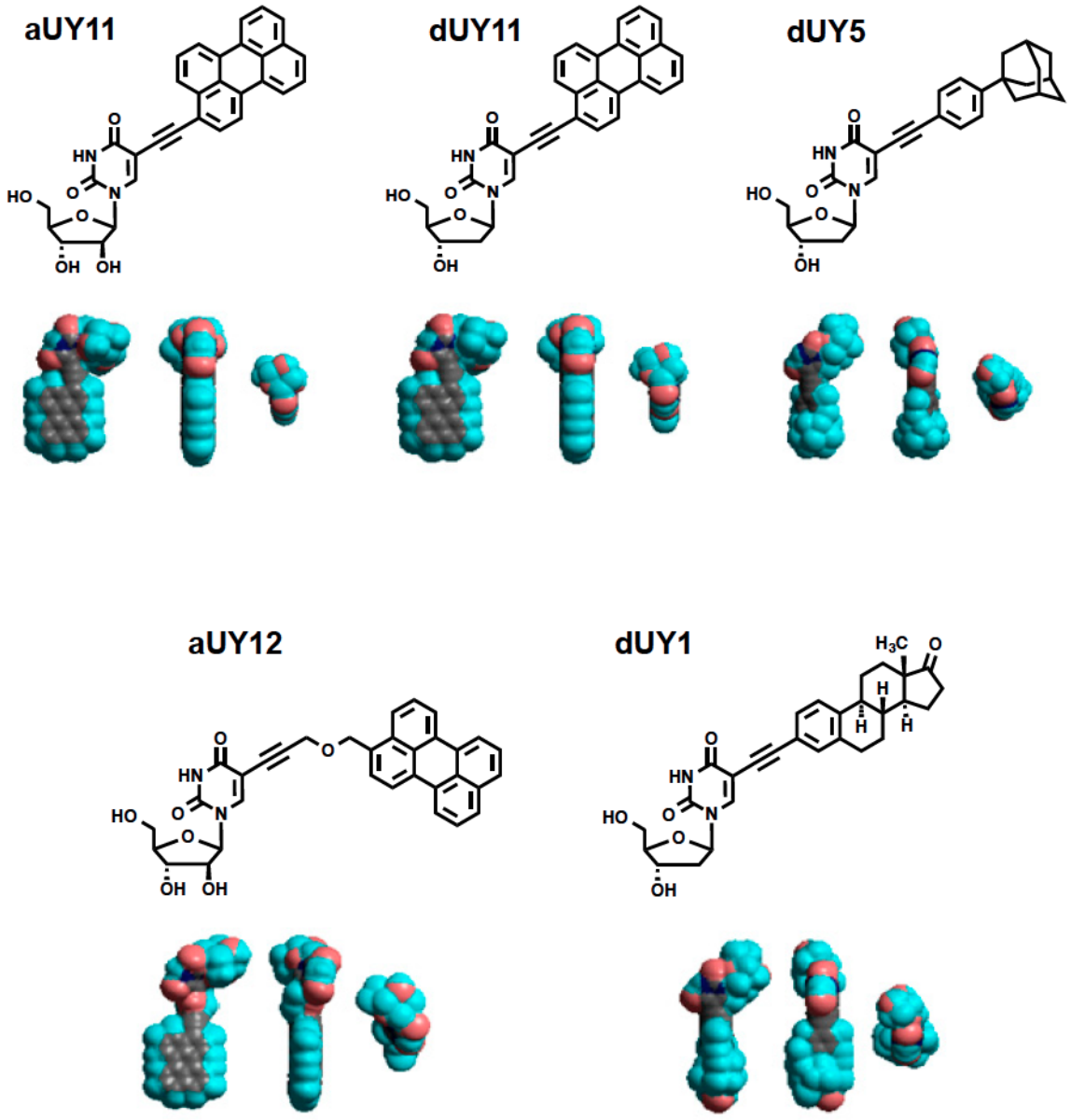

Figure 4.2. Chemical and three-dimensional structures of the RAFIs aUY11, dUY11, aUY12, dUY5 and dUY1. 3D structures are displayed in three orthogonal perspectives (gray, carbon; blue, hydrogen; red, oxygen; dark blue, nitrogen).

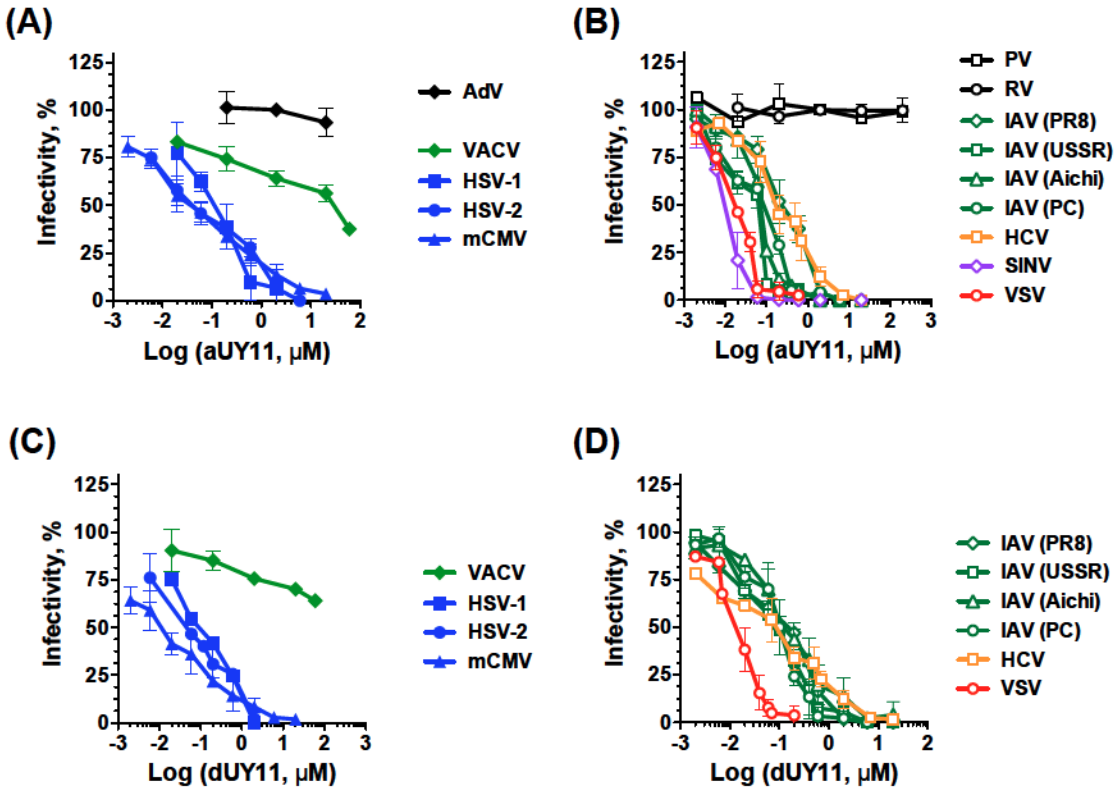

Figure 4.3. The RAFIs aUY11 and dUY11 inhibit the infectivity of enveloped but otherwise unrelated viruses. Infectivity of unrelated DNA **(A, C)** or RNA **(B, D)** viruses pre-exposed to aUY11 **(A, B)** or dUY11 **(C, D)**. Infectivity of treated virions was evaluated by plaquing efficiency or focus-forming efficiency (average ± SD; n = 3).

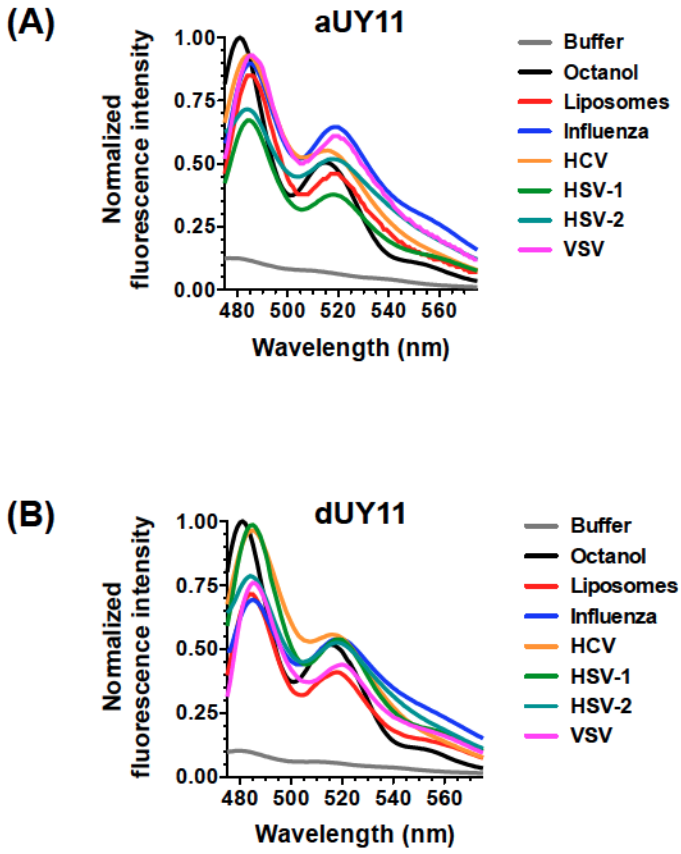

Figure 4.4. **The RAFIs aUY11 and dUY11 localize to the hydrophobic core of virion envelopes.** The emission spectra of aUY11 **(A)** and dUY11 **(B)** are most similar in virions or protein-free liposomes, and closely resemble their spectra in hydrophobic environments. aUY11 or dUY11 was added to aqueous buffer (grey) or to 1-octanol (black), to a final concentration of 48 nM or 0.48 nM, respectively. aUY11 or dUY11 (48 nM final concentration) was also added to 10^6 pfu of IAV (blue), 10^6 ffu of HCV (orange), 10^7 pfu of HSV-1 (green), 10^7 pfu of HSV-2 (teal) or 10^7 pfu of VSV (pink) or 2 nmol liposomes (red) in 2.5 mL of aqueous buffer. Fluorescence was excited at 455 nm.

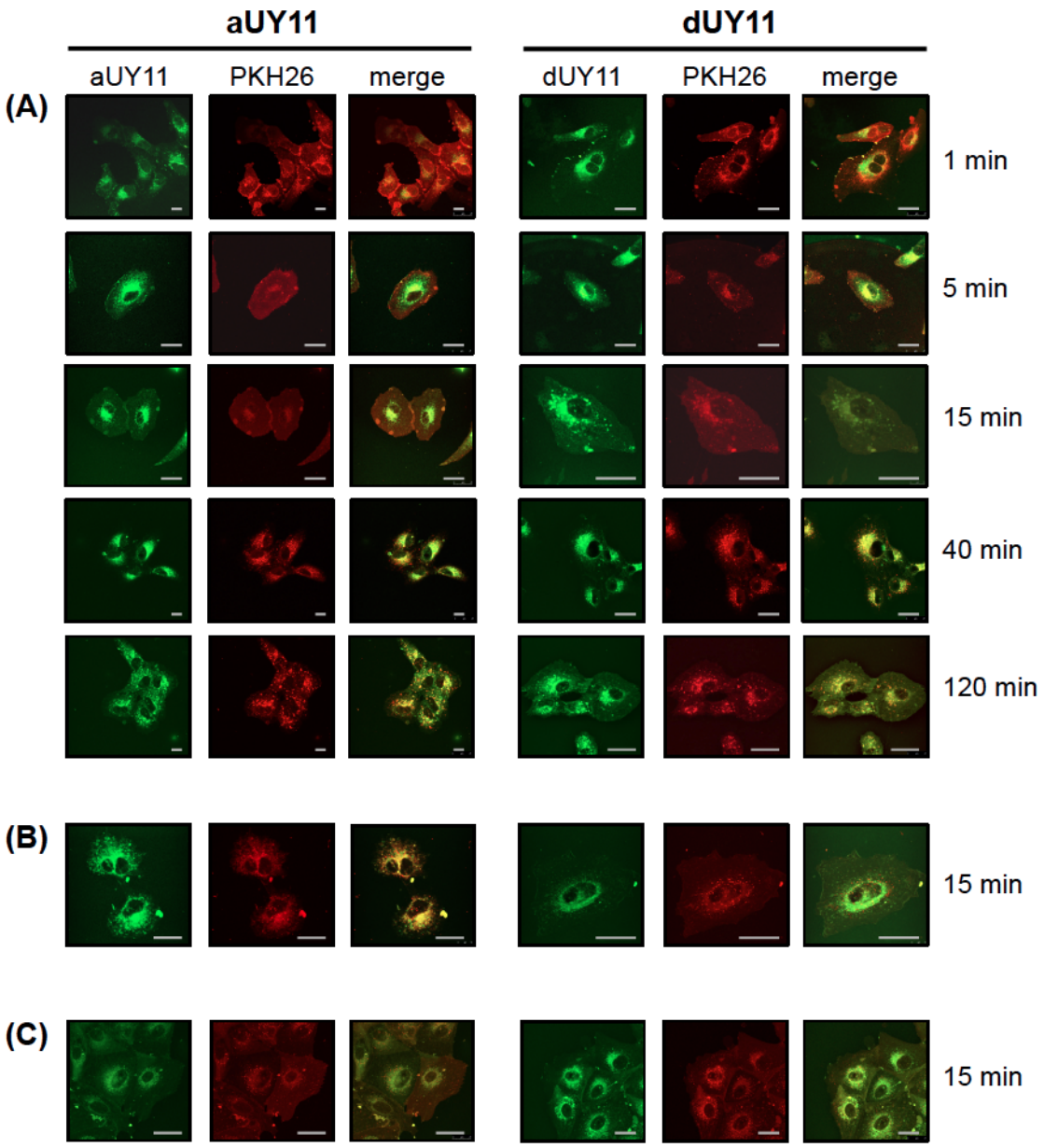

Figure 4.5. The RAFI aUY11 localizes to cellular lipid membranes. Vero **(A)**, Huh7.5 **(B)** or MDCK **(C)** cell monolayers were exposed to PKH26 general membrane dye for 10 minutes at 37°C. Cells were then washed and exposed to aUY11 (left panel) or dUY11 (right panel) for 1, 5, 15, 40, or 120 minutes at 37°C. Shown are confocal microscopy images; scale bars, 25 μm.

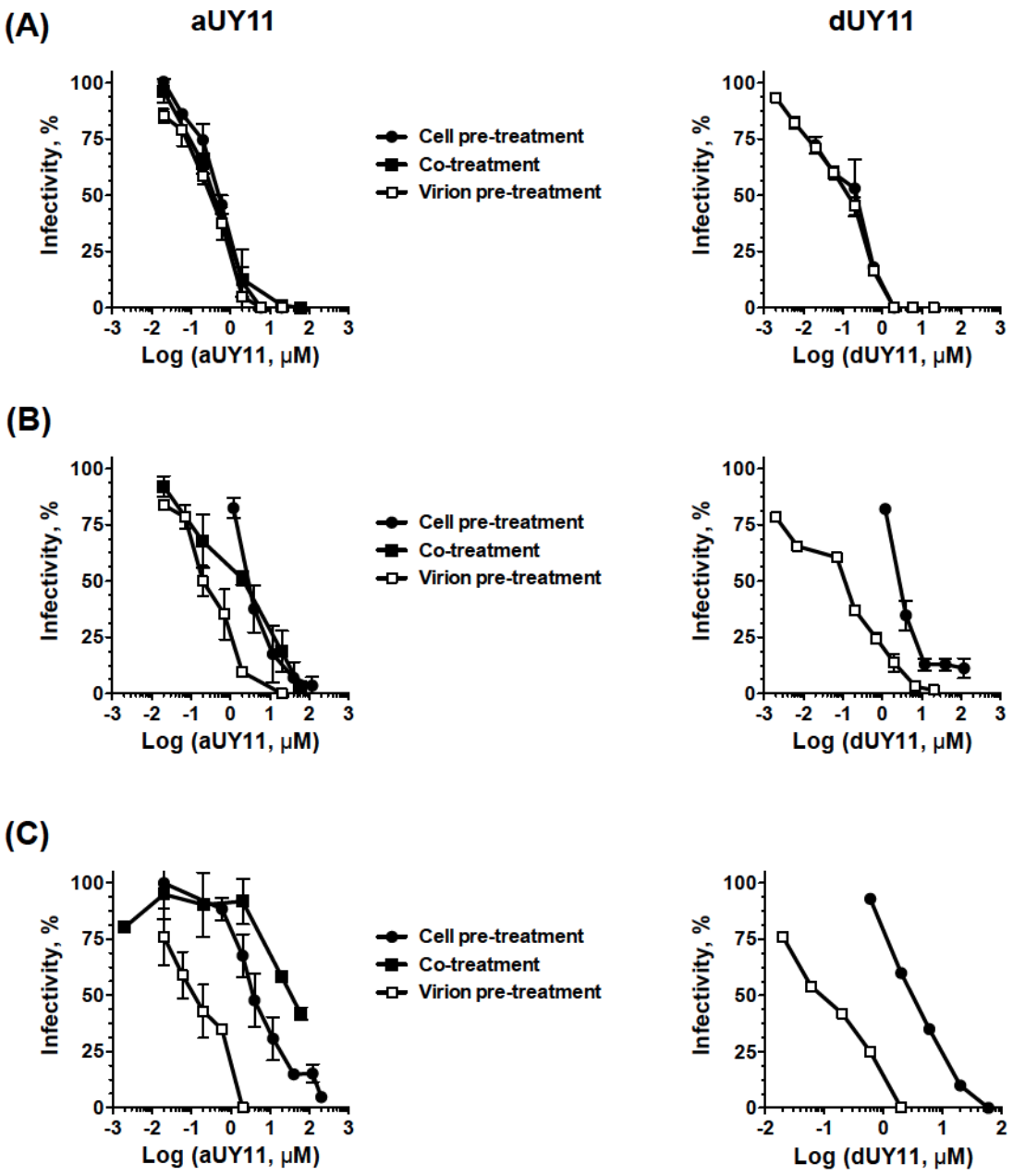

Figure 4.6. The RAFIs aUY11 and dUY11 protect cells from infection with IAV, HCV and HSV-1. MDCK, Huh7.5 or Vero cells were treated with aUY11 (left) or dUY11 (right) for 1 hour prior to infection with IAV **(A)**, HCV **(B)** or HSV-1 **(C)**, respectively (cell pre-treatment, filled circles). Alternately, virions were pre-exposed to aUY11 or dUY11 prior to infection of cells (virion pre-treatment, open squares) or exposed to aUY11 or dUY11 at the time of infection (co-treatment, filled squares). Infectivity was evaluated by plaquing or focus forming efficiency (for aUY11, average ± SD, n = 3; for dUY11, average ± range, n = 2).

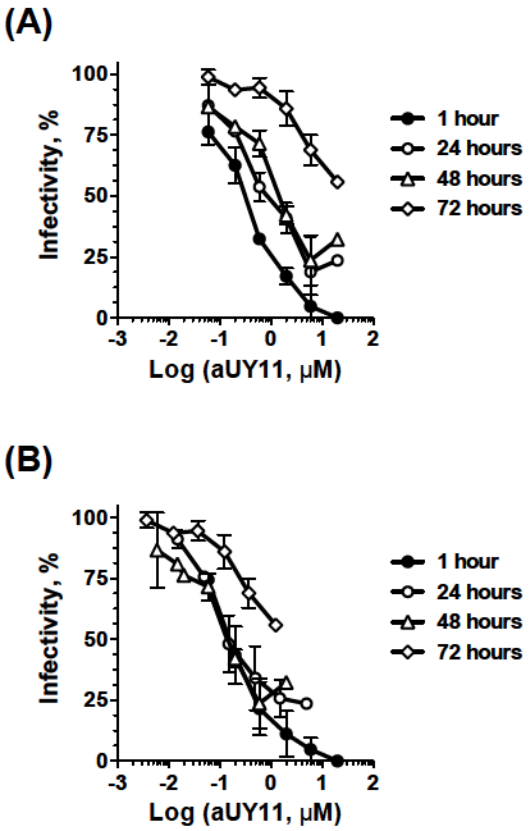

Figure 4.7. The RAFI aUY11 protects cells from infection with IAV for as long as 72 hours. MDCK cells were treated with aUY11 for 1 hour, and then washed three times and overlaid with aUY11-free DMEM-5% FBS. Cells were then infected with IAV immediately (1 hour), or after 24, 48 or 72 hours. Infectivity was evaluated by plaquing efficiency **(A)**. In **(B)**, the concentrations of aUY11 were corrected for cell division. Graphs show the average ± range, n = 2.

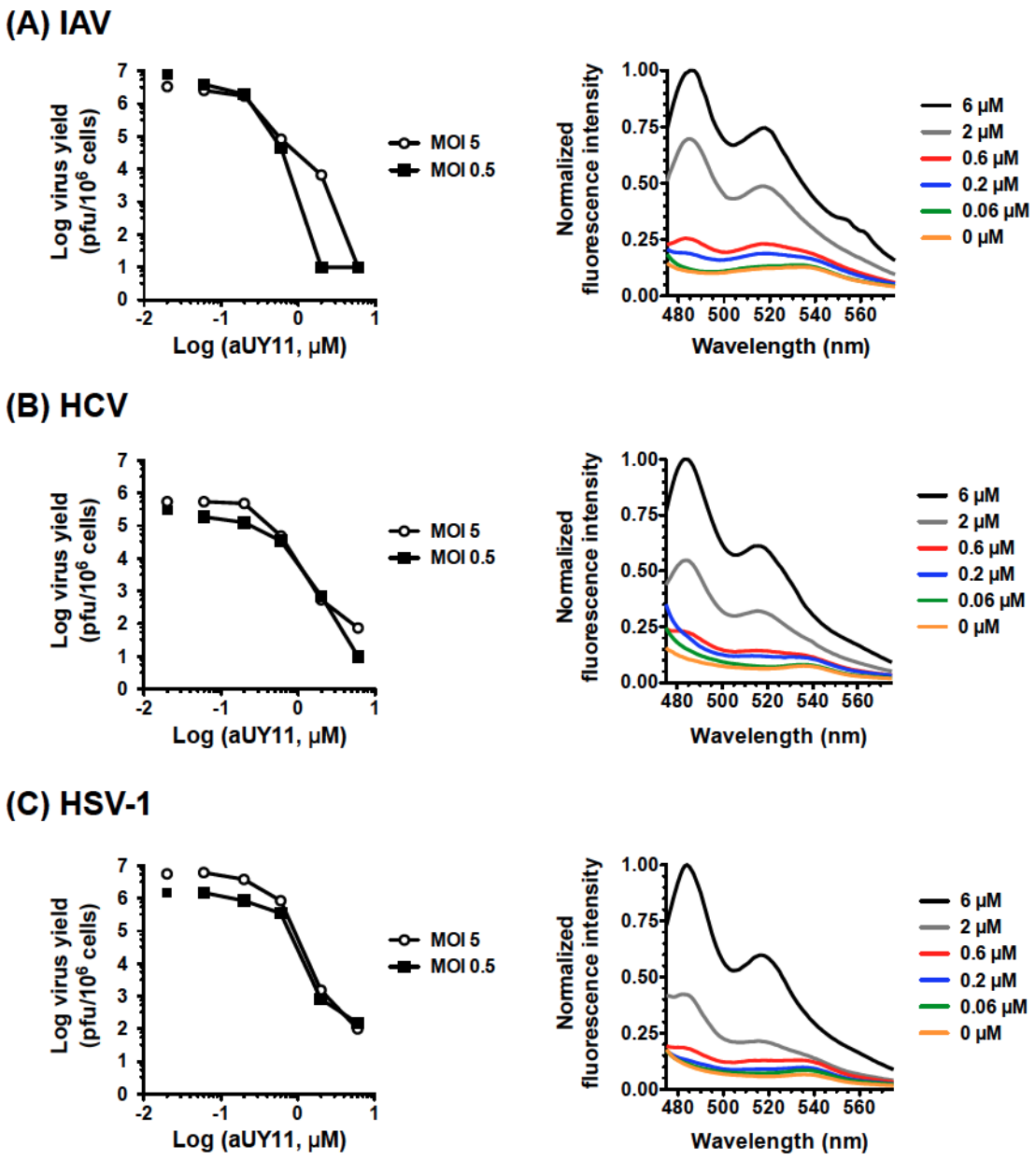

Figure 4.8. The RAFI aUY11 inhibits the infectivity of IAV, HCV and HSV-1 virions produced by infected cells. Cells infected with 5 or 0.5 PFU or FFU per cell of IAV **(A)**, HCV **(B)**, or HSV-1 **(C)** were incubated in the presence of aUY11 for 23 h (IAV and HSV-1) or 44 h (HCV). Supernatants and cell lysates were harvested and titrated for the presence of infectious virus. Harvested virions (from graphs on the left panel) for each concentration of aUY11 were tested for the presence of aUY11 by examining its fluorescence spectra (right panel). aUY11 fluorescence was excited at 455 nm.

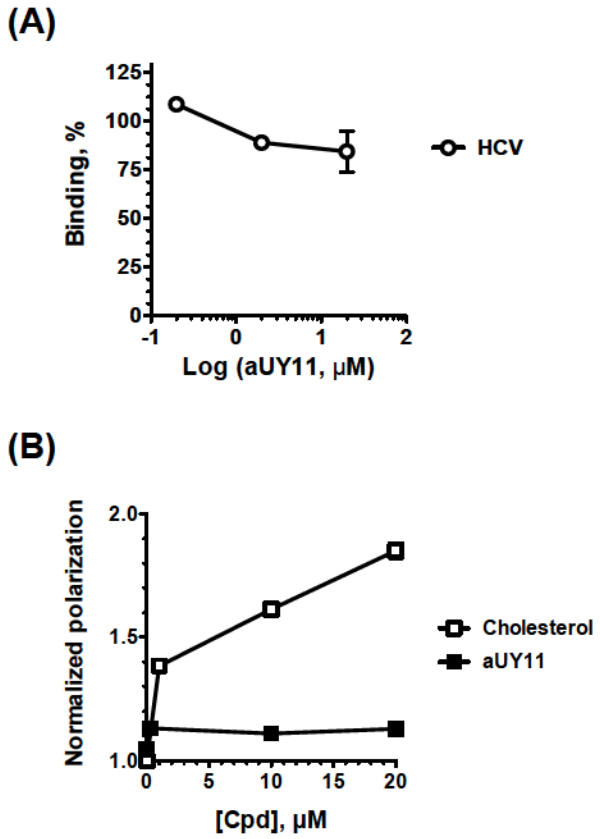

Figure 4.9. The RAFI aUY11 has only minimal effects on virion binding and membrane fluidity. (A) HCV virions pre-exposed to aUY11 were adsorbed onto Huh7.5 cells for 1 hour at 4°C. The fluorescence attached to the cells was then measured, normalized to total input, and is presented as a percentage relative to attachment of DMSO vehicle-treated control virions (average ± range; n = 2). **(B)** DPH-labelled liposomes were treated with aUY11 for 10 minutes at 37°C. DPH fluorescence polarization was measured. An increase in polarization indicates a decrease in membrane fluidity. The graph shows the result of two independent experiments (average ± range; n = 2). Several error bars are too small to be seen at this scale.

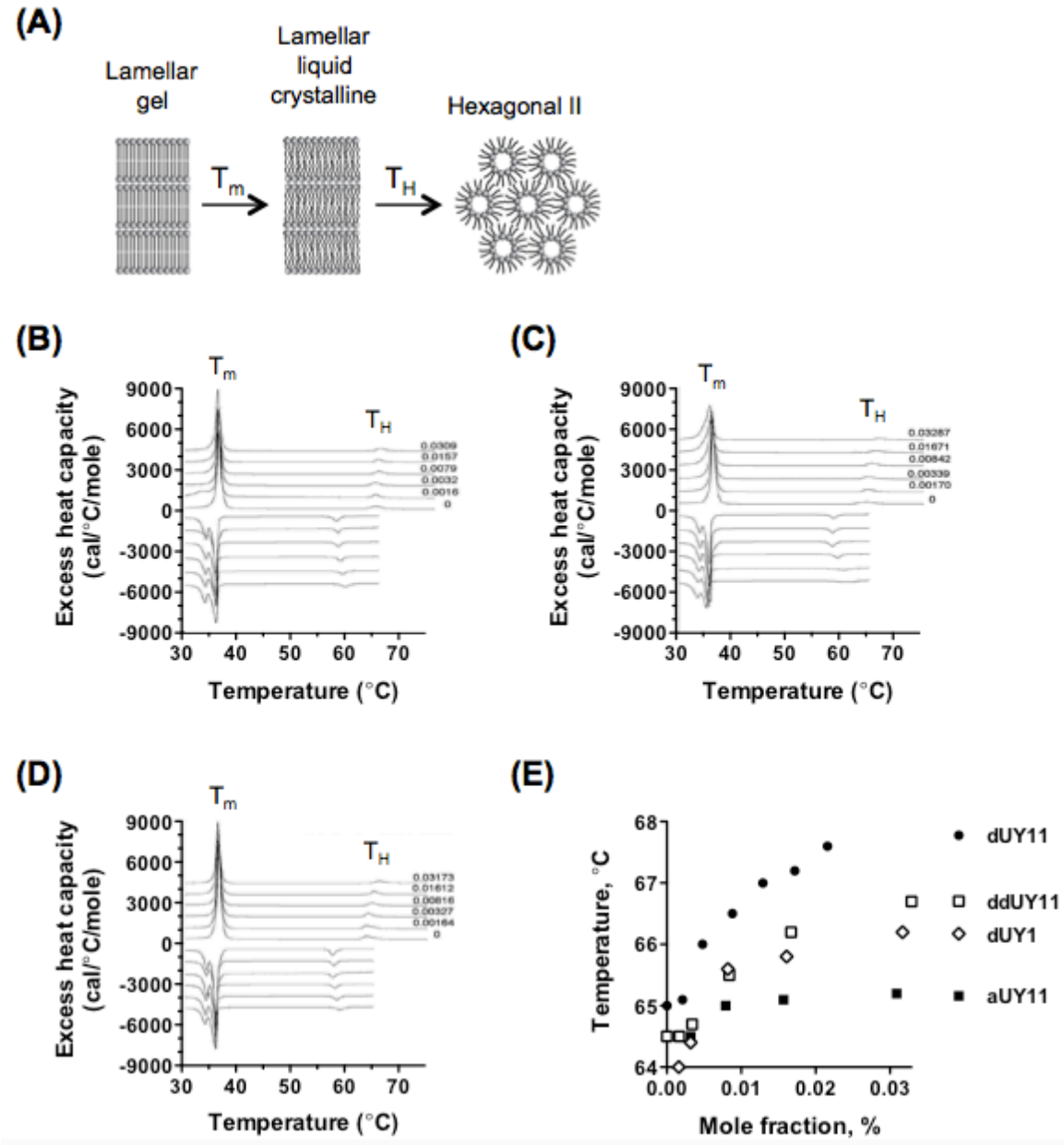

Figure 4.10. The RAFIs aUY11, dUY11, ddUY11 and dUY1 prevent the formation of negative curvature in lipid structures. (A) Schematic representation of the lipid phase transitions measured by DSC. The transition from lamellar gel to lamellar liquid crystalline occurs at melting temperature (Tm); the transition from lamellar liquid crystalline to hexagonal phase occurs at temperature T_H. Shown are DSC of the RAFIs aUY11 **(B)**, ddUY11 **(C)** and dUY1 **(D)** in DEPE. The heating scans are shown with positive values and the corresponding cooling scans with negative values. **(E)** Increasing concentrations of RAFIs in DEPE increased the transition temperature from the lamellar to the hexagonal phase. DSC experiments were conducted by Drs. Richard and Raquel Epand (McMaster University, Hamilton, Canada).

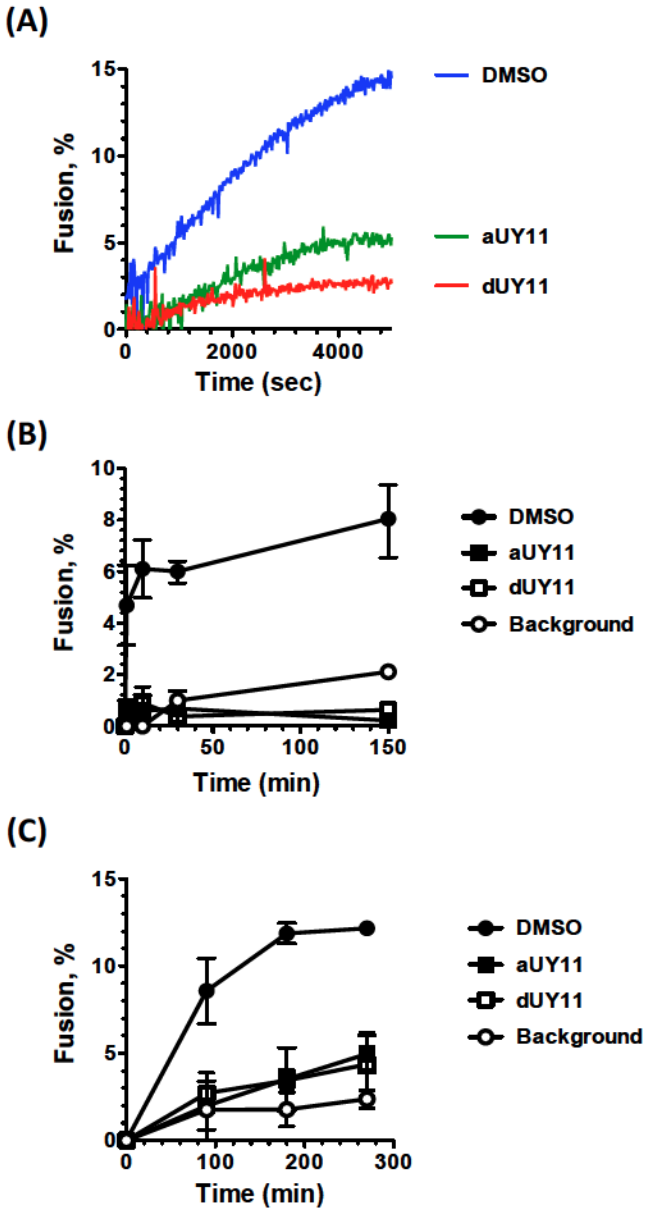

Figure 4.11. The RAFIs aUY11 and dUY11 inhibit IAV, HCV and VSV fusion. R18-labelled VSV **(A)**, IAV **(B)** or HCV **(C)** virions pre-exposed to aUY11 or dUY11 were adsorbed onto Vero, MDCK or Huh7.5 cells for 1 hour at 4°C. Fusion was triggered by increasing the temperature to 37°C and lowering the pH to 5. Fusion was evaluated by fluorescence dequenching of R18. For **(A)**, the background has been subtracted from each curve.

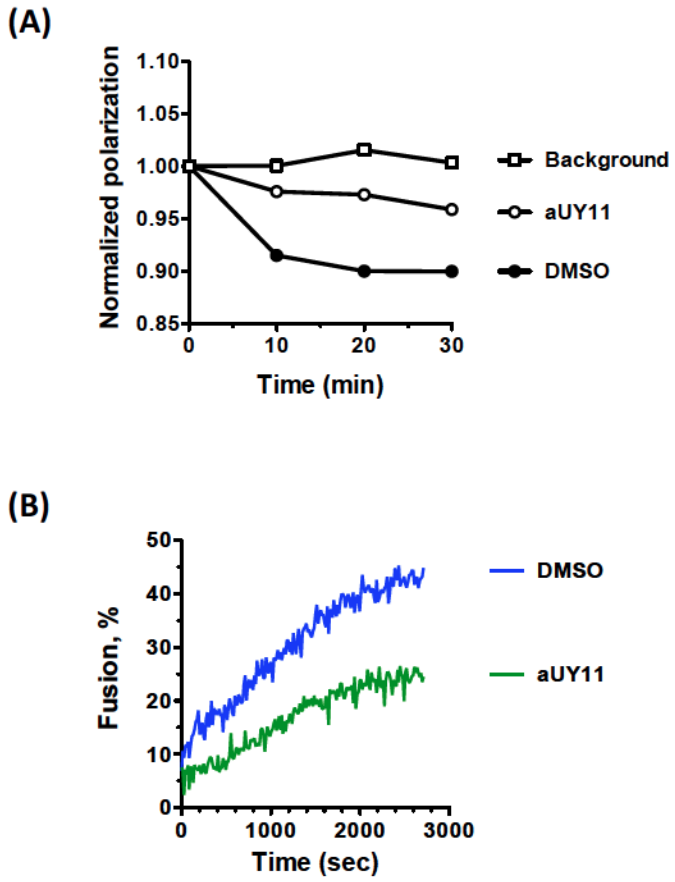

Figure 4.12. The RAFI aUY11 inhibits virus-liposome and liposome-cell fusions. **(A)** DPH-labeled VSV virions were treated with aUY11 or DMSO vehicle for 10 minutes at 37°C. DOPC/cholesterol liposomes were then added, and fusion was triggered by increasing the temperature to 37°C and lowering the pH to 5. The polarization of DPH fluorescence was then tested, as a measure of fusion. DPH is more polarized in membranes with higher rigidity/lower fluidity (such as the pre-fusion environment of the virion envelope) and less so in membranes with lower rigidity/higher fluidity (such as the post-fusion environment of the liposome membrane). **(B)** aUY11 inhibits acid-induced liposome fusion to cells. Shown is fluorescence dequenching of R18-labeled DOPC-cholesterol liposomes preexposed to 2 μM aUY11 or DMSO vehicle during acid-induced fusion to Vero cells.

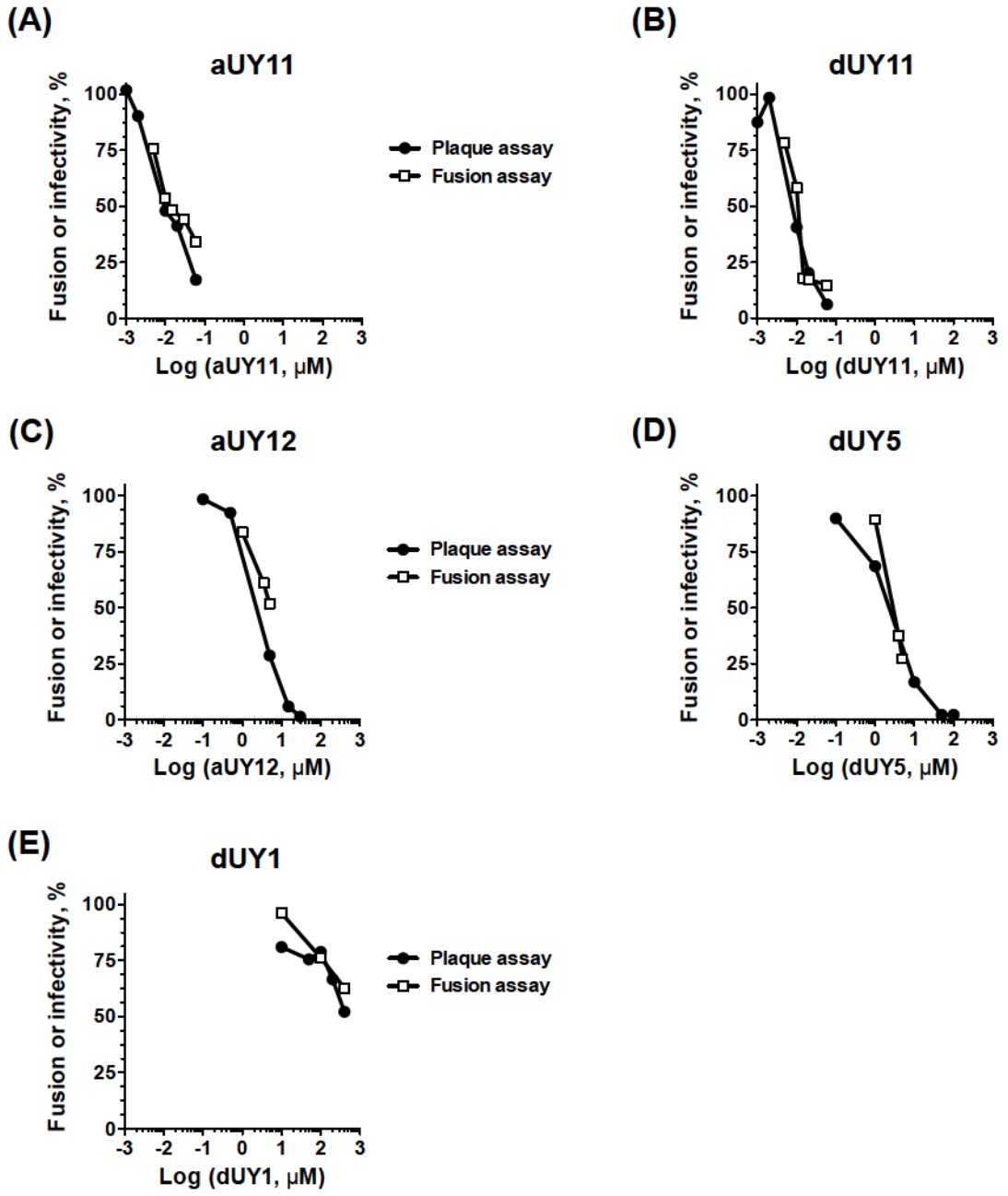

Figure 4.13. The RAFIs inhibit VSV plaquing efficiency and fusion to Vero cells at similar concentrations. Shown are comparisons of inhibition of fusion (open squares) or infectivity (filled circles) by RAFIs. For plaquing assays, approximately 200 VSV virions were exposed to increasing concentrations of aUY11 **(A)**, dUY11 **(B)**, aUY12 **(C)**, dUY5 **(D)**, or dUY1 **(E)** for 10 minutes at 37°C. The exposed virions were then used to infect 5 x 10^6 Vero cells seeded in 6-well plates. Plaquing efficiency was calculated as a percentage of plaques formed by virions exposed to DMSO vehicle.

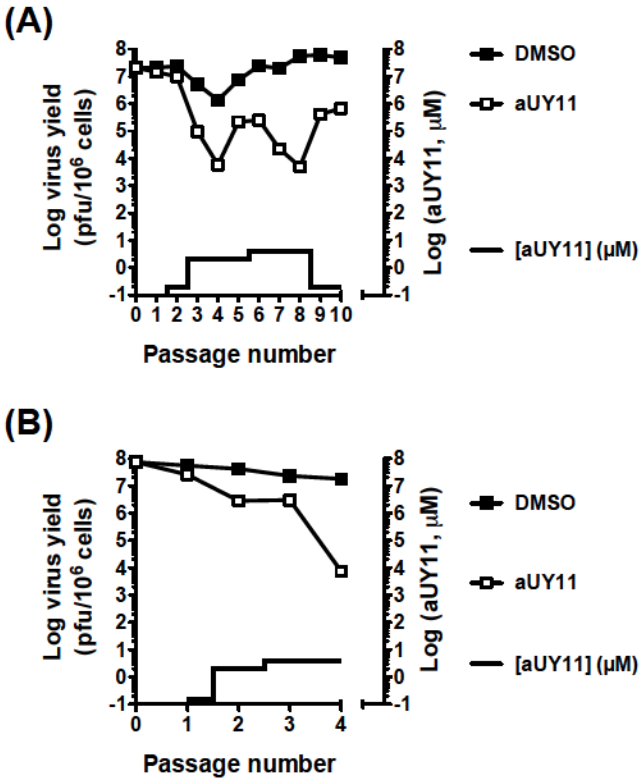

Figure 4.14. Viral titers under aUY11 selection pressure. IAV PR8 (**A**) and HSV-1 KOS (**B**) were passaged in the presence of DMSO vehicle or aUY11 and harvested at full cytopathic effect. Viral titers were evaluated by plaque assay.

CHAPTER 5: CHARACTERIZATION OF SMALL MOLECULE COMPOUNDS THAT MODULATE VIRAL OR CELLULAR MEMBRANE FLUIDITY TO INHIBIT THE INFECTIVITY OF ENVELOPED VIRUSES

Data in this chapter were published in *Gut*:

Anggakusuma, **Colpitts, C.C.**, Schang, L.M., Rachmawati, H., Frentzen, A., Pfaender, S., Behrendt, P., Brown, R.J., Bankwitz, D., Steinmann, J., Ott, M., Meuleman, P., Rice, C.M., Ploss, A., Pietschmann, T. and Steinmann, E. **(2014)** Turmeric curcumin inhibits entry of all hepatitis C virus genotypes into human liver cells. ***Gut*** *63(7):*1137-49

I performed all of the experiments described in this chapter. I wrote the sections of the Gut manuscript corresponding to my experiments.

5.1 INTRODUCTION

Appropriate fluidity of virion lipid envelopes is critical for the infectivity of enveloped viruses. It is essential for both binding and fusion. Compounds that modulate virion envelope fluidity affect their infectivity (Harada *et al.*, 2005). For example, glycyrrhizin, a natural product from licorice roots, inhibits human immunodeficiency virus (HIV)-1 fusion by decreasing HIV-1 envelope fluidity. Similarly, excess cholesterol in virion envelopes also inhibits infectivity (Harada, 2005). Increased fluidity is also deleterious for infectivity. Virions depleted of cholesterol (and thus with increased envelope fluidity) are also impaired in their fusogenic abilities (Moore *et al.*, 1978; Campbell *et al.*, 2002; Graham *et al.*, 2003; Sun and Whittaker, 2003; Huang *et al.*, 2006; Carro and Damonte, 2013).

Appropriate fluidity of cellular membranes is also important for the entry of enveloped viruses (Howell *et al.*, 1972; Breisblatt and Ohki, 1976). Many viruses require cholesterol-rich domains in cellular membranes for entry. Many enveloped viruses, such as vaccinia virus (VACV) (Chung *et al.*, 2005), varicella zoster virus (VZV) (Hambleton

et al., 2007), hepatitis C virus (HCV) (Kapadia *et al.*, 2007), severe acute respiratory syndrome (SARS)-coronavirus (Lu *et al.*, 2008) and HIV (Waheed and Freed, 2009) bind to receptors embedded within cholesterol-enriched microdomains or even fuse to these microdomains (Schroeder, 2010). Some nonenveloped viruses also require cholesterol-rich domains for cell penetration (Marjomaki *et al.*, 2002; Danthi and Chow, 2004). Compounds that disrupt these domains or modulate cellular cholesterol levels could have potential as antivirals, if cytotoxicity could be avoided. Cyclodextrins globally deplete cells of cholesterol and have broad antiviral activity. However, as expected, these activities are accompanied by the cytotoxic effects associated with cholesterol depletion (Kiss *et al.*, 2010). More subtle modifications of cholesterol-rich domains still have antiviral effects and are better tolerated. For example, some phenothiazines active against HCV localize to cellular cholesterol-rich domains and increase their local fluidity, thereby impairing HCV entry (Chamoun-Emanuelli *et al.*, 2013).

Many viruses require cholesterol-rich membrane structures within cells for replication and assembly steps beyond entry. Flaviviruses, such as HCV and West Nile virus, for example, form replication complexes on cholesterol-rich membranous web structures (Mackenzie *et al.*, 2007; Alvisi *et al.*, 2011; Chatel-Chaix and Bartenschlager, 2014). The glycoproteins of many enveloped viruses localize to cholesterol-rich domains, from which the virions are generally thought to bud (Pessin and Glaser, 1980; Scheiffele *et al.*, 1999; Manie *et al.*, 2000; Nguyen and Hildreth, 2000). Virion envelopes, therefore, are derived from specific subdomains of host cell membranes and consequently have lipid compositions distinct from that of the overall host cell membranes (Chazal and Gerlier, 2003). Under physiological conditions, the virion envelopes are mostly in the

liquid disordered phase (with some liquid ordered regions) under physiological conditions. Virion envelopes are commonly more ordered than typical cellular membranes (Polozov *et al.*, 2008). Proteins embedded within the virion envelopes further decrease the fluidity of the envelopes (Schaap *et al.*, 2012). As for any bilayer, decreased temperature or excessive sterol incorporation at physiological temperatures decrease virion envelope fluidity (Harada *et al.*, 2005; Bales and Leon, 1978).

Cholesterol content is critical for membrane fluidity. Cholesterol **(Figure 5.1)** has a tetracyclic ring system fused in the trans configuration, conferring planarity and rigidity (Ohvo-Rekila *et al.*, 2002). Cholesterol has a single hydroxyl group at carbon 3 and a hydrocarbon chain at carbon 17 (Ohvo-Rekila *et al.*, 2002). The polar hydroxyl group of cholesterol can interact with the aqueous phase or polar head groups of phospholipids and sphingolipids, whereas the steroid and hydrocarbon chain are buried in the hydrophobic core of the membrane. At physiological temperatures, which are above the gel to liquid-crystalline phase transition temperature, the resulting interactions with phospholipid fatty acid chains, and the rigid and planar shape of cholesterol, increase membrane packing (Ohvo-Rekila *et al.*, 2002), which reduces the membrane fluidity. These effects depend on the membrane composition. Overall, however, enrichment of sterols or sterol-like compounds into virion envelopes decreases envelope fluidity and inhibits infectivity.

Viruses acquire their envelopes during budding from host cell membranes. Virions themselves have no enzymes or energy sources, and therefore cannot modify the envelope composition or fluidity. In contrast, cells actively regulate the composition and fluidity of their membranes. Cholesterol is internalized from exogenous sources (low-density lipoprotein particles) by lipoprotein receptors (Brown and Goldstein, 1986). The

expression of these receptors is tightly regulated. Multiple sterol-response pathways that regulate cholesterol biosynthesis tightly control cholesterol homeostasis (Goldstein and Brown, 1990; Lange *et al.*, 2004). Perturbation of the cholesterol regulatory mechanisms affects the sterol content in membranes, thereby altering membrane fluidity. Cellular membrane fluidity also depends on the length of the fatty acid chains and their degree of unsaturation, which is regulated by cellular proteins such as lipid desaturases (Aguilar and de Mendoza, 2006).

I propose that modulators of membrane lipid bilayer fluidity can inhibit the infectivity of enveloped but otherwise unrelated viruses, including clinically important pathogens such as HCV. My objectives were to evaluate the antiviral mechanisms of viral- or host-targeted modulators of membrane fluidity. HCV was chosen as a primary model for these studies because it replicates within hepatocytes, which are the main cholesterol-synthesizing cells. Furthermore, the replication cycle of HCV is closely linked to cholesterol and lipid metabolism, as well as to intracellular membrane structures (Felmlee *et al.*, 2013).

The anti-HIV activities of the natural product glycyrrhizin (found in the roots of the licorice plant, *Glycyrrhiza glabra*) are the result of its effects on virion envelope fluidity (Harada, 2005). Glycyrrhizin is one of many secondary metabolites produced by plant species for protection against pathogens. As appropriate membrane fluidity is required by many pathogens, the production of secondary metabolites that modulate membrane fluidity may well have evolved as a broad defense mechanism against enveloped pathogens. Therefore, we sought to identify other natural products that have antiviral activity by modulating membrane fluidity. Curcumin **(Figure 5.1)**, the principal

curcuminoid produced by the roots of *Curcuma longa* (turmeric), had been identified as a modulator of the fluidity of model lipid bilayers (Barry *et al.*, 2009). Curcumin decreases membrane fluidity at physiological temperatures by inserting into lipid membranes in a transbilayer orientation (Barry *et al.*, 2009). Curcumin also interferes with the activity of many diverse unrelated membrane proteins, likely through modifications of the physical properties of membranes (Ingolfsson *et al*., 2007).

Curcumin has broad inhibitory activity against a number of enveloped viruses, including herpes simplex virus 1 (HSV-1) (Bourne *et al*., 1999; Kutluay *et al*., 2008; Zandi *et al*., 2010), HIV (Mazumder *et al*., 1995), Rift Valley fever virus (Narayanan *et al*., 2012), HCV (Kim *et al*., 2010; Chen *et al*., 2012), Japanese encephalitis virus (JEV) (Dutta *et al*., 2009), hepatitis B virus (HBV) (Rechtman *et al*., 2010), influenza A virus (IAV) (Chen *et al*., 2013) and Dengue virus (DENV) (Padilla *et al*., 2014). The antiviral mechanisms were unclear, but were proposed to involve the direct inhibition of viral replication machinery (Mazumder *et al*., 1995) or modulation of cellular signaling pathways involved in viral replication (Kutluay *et al*., 2008; Dutta *et al*., 2009; Kim *et al*., 2010; Chen *et al*., 2012). However, the virion glycoproteins involved in entry steps are also membrane proteins, inserted into virion envelopes. Surprisingly, the potential effects of curcumin on envelope fluidity had not been examined. The broad activity of curcumin against unrelated enveloped viruses, but not against nonenveloped viruses (Chen *et al.*, 2012), suggests that the target may well be the conserved virion envelope. My hypothesis was that curcumin inhibits the infectivity of HCV and other enveloped viruses by decreasing the virion envelope fluidity.

Unlike plants, mammals are not known to produce secondary metabolites as a

defensive strategy. However, innate immune mechanisms that modulate cellular metabolic pathways have evolved to contribute to pathogen defense. It would not be that surprising if mammals had also evolved broadly acting antiviral defenses targeting virion envelopes.

Cholesterol-25-hydroxylase is an interferon-stimulated protein involved in establishing an antiviral state (Liu *et al.*, 2013). Cholesterol-25-hydroxylase oxidizes cholesterol to 25-hydroxycholesterol (25HC). 25HC downregulates expression of the low-density lipoprotein receptor (LDL-R) and inhibits 3-hydroxyl-3-methyl-glutaryl-CoA reductase (HMG-CoA reductase) to decrease cellular cholesterol levels (Pezacki *et al.*, 2009). In mammalian cells, cholesterol is the most critical regulator of membrane fluidity. Therefore, my hypothesis was that induction of 25HC production inhibits HCV infectivity by modulating cellular membrane fluidity. 25HC was shown to be active against HCV replication (Pezacki *et al.*, 2009), but its specific antiviral mechanisms remain unclear. More recently, 25HC was found to inhibit the entry of unrelated enveloped viruses by interfering with viral fusion (Liu *et al.*, 2013). My objectives were to characterize the antiviral mechanisms of 25HC against HCV.

5.2 RESULTS

5.2.1 Curcumin inhibits the infectivity of HCV and other enveloped viruses. HCV, HSV-1, VSV or PV virions (~100 infectious particles) were exposed to curcumin, THC or DMSO vehicle control in serum-free medium for 10 minutes at 37°C prior to infecting Huh7.5 cell monolayers. The foci of infected cells were detected by focus-forming or plaquing efficiency, and the infectivity was expressed as a percentage of the infectivity of virions treated with vehicle control. Curcumin inhibited the infectivity of the enveloped HCV, HSV-1 and VSV (EC_{50}, 8.18 μM, 4.78 μM and 14.9 μM, respectively), but not the infectivity of the nonenveloped PV **(Figure 5.2A)**. In contrast, THC did not inhibit the infectivity of any virus, even at concentrations up to 60 μM **(Figure 5.2B)**.

Curcumin inhibits virion infectivity when virions are pre-exposed **(Figure 5.2)**. Time-of-addition experiments conducted by our collaborators (Dr. Eike Steinmann and colleagues, Twincore, Hannover, Germany) showed that curcumin did not inhibit HCV infection when cells were pre-treated, or treated after infection (Anggakusuma *et al.*, 2013). Curcumin inhibited HCV infection only when present at the time of infection (Anggakusuma *et al.*, 2013), or when virions were pre-exposed **(Figure 5.2)**, suggesting that it directly targets the virions.

Curcumin derivatives desmethoxycurcumin and bis-desmethoxycurcumin lack either one or both of the methoxy groups in the phenyl rings but have the same α, β-unsaturated ketone groups as curcumin **(Figure 5.1).** Our collaborators further showed that they also inhibit HCV infectivity (Anggakusuma *et al.*, 2013). I showed that THC, the only curcuminoid that lacks α, β-unsaturated ketone groups, did not inhibit HCV infectivity **(Figure 5.2B)**. The methoxy groups, on the other hand, were dispensable.

Therefore, we postulated that the rigidity and planarity of curcuminoids, conferred by the α, β-unsaturated ketone groups, was critical for their antiviral activity.

5.2.2 Curcumin decreases the fluidity of liposome membranes and virion envelopes. Other rigid and planar compounds, such as cholesterol, decrease membrane fluidity. I tested the effects of curcumin, THC and cholesterol on membrane fluidity using DPH fluorescence polarization (Lentz, 1989). The polarization of DPH increases as membrane fluidity decreases. The addition of curcumin to liposomes increased DPH polarization. As expected, so did the positive control, cholesterol (**Figure 5.3A**). Curcumin also decreased the fluidity of HCV and VSV envelopes **(Figure 5.3B and 5.3C)**, whereas THC did not affect the fluidity of any tested membranes **(Figure 5.3)**. Due the extended conjugation of curcumin, it has a more planar shape than THC. The planar shape of curcumin is consistent with the shape of other compounds that decrease membrane fluidity, such as cholesterol.

5.2.3 Curcumin inhibits HCV binding to Huh7.5 cells. Binding requires appropriate membrane fluidity to allow for movements of viral glycoproteins in the envelope. If the antiviral activities of curcumin were a result of its effects on fluidity, then it should affect virion binding. I next evaluated the effects of curcumin on HCV virion attachment. R18-labelled HCV virions pre-exposed to curcumin, THC or DMSO vehicle, were adsorbed onto Huh7.5 cell monolayers at 4°C. Unbound virions were removed by three washes, and the level of R18 fluorescence bound to cells was measured. Binding was expressed as a percentage relative to the binding of the DMSO vehicle control. Curcumin inhibited HCV binding in the absence or presence of serum (IC_{50}, 35.1 μM or 11.4 μM, respectively), whereas THC did not **(Figure 5.4A and 5.4B)**.

5.2.4 Curcumin inhibits HCV fusion to background levels. Like binding, viral fusion depends on appropriate membrane fluidity. Therefore, I tested the effects of curcumin on the fusion of HCV to Huh7.5 cells. R18-labelled HCV JFH-1 virions were exposed to curcumin, THC or DMSO vehicle prior to mixing with Huh7.5 cells. Fluorescence was dequenched by approximately 18% for HCV virions treated with DMSO vehicle, but by only 8% for HCV virions treated with 200 or 20 μM curcumin (EC_{99} or EC_{90} in infectivity assays, respectively) **(Figure 5.55A)**. This low level of dequenching overlapped with the background dequenching at neutral pH in the assays **(Figure 5.5A)**. As expected, THC did not inhibit HCV fusion (**Figure 5.5B**). These results could indicate that curcumin inhibits fusion directly or as a result of inhibiting attachment. To test these possibilities, virions were treated with curcumin following virion attachment at 4°C. Curcumin also inhibited fusion to background levels under these conditions (**Figure 5.5A**).

5.2.5 The cellular metabolite 25-hydroxycholesterol inhibits HCV infectivity. Curcumin, a plant natural product, inhibits viral infectivity by modulating membrane fluidity. Therefore, we proposed that mammalian cells could have similar natural antiviral defenses modulating virion membrane fluidity. Cholesterol metabolism is critical for the maintenance of membrane fluidity in cells. Therefore, we tested 25HC, a cholesterol metabolite induced in response to interferon and with known antiviral properties (Liu *et al.*, 2013). HCV virions were pre-exposed to 25HC prior to infection of Huh7.5 cells, and focus formation was evaluated 72 hours later by immunocytochemistry. Pre-treatment of the virions inhibited their infectivity to cells (EC_{50}, 4.31 μM) (**Figure 5.6**), at similar concentrations as curcumin did (EC_{50}, 8.18 μM) **(Figure 5.2)**.

5.2.6 25HC decreases membrane fluidity, but does not inhibit HCV fusion when virions are pre-exposed. DPH-labeled HCV virions were exposed to 25HC, cholesterol, curcumin or vehicle control. 25HC exposure increased the fluorescence polarization of the DPH probe, demonstrating a decrease in the envelope fluidity **(Figure 5.7A).** However, 25HC decreased the envelope fluidity to a lesser extent than cholesterol or curcumin did (**Figure 5.7A**, $P<0.01$ or $P<0.05$, respectively, two-tailed unpaired *t*-test). It was unclear if this degree of fluidity decrease could affect fusion. I thus tested the effects of 25HC on fusion. R18-labelled HCV JFH-1 virions were exposed to 25HC or ethanol vehicle prior to mixing with Huh7.5 cells. 25HC did not inhibit HCV fusion when virions were pre-exposed, and only minimally inhibited fusion when the cells were pre-exposed (**Figure 5.7B**). Fusion was inhibited the most when the cells were treated after virion binding (**Figure 5.7B**), suggesting a cellular target, or a viral target exposed after virion binding to the cell. It is also possible that 25HC is rapidly metabolized (or stripped from the virions) upon exposure to cells. In such cases, 25HC would only affect fusion if added at the time of fusion.

5.2.7 25HC inhibits the formation of HCV foci when cells are pre-treated, or treated after infection. 25HC modulates cholesterol levels in cells, which could affect HCV infectivity, replication, assembly or the infectivity of the progeny virions. Huh7.5 cells were pre-exposed to 25HC for 1 hour prior to infection, or cells were infected and then treated with 25HC for 4 hours or 72 hours. Pre-treatment of cells inhibited infection with HCV (EC_{50}, 2.00 μM) (**Figure 5.8A**). Similarly, 25HC inhibited focus formation when cells were treated after infection for either 4 or 72 hours (EC_{50}, 1.17 μM or 0.607 μM, respectively) (**Figure 5.8B**). The mechanisms of 25HC therefore differ from those of

curcumin, which was only effective when virions were pre-exposed or when added at the time of infection (Anggakusuma *et al.*, 2013).

5.2.8 25HC inhibits the production of infectious HCV particles. Huh7.5 cells were infected with 3 ffu/cell of HCV JFH-1 and incubated in the presence of 6 μM 25HC. Supernatant and cell-associated virions were harvested after 12, 24, 48 and 72 hours. 25HC treatment inhibited the production of released and cell-associated infectious virions **(Figure 5.9A and 5.9B)**. I then compared the infectious particles (FFU) and HCV RNA copies present in the infected cells and supernatants. 25HC caused a similar decrease in the cell-associated FFU and RNA copies (**Figure 5.9C**). However, 25HC inhibited the infectivity of the released particles to a greater extent than it inhibited the release of viral RNA copies into the supernatant **(Figure 5.9C).** There was a 10-fold decrease in the specific infectivity of cell-associated virions, and approximately a 500-fold decrease in the specific infectivity of virions released into the supernatant.

5.2.9 HCV virions produced by 25HC-treated cells are still able to bind and fuse.

I next evaluated the cholesterol levels in cells treated with 25HC, and in virions produced by the treated cells. Huh7.5 cells were infected with 3 ffu/cell of HCV and treated with 6 μM, 2 μM, 0.6 μM 25HC or vehicle control for 72 hours. Virions harvested from the supernatant were purified through a sucrose cushion. Cholesterol levels in virions or cells were determined using the Amplex Red cholesterol assay, according to manufacturer instructions. As expected, 25HC treatment decreased both cellular cholesterol levels and virion-associated cholesterol in the supernatant **(Figure 5.10A)**. Although total virion-associated cholesterol levels decreased, they were actually increased relative to the RNA copies present **(Figure 5.10B)**. However, the overall fluidity of the envelopes of the

virions produced by cells treated with 25HC was similar to the vehicle-treated control **(Figure 5.10C)**.

HCV virion-associated cholesterol is critical for infectivity (Aizaki *et al.*, 2008; Yamamoto *et al.*, 2011). Since 25HC treatment decreases cellular cholesterol levels, I proposed as a model that less cholesterol would be incorporated into HCV virions, thereby inhibiting the infectivity of the progeny virions. To characterize the infectivity defect of virions produced by 25HC-treated cells, I tested their ability to bind and fuse to cells. Virions produced from the 25HC-treated cells were harvested after 72 hours and labeled with R18 to evaluate binding and fusion. Neither binding **(Figure 5.11A)** nor fusion (induced at the plasma membrane by lowered pH) **(Figure 5.11B)** was inhibited.

5.3 DISCUSSION

In these studies, I showed that curcumin acts mainly on virion envelopes to decrease their fluidity, impairing both binding and fusion. In contrast, the main antiviral effects of 25HC result from modulation of cellular factors and not direct activities on virions.

Curcumin had been recognized previously as a broad inhibitor of the infectivity of enveloped viruses (Chen *et al.*, 2013). Curcumin inhibited the infectivity of representative enveloped viruses (IAV, JEV, DENV, and a herpesvirus, pseudorabies virus) when exposed to virions at the time of infection. However, curcumin did not inhibit replication if added after entry (Chen *et al.*, 2013). EC_{50} in these studies were from ~1-5 μM, in the same range that I found for HCV, HSV-1 and vesicular stomatitis virus (VSV). Curcumin inhibited the infectivity of VACV, but only by 70% at the highest concentration tested (60 μM) (Chen *et al.*, 2013). As for other compounds that target the lipid envelope (*e.g.*, aUY11, **Chapter 4**), the decreased efficacy against VACV may be the result of its second envelope, which is shed by nonfusogenic mechanisms prior to fusion (Law *et al.*, 2006). Curcumin was not active against a nonenveloped virus, enterovirus 71, which is consistent with its lack of activity against the nonenveloped PV as presented in this thesis **(Figure 5.2A)**. Curcumin (60 μM) disrupted the integrity of liposomal membranes and increased their permeability (Chen *et al.*, 2013), but its specific effects on membrane fluidity were not tested. Changes in membrane fluidity often affect permeability (Lande *et al.*, 1995). The inhibitory effects of curcumin on IAV infectivity were irreversible (Chen *et al.*, 2013), as expected from its affinity for

membrane bilayers. Curcumin interfered with the HA activity of IAV (Chen *et al.*, 2010), as expected for a modulator of envelope fluidity.

Other groups reported that curcumin was active against other enveloped viruses, such as HIV, HSV-1 and HBV. Curcumin inhibited HIV replication, perhaps through interactions with viral integrase or protease (Mazumder *et al.*, 1995; Vajragupta *et al.*, 2005). However, the antiviral activities of curcumin have been mainly attributed to modulation of cellular signaling pathways. Curcumin modulates signaling through several pathways, including the mitogen-activated protein kinase (Squires *et al.*, 2003), phosphoinositide 3-kinase/protein kinase B/Akt (Chaudhary and Hruska, 2003) and nuclear factor kappa B (Bharti *et al.*, 2003) pathways. These pathways are involved in the replication of viruses such as IAV (Nimmerjahn *et al.*, 2004; Hirata *et al.*, 2014). Curcumin was also reported to inhibit the replication of HCV replicons by affecting cell signaling, through mechanisms proposed to involve suppression of the Akt-SREBP-1 pathway (Kim *et al.*, 2010). Membrane-bound receptors or activators induce signaling through these pathways. Therefore, modulation of membrane fluidity may affect downstream activities of these signaling pathways. The effects of curcumin against HSV-1 involved inhibition of VP16-dependent transcription activity by interfering with appropriate recruitment of RNA polymerase II to immediate-early gene promoters (Kutluay *et al.*, 2008). However, the mechanisms are not clear. Curcumin was even reported to be active against one nonenveloped virus, coxsackievirus B3 (CBV3), but did not affect viral binding (Si *et al.*, 2007). Instead, the antiviral activities of curcumin were attributed to modulation of the ubiquitin-proteasome system. Curcumin promotes the

polyubiquitination of cellular proteins, thereby decreasing the free ubiquitin pools in cells that are required for the replication of CVB3 (Si *et al.*, 2007).

None of the studies cited in the previous paragraph directly tested the effects of curcumin on virion infectivity. Typically, curcumin was added to cell cultures before infection or during the course of infection. The effects on viral replication or yield could be the result of activities against cellular factors as proposed, or alternatively could result from the direct effects on virion infectivity during the early stages of infection. Time-of-addition studies should be used to differentiate between direct effects on virions and potential effects on cellular factors. In this thesis, I showed that curcumin directly inhibits the infectivity of unrelated enveloped viruses HCV, HSV-1 and VSV **(Figure 5.2A).** I also showed that curcumin directly decreases the fluidity of virion envelopes **(Figures 5.3B and 5.3C)** to inhibit binding and fusion.

Glycyrrhizin, the major component of licorice root extract, is another natural product with broad antiviral effects and which modulates membrane fluidity. Glycyrrhizin inhibits the infectivity of IAV (Wolkerstorfer *et al.*, 2009), HIV-1 (Harada, 2005), hepatitis A virus (HAV) (Crance *et al.*, 1994) and SARS-CoV (Hoever *et al.*, 2005) by targeting entry steps. Like cholesterol and curcumin, glycyrrhizin decreases membrane fluidity. This effect is responsible for its inhibitory effects on HIV fusion (Harada, 2005). Unexpectedly, glycyrrhizin only inhibited entry of HCV pseudoparticles at high micromolar concentrations (as measured by luciferase activity after 48 hours). However, direct effects on HCV virion infectivity were not tested (Matsumoto *et al.*, 2013). Glycyrrhizin was shown to inhibit the release of infectious HCV particles, without affecting cell-associated infectivity (Matsumoto *et al.*, 2013). Glycyrrhizin treatment

resulted in the accumulation of HCV core protein on lipid droplets (the platform for virion assembly) and on endoplasmic reticulum attached to lipid droplets (Matsumoto *et al.*, 2013). The effects of glycyrrhizin on release of infectious HCV particles were attributed to inhibition of phospholipase A2, a known target of glycyrrhizin (Okimasu *et al.*, 1983). In part, the inhibitory effects of glycyrrhizin on PLA2 are the result of its effects on the physical state of the membrane (which is the PLA2 substrate) (Okimasu *et al.*, 1983). Glycyrrhizin may well also affect the composition or fluidity of intracellular membrane compartments to contribute to the inhibition of the release of infectious HCV particles. Of course, other mechanisms are also possible, and other specific inhibitors of PLA2 also affected HCV secretion (Matsumoto *et al.*, 2013).

Curcumin and glycyrrhizin are two examples of plant natural products that target lipid membranes. Not surprisingly, the mammalian innate immune system has evolved similar antiviral approaches that modulate the lipid composition and fluidity of membranes. Interferon-stimulated genes (ISGs) encode proteins with activities that generate a general antiviral state in cells. One such ISG encodes cholesterol-25-hydroxylase, which oxidizes cholesterol to 25HC (Park and Scott, 2010). 25HC is a regulatory factor involved in cholesterol homeostasis **(Figure 5.12)**. 25HC suppresses SREBP-2, which regulates the sterol biosynthesis pathway (Brown and Goldstein, 1999). It also activates the liver X receptor (LXR), a nuclear receptor which downregulates the LDL receptor under conditions of excess cholesterol (Ma *et al.*, 2008). 25HC also suppresses the mevalonate pathway by inhibiting the critical regulatory enzyme, HMG-CoA reductase (Brown and Goldstein, 1997; Pezacki *et al.*, 2009). 25HC also downregulates expression of the LDL receptor, which decreases the uptake of exogenous

cholesterol into cells (Pezacki *et al.*, 2009). The overall effects of 25HC result in inhibition of HCV infection (Su *et al.*, 2002; Pezacki *et al.*, 2009; Owen *et al.*, 2009).

25HC was only recently connected to interferon-mediated antiviral immunity (Blanc *et al.*, 2013; Liu *et al.*, 2013). Induction of 25HC production inhibited the infectivity of enveloped viruses (IAV, HSV-1, VZV, HIV-1, VSV, Ebola virus, Nipah virus and Rift Valley fever virus) but not that of a nonenveloped virus, adenovirus (Blanc *et al.*, 2013; Liu *et al.*, 2013; Gold *et al.*, 2014). 25HC was also shown to amplify inflammatory signalling, thereby modulating immune responses (Gold *et al.*, 2014). Blanc *et al*. found that 25HC acted by different mechanisms for different viruses. Its effects also depended on the cell type, suggesting effects on cellular factors (Blanc *et al.*, 2013). Liu *et al*. characterized the effects of 25HC on viral entry. They proposed that 25HC blocked the fusion of HIV and VSV by altering the properties of the host cell membrane (Liu *et al.*, 2013).

My findings in the context of HCV are in agreement with the published data. Although 25HC did inhibit HCV infectivity when virions were pre-exposed, it was tenfold more potent when cells were pre-treated, or treated after infection. Therefore, the main antiviral mechanisms of 25HC likely involve effects on cellular factors during fusion or subsequent replication steps, particularly in the production and secretion of infectious virions. Most notably, HCV virions produced by 25HC-treated cells had decreased specific infectivity **(Figure 5.9C)**, suggesting that the progeny virions were defective in their ability to infect cells. Virions produced by 25HC-treated cells were still able to bind and fuse to cells normally when fusion was induced at the plasma membrane by exposure to low pH **(Figure 5.10A and 5.10B)**. The cholesterol levels relative to the

RNA copies in virions produced by 25HC-treated cells were increased **(Figure 5.11B)**, although the overall fluidity of the virion envelopes was unaffected by 25HC treatment **(Figure 5.11C)**.

Direct exposure of HCV virions to 25HC decreased the envelope fluidity. However, 25HC decreased HCV envelope fluidity to a lesser extent than either cholesterol or curcumin **(Figure 5.7A)**, and the effect was not sufficient to inhibit infectivity. Cholesterol and curcumin are both planar and rigid, and insert similarly into membranes in a transbilayer orientation (Barry *et al.*, 2009). Both induce ordering in membranes, which contributes to decreased fluidity (Barry *et al.*, 2009). In contrast, 25HC has a bent shape and orients in membranes differently from cholesterol, with the sterol tail angled towards the bilayer surface such that both hydroxyl groups interact with phospholipid headgroups (Olsen *et al.*, 2009). 25HC also alters membrane structure in different ways from cholesterol (Olsen *et al*., 2011). For example, oxysterols such as 25HC are thought to increase membrane permeability and induce membrane expansion or membrane thinning by forming a network of hydrogen bonded oxysterols (Olsen *et al*., 2012). Such perturbations in the membrane could induce packing of cholesterol molecules to generate localized regions of decreased fluidity within the membrane. However, the potential effects of 25HC on membrane fluidity have not been fully characterized.

Alterations of host cell lipid and cholesterol metabolism are known to disrupt HCV replication complexes (Sagan *et al.*, 2006). HCV replication relies on appropriate cholesterol content in intracellular membranes, particularly for the formation of membranous webs (where replication occurs) and lipid droplet integrity (where assembly

occurs). Inappropriate fluidity of these membrane structures could impair genome replication, through improper localization of viral and cellular proteins. It could also result in retention of HCV proteins on lipid droplets, as in glycyrrhizin-treated cells (Matsumoto *et al.*, 2013).

Other innate immune mechanisms targeting cellular cholesterol homeostasis have been described. Interferon-inducible transmembrane (IFITM) proteins also inhibit the entry of several unrelated enveloped viruses (Bailey *et al.*, 2012; Brass *et al.*, 2009; Feeley *et al.*, 2011; Huang *et al.*, 2011). Several IFITMs were shown to interact with two oxysterol regulators (vehicle-associated membrane protein-associated protein A and oxysterol-binding protein) involved in cholesterol homeostasis (Amini-Bavil-Olyaee *et al.*, 2013). These interactions resulted in accumulation of cholesterol in endosomal compartments and blocked viral entry into the cytosol (Amini-Bavil-Olyaee *et al.*, 2013). Consistently, IFITM-mediated inhibition of viral entry could be bypassed by inducing viral fusion at the plasma membrane (Huang *et al.*, 2011), as I found for 25HC. Since 25HC and other oxysterols are known to trigger cholesterol trafficking from the plasma membrane (Olsen *et al.*, 2011), 25HC-induced accumulation of cholesterol in intracellular compartments may block viral entry by similar mechanisms as the IFITMs.

Curcumin and 25HC are not ideal drug candidates. Their pharmacological properties are unfavourable for further development as drugs. Curcumin is not stable in aqueous solution under physiological conditions, being readily degraded to ferulic acid, feruloylmethane, vanillin and acetone (Anand *et al.*, 2007). Curcumin has low bioavailability. The levels of curcumin in the plasma reach only ~10 nM in patients administered several grams of curcumin per day (Anand *et al.*, 2007). Incorporation of

curcumin into liposomes improves its stability (Barry *et al.*, 2009) and confers enhanced clinical efficacy, at least in cancer trials (Wang *et al.*, 2008a). Novel delivery strategies, such as nanoparticles, may further improve the bioavailability of curcumin. 25HC is likely too rapidly metabolized to be useful as a drug (Taylor and Kandutsch, 1989). 25HC also broadly disrupts cellular cholesterol homeostasis and would likely affect too many signaling pathways, resulting in cytotoxic effects (Clare *et al.*, 1995).

Although curcumin and 25HC are not drug candidates themselves, they are useful as probes to characterize the requirements for appropriate membrane fluidity during viral entry and subsequent replication steps. Identification of their antiviral mechanisms may lead to the rational design of small molecules that modulate membrane fluidity and lipid composition. Such molecules could be designed to selectively affect viral replication steps, with enhanced antiviral activities and better pharmacological profiles.

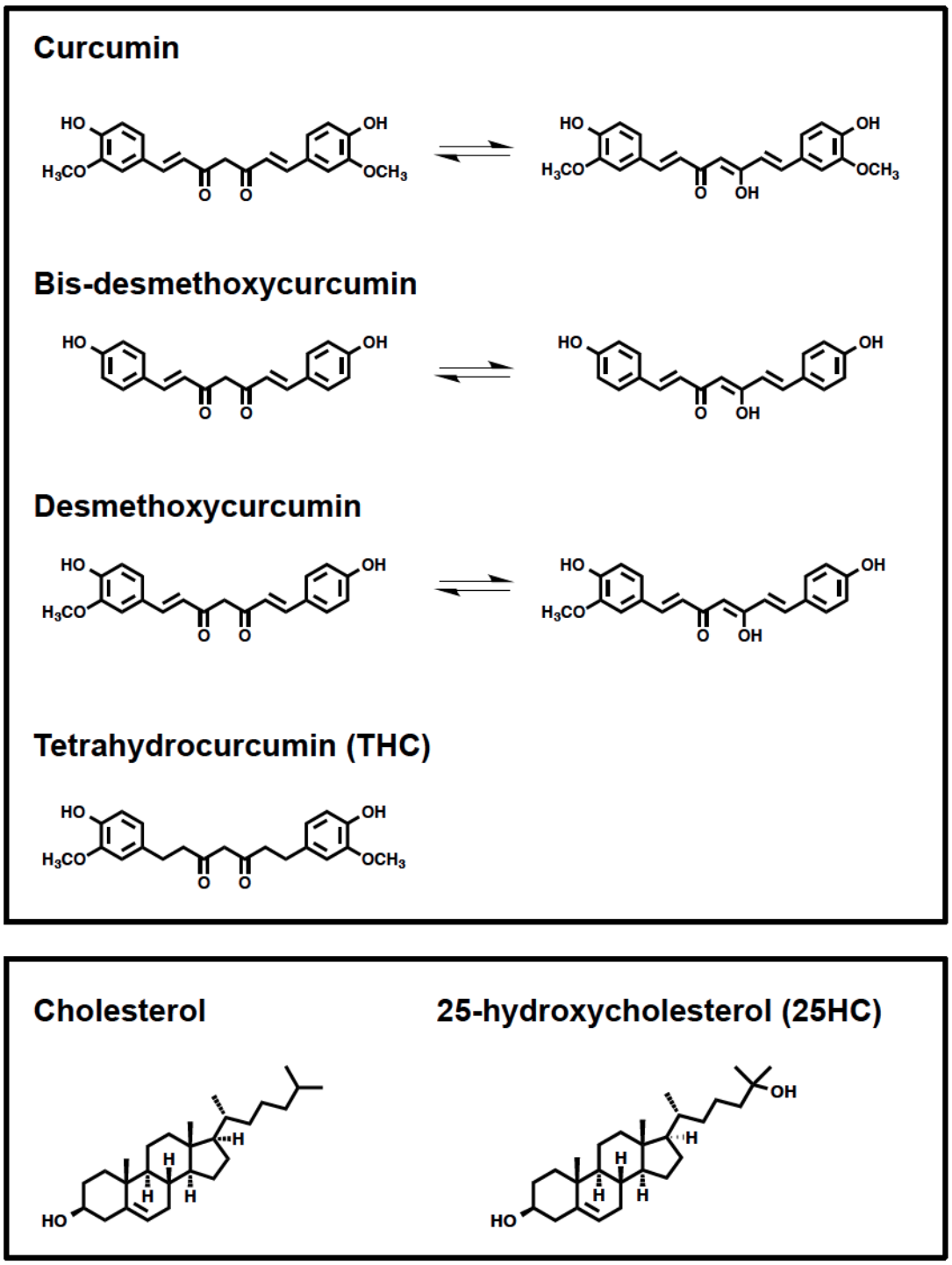

Figure 5.1. Structures of curcuminoids, cholesterol and 25-hydroxycholesterol (25HC). Curcuminoids include curcumin, bis-desmethoxycurcumin, desmethoxycurcumin and tetrahydrocurcumin (THC). Curcumin, bis-desmethoxycurcumin and desmethoxycurcumin exist as keto-enol tautomers.

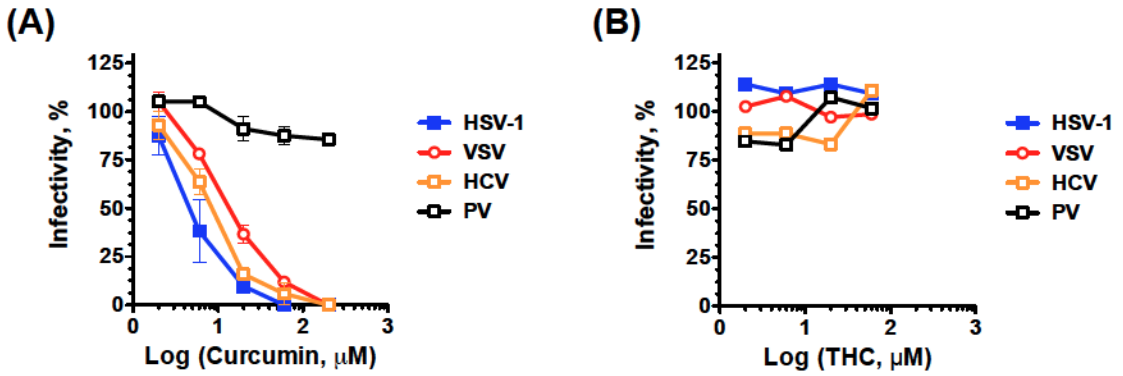

Figure 5.2. Curcumin, but not THC, inhibits the infectivity of enveloped viruses. Infectivity of unrelated enveloped (HSV-1, HCV and VSV) or nonenveloped (PV) viruses pre-exposed to curcumin **(A)** or THC **(B)**. Infectivity of treated virions was evaluated by plaquing efficiency or focus-forming efficiency (average ± SD; n = 3). THC was cytotoxic at concentrations above 60 μM.

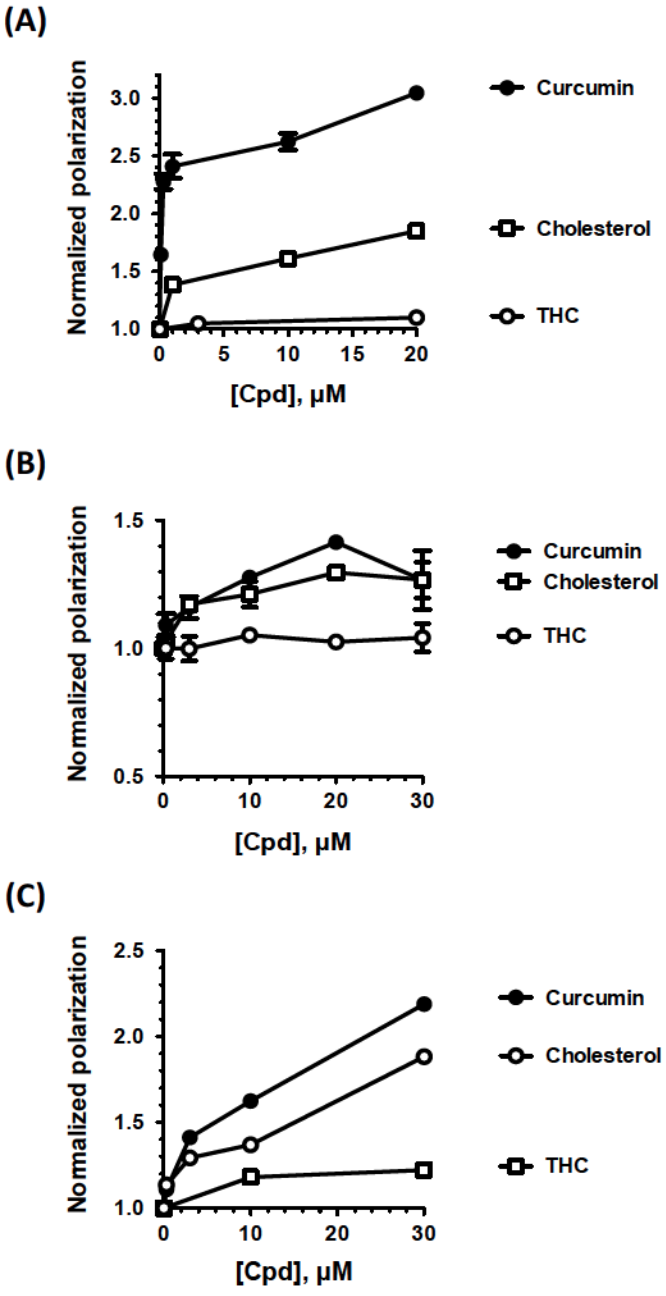

Figure 5.3. Like cholesterol, curcumin decreases membrane fluidity. DPH-labelled liposomes (A), HCV virions (B) or VSV virions (C) were exposed to increasing concentrations of curcumin, cholesterol or THC for 10 minutes at 37°C. DPH fluorescence polarization was measured. An increase in polarization indicates a decrease in membrane fluidity. The graph shows the result of two independent experiments (average ± range; n = 2). Several error bars are too small to be seen at this scale.

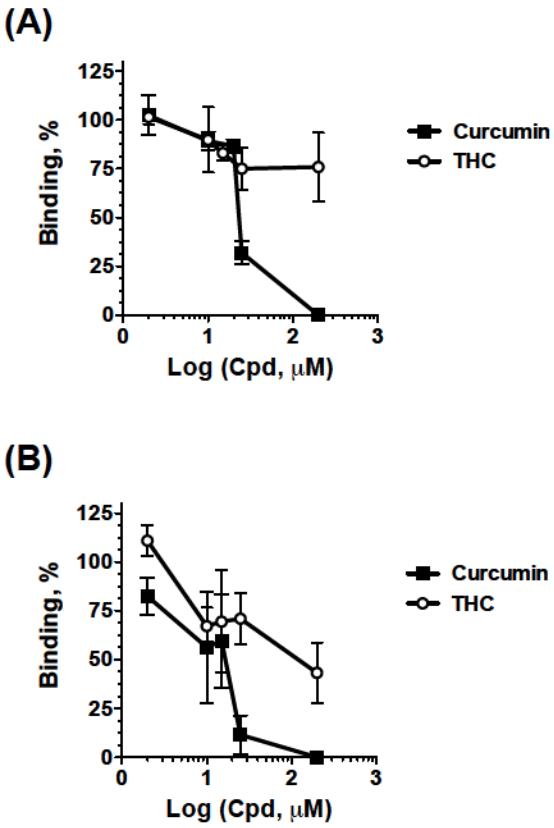

Figure 5.4. Curcumin inhibits binding of HCV JFH-1 virions to Huh7.5 cells. Binding of HCV virions exposed to curcumin or tetrahydrocurcumin (THC) in the absence **(A)** or presence **(B)** of serum. R18-labeled HCV virions (1,500 ffu) were exposed to the test compound for 10 minutes at 37°C, and then cooled to 4°C prior to being added to pre-chilled Huh7.5 cell monolayers (1.5 x 10^5 cells). Cells and virions were then incubated at 4°C for 1 hour, then washed three times with cold PBS. Cells and attached virions were lysed, and lysates were examined for R18 fluorescence. Binding is expressed as a percentage relative to the R18 fluorescence of DMSO vehicle-treated virions after standardization to the total amount of fluorescence detected for each sample. A, average ± S.D.; n = 4. B, average ± range; n = 2.

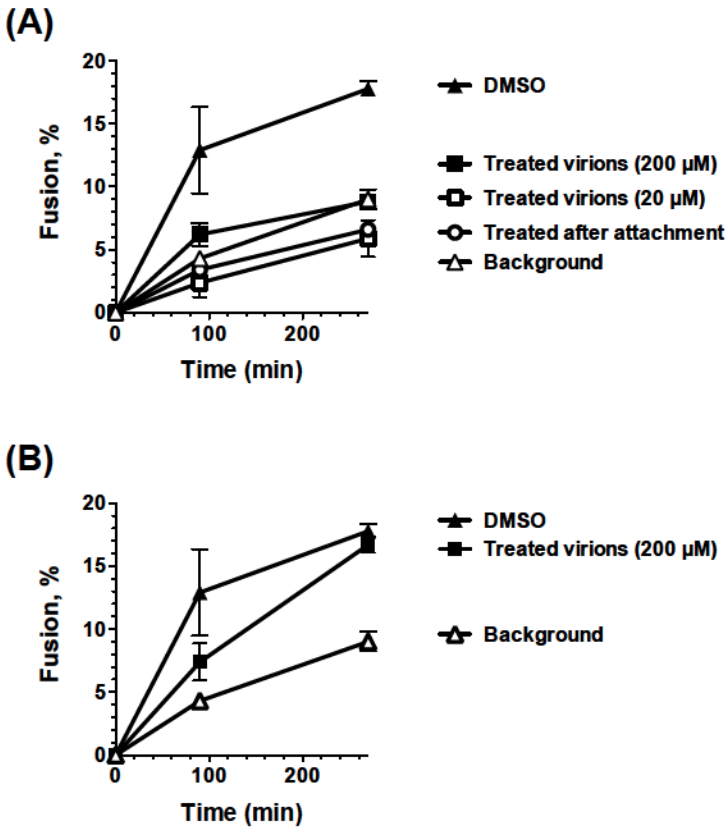

Figure 5.5. Curcumin inhibits the fusion of HCV JFH-1 virions to Huh7.5 cells. Fluorescence dequenching of HCV exposed to curcumin **(A)** or THC **(B)** (average ± range; n = 2). R18-labeled HCV virions (10^4 ffu) were exposed to DMSO vehicle, curcumin or THC for 10 minutes at 37°C, and then cooled to 4°C prior to being added to pre-chilled Huh7.5 cells (1 x 10^6 cells). Alternatively, virions were first allowed to attach to cells at 4°C, and then virion-cell complexes were exposed to curcumin. Fusion was triggered by increasing the temperature and lowering the pH.

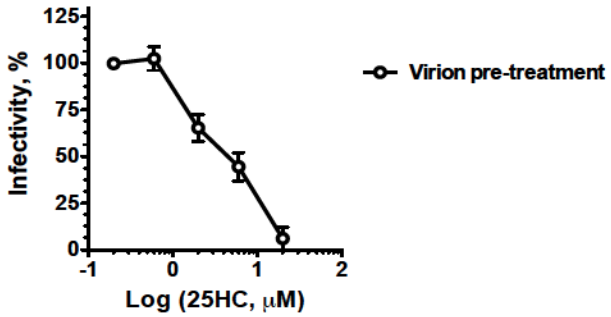

Figure 5.6. 25HC inhibits HCV infectivity to Huh7.5 cells. Infectivity of HCV virions exposed to 25HC (*virion treatment, open circles*) was tested by focus-forming efficiency. HCV virions (~100 ffu) were exposed to 25HC for 10 minutes at 37°C, prior to infection of Huh7.5 cell monolayers At 72 hours post-infection, cells were fixed and foci of infected cells were detected by immunocytochemistry. Dose-response line graphs present the average ± range (n = 2).

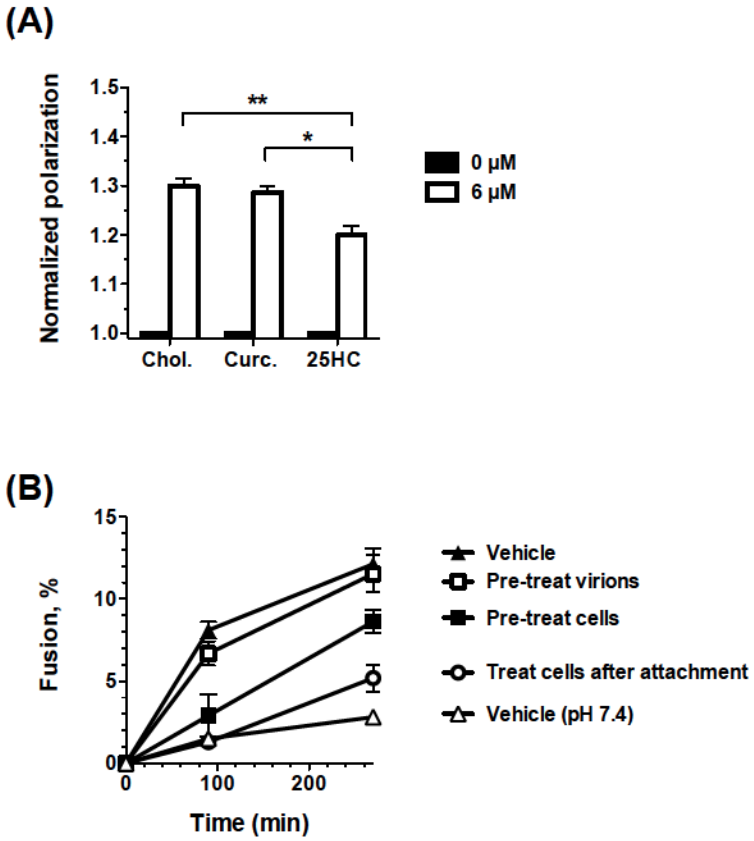

Figure 5.7. 25HC decreases the fluidity of HCV envelopes, but not enough to affect fusion when virions are pre-exposed. (A) DPH-labelled HCV virions exposed to 25HC or cholesterol were tested for DPH fluorescence polarization. 25HC reduced the fluidity of the virion envelopes, as shown by an increase in DPH polarization, but not to the same extent as cholesterol (chol.) or curcumin (curc.). Bar graphs present the average ± S.D. (n = 3) (**, $P<0.01$; *, $P<0.05$; two-tailed unpaired *t*-test). **(B)** R18-labelled HCV JFH-1 virions or Huh.75 cells were pre-exposed to 20 µM 25HC for 10 minutes at 37°C. Alternatively, virions were allowed to attach to Huh7.5 cells at 4°C for 1 hour, and then virion-cell complexes were exposed to 20 µM 25HC for 10 minutes at 37°C. Fusion was inhibited to the greatest extent when cells were treated after attachment of virions. Graphs present the average ± range (n = 2).

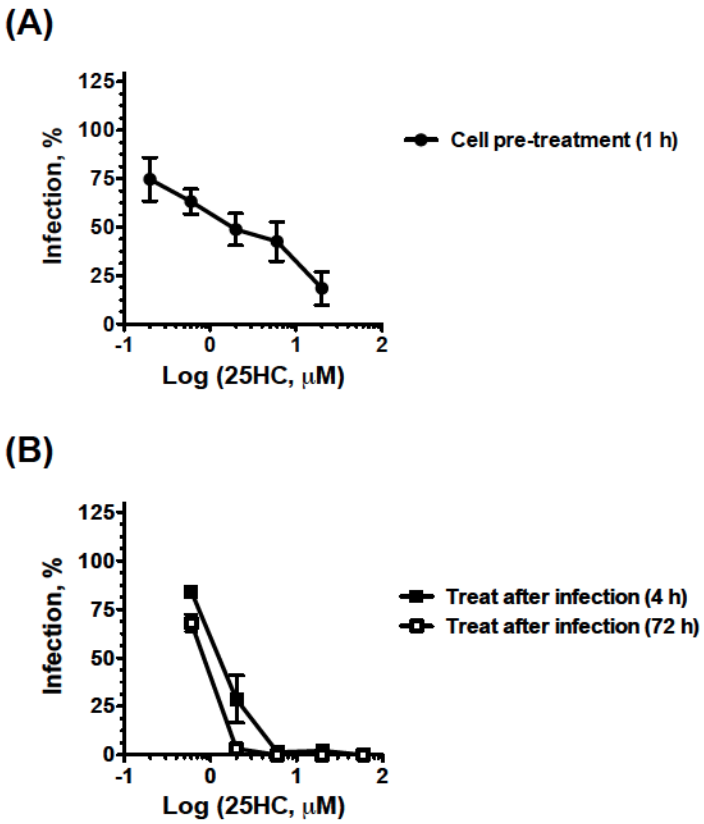

Figure 5.8. 25HC inhibits HCV focus formation when Huh7.5 cells are pre-treated, or treated after infection. Huh7.5 cell monolayers were first exposed to 25HC for 1 hour at 37°C (*cell pre-treatment, filled diamond*) **(A)** or untreated (treat after infection) prior to infection with HCV virions (~100 ffu). After 4 hours, inocula were removed, and cells were washed twice with DMEM prior to being overlaid with DMEM-10% FBS, or DMEM-10% FBS containing 25HC for 4 hours or 72 hours (*treat after infection, filled circles or squares, respectively*) **(B)**. At 72 hours post-infection, cells were fixed and foci of infected cells were detected by immunocytochemistry. Dose-response line graphs present the average ± range (n = 2).

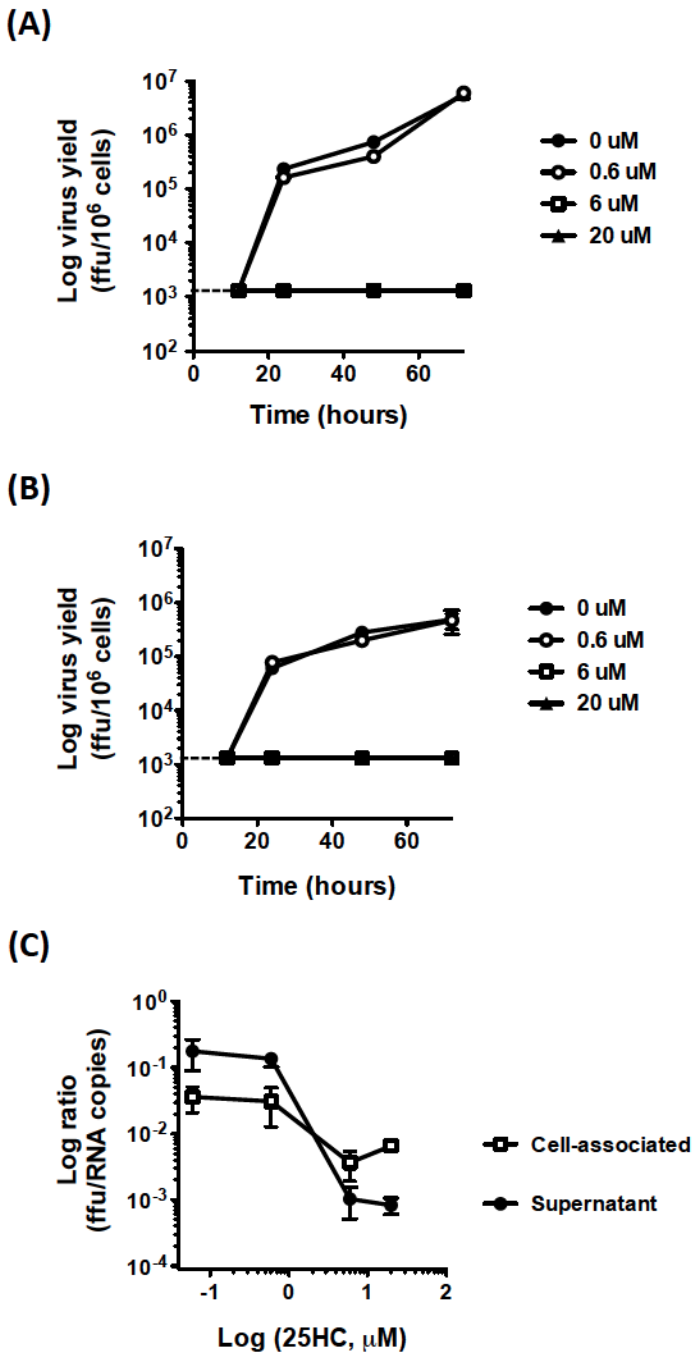

Figure 5.9. 25HC decreases the specific infectivity of HCV JFH-1 virions released into the supernatant. Huh7.5 cell monolayers were infected with HCV JFH-1 (MOI of 3). After 3 hours, the inoculum was replaced with DMEM-10% FBS containing 25HC. At 12, 24, 48 and 72 hpi, supernatant **(A)** and cell-associated **(B)** virions were harvested and titrated. At 72 hpi, supernatant and cell-associated RNA copies were titrated and compared to FFU **(C)**. Line graphs present the average ± range (n = 2) (dashed line, detection limit)

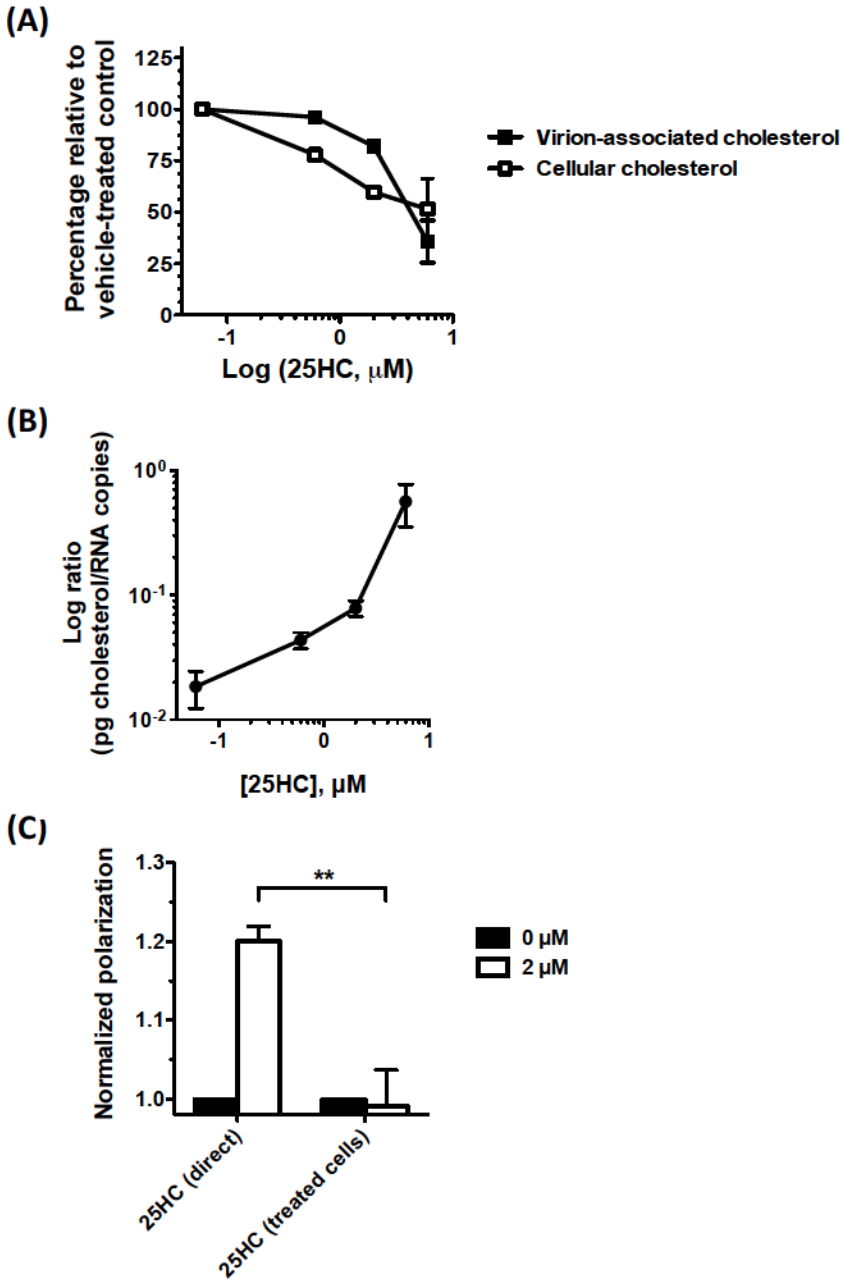

Figure 5.10. 25HC treatment of cells does not specifically decrease virion cholesterol content. Huh7.5 cells infected with HCV (MOI, 3 ffu/cell) were treated with 25HC for 72 hours. Cholesterol levels in cells or virions purified from the supernant were then measured **(A)**. Virion-associated cholesterol decreased proportionally to virion RNA **(B)**. The fluidity of the envelopes of virions produced by 25HC-treated cells was unaffected, in contrast to the direct exposure of HCV virions to 25H (**, $P<0.01$; two-tailed unpaired *t*-test) **(C)**. Graphs present the average ± range (n = 2) of two independent experiments.

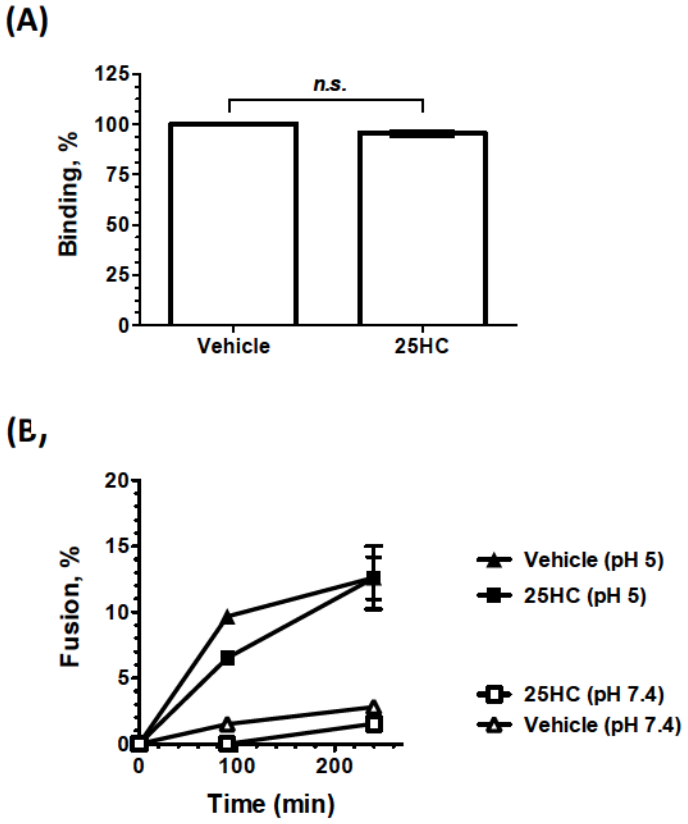

Figure 5.11. Effects of 25HC on binding and fusion of virions produced by treated cells. Huh7.5 cells infected with HCV (MOI, 3 ffu/cell) were treated with 6 μM 25HC for 72 hours. Virions were then harvested from the supernatants, labeled with R18 membrane dye, and tested for their ability to bind and fuse to cells **(A)**. Neither binding nor fusion (induced at the plasma membrane by low pH) was affected.

CHAPTER 6: DISCUSSION AND FUTURE DIRECTIONS

6.1 CHARACTERIZATION OF ANTI-ENTRY MECHANISMS

Most antivirals in current clinical use have some limitations, such as selection for resistance, toxicity and a narrow spectrum of activity. Ideally, new antiviral strategies will circumvent some of these limitations. In this thesis, I describe the characterization of the mechanisms of small molecule inhibitors of viral entry. Entry inhibitors prevent infection of uninfected cells and inhibit virus replication at a step before persistent reservoirs are established. Entry steps are also conserved among many unrelated viruses. Despite these advantages, only two antiviral drugs that target binding or fusion are currently in clinical use, maraviroc and enfuvirtide. They inhibit binding and fusion, respectively, but both are active only against HIV (Dorr *et al.*, 2005; Wild *et al.*, 1994). No truly broad-spectrum entry inhibitors have yet been approved for clinical use.

Using small molecules as probes, I have identified and characterized three mechanisms by which it is possible to inhibit entry of several unrelated viruses. Some of the small molecules that I used are themselves not ideal drug candidates. Nonetheless, the identification of their antiviral mechanisms opens the possibility for the design of novel antiviral candidates that may overcome some limitations of current therapies.

6.1.1 Virion attachment to heparan sulfate- or sialic acid-containing glycans. The initial binding of virions to cellular glycans is a conserved step in the entry of most human viruses. I showed that epigallocatechin gallate (EGCG), a polyphenol from green tea, is active against all viruses that I tested that bind to glycans. Glycan-binding viruses account for the vast majority of human viruses. The data in this thesis support a model in which EGCG competes with cellular HS or SA for binding to virion glycoproteins

(Figure 6.1). The majority of human viruses bind to either HS or SA, which accounts for the remarkable broad-spectrum activities described for EGCG.

The proposed targets of EGCG are highly mutable virally encoded proteins. Therefore, EGCG suffers from the same major limitation as targeting any viral protein, the prompt selection for resistance. EGCG resistance emerged after only five passages of IAV in the presence of increasing concentrations of EGCG. Mutations conferring resistance mapped to the stalk region of hemagglutinin (HA) from both H1N1 (A/Puerto Rico/8/34) and H3N2 (A/Aichi/2/68) strains. However, EGCG (or other compounds acting by similar mechanisms) could be combined with other antiviral agents to limit the selection for resistance. EGCG targets an entry step, which is complementary to the targets of most currently approved antivirals. Cross resistance is therefore less likely to be selected for. In the context of HCV, combinations of entry inhibitors with current direct acting antivirals were found to be promising treatment strategies (Xiao *et al.*, 2014). Our collaborators tested EGCG in combination with other anti-HCV drugs and observed a strong additive effect (Ciesek *et al.*, 2011), indicating that EGCG (or related compounds acting by similar mechanisms) could be used in combination therapy. Combination regimens are already commonly used in the treatment of HCV and HIV infections, to limit the selection for resistant variants (Liang and Ghany, 2013; Henrich and Kuritzkes, 2013).

6.1.2. Modulation of membrane curvature. The rigid amphipathic fusion inhibitors (RAFIs) such as aUY11 and dUY11 inhibit the fusion of enveloped but otherwise unrelated viruses by preventing the formation of the negative membrane curvature required for fusion **(Figure 6.2)**. Enrichment in the outer leaflet of phospholipids with

hydrophilic headgroups larger than their hydrophobic tails has been known for many years to prevent fusion of enveloped viruses (Chernomordik *et al.*, 1998; Gunther-Ausborn *et al.*, 1995; Gaudin, 2000b). These phosopholipids, however, are not useful as drugs. They are disruptive to all membranes, having signalling activities, and are too rapidly metabolized. The RAFIs, on the other hand, are synthetic compounds that have the same antiviral activities as phospholipids, but do not suffer from the same limitations.

The RAFI aUY11 is neither cytotoxic nor cytostatic (St Vincent *et al.*, 2010), with no apparent effects on cellular fusions. Virions and cells (and cellular vesicles) differ in size, curvature, lipid composition and, most critically, the energy available for fusion. Virions are metabolically inert and viral fusion depends solely on the energy provided by binding and rearrangements of the virion glycoproteins. In contrast, cells use energy-consuming processes (described in **Chapter 1**) to overcome the energy barriers required for fusion. Virions (~100 nm) are smaller than most cellular vesicles that are involved in endocytotic processes (~500-1000 nm), although other intracellular vesicles are similar in size to virions. Interestingly, aUY11 was most potent against Sindbis virus (EC_{50}, 0.009 μM) and least potent against HSV-1 (EC_{50}, 0.258 μM). These differences correlate somewhat with virion size **(Figure 6.3)**. aUY11 was even less potent against VACV (EC_{50}, 24.6 μM), which could be the result of its second envelope, which is shed by nonfusogenic mechanisms (Law *et al.*, 2006). VACV is larger than all other enveloped viruses I tested (Benhnia *et al.*, 2013), which could contribute also to its decreased sensitivity to aUY11. Smaller virions, such as Sindbis virus, have stronger positive curvature and may require more energy for the formation of the negatively curved stalk.

Consequently, virions of smaller size would be more sensitive than larger virions (or cellular vesicles) to increases in the energy barrier to fusion posed by RAFIs.

Virions and cellular vesicles differ also in their membrane compositions. Virion envelopes have a high membrane protein content and are rich in cholesterol. Consequently, virion envelopes have decreased fluidity relative to most cellular membranes. The outer leaflet of virion envelopes is often enriched in lipids of appropriate shape to favour positive curvature (Chan *et al.*, 2008). For example, viral envelopes often contain a higher proportion of sphingomyelin relative to cellular membranes (Brugger *et al.*, 2006; Quigley *et al.*, 1971). The localization of RAFIs may also differ in virion and vesicle membranes. Since the large polar head group of aUY11 likely precludes its translocation across leaflets, aUY11 would preferentially localize to the outer leaflets of virions. Any aUY11 in intracellular vesicles would instead reside in the inner leaflet as the result of membrane inversion during endocytosis. RAFIs localized to inner leaflets are not expected to affect stalk formation. Molecules of inverted cone shape only inhibit fusion when localized to the external leaflet of fusing vesicles. These factors likely all contribute to the selectivity of aUY11 and other RAFIs for inhibiting viral fusion without affecting cellular fusions.

Since lipids are not virally encoded, antivirals that target lipids and act through non-biochemical mechanisms are expected to have a higher barrier to selection for resistance. Resistance to other lipid-targeting antivirals (such as LJ001, PD404182, curcumin and glycyrrhizin) has not yet been documented in the public literature. Arbidol interacts with both lipid membranes and tryptophan residues of viral proteins and is thought to inhibit fusion by stabilizing the interactions between virion glycoproteins and

lipid membranes (Teissier *et al.*, 2011b). In the case of IAV, arbidol stabilizes HA to inhibit the low pH-induced conformational changes that promote fusion (Leneva *et al.*, 2009). As expected for a compound that at least partially targets a virally encoded protein, arbidol does select for resistance mutations in the HA2 stalk region of IAV HA (Leneva *et al.*, 2009). Single amino acid substitutions in HA2 increase the pH required for fusion, thereby allowing fusion to proceed despite the arbidol-induced stabilization. In another study, arbidol selected for resistant Chikungunya virus mutant with a similar single amino acid substitution in the E2 envelope protein (Delogu *et al.*, 2011).

I was not able to select for IAV resistance to aUY11 after 10 passages (**Chapter 4**), and dUY11 did not select for HSV-1 resistance after 11 passages (Dr. Mireille St.Vincent, unpublished). Therefore, neither IAV nor HSV-1 readily selected for RAFI-resistant variants. Theoretically, mutant strains with increased fusion efficiencies could overcome the effects of RAFIs. For example, mutations in virion fusion proteins could help to overcome the increased energy barrier for fusion (perhaps by mechanisms similar to those that confer resistance against arbidol). An increased number of virion glycoproteins could also provide increased energy to overcome the barrier posed by RAFIs. In the case of IAV, at least three hemagglutinin trimers are required for hemifusion (Danieli *et al.*, 1996). The extent and rate of fusion depends on the surface density of fusion proteins (Dutch *et al.*, 1998; Clague *et al.*, 1991). Variants with higher densities of fusion proteins could potentially be resistant to RAFIs. Viral variants with altered lipid envelope compositions could also be resistant, if enriched in the presence of lipids that promote negative curvature and thereby promote fusion (Stiasny and Heinz, 2004; Chernomordik, 1996). Such modifications likely require a number of critical

mutations, however, resulting in a higher barrier to resistance than traditional antiviral approaches targeting viral proteins. In summary, RAFIs are less likely to select for resistance than drugs targeting viral proteins, a most desirable property for an antiviral drug candidate.

6.1.3 Modulation of membrane fluidity and composition. My studies with curcumin demonstrate the importance of appropriate virion envelope fluidity for binding and fusion. Modulation of membrane fluidity is another example of a biophysical mechanism that targets lipid membranes, instead of virally encoded proteins. Like other lipid-targeted approaches, there is likely a higher barrier to resistance against curcumin than against traditional antivirals (as I described for RAFIs). Not unexpectedly, resistance to curcumin or glycyrrhizin, which also targets membrane fluidity (Harada, 2005), has not yet been reported. It is possible to envision some potential resistance mechanisms. Virions with altered lipid composition may be able to overcome the effects of curcumin. For example, virions with higher envelope fluidity may be less sensitive to the fluidity decreases imposed by curcumin. The lipid composition of virion envelopes typically reflects the membrane where budding took place. Viruses resistant to curcumin could potentially bud from different membranes, although this would require altered localization of viral structural proteins and would likely require a number of mutations. In the event of resistance, curcumin (or molecules acting by similar mechanisms) could be used in combination therapy, as described for EGCG. Our collaborators tested several HCV antiviral agents in combination with curcumin, and showed that the presence of curcumin increased their efficacy up to 10-fold (Anggakusuma *et al.*, 2013).

Curcumin has cytotoxic effects in the micromolar range (Sharma *et al.*, 2005),

only slightly above its antiviral concentrations (EC_{50}, ~10 μM). It was shown to induce apoptosis through multiple processes related to p53 stability, cytochrome C release (and subsequent activation of caspases), and generation of reactive oxygen species (Woo *et al.*, 2003). However, the specific mechanisms are unclear. Curcumin oxidizes thiol residues in membrane proteins at the mitochondrial transition pore, causing mitochondrial dysfunction (Morin *et al.*, 2001; Ligeret *et al.*, 2004), which could contribute to cytochrome C release. The α, β-unsaturated carbonyl group of curcumin is a highly reactive Michael acceptor, commonly associated with toxicity (Mulliner *et al.*, 2011). Nonetheless, curcumin was well-tolerated in a number of human trials, although its pharmacokinetic and pharmacodynamic properties are not favourable (Sharma *et al.*, 2005). From an antiviral perspective, the mechanisms responsible for the cytotoxicity of curcumin are not necessarily involved in its antiviral activities, which depend on the rigid and planar shape of the molecule and not on specific chemical groups or reactivities. Structure-activity relationship (SAR) studies of curcumin and other fluidity modulators would be required to explore its antiviral potential.

6.2 CHEMICAL BIOLOGY AND VIRAL ENTRY MECHANISMS

In addition to their potential as antivirals, small molecules are useful as probes to study viral or cellular activities and host-virus interactions. In this thesis, the use of small molecules to probe anti-entry mechanisms led to the identification of novel functions in viral entry.

6.2.1 Virion attachment to heparan sulfate- or sialic acid-containing glycans. Although most human viruses bind to cellular glycans, the specific requirements for

binding were thought to be different. One group of viruses binds to heparan sulfate (HS) in cellular glycosaminoglycans, whereas another group binds to terminal sialic acid (SA) moieties in cellular sialoglycans. No small molecule had previously been identified that could inhibit the binding of both groups. Most unexpectedly, I found that EGCG inhibited the attachment of both groups of viruses, providing the first evidence of common requirements for binding of viruses to HS- or SA-containing glycans.

EGCG-resistant IAV variants had mutations in the HA2 stalk region **(Figure 3.13)**, which is known to be in involved in fusion but not thought to have roles in binding. HA2 is relatively well conserved amongst IAV and influenza B virus (IBV) (Krystal *et al.*, 1982). As such, monoclonal antibodies that bind the HA stalk domain are broadly cross-reactive and neutralizing (Ekiert *et al.*, 2009). Such antibodies were proposed to block the conformational rearrangements of HA required for membrane fusion. It may be, however, that HA binding is impaired as well. The epitopes for the cross-reactive antibodies are the membrane proximal portions of HA2, in the same region as the mutations that confer resistance to EGCG. The EGCG mutations suggest that the stalk region of HA may also contribute to binding, either directly or through effects on the overall structure of HA. Like IAV HA, the reovirus (RV) sigma 1 protein is responsible for attachment to SA-containing glycans. Sigma 1 has an alpha-helical stalk and a globular head domain, and like HA, exists as a trimer. Structural and functional studies showed that the globular head engages junctional adhesion molecule-A (JAM-A), the specific secondary receptor for RV (Kirchner *et al.*, 2008). Interestingly, sequences in the membrane proximal region of the sigma 1 stalk bind to SA-containing glycans (Reiter *et*

al., 2011). It may be that the corresponding membrane proximal regions of IAV HA also contribute to SA binding.

6.2.2. Membrane curvature and viral fusion. Historically, virus-to-cell fusion has been widely used as a model for cellular fusions, on the assumption that both types of fusions involve the same basic mechanisms. The data in this thesis support a model in which RAFIs inhibit fusion by preventing formation of the negative curvature in the hemifusion stalk, which was thought to be a conserved requirement (that was formed by similar lipid rearrangements) for both viral and cellular fusion. However, RAFIs inhibited virus-to-cell, virus-to-liposome and liposome-to-cell fusions, but had no apparent effects on cellular fusions, suggesting critical differences between viral (or liposome) and cellular fusions. As described above, differences in energy availability, vesicle size and curvature, and lipid composition may be involved. RAFIs could be used as probes to characterize the differential requirements for virus-to-cell fusion and cellular fusions.

6.2.3 Membrane fluidity and viral entry. Membrane fluidity depends on many factors, including lipid composition and temperature. The decreases in membrane fluidity resulting from curcumin insertion into membranes were sufficient to inhibit the entry steps of HCV and the infectivity of other enveloped viruses. In contrast, the (lesser) decreases in membrane fluidity induced by 25HC (likely through different mechanisms) did not correspond with anti-entry activities. To a certain extent, therefore, virions can apparently overcome decreases in virion envelope fluidity to bind and fuse. These findings suggest specific requirements for fluidity and lipid composition for viral entry. The relationship between membrane fluidity and viral infectivity has not been well-

characterized. Curcumin, 25HC, and other related compounds could be used as probes to identify these requirements.

6.3 FUTURE DIRECTIONS

6.3.1 Virion attachment to heparan sulfate- or sialic acid-containing glycans. I showed in my thesis that EGCG and some other gallate-containing compounds (alkyl gallate derivatives and pentagalloylglucose, PGG) inhibited the infectivity of HS- and SA-binding viruses. I proposed that the gallate moiety is the critical determinant for antiviral activity, but the adjoining moieties contribute to potency. To test this model, SAR studies will be done with a series of chemically synthesized gallate derivatives. These will include digallate and trigallate compounds, with the gallate moieties connected by different linkers. Linkers lacking the reactive gallate carbonyl are expected to be more stable. However, it is yet unknown whether the gallate carbonyl is important for antiviral activity. The SAR studies may result in a lead compound for further antiviral optimization and development, but could also be used to probe the binding requirements of HS and SA binding viruses. EGCG inhibited the binding of HS-binding viruses at lower concentrations than SA-binding viruses, although the alkyl gallates inhibited infectivity of both groups at similar concentrations. Differential activities of gallate-containing compounds could highlight subtle differences in binding mechanisms.

I isolated H1N1 and H3N2 IAV variants that were resistant to EGCG, with single amino acid substitutions mapping to the HA stalk. To validate that the mutation is responsible for resistance, marker rescue experiments should be performed. We could also use reverse genetics approaches to introduce the mutations into wild-type IAV

strains, and test their susceptibility to EGCG. Another objective is to select for resistance in HS-binding viruses (such as HSV-1) or other SA-binding viruses (such as RV). Comparisons of resistant viruses would provide insights into the antiviral mechanisms of EGCG, and perhaps also into the binding mechanisms of HS- and SA-binding viruses.

We should also attempt more direct approaches to identify the binding site of EGCG. Although modelling studies indicated that EGCG could fit into the globular receptor-binding domain of IAV HA (Ge *et al.*, 2014), EGCG may well bind elsewhere. We could heterologously overexpress and purify virion proteins (such as IAV HA or HSV-1 gC) and use mass spectrometry methods to identify the specific binding sites of EGCG, based on deuterium exchange (Chalmers *et al.*, 2011).

6.3.2. Membrane curvature and viral fusion. As described in earlier sections, the RAFIs selectively inhibit viral fusions without apparent effects on cellular fusions. Virion envelopes and cellular vesicles differ in size, curvature, lipid composition and the energy available for fusion, all of which may contribute to the selectivity of RAFIs for viral fusions. These possibilities could be tested by liposome fusion assays, such as those I described in **Chapter 4**, using liposomes of different diameters and different lipid compositions that more close resemble either virions or cellular vesicles. To test the hypothesis that RAFIs localized in the inner leaflet (of intracellular vesicles) does not inhibit fusion, asymmetrical liposomes that contain aUY11 only in the inner leaflet could be tested for their ability to fuse.

The most critical difference between cellular and viral fusions is likely the energy available for fusion. Yeast vacuole fusion assays, a model for eukaryotic vesicular fusions, could be used to examine the effects of cellular fusion factors (and energy) on

the activity of RAFIs. Yeast vacuole fusion depends on conserved cellular factors that include SNAREs. RAFIs may inhibit yeast vacuole fusion in the absence of cellular fusion factors and under limiting ATP. We could also test if increased energy availability during viral fusion would overcome the effects of RAFIs, using liposomes reconstituted with IAV HA (Gunther-Ausborn *et al.*, 1995). In such a system, energy can be regulated by the number of HA trimers, pH and temperature. For example, exposure to low pH overcomes the IFITM3-mediated inhibition of IAV fusion (Desai *et al.*, 2014).

Using conventional serial passage approaches, we were not yet able to select for aUY11- or dUY11-resistant viruses. We may still be able to select for resistance with more passages. If not, we could attempt to select for resistance with weaker, less potent RAFIs, or use chemical mutagenesis approaches to mutagenize the viruses prior to selection. These methods could facilitate the selection of RAFI-resistant variants. Analysis of the resistant variants would contribute to our understanding of the antiviral mechanism of RAFIs, and also viral fusion mechanisms.

6.3.3 Membrane fluidity and composition. My characterization of the mechanisms of curcumin in this thesis was focused on HCV. However, curcumin has broad activity against enveloped viruses (Chen *et al.*, 2013), and my model is that the antiviral effects of curcumin depend on its modulation of virion envelope fluidity. Accordingly, I expect curcumin to act by similar mechanisms against all enveloped viruses. To test this model, we should next evaluate the effects of curcumin on the fluidity and entry steps of other enveloped viruses, using the binding and fusion assays described in this thesis. These experiments would test our model for the antiviral mechanisms of curcumin and could

also point to differential fluidity requirements for the entry steps of different enveloped viruses.

Resistance to curcumin has not been documented in the literature. Based on the proposed mechanism, I expect curcumin to have a high barrier to resistance. Nonetheless, resistance mechanisms are of course possible to envision. Future studies should be done to isolate resistant viruses by serial passage in the presence of increasing curcumin concentrations, using an RNA virus such as IAV (as I have done for EGCG and aUY11, **Chapters 3 and 4**). One potential resistance mechanism is alteration of lipid composition in virion envelopes. To test that possibility, liposomes of different lipid composition could be prepared, treated with curcumin, and induced to fuse (as described in **section 6.3.2** for RAFIs).

Curcumin is planar and rigid, and inserts into membranes in a transbilayer orientation similar to cholesterol (Barry *et al.*, 2009). It induces ordering in membranes, which influences many membrane properties, including fluidity. Curcumin, glycyrrhizin and cholesterol all decrease membrane fluidity, with corresponding broad antiviral activities *(***Chapter 5,** Chen *et al.*, 2013; Harada, 2005). Their structures share the common features of rigidity, planarity and at least one terminal hydrophilic moiety. 25HC, in contrast, has a bent shape and affects membrane fluidity to a lesser extent, likely by mechanisms distinct from those of curcumin or cholesterol (discussed in **Chapter 5**). To my knowledge, structure-activity relationship studies for membrane fluidity-modulating antivirals have not been done. Such studies would be useful to identify and optimize antiviral candidates, and to elucidate the specific fluidity requirements for the entry steps of enveloped viruses.

25HC broadly affects cellular membrane fluidity and lipid composition. Its effects on virion envelope fluidity were not sufficient to inhibit entry, but its effects on cellular membranes and signalling impact the production of infectious HCV particles. HCV replication and assembly rely on appropriate cholesterol content in intracellular membranes. Inappropriate fluidity or lipid composition of these membrane structures could impair genome replication, through improper localization of viral and cellular proteins. Cellular imaging studies could be used to examine the integrity and localization of subcellular membrane compartments, and the localization of viral proteins to these compartments, when infected cells are treated with 25HC.

Treatment of cells with 25HC and other oxysterols triggers cholesterol trafficking from the plasma membrane to the endoplasmic reticulum (Lange *et al.*, 1999; Lange *et al.*, 2004; Olsen *et al.*, 2011), from which HCV virions bud. Such modifications to the lipid composition of the endoplasmic reticulum could therefore affect the composition of virion envelopes. These possibilities could be tested by lipidomics approaches to evaluate the lipid content of purified HCV virions, with or without 25HC treatment.

Other sterol-derived small molecules with antiviral activities may also act similarly to 25HC by modifying the fluidity or composition of cellular membranes. For example, 25-hydroxyvitamin D3 inhibits the production of infectious HCV particles similarly to 25HC (Matsumura *et al.*, 2012). Identification of other natural products and innate small molecules with effects on membrane composition and fluidity would be useful to characterize the potential antiviral mechanisms involved and to better understand their roles in innate immunity.

6.4 CONCLUSIONS

Overall, I have identified three distinct mechanisms to inhibit different entry steps of unrelated viruses. Identification of these mechanisms opens the possibility for the rational design of small molecule entry inhibitors with broad-spectrum activities and appropriate pharmacological properties. Furthermore, the small molecules described in this thesis are useful as probes to characterize viral entry steps.

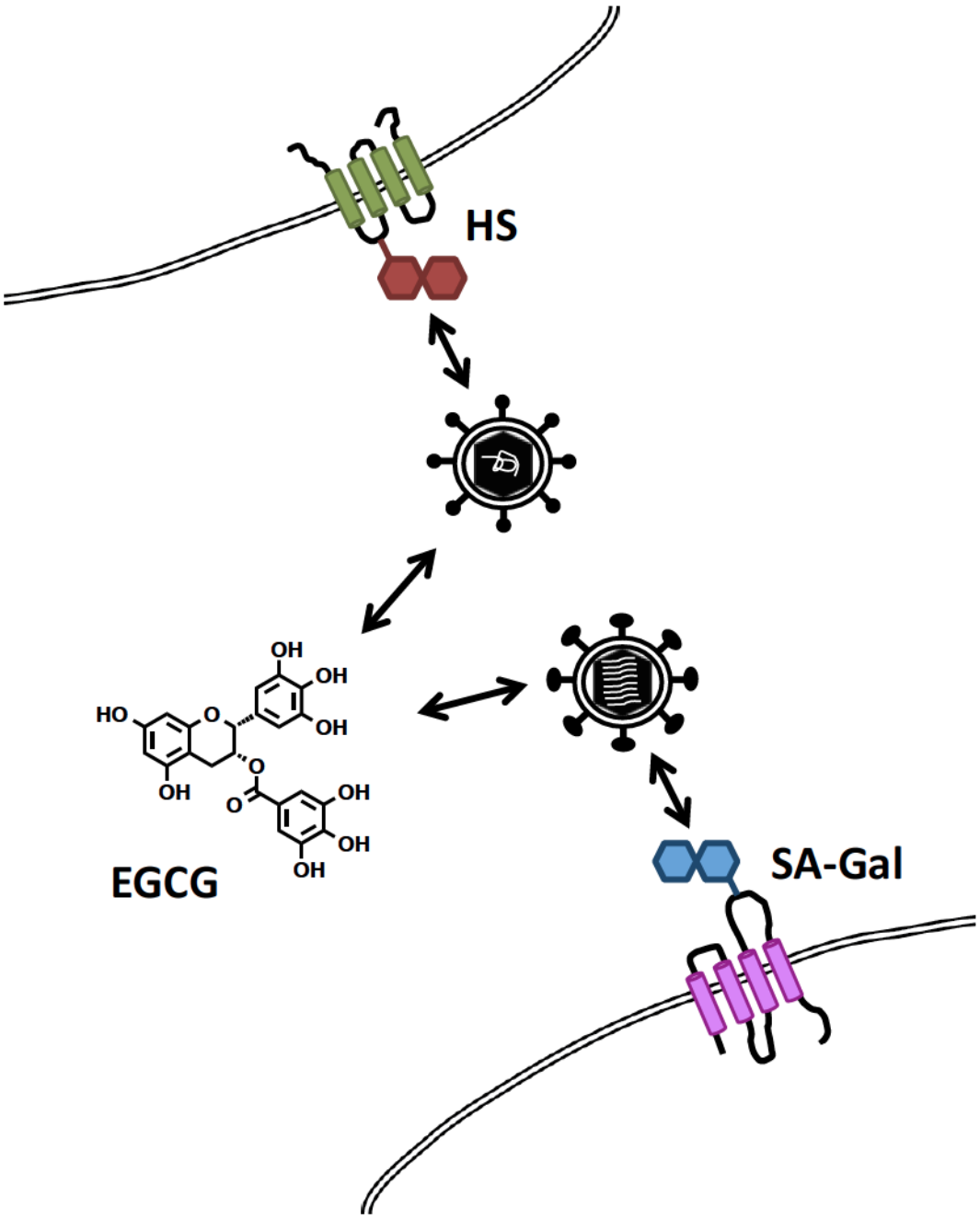

Figure 6.1. Model for the proposed antiviral mechanism of EGCG and other gallate-containing compounds. EGCG competes with cellular HS or SA for binding to virion glycoproteins.

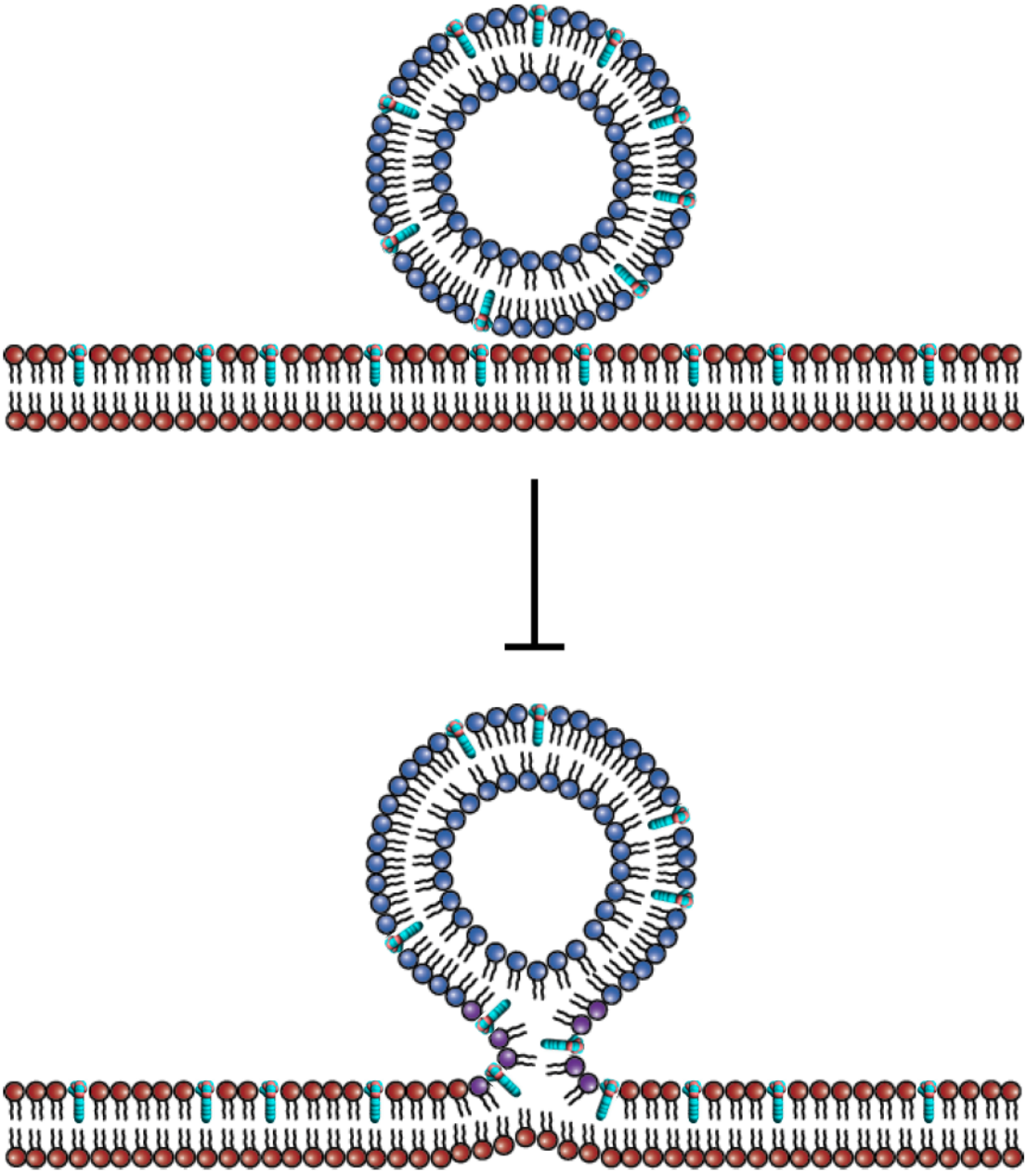

Figure 6.2. Proposed model for the antiviral mechanism of RAFIs. The RAFIs insert into the outer leaflet of virion envelopes to inhibit formation of the negative membrane curvature required to form the hemifusion stalk intermediate.

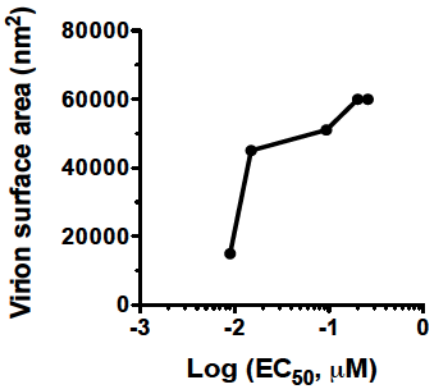

Figure 6.3. The EC_{50} of aUY11 increases with the virion surface area. Shown on the graph (from lowest EC_{50} to highest) are Sindbis virus, VSV, IAV (average of four strains), HSV-2 and HSV-1.

REFERENCES

1. Abban CY, Bradbury NA, Meneses PI. 2008. HPV16 and BPV1 infection can be blocked by the dynamin inhibitor dynasore. Am J Ther **15**:304–311.

2. Acton S, Rigotti A, Landschulz KT, Xu S, Hobbs HH, Krieger M. 1996. Identification of scavenger receptor SR-BI as a high density lipoprotein receptor. Science **271**:518–520.

3. Agnello V, Abel G, Elfahal M, Knight GB, Zhang QX. 1999. Hepatitis C virus and other flaviviridae viruses enter cells via low density lipoprotein receptor. Proc Natl Acad Sci USA **96**:12766–12771.

4. Aguilar JS, Rice M, Wagner EK. 1999. The polysulfonated compound suramin blocks adsorption and lateral difusion of herpes simplex virus type-1 in vero cells. Virology **258**:141–151.

5. Aguilar PS, de Mendoza D. 2006. Control of fatty acid desaturation: a mechanism conserved from bacteria to humans. Mol Microbiol **62**:1507–1514.

6. Aizaki H, Morikawa K, Fukasawa M, Hara H, Inoue Y, Tani H, Saito K, Nishijima M, Hanada K, Matsuura Y, Lai MM, Miyamura T, Wakita T, Suzuki T. 2008. Critical role of virion-associated cholesterol and sphingolipid in hepatitis C virus infection. J Virol **82**:5715–5724.

7. Akkarawongsa R, Pocaro NE, Case G, Kolb AW, Brandt CR. 2009. Multiple peptides homologous to herpes simplex virus type 1 glycoprotein B inhibit viral infection. Antimicrob Agents Chemother **53**:987–996.

8. Alagaili AN, Briese T, Mishra N, Kapoor V, Sameroff SC, Burbelo PD, de Wit E, Munster VJ, Hensley LE, Zalmout IS, Kapoor A, Epstein JH, Karesh WB, Daszak P, Mohammed OB, Lipkin WI. 2014. Middle East respiratory syndrome coronavirus infection in dromedary camels in Saudi Arabia. MBio **5**:e00884–e00814.

9. Albecka A, Belouzard S, Op de Beeck A, Descamps V, Goueslain L, Bertrand-Michel J, Terce F, Duverlie G, Rouille Y, Dubuisson J. 2012. Role of low-density lipoprotein receptor in the hepatitis C virus life cycle. Hepatology **55**:998–1007.

10. Allaudeen HS, Kozarich JW, Bertino JR, De Clercq E. 1981. On the mechanism of selective inhibition of herpesvirus replication by (E)-5-(2-bromovinyl)-2'-deoxyuridine. Proc Natl Acad Sci U S A **78**:2698–2702.

11. Alvisi G, Madan V, Bartenschlager R. 2011. Hepatitis C virus and host cell lipids: an intimate connection. RNA Biol **8**:258–269.

12. Amini-Bavil-Olyaee S, Choi YJ, Lee JH, Shi M, Huang IC, Farzan M, Jung JU. 2013. The antiviral effector IFITM3 disrupts intracellular cholesterol homeostasis to block viral entry. Cell Host Microbe **13**:452–464.

13. Anafu AA, Bowen CH, Chin CR, Brass AL, Holm GH. 2013. Interferon-inducible transmembrane protein 3 (IFITM3) restricts reovirus cell entry. J Biol Chem **288**:17261–17271.

14. Anand P, Kunnumakkara AB, Newman RA, Aggarwal BB. 2007. Bioavailability of curcumin: problems and promises. Mol Pharm **4**:807–818.

15. Andersen JH, Jenssen H, Gutteberg TJ. 2003. Lactoferrin and lactoferricin inhibit Herpes simplex 1 and 2 infection and exhibit synergy when combined with acyclovir. Antiviral Res **58**:209–215.

16. Anggakusuma, Colpitts CC, Schang LM, Rachmawati H, Frentzen A, Pfaender S, Behrendt P, Brown RJ, Bankwitz D, Steinmann J, Ott M, Meuleman P, Rice CM, Ploss A, Pietschmann T, Steinmann E. 2014. Turmeric curcumin inhibits entry of all hepatitis C virus genotypes into human liver cells. Gut 63:1137-49.

17. Arnberg N, Edlund K, Kidd AH, Wadell G. 2000. Adenovirus type 37 uses sialic acid as a cellular receptor. J Virol **74**:42–48.

18. Arnberg N, Kidd AH, Edlund K, Nilsson J, Pring-Akerblom P, Wadell G. 2002. Adenovirus type 37 binds to cell surface sialic acid through a charge-dependent interaction. Virology **302**:33–43.

19. Arnold D, Di Biase AM, Marchetti M, Pietrantoni A, Valenti P, Seganti L, Superti F. 2002. Antiadenovirus activity of milk proteins: lactoferrin prevents viral infection. Antiviral Res **53**:153–158.

20. Asselah T, Lada O, Moucari R, Martinot M, Boyer N, Marcellin P. 2007. Interferon therapy for chronic hepatitis B. Clinics in liver disease **11**:839–849.

21. Atanasiu D, Whitbeck JC, de Leon MP, Lou H, Hannah BP, Cohen GH, Eisenberg RJ. 2010. Bimolecular complementation defines functional regions of Herpes simplex virus gB that are involved with gH/gL as a necessary step leading to cell fusion. J Virol **84**:3825–3834.

22. Azad RF, Driver VB, Tanaka K, Crooke RM, Anderson KP. 1993. Antiviral activity of a phosphorothioate oligonucleotide complementary to RNA of the human cytomegalovirus major immediate-early region. Antimicrob Agents Chemother **37**:1945–1954.

23. Azhar EI, El-Kafrawy SA, Farraj SA, Hassan AM, Al-Saeed MS, Hashem AM, Madani TA. 2014. Evidence for camel-to-human transmission of MERS coronavirus. N Engl J Med **370**:2499–2505.

24. Baba M, De Clercq E, Schols D, Pauwels R, Snoeck R, Van Boeckel C, Van Dedem G, Kraaijeveld N, Hobbelen P, Ottenheijm H. 1990. Novel sulfated polysaccharides: dissociation of anti-human immunodeficiency virus activity from antithrombin activity. J Infect Dis **161**:208–213.

25. Baba M, Miyake H, Wang X, Okamoto M, Takashima K. 2007. Isolation and characterization of human immunodeficiency virus type 1 resistant to the small-molecule CCR5 antagonist TAK-652. Antimicrob Agents Chemother **51**:707–715.

26. Baba M, Shigeta S. 1987. Antiviral activity of glycyrrhizin against varicella-zoster virus in vitro. Antiviral Res **7**:99–107.

27. Baba M, Snoeck R, Pauwels R, de Clercq E. 1988. Sulfated polysaccharides are potent and selective inhibitors of various enveloped viruses, including herpes simplex virus, cytomegalovirus, vesicular stomatitis virus, and human immunodeficiency virus. Antimicrob Agents Chemother **32**:1742–1745.

28. Bailey CC, Huang IC, Kam C, Farzan M. 2012. Ifitm3 limits the severity of acute influenza in mice. PLoS Pathog **8**:e1002909.

29. Bales BL, Leon V. 1978. Magnetic resonance studies of eukaryotic cells. III. Spin labeled fatty acids in the plasma membrane. Biochim Biophys Acta **509**:90–99.

30. Bankwitz D, Steinmann E, Bitzegeio J, Ciesek S, Friesland M, Herrmann E, Zeisel MB, Baumert TF, Keck ZY, Foung SK, Pecheur EI, Pietschmann T. 2010. Hepatitis C virus hypervariable region 1 modulates receptor interactions, conceals the CD81 binding site, and protects conserved neutralizing epitopes. J Virol **84**:5751–5763.

31. Barr FA, Short B. 2003. Golgins in the structure and dynamics of the Golgi apparatus. Curr Opin Cell Biol **15**:405–413.

32. Barrientos LG, O'Keefe BR, Bray M, Sanchez A, Gronenborn AM, Boyd MR. 2003. Cyanovirin-N binds to the viral surface glycoprotein, GP1,2 and inhibits infectivity of Ebola virus. Antiviral Res **58**:47–56.

33. Barry J, Fritz M, Brender JR, Smith PE, Lee DK, Ramamoorthy A. 2009. Determining the effects of lipophilic drugs on membrane structure by solid-state NMR spectroscopy: the case of the antioxidant curcumin. J Am Chem Soc **131**:4490–4498.

34. Barth H, Schafer C, Adah MI, Zhang F, Linhardt RJ, Toyoda H, Kinoshita-Toyoda A, Toida T, Van Kuppevelt TH, Depla E, Von Weizsacker F, Blum HE, Baumert TF. 2003. Cellular binding of hepatitis C virus envelope glycoprotein E2 requires cell surface heparan sulfate. J Biol Chem **278**:41003–41012.

35. Barton ES, Forrest JC, Connolly JL, Chappell JD, Liu Y, Schnell FJ, Nusrat A, Parkos CA, Dermody TS. 2001. Junction adhesion molecule is a receptor for reovirus. Cell **104**:441–451.

36. Bartosch B, Vitelli A, Granier C, Goujon C, Dubuisson J, Pascale S, Scarselli E, Cortese R, Nicosia A, Cosset FL. 2003. Cell entry of hepatitis C virus requires a set of co-receptors that include the CD81 tetraspanin and the SR-B1 scavenger receptor. J Biol Chem **278**:41624–41630.

37. Barzu T, Level M, Petitou M, Lormeau JC, Choay J, Schols D, Baba M, Pauwels R, Witvrouw M, De Clercq E. 1993. Preparation and anti-HIV activity of O-acylated heparin and dermatan sulfate derivatives with low anticoagulant effect. J Med Chem **36**:3546–3555.

38. Basu A, Antanasijevic A, Wang M, Li B, Mills DM, Ames JA, Nash PJ, Williams JD, Peet NP, Moir DT, Prichard MN, Keith KA, Barnard DL, Caffrey M, Rong L, Bowlin TL. 2014. New small molecule entry inhibitors targeting hemagglutinin-mediated influenza a virus fusion. J Virol **88**:1447–1460.

39. Basu A, Kanda T, Beyene A, Saito K, Meyer K, Ray R. 2007. Sulfated homologues of heparin inhibit hepatitis C virus entry into mammalian cells. J Virol **81**:3933–3941.

40. Belshe RB, Smith MH, Hall CB, Betts R, Hay AJ. 1988. Genetic basis of resistance to rimantadine emerging during treatment of influenza virus infection. J Virol **62**:1508–1512.

41. Benedicto I, Molina-Jimenez F, Bartosch B, Cosset FL, Lavillette D, Prieto J, Moreno-Otero R, Valenzuela-Fernandez A, Aldabe R, Lopez-Cabrera M, Majano PL. 2009. The tight junction-associated protein occludin is required for a postbinding step in hepatitis C virus entry and infection. J Virol **83**:8012–8020.

42. Bengali Z, Townsley AC, Moss B. 2009. Vaccinia virus strain differences in cell attachment and entry. Virology **389**:132–140.

43. Benhnia MR, Maybeno M, Blum D, Aguilar-Sino R, Matho M, Meng X, Head S, Felgner PL, Zajonc DM, Koriazova L, Kato S, Burton DR, Xiang Y, Crowe JEJ, Peters B, Crotty S. 2013. Unusual features of vaccinia virus extracellular virion form neutralization resistance revealed in human antibody responses to the smallpox vaccine. J Virol **87**:1569–1585.

44. Berger SJ, Gupta S, Belfi CA, Gosky DM, Mukhtar H. 2001. Green tea constituent (--)-epigallocatechin-3-gallate inhibits topoisomerase I activity in human colon carcinoma cells. Biochem Biophys Res Commun **288**:101–105.

45. Berlutti F, Pantanella F, Natalizi T, Frioni A, Paesano R, Polimeni A, Valenti P. 2011. Antiviral properties of lactoferrin--a natural immunity molecule. Molecules **16**:6992–7018.

46. Bernfield M, Kokenyesi R, Kato M, Hinkes MT, Spring J, Gallo RL, Lose EJ. 1992. Biology of the syndecans: a family of transmembrane heparan sulfate proteoglycans. Annu Rev Cell Biol **8**:365–393.

47. Bertaux C, Dragic T. 2006. Different domains of CD81 mediate distinct stages of hepatitis C virus pseudoparticle entry. J Virol **80**:4940–4948.

48. Bharti AC, Donato N, Singh S, Aggarwal BB. 2003. Curcumin (diferuloylmethane) down-regulates the constitutive activation of nuclear factor-kappa B and IkappaBalpha kinase in human multiple myeloma cells, leading to suppression of proliferation and induction of apoptosis. Blood **101**:1053–1062.

49. Blaising J, Levy PL, Gondeau C, Phelip C, Varbanov M, Teissier E, Ruggiero F, Polyak SJ, Oberlies NH, Ivanovic T, Boulant S, Pecheur EI. 2013a. Silibinin inhibits hepatitis C virus entry into hepatocytes by hindering clathrin-dependent trafficking. Cell Microbiol **15**:1866–1882.

50. Blaising J, Levy PL, Polyak SJ, Stanifer M, Boulant S, Pecheur EI. 2013b. Arbidol inhibits viral entry by interfering with clathrin-dependent trafficking. Antiviral Res **100**:215–219.

51. Blaising J, Polyak SJ, Pecheur EI. 2014. Arbidol as a broad-spectrum antiviral: An update. Antiviral Res

52. Blanc M, Hsieh WY, Robertson KA, Kropp KA, Forster T, Shui G, Lacaze P, Watterson S, Griffiths SJ, Spann NJ, Meljon A, Talbot S, Krishnan K, Covey DF, Wenk MR, Craigon M, Ruzsics Z, Haas J, Angulo A, Griffiths WJ, Glass CK, Wang Y, Ghazal P. 2013. The transcription factor STAT-1 couples macrophage synthesis of 25-hydroxycholesterol to the interferon antiviral response. Immunity **38**:106–118.

53. Blanchard E, Belouzard S, Goueslain L, Wakita T, Dubuisson J, Wychowski C, Rouille Y. 2006. Hepatitis C virus entry depends on clathrin-mediated endocytosis. J Virol **80**:6964–6972.

54. Bleul CC, Farzan M, Choe H, Parolin C, Clark-Lewis I, Sodroski J, Springer TA. 1996. The lymphocyte chemoattractant SDF-1 is a ligand for LESTR/fusin and blocks HIV-1 entry. Nature **382**:829–833.

55. Bloor S, Maelfait J, Krumbach R, Beyaert R, Randow F. 2010. Endoplasmic reticulum chaperone gp96 is essential for infection with vesicular stomatitis virus. Proc Natl Acad Sci USA **107**:6970–6975.

56. Blumenthal R, Bali-Puri A, Walter A, Covell D, Eidelman O. 1987. pH-dependent fusion of vesicular stomatitis virus with Vero cells. Measurement by dequenching of octadecyl rhodamine fluorescence. J Biol Chem **262**:13614–13619.

57. Blumenthal R, Clague MJ, Durell SR, Epand RM. 2003. Membrane fusion. Chem Rev **103**:53–69.

58. Bobardt MD, Cheng G, de Witte L, Selvarajah S, Chatterji U, Sanders-Beer BE, Geijtenbeek TB, Chisari FV, Gallay PA. 2008. Hepatitis C virus NS5A anchor peptide disrupts human immunodeficiency virus. Proc Natl Acad Sci USA **105**:5525–5530.

59. Bolmstedt AJ, O'Keefe BR, Shenoy SR, McMahon JB, Boyd MR. 2001. Cyanovirin-N defines a new class of antiviral agent targeting N-linked, high-mannose glycans in an oligosaccharide-specific manner. Mol Pharmacol **59**:949–954.

60. Boriskin YS, Leneva IA, Pecheur EI, Polyak SJ. 2008. Arbidol: a broad-spectrum antiviral compound that blocks viral fusion. Curr Med Chem **15**:997–1005.

61. Bosch BJ, van der Zee R, de Haan CAM, Rottier PJM. 2003. The coronavirus spike protein is a class I virus fusion protein: structural and functional characterization of the fusion core complex. Journal of virology **77**:8801–8811.

62. Bose S, Banerjee AK. 2002. Role of heparan sulfate in human parainfluenza virus type 3 infection. Virology **298**:73–83.

63. Boulant S, Targett-Adams P, McLauchlan J. 2007. Disrupting the association of hepatitis C virus core protein with lipid droplets correlates with a loss in production of infectious virus. J Gen Virol **88**:2204–2213.

64. Bourne KZ, Bourne N, Reising SF, Stanberry LR. 1999. Plant products as topical microbicide candidates: assessment of in vitro and in vivo activity against herpes simplex virus type 2. Antiviral Res **42**:219–226.

65. Boyd MR, Gustafson KR, McMahon JB, Shoemaker RH, O'Keefe BR, Mori T, Gulakowski RJ, Wu L, Rivera MI, Laurencot CM, Currens MJ, Cardellina JH, Buckheit RWJ, Nara PL, Pannell LK, Sowder RC, Henderson LE. 1997. Discovery of cyanovirin-N, a novel human immunodeficiency virus-inactivating protein that binds viral surface envelope glycoprotein gp120: potential applications to microbicide development. Antimicrob Agents Chemother **41**:1521–1530.

66. Brass AL, Huang IC, Benita Y, John SP, Krishnan MN, Feeley EM, Ryan BJ, Weyer JL, van der Weyden L, Fikrig E, Adams DJ, Xavier RJ, Farzan M, Elledge SJ. 2009. The IFITM proteins mediate cellular resistance to influenza A H1N1 virus, West Nile virus, and dengue virus. Cell **139**:1243–1254.

67. Brazzoli M, Bianchi A, Filippini S, Weiner A, Zhu Q, Pizza M, Crotta S. 2008. CD81 is a central regulator of cellular events required for hepatitis C virus infection of human hepatocytes. J Virol **82**:8316–8329.

68. Breisblatt W, Ohki S. 1976. Fusion in phospholipid spherical membranes. II. Effect of cholesterol, divalent ions and pH. J Membr Biol **29**:127–146.

69. Brown DA, London E. 1998. Functions of lipid rafts in biological membranes. Annu Rev Cell Dev Biol **14**:111–136.

70. Brown MS, Goldstein JL. 1999. A proteolytic pathway that controls the cholesterol content of membranes, cells, and blood. Proc Natl Acad Sci USA **96**:11041–11048.

71. Brown MS, Goldstein JL. 1986. A receptor-mediated pathway for cholesterol homeostasis. Science **232**:34–47.

72. Brown MS, Goldstein JL. 1997. The SREBP pathway: regulation of cholesterol metabolism by proteolysis of a membrane-bound transcription factor. Cell **89**:331–340.

73. Brugger B, Glass B, Haberkant P, Leibrecht I, Wieland FT, Krausslich HG. 2006. The HIV lipidome: a raft with an unusual composition. Proc Natl Acad Sci USA **103**:2641–2646.

74. Buck CB, Day PM, Thompson CD, Lubkowski J, Lu W, Lowy DR, Schiller JT. 2006. Human alpha-defensins block papillomavirus infection. Proc Natl Acad Sci USA **103**:1516–1521.

75. Bui M, Whittaker G, Helenius A. 1996. Effect of M1 protein and low pH on nuclear transport of influenza virus ribonucleoproteins. J Virol **70**:8391–8401.

76. Bullough PA, Hughson FM, Skehel JJ, Wiley DC. 1994. Structure of influenza haemagglutinin at the pH of membrane fusion. Nature **371**:37–43.

77. Byrnes AP, Griffin DE. 1998. Binding of Sindbis virus to cell surface heparan sulfate. J Virol **72**:7349–7356.

78. Cabrera C, Artacho R, Gimenez R. 2006. Beneficial effects of green tea--a review. J Am Coll Nutr **25**:79–99.

79. Calland N, Albecka A, Belouzard S, Wychowski C, Duverlie G, Descamps V, Hober D, Dubuisson J, Rouille Y, Seron K. 2012. (-)-Epigallocatechin-3-gallate is a new inhibitor of hepatitis C virus entry. Hepatology **55**:720–729.

80. Campbell SM, Crowe SM, Mak J. 2002. Virion-associated cholesterol is critical for the maintenance of HIV-1 structure and infectivity. AIDS **16**:2253–2261.

81. Cardin AD, Weintraub HJ. 1989. Molecular modeling of protein-glycosaminoglycan interactions. Arteriosclerosis **9**:21–32.

82. Carneiro FA, Ferradosa AS, Da Poian AT. 2001. Low pH-induced conformational changes in vesicular stomatitis virus glycoprotein involve dramatic structure reorganization. J Biol Chem **276**:62–67.

83. Carro AC, Damonte EB. 2013. Requirement of cholesterol in the viral envelope for dengue virus infection. Virus Res **174**:78–87.

84. Chalmers MJ, Busby SA, Pascal BD, West GM, Griffin PR. 2011. Differential hydrogen/deuterium exchange mass spectrometry analysis of protein-ligand interactions. Expert Rev Proteomics **8**:43–59.

85. Chamoun-Emanuelli AM, Bobardt M, Moncla B, Mankowski MK, Ptak RG, Gallay P, Chen Z. 2014. Evaluation of PD 404,182 as an anti-HIV and anti-herpes simplex virus microbicide. Antimicrob Agents Chemother **58**:687–697.

86. Chamoun-Emanuelli AM, Pecheur EI, Simeon RL, Huang D, Cremer PS, Chen Z. 2013. Phenothiazines inhibit hepatitis C virus entry, likely by increasing the fluidity of cholesterol-rich membranes. Antimicrob Agents Chemother **57**:2571–2581.

87. Chamoun AM, Chockalingam K, Bobardt M, Simeon R, Chang J, Gallay P, Chen Z. 2012. PD 404,182 is a virocidal small molecule that disrupts hepatitis C virus and human immunodeficiency virus. Antimicrob Agents Chemother **56**:672–681.

88. Chan C-H, Lin K-L, Chan Y, Wang Y-L, Chi Y-T, Tu H-L, Shieh H-K, Liu W-T. 2006. Amplification of the entire genome of influenza A virus H1N1 and H3N2 subtypes by reverse-transcription polymerase chain reaction. Journal of virological methods **136**:38–43.

89. Chan DC, Fass D, Berger JM, Kim PS. 1997. Core structure of gp41 from the HIV envelope glycoprotein. Cell **89**:263–273.

90. Chan R, Uchil PD, Jin J, Shui G, Ott DE, Mothes W, Wenk MR. 2008. Retroviruses human immunodeficiency virus and murine leukemia virus are enriched in phosphoinositides. J Virol **82**:11228–11238.

91. Chandran K, Farsetta DL, Nibert ML. 2002. Strategy for nonenveloped virus entry: a hydrophobic conformer of the reovirus membrane penetration protein micro 1 mediates membrane disruption. J Virol **76**:9920–9933.

92. Chang LK, Wei TT, Chiu YF, Tung CP, Chuang JY, Hung SK, Li C, Liu ST. 2003. Inhibition of Epstein-Barr virus lytic cycle by (-)-epigallocatechin gallate. Biochem Biophys Res Commun **301**:1062–1068.

93. Chatel-Chaix L, Bartenschlager R. 2014. Dengue virus- and hepatitis C virus-induced replication and assembly compartments: the enemy inside--caught in the web. J Virol **88**:5907–5911.

94. Chaudhary LR, Hruska KA. 2003. Inhibition of cell survival signal protein kinase B/Akt by curcumin in human prostate cancer cells. J Cell Biochem **89**:1–5.

95. Chazal N, Gerlier D. 2003. Virus entry, assembly, budding, and membrane rafts. Microbiol Mol Biol Rev **67**:226–37.

96. Chen C, Zhuang X. 2008. Epsin 1 is a cargo-specific adaptor for the clathrin-mediated endocytosis of the influenza virus. Proc Natl Acad Sci USA **105**:11790–11795.

97. Chen D-Y, Shien J-H, Tiley L, Chiou S-S, Wang S-Y, Chang T-J, Lee Y-J, Chan K-W, Hsu W-L. 2010. Curcumin inhibits influenza virus infection and haemagglutination activity. Food chemistry **119**:1346–1351.

98. Chen J, Lee KH, Steinhauer DA, Stevens DJ, Skehel JJ, Wiley DC. 1998a. Structure of the hemagglutinin precursor cleavage site, a determinant of influenza pathogenicity and the origin of the labile conformation. Cell **95**:409–417.

99. Chen MH, Lee MY, Chuang JJ, Li YZ, Ning ST, Chen JC, Liu YW. 2012. Curcumin inhibits HCV replication by induction of heme oxygenase-1 and suppression of AKT. Int J Mol Med **30**:1021–1028.

100. Chen TY, Chen DY, Wen HW, Ou JL, Chiou SS, Chen JM, Wong ML, Hsu WL. 2013. Inhibition of enveloped viruses infectivity by curcumin. PLoS One **8**:e62482.

101. Chen Y, Gotte M, Liu J, Park PW. 2008. Microbial subversion of heparan sulfate proteoglycans. Mol Cells **26**:415–426.

102. Chen Y, Maguire T, Hileman RE, Fromm JR, Esko JD, Linhardt RJ, Marks RM. 1997. Dengue virus infectivity depends on envelope protein binding to target cell heparan sulfate. Nat Med **3**:866–871.

103. Chen YA, Scheller RH. 2001. SNARE-mediated membrane fusion. Nat Rev Mol Cell Biol **2**:98–106.

104. Chen ZP, Schell JB, Ho C-T, Chen KY. 1998b. Green tea epigallocatechin gallate shows a pronounced growth inhibitory effect on cancerous cells but not on their normal counterparts. Cancer Letters **129**:173–179.

105. Cheng G, Montero, A Gastaminza P, Whitten-Bauer C, Wieland SF, Isogawa M, Fredericksen B, Selvarajah S, Gallay PA, Ghadiri MR, Chisari FV. 2008. A virocidal amphipathic alpha-helical peptide that inhibits hepatitis C virus infection in vitro. Proc Natl Acad Sci USA **105**:3088–3093.

106. Chernomordik L. 1996. Non-bilayer lipids and biological fusion intermediates. Chem Phys Lipids **81**:203–213.

107. Chernomordik L, Chanturiya A, Green J, Zimmerberg J. 1995. The hemifusion intermediate and its conversion to complete fusion: regulation by membrane composition. Biophys J **69**:922–929.

108. Chernomordik LV, Kozlov MM. 2005. Membrane hemifusion: crossing a chasm in two leaps. Cell **123**:375–382.

109. Chernomordik LV, Frolov VA, Leikina E, Bronk P, Zimmerberg J. 1998. The pathway of membrane fusion catalyzed by influenza hemagglutinin: restriction of lipids, hemifusion, and lipidic fusion pore formation. J Cell Biol **140**:1369–1382.

110. Chernomordik LV, Leikina E, Frolov V, Bronk P, Zimmerberg J. 1997. An early stage of membrane fusion mediated by the low pH conformation of influenza hemagglutinin depends upon membrane lipids. J Cell Biol **136**:81–93.

111. Cheshenko N, Herold BC. 2002. Glycoprotein B plays a predominant role in mediating herpes simplex virus type 2 attachment and is required for entry and cell-to-cell spread. J Gen Virol **83**:2247–2255.

112. Choi S-K, Mammen M, Whitesides GM. 1997. Generation and in situ evaluation of libraries of poly (acrylic acid) presenting sialosides as side chains as polyvalent inhibitors of influenza-mediated hemagglutination. J Am Chem Soc **119**:4103–4111.

113. Chow J, Liu Y, Comstock K, Brandl M, Lin F, Li F, Sarma K, Alfredson T. 2010. Isolation and identification of ester impurities in RG7128, an HCV polymerase inhibitor. J Pharm Biomed Anal **53**:710–716.

114. Chowdary TK, Cairns TM, Atanasiu D, Cohen GH, Eisenberg RJ, Heldwein EE. 2010. Crystal structure of the conserved herpesvirus fusion regulator complex gH-gL. Nat Struct Mol Biol **17**:882–888.

115. Christoforidis S, McBride HM, Burgoyne RD, Zerial M. 1999. The Rab5 effector EEA1 is a core component of endosome docking. Nature **397**:621–625.

116. Chung CS, Hsiao JC, Chang YS, Chang W. 1998. A27L protein mediates vaccinia virus interaction with cell surface heparan sulfate. J Virol **72**:1577–1585.

117. Chung CS, Huang CY, Chang W. 2005. Vaccinia virus penetration requires cholesterol and results in specific viral envelope proteins associated with lipid rafts. J Virol **79**:1623–1634.

118. Ciesek S, von Hahn T, Colpitts CC, Schang LM, Friesland M, Steinmann J, Manns MP, Ott M, Wedemeyer H, Meuleman P, Pietschmann T, Steinmann E. 2011. The green tea polyphenol, epigallocatechin-3-gallate, inhibits hepatitis C virus entry. Hepatology **54**:1947–1955.

119. Cinatl J, Morgenstern B, Bauer G, Chandra P, Rabenau H, Doerr HW. 2003. Glycyrrhizin, an active component of liquorice roots, and replication of SARS-associated coronavirus. Lancet **361**:2045–2046.

120. Cladera J, Martin I, O'Shea P. 2001. The fusion domain of HIV gp41 interacts specifically with heparan sulfate on the T-lymphocyte cell surface. EMBO J **20**:19–26.

121. Clague MJ, Schoch C, Blumenthal R. 1991. Delay time for influenza virus hemagglutinin-induced membrane fusion depends on hemagglutinin surface density. J Virol **65**:2402–2407.

122. Clanton DJ, Moran RA, McMahon JB, Weislow OS, Buckheit RWJ, Hollingshead MG, Ciminale V, Felber BK, Pavlakis GN, Bader JP. 1992. Sulfonic acid dyes: inhibition of the human immunodeficiency virus and mechanism of action. J Acquir Immune Defic Syndr **5**:771–781.

123. Clare K, Hardwick SJ, Carpenter KL, Weeratunge N, Mitchinson MJ. 1995. Toxicity of oxysterols to human monocyte-macrophages. Atherosclerosis **118**:67–75.

124. Coakley E, Petropoulos CJ, Whitcomb JM. 2005. Assessing chemokine co-receptor usage in HIV. Curr Opin Infect Dis **18**:9–15.

125. Cocchi F, Fusco D, Menotti L, Gianni T, Eisenberg RJ, Cohen GH, Campadelli-Fiume G. 2004. The soluble ectodomain of herpes simplex virus gD contains a membrane-proximal pro-fusion domain and suffices to mediate virus entry. Proc Natl Acad Sci USA **101**:7445–7450.

126. Coelmont L, Kaptein S, Paeshuyse J, Vliegen I, Dumont JM, Vuagniaux G, Neyts J. 2009. Debio 025, a cyclophilin binding molecule, is highly efficient in clearing hepatitis C virus (HCV) replicon-containing cells when used alone or in combination with specifically targeted antiviral therapy for HCV (STAT-C) inhibitors. Antimicrob Agents Chemother **53**:967–976.

127. Coen DM, Schaffer PA. 1980. Two distinct loci confer resistance to acycloguanosine in herpes simplex virus type 1. Proc Natl Acad Sci USA **77**:2265–2269.

128. Coil DA, Miller AD. 2004. Phosphatidylserine is not the cell surface receptor for vesicular stomatitis virus. J Virol **78**:10920–10926.

129. Colpitts CC, Schang LM. 2014. A small molecule inhibits virion attachment to heparan sulfate- or sialic Acid-containing glycans. J Virol **88**:7806–7817.

130. Colpitts CC, Ustinov AV, Epand RF, Epand RM, Korshun VA, Schang LM. 2013. 5-(Perylen-3-yl)ethynyl-arabino-uridine (aUY11), an arabino-based rigid amphipathic fusion inhibitor, targets virion envelope lipids to inhibit fusion of influenza virus, hepatitis C virus, and other enveloped viruses. J Virol **87**:3640–3654.

131. Compton T, Nowlin DM, Cooper NR. 1993. Initiation of human cytomegalovirus infection requires initial interaction with cell surface heparan sulfate. Virology **193**:834–841.

132. Connaris H, Takimoto T, Russell R, Crennell S, Moustafa I, Portner A, Taylor G. 2002. Probing the sialic acid binding site of the hemagglutinin-neuraminidase of Newcastle disease virus: identification of key amino acids involved in cell binding, catalysis, and fusion. J Virol **76**:1816–1824.

133. Connor J, Yatvin MB, Huang L. 1984. pH-sensitive liposomes: acid-induced liposome fusion. Proc Natl Acad Sci USA **81**:1715–1718.

134. Conti C, Mastromarino P, Riccioli A, Orsi N. 1991. Electrostatic interactions in the early events of VSV infection. Res Virol **142**:17–24.

135. Cormier EG, Tsamis F, Kajumo F, Durso RJ, Gardner JP, Dragic T. 2004. CD81 is an entry coreceptor for hepatitis C virus. Proc Natl Acad Sci USA **101**:7270–7274.

136. Crance JM, Leveque F, Biziagos E, van Cuyck-Gandre H, Jouan A, Deloince R. 1994. Studies on mechanism of action of glycyrrhizin against hepatitis A virus replication in vitro. Antiviral Res **23**:63–76.

137. Croteau G, Doyon L, Thibeault D, McKercher G, Pilote L, Lamarre D. 1997. Impaired fitness of human immunodeficiency virus type 1 variants with high-level resistance to protease inhibitors. J Virol **71**:1089–1096.

138. Crublet E, Andrieu JP, Vives RR, Lortat-Jacob H. 2008. The HIV-1 envelope glycoprotein gp120 features four heparan sulfate binding domains, including the co-receptor binding site. J Biol Chem **283**:15193–15200.

139. Crumpacker CS. 1992. Mechanism of action of foscarnet against viral polymerases. Am J Med **92**:3S–7S.

140. Cureton DK, Massol RH, Saffarian S, Kirchhausen TL, Whelan SP. 2009. Vesicular stomatitis virus enters cells through vesicles incompletely coated with clathrin that depend upon actin for internalization. PLoS Pathog **5**:e1000394.

141. Daher KA, Selsted ME, Lehrer RI. 1986. Direct inactivation of viruses by human granulocyte defensins. J Virol **60**:1068–1074.

142. Danieli T, Pelletier SL, Henis YI, White JM. 1996. Membrane fusion mediated by the influenza virus hemagglutinin requires the concerted action of at least three hemagglutinin trimers. J Cell Biol **133**:559–569.

143. Danthi P, Chow M. 2004. Cholesterol removal by methyl-beta-cyclodextrin inhibits poliovirus entry. J Virol **78**:33–41.

144. Danthi P, Guglielmi KM, Kirchner E, Mainou B, Stehle T, Dermody TS. 2010. From touchdown to transcription: the reovirus cell entry pathway. Curr Top Microbiol Immunol **343**:91–119.

145. Dao Thi VL, Dreux M, Cosset FL. 2011. Scavenger receptor class B type I and the hypervariable region-1 of hepatitis C virus in cell entry and neutralisation. Expert Rev Mol Med **13**:e13.

146. Datta S, Hazari S, Chandra PK, Samara M, Poat B, Gunduz F, Wimley WC, Hauser H, Koster M, Lamaze C, Balart LA, Garry RF, Dash S. 2011. Mechanism of HCV's resistance to IFN-alpha in cell culture involves expression of functional IFN-alpha receptor 1. Virol J **8**:351.

147. David G. 1993. Integral membrane heparan sulfate proteoglycans. FASEB J **7**:1023–1030.

148. Davies WL, Grunert RR, Haff RF, McGahen JW, Neumayer EM, Paulshock M, Watts JC, Wood TR, Hermann EC, Hoffmann CE. 1964. Antiviral activity of 1-adamantanamine (amantadine). Science **144**:862–863.

149. Day PM, Lowy DR, Schiller JT. 2003. Papillomaviruses infect cells via a clathrin-dependent pathway. Virology **307**:1–11.

150. de Bethune MP. 2010. Non-nucleoside reverse transcriptase inhibitors (NNRTIs), their discovery, development, and use in the treatment of HIV-1 infection: a review of the last 20 years (1989-2009). Antiviral Res **85**:75–90.

151. de Boer SM, Kortekaas J, de Haan CA, Rottier PJ, Moormann RJ, Bosch BJ. 2012. Heparan sulfate facilitates Rift Valley fever virus entry into the cell. J Virol **86**:13767–13771.

152. De Clercq E. 2010. Antiretroviral drugs. Curr Opin Pharmacol **10**:507–515.

153. De Clercq E, Holy A. 1991. Efficacy of (S)-1-(3-hydroxy-2-phosphonylmethoxypropyl)cytosine in various models of herpes simplex virus infection in mice. Antimicrob Agents Chemother **35**:701–706.

154. De Clercq E. 2004. Antiviral drugs in current clinical use. Journal of Clinical Virology **30**:115–133.

155. de la Vega M, Marin M, Kondo N, Miyauchi K, Kim Y, Epand RF, Epand RM, Melikyan GB. 2011. Inhibition of HIV-1 endocytosis allows lipid mixing at the plasma membrane, but not complete fusion. Retrovirology **8**:99.

156. de Oliveira A, Adams SD, Lee LH, Murray SR, Hsu SD, Hammond JR, Dickinson D, Chen P, Chu TC. 2013. Inhibition of herpes simplex virus type 1 with the modified green tea polyphenol palmitoyl-epigallocatechin gallate. Food Chem Toxicol **52**:207–215.

157. de Oliveria Andrade LJ, D'Oliveira A, Melo RC, De Souza EC, Costa Silva CA, Parana R. 2009. Association between hepatitis C and hepatocellular carcinoma. J Glob Infect Dis **1**:33–37.

158. de Vries E, Tscherne DM, Wienholts MJ, Cobos-Jimenez V, Scholte F, Garcia-Sastre A, Rottier PJ, de Haan CA. 2011. Dissection of the influenza A virus endocytic routes reveals macropinocytosis as an alternative entry pathway. PLoS Pathog **7**:e1001329.

159. Dechecchi MC, Melotti P, Bonizzato A, Santacatterina M, Chilosi M, Cabrini G. 2001. Heparan sulfate glycosaminoglycans are receptors sufficient to mediate the initial binding of adenovirus types 2 and 5. J Virol **75**:8772–8780.

160. Dechecchi MC, Tamanini A, Bonizzato A, Cabrini G. 2000. Heparan sulfate glycosaminoglycans are involved in adenovirus type 5 and 2-host cell interactions. Virology **268**:382–390.

161. Delogu I, Pastorino B, Baronti C, Nougairede A, Bonnet E, de Lamballerie X. 2011. In vitro antiviral activity of arbidol against Chikungunya virus and characteristics of a selected resistant mutant. Antiviral Res **90**:99–107.

162. Demirkhanyan LH, Marin M, Padilla-Parra S, Zhan C, Miyauchi K, Jean-Baptiste M, Novitskiy G, Lu W, Melikyan GB. 2012. Multifaceted mechanisms of HIV-1 entry inhibition by human alpha-defensin. J Biol Chem **287**:28821–28838.

163. Desai TM, Marin M, Chin CR, Savidis G, Brass AL, Melikyan GB. 2014. IFITM3 restricts influenza A virus entry by blocking the formation of fusion pores following virus-endosome hemifusion. PLoS Pathog **10**:e1004048.

164. Dessau M, Modis Y. 2013. Crystal structure of glycoprotein C from Rift Valley fever virus. Proc Natl Acad Sci USA **110**:1696–1701.

165. DeTulleo L, Kirchhausen T. 1998. The clathrin endocytic pathway in viral infection. EMBO J **17**:4585–4593.

166. Di Giovine P, Settembre EC, Bhargava AK, Luftig MA, Lou H, Cohen GH, Eisenberg RJ, Krummenacher C, Carfi A. 2011. Structure of herpes simplex virus glycoprotein D bound to the human receptor nectin-1. PLoS Pathog **7**:e1002277.

167. Diallo K, Gotte M, Wainberg MA. 2003. Molecular impact of the M184V mutation in human immunodeficiency virus type 1 reverse transcriptase. Antimicrob Agents Chemother **47**:3377–3383.

168. Diamond MS, Farzan M. 2013. The broad-spectrum antiviral functions of IFIT and IFITM proteins. Nat Rev Immunol **13**:46–57.

169. Dorr P, Westby M, Dobbs S, Griffin P, Irvine B, Macartney M, Mori J, Rickett G, Smith-Burchnell C, Napier C, Webster R, Armour D, Price D, Stammen B, Wood A, Perros M. 2005. Maraviroc (UK-427,857), a potent, orally bioavailable, and selective small-molecule inhibitor of chemokine receptor CCR5 with broad-spectrum anti-human immunodeficiency virus type 1 activity. Antimicrob Agents Chemother **49**:4721–4732.

170. Douam F, Dao Thi VL, Maurin G, Fresquet J, Mompelat D, Zeisel MB, Baumert TF, Cosset FL, Lavillette D. 2014. Critical interaction between E1 and E2 glycoproteins determines binding and fusion properties of hepatitis C virus during cell entry. Hepatology **59**:776–788.

171. Douglas JL, Panis ML, Ho E, Lin KY, Krawczyk SH, Grant DM, Cai R, Swaminathan S, Cihlar T. 2003. Inhibition of respiratory syncytial virus fusion by the small molecule VP-14637 via specific interactions with F protein. J Virol **77**:5054–5064.

172. Dragic T, Litwin V, Allaway GP, Martin SR, Huang Y, Nagashima KA, Cayanan C, Maddon PJ, Koup RA, Moore JP, Paxton WA. 1996. HIV-1 entry into CD4+ cells is mediated by the chemokine receptor CC-CKR-5. Nature **381**:667–673.

173. DuBois RM, Vaney MC, Tortorici MA, Kurdi RA, Barba-Spaeth G, Krey T, Rey FA. 2013. Functional and evolutionary insight from the crystal structure of rubella virus protein E1. Nature **493**:552–556.

174. Dugan AS, Eash S, Atwood WJ. 2005. An N-linked glycoprotein with alpha(2,3)-linked sialic acid is a receptor for BK virus. J Virol **79**:14442–14445.

175. Dugan AS, Eash S, Atwood WJ. 2006. Update on BK virus entry and intracellular trafficking. Transpl Infect Dis **8**:62–67.

176. Dutch RE, Joshi SB, Lamb RA. 1998. Membrane fusion promoted by increasing surface densities of the paramyxovirus F and HN proteins: comparison of fusion reactions mediated by simian virus 5 F, human parainfluenza virus type 3 F, and influenza virus HA. J Virol **72**:7745–7753.

177. Dutta K, Ghosh D, Basu A. 2009. Curcumin protects neuronal cells from Japanese encephalitis virus-mediated cell death and also inhibits infective viral particle formation by dysregulation of ubiquitin-proteasome system. J Neuroimmune Pharmacol **4**:328–337.

178. Dwyer JJ, Wilson KL, Davison DK, Freel SA, Seedorff JE, Wring SA, Tvermoes NA, Matthews TJ, Greenberg ML, Delmedico MK. 2007. Design of helical, oligomeric HIV-1 fusion inhibitor peptides with potent activity against enfuvirtide-resistant virus. Proc Natl Acad Sci USA **104**:12772–12777.

179. Earp LJ, Delos SE, Park HE, White JM. 2005. The many mechanisms of viral membrane fusion proteins. Curr Top Microbiol Immunol **285**:25–66.

180. Eckert DM, Kim PS. 2001. Mechanisms of viral membrane fusion and its inhibition. Annu Rev Biochem **70**:777–810.

181. Edinger TO, Pohl MO, Stertz S. 2014. Entry of influenza A virus: host factors and antiviral targets. J Gen Virol **95**:263–277.

182. Egger D, Wolk B, Gosert R, Bianchi L, Blum HE, Moradpour D, Bienz K. 2002. Expression of hepatitis C virus proteins induces distinct membrane alterations including a candidate viral replication complex. J Virol **76**:5974–5984.

183. Ekiert DC, Bhabha G, Elsliger MA, Friesen RH, Jongeneelen M, Throsby M, Goudsmit J, Wilson IA. 2009. Antibody recognition of a highly conserved influenza virus epitope. Science **324**:246–251.

184. El Omari K, Iourin O, Harlos K, Grimes JM, Stuart DI. 2013. Structure of a pestivirus envelope glycoprotein E2 clarifies its role in cell entry. Cell Rep **3**:30–35.

185. El Yazidi-Belkoura I, Legrand D, Nuijens J, Slomianny MC, van Berkel P, Spik G. 2001. The binding of lactoferrin to glycosaminoglycans on enterocyte-like HT29-18-C1 cells is mediated through basic residues located in the N-terminus. Biochim Biophys Acta **1568**:197–204.

186. Epand RM. 1986. Virus replication inhibitory peptide inhibits the conversion of phospholipid bilayers to the hexagonal phase. Biosci Rep **6**:647–653.

187. Epand RM, Epand RF. 1988. Kinetic effects in the differential scanning calorimetry cooling scans of phosphatidylethanolamines. Chemistry and Physics of Lipids **49**:101–104.

188. Esko JD, Kimata K, Lindahl U. 2009. Proteoglycans and Sulfated Glycosaminoglycans. **Essentials of Glycobiology**

189. Evans MJ, von Hahn T, Tscherne DM, Syder AJ, Panis M, Wolk B, Hatziioannou T, McKeating JA, Bieniasz PD, Rice CM. 2007. Claudin-1 is a hepatitis C virus co-receptor required for a late step in entry. Nature **446**:801–805.

190. Everitt AR, Clare S, Pertel T, John SP, Wash RS, Smith SE, Chin CR, Feeley EM, Sims JS, Adams DJ, Wise HM, Kane L, Goulding D, Digard P, Anttila V, Baillie JK, Walsh TS, Hume DA, Palotie A, Xue Y, Colonna V, Tyler-Smith C, Dunning J, Gordon SB, Smyth RL, Openshaw PJ, Dougan G, Brass AL, Kellam P. 2012. IFITM3 restricts the morbidity and mortality associated with influenza. Nature **484**:519–523.

191. Farge E, Ojcius DM, Subtil A, Dautry-Varsat A. 1999. Enhancement of endocytosis due to aminophospholipid transport across the plasma membrane of living cells. Am J Physiol **276**:C725–C733.

192. Farquhar MJ, Hu K, Harris HJ, Davis C, Brimacombe CL, Fletcher SJ, Baumert TF, Rappoport JZ, Balfe P, McKeating JA. 2012. Hepatitis C virus induces CD81 and claudin-1 endocytosis. J Virol **86**:4305–4316.

193. Fasshauer D. 2003. Structural insights into the SNARE mechanism. Biochim Biophys Acta **1641**:87–97.

194. Fassina G, Buffa A, Benelli R, Varnier OE, Noonan DM, Albini A. 2002. Polyphenolic antioxidant (-)-epigallocatechin-3-gallate from green tea as a candidate anti-HIV agent. AIDS **16**:939–941.

195. Fazli A, Bradley SJ, Kiefel MJ, Jolly C, Holmes IH, von Itzstein M. 2001. Synthesis and biological evaluation of sialylmimetics as rotavirus inhibitors. J Med Chem **44**:3292–3301.

196. Feeley EM, Sims JS, John SP, Chin CR, Pertel T, Chen LM, Gaiha GD, Ryan BJ, Donis RO, Elledge SJ, Brass AL. 2011. IFITM3 inhibits influenza A virus infection by preventing cytosolic entry. PLoS Pathog **7**:e1002337.

197. Feldman SA, Audet S, Beeler JA. 2000. The fusion glycoprotein of human respiratory syncytial virus facilitates virus attachment and infectivity via an interaction with cellular heparan sulfate. J Virol **74**:6442–6447.

198. Feldman SA, Hendry RM, Beeler JA. 1999. Identification of a linear heparin binding domain for human respiratory syncytial virus attachment glycoprotein G. J Virol **73**:6610–6617.

199. Felmlee DJ, Hafirassou ML, Lefevre M, Baumert TF, Schuster C. 2013. Hepatitis C virus, cholesterol and lipoproteins--impact for the viral life cycle and pathogenesis of liver disease. Viruses **5**:1292–1324.

200. Finkelshtein D, Werman A, Novick D, Barak S, Rubinstein M. 2013. LDL receptor and its family members serve as the cellular receptors for vesicular stomatitis virus. Proc Natl Acad Sci USA **110**:7306–7311.

201. Flexner C, Barditch-Crovo PA, Kornhauser DM, Farzadegan H, Nerhood LJ, Chaisson RE, Bell KM, Lorentsen KJ, Hendrix CW, Petty BG. 1991. Pharmacokinetics, toxicity, and activity of intravenous dextran sulfate in human immunodeficiency virus infection. Antimicrob Agents Chemother **35**:2544–2550.

202. Ford MG, Mills IG, Peter BJ, Vallis Y, Praefcke GJ, Evans PR, McMahon HT. 2002. Curvature of clathrin-coated pits driven by epsin. Nature **419**:361–366.

203. Frey G, Rits-Volloch S, Zhang XQ, Schooley RT, Chen B, Harrison SC. 2006. Small molecules that bind the inner core of gp41 and inhibit HIV envelope-mediated fusion. Proc Natl Acad Sci USA **103**:13938–13943.

204. Furuse M, Fujita K, Hiiragi T, Fujimoto K, Tsukita S. 1998. Claudin-1 and -2: novel integral membrane proteins localizing at tight junctions with no sequence similarity to occludin. J Cell Biol **141**:1539–1550.

205. Furuse M, Hirase T, Itoh M, Nagafuchi A, Yonemura S, Tsukita S, Tsukita S. 1993. Occludin: a novel integral membrane protein localizing at tight junctions. J Cell Biol **123**:1777–1788.

206. Gaggar A, Shayakhmetov DM, Lieber A. 2003. CD46 is a cellular receptor for group B adenoviruses. Nat Med **9**:1408–1412.

207. Gallo SA, Wang W, Rawat SS, Jung G, Waring AJ, Cole AM, Lu H, Yan X, Daly NL, Craik DJ, Jiang S, Lehrer RI, Blumenthal R. 2006. Theta-defensins prevent HIV-1 Env-mediated fusion by binding gp41 and blocking 6-helix bundle formation. J Biol Chem **281**:18787–18792.

208. Gamblin SJ, Haire LF, Russell RJ, Stevens DJ, Xiao B, Ha Y, Vasisht N, Steinhauer DA, Daniels RS, Elliot A, Wiley DC, Skehel JJ. 2004. The structure and receptor binding properties of the 1918 influenza hemagglutinin. Science **303**:1838–1842.

209. Gane EJ, Stedman CA, Hyland RH, Ding X, Svarovskaia E, Symonds WT, Hindes RG, Berrey MM. 2013. Nucleotide polymerase inhibitor sofosbuvir plus ribavirin for hepatitis C. N Engl J Med **368**:34–44.

210. Gastaminza P, Cheng G, Wieland S, Zhong J, Liao W, Chisari FV. 2008. Cellular determinants of hepatitis C virus assembly, maturation, degradation, and secretion. J Virol **82**:2120–2129.

211. Gaudin Y. 2000a. Reversibility in fusion protein conformational changes. The intriguing case of rhabdovirus-induced membrane fusion. Subcell Biochem **34**:379–408.

212. Gaudin Y. 2000b. Rabies virus-induced membrane fusion pathway. J Cell Biol **150**:601–612.

213. Ge H, Liu G, Xiang YF, Wang Y, Guo CW, Chen NH, Zhang YJ, Wang YF, Kitazato K, Xu J. 2014. The mechanism of poly-galloyl-glucoses preventing Influenza A virus entry into host cells. PLoS One **9**:e94392.

214. Ge XY, Li JL, Yang XL, Chmura AA, Zhu G, Epstein JH, Mazet JK, Hu B, Zhang W, Peng C, Zhang YJ, Luo CM, Tan B, Wang N, Zhu Y, Crameri G, Zhang SY, Wang LF, Daszak P, Shi ZL. 2013. Isolation and characterization of a bat SARS-like coronavirus that uses the ACE2 receptor. Nature **503**:535–538.

215. Gentsch JR, Pacitti AF. 1985. Effect of neuraminidase treatment of cells and effect of soluble glycoproteins on type 3 reovirus attachment to murine L cells. J Virol **56**:356–364.

216. Germi R, Crance JM, Garin D, Guimet J, Lortat-Jacob H, Ruigrok RW, Zarski JP, Drouet E. 2002. Heparan sulfate-mediated binding of infectious dengue virus type 2 and yellow fever virus. Virology **292**:162–168.

217. Ghany MG, Strader DB, Thomas DL, Seeff LB. 2009. Diagnosis, management, and treatment of hepatitis C: an update. Hepatology **49**:1335–1374.

218. Giroglou T, Florin L, Schafer F, Streeck RE, Sapp M. 2001. Human papillomavirus infection requires cell surface heparan sulfate. J Virol **75**:1565–1570.

219. Goffard A, Callens N, Bartosch B, Wychowski C, Cosset FL, Montpellier C, Dubuisson J. 2005. Role of N-linked glycans in the functions of hepatitis C virus envelope glycoproteins. J Virol **79**:8400–8409.

220. Gold ES, Diercks AH, Podolsky I, Podyminogin RL, Askovich PS, Treuting PM, Aderem A. 2014. 25-Hydroxycholesterol acts as an amplifier of inflammatory signaling. Proc Natl Acad Sci USA: pii: 201404271.

221. Goldstein JL, Brown MS. 1990. Regulation of the mevalonate pathway. Nature **343**:425–430.

222. Goodfellow IG, Sioofy AB, Powell RM, Evans DJ. 2001. Echoviruses bind heparan sulfate at the cell surface. J Virol **75**:4918–4921.

223. Gotte M. 2012. The distinct contributions of fitness and genetic barrier to the development of antiviral drug resistance. Curr Opin Virol **2**:644–650.

224. Graham DR, Chertova E, Hilburn JM, Arthur LO, Hildreth JE. 2003. Cholesterol depletion of human immunodeficiency virus type 1 and simian immunodeficiency virus with beta-cyclodextrin inactivates and permeabilizes the virions: evidence for virion-associated lipid rafts. J Virol **77**:8237–8248.

225. Graham RL, Donaldson EF, Baric RS. 2013. A decade after SARS: strategies for controlling emerging coronaviruses. Nat Rev Microbiol **11**:836–848.

226. Greber UF, Willetts M, Webster P, Helenius A. 1993. Stepwise dismantling of adenovirus 2 during entry into cells. Cell **75**:477–486.

227. Greenberg ML, Cammack N. 2004. Resistance to enfuvirtide, the first HIV fusion inhibitor. J Antimicrob Chemother **54**:333–340.

228. Grunewald K, Desai P, Winkler DC, Heymann JB, Belnap DM, Baumeister W, Steven AC. 2003. Three-dimensional structure of herpes simplex virus from cryo-electron tomography. Science **302**:1396–1398.

229. Guinea R, Carrasco L. 1994a. Concanamycin A blocks influenza virus entry into cells under acidic conditions. FEBS Lett **349**:327–330.

230. Guinea R, Carrasco L. 1994b. Concanamycin A: a powerful inhibitor of enveloped animal-virus entry into cells. Biochem Biophys Res Commun **201**:1270–1278.

231. Gunther-Ausborn S, Praetor A, Stegmann T. 1995. Inhibition of influenza-induced membrane fusion by lysophosphatidylcholine. J Biol Chem **270**:29279–29285.

232. Guo CT, Sun XL, Kanie O, Shortridge KF, Suzuki T, Miyamoto D, Hidari KI, Wong CH, Suzuki Y. 2002. An O-glycoside of sialic acid derivative that inhibits both hemagglutinin and sialidase activities of influenza viruses. Glycobiology **12**:183–190.

233. Guo Q, Ho HT, Dicker I, Fan L, Zhou N, Friborg J, Wang T, McAuliffe BV, Wang HG, Rose RE, Fang H, Scarnati HT, Langley DR, Meanwell NA, Abraham R, Colonno RJ, Lin PF. 2003. Biochemical and genetic characterizations of a novel human immunodeficiency virus type 1 inhibitor that blocks gp120-CD4 interactions. J Virol **77**:10528–10536.

234. Gupta S, Hastak K, Afaq F, Ahmad N, Mukhtar H. 2004. Essential role of caspases in epigallocatechin-3-gallate-mediated inhibition of nuclear factor kappa B and induction of apoptosis. Oncogene **23**:2507–2522.

235. Haff RF, Stewart RC. 1965. Role of sialic acid receptors in adsorption of influenza virus to chick embryo cells. J Immunol **94**:842–851.

236. Hambleton S, Steinberg SP, Gershon MD, Gershon AA. 2007. Cholesterol dependence of varicella-zoster virion entry into target cells. J Virol **81**:7548–7558.

237. Hara K, Ikeda M, Saito S, Matsumoto S, Numata K, Kato N, Tanaka K, Sekihara H. 2002. Lactoferrin inhibits hepatitis B virus infection in cultured human hepatocytes. Hepatol Res **24**:228.

238. Harada S. 2005. The broad anti-viral agent glycyrrhizin directly modulates the fluidity of plasma membrane and HIV-1 envelope. Biochem J **392**:191–199.

239. Harada S, Yusa K, Monde K, Akaike T, Maeda Y. 2005. Influence of membrane fluidity on human immunodeficiency virus type 1 entry. Biochem Biophys Res Commun **329**:480–486.

240. Harden EA, Falshaw R, Carnachan SM, Kern ER, Prichard MN. 2009. Virucidal activity of polysaccharide extracts from four algal species against herpes simplex virus. Antiviral Res **83**:282–289.

241. Harmsen MC, Swart PJ, de Bethune MP, Pauwels R, De Clercq E, The TH, Meijer DK. 1995. Antiviral effects of plasma and milk proteins: lactoferrin shows potent activity against both human immunodeficiency virus and human cytomegalovirus replication in vitro. J Infect Dis **172**:380–388.

242. Harris HJ, Davis C, Mullins JG, Hu K, Goodall M, Farquhar MJ, Mee CJ, McCaffrey K, Young S, Drummer H, Balfe P, McKeating JA. 2010. Claudin association with CD81 defines hepatitis C virus entry. J Biol Chem **285**:21092–21102.

243. Harrison SC. 2008. Viral membrane fusion. Nat Struct Mol Biol **15**:690–698.

244. Haudecoeur R, Peuchmaur M, Ahmed-Belkacem A, Pawlotsky JM, Boumendjel A. 2013. Structure-activity relationships in the development of allosteric hepatitis C virus RNA-dependent RNA polymerase inhibitors: ten years of research. Med Res Rev **33**:934–984.

245. Hay JC, Scheller RH. 1997. SNAREs and NSF in targeted membrane fusion. Curr Opin Cell Biol **9**:505–512.

246. Hazrati E, Galen B, Lu W, Wang W, Ouyang Y, Keller MJ, Lehrer RI, Herold BC. 2006. Human alpha- and beta-defensins block multiple steps in herpes simplex virus infection. J Immunol **177**:8658–8666.

247. He W, Li LX, Liao QJ, Liu CL, Chen XL. 2011. Epigallocatechin gallate inhibits HBV DNA synthesis in a viral replication - inducible cell line. World J Gastroenterol **17**:1507–1514.

248. Helbig B, Klöcking R, Wutzler P. 1997. Anti-herpes simplex virus type 1 activity of humic acid-like polymers and their o-diphenolic starting compounds. Antiviral Chem Chemother **8**:265–273.

249. Heldwein EE, Lou H, Bender FC, Cohen GH, Eisenberg RJ, Harrison SC. 2006. Crystal structure of glycoprotein B from herpes simplex virus 1. Science **313**:217–220.

250. Helle F, Wychowski C, Vu-Dac N, Gustafson KR, Voisset C, Dubuisson J. 2006. Cyanovirin-N inhibits hepatitis C virus entry by binding to envelope protein glycans. J Biol Chem **281**:25177–25183.

251. Henrich TJ, Kuritzkes DR. 2013. HIV-1 entry inhibitors: recent development and clinical use. Curr Opin Virol **3**:51–57.

252. Herold BC, Visalli RJ, Susmarski N, Brandt CR, Spear PG. 1994. Glycoprotein C-independent binding of herpes simplex virus to cells requires cell surface heparan sulphate and glycoprotein B. J Gen Virol **75**:1211–1222.

253. Herold BC, WuDunn D, Soltys N, Spear PG. 1991. Glycoprotein C of herpes simplex virus type 1 plays a principal role in the adsorption of virus to cells and in infectivity. J Virol **65**:1090–1098.

254. Herz C, Stavnezer E, Krug R, Gurney TJ. 1981. Influenza virus, an RNA virus, synthesizes its messenger RNA in the nucleus of infected cells. Cell **26**:391–400.

255. Hidari KI, Murata T, Yoshida K, Takahashi Y, Minamijima YH, Miwa Y, Adachi S, Ogata M, Usui T, Suzuki Y, Suzuki T. 2008. Chemoenzymatic synthesis, characterization, and application of glycopolymers carrying lactosamine repeats as entry inhibitors against influenza virus infection. Glycobiology **18**:779–788.

256. Hirata N, Suizu F, Matsuda-Lennikov M, Edamura T, Bala J, Noguchi M. 2014. Inhibition of Akt kinase activity suppresses entry and replication of influenza virus. Biochem Biophys Res Commun doi: 10.1016/j.bbrc.2014.06.077.

257. Hirst GK. 1941. The agglutination of red cells by allantoic fluid of chick embryos infected with influenza virus. Science **94**:22–23.

258. Ho HY, Cheng ML, Weng SF, Leu YL, Chiu DT. 2009. Antiviral effect of epigallocatechin gallate on enterovirus 71. J Agric Food Chem **57**:6140–6147.

259. Ho Y, Hsiao JC, Yang MH, Chung CS, Peng YC, Lin TH, Chang W, Tzou DL. 2005. The oligomeric structure of vaccinia viral envelope protein A27L is essential for binding to heparin and heparan sulfates on cell surfaces: a structural and functional approach using site-specific mutagenesis. J Mol Biol **349**:1060–1071.

260. Hoever G, Baltina L, Michaelis M, Kondratenko R, Baltina L, Tolstikov GA, Doerr HW, Cinatl JJ. 2005. Antiviral activity of glycyrrhizic acid derivatives against SARS-coronavirus. J Med Chem **48**:1256–1259.

261. Hosoya M, Shigeta S, Nakamura K, De Clercq E. 1989. Inhibitory effect of selected antiviral compounds on measles (SSPE) virus replication in vitro. Antiviral Res **12**:87–97.

262. Howard CR, Fletcher NF. 2012. Emerging virus diseases: can we ever expect the unexpected? Emerg Microbes & Infect doi:10.1038/emi.2012.47

263. Howell JI, Ahkong QF, Cramp FC, Fisher D, Tampion W, Lucy JA. 1972. Membrane fluidity and membrane fusion. Biochem J **130**:44P.

264. Hrobowski YM, Garry RF, Michael SF. 2005. Peptide inhibitors of dengue virus and West Nile virus infectivity. Virol J **2**:49.

265. Hsiao JC, Chung CS, Chang W. 1998. Cell surface proteoglycans are necessary for A27L protein-mediated cell fusion: identification of the N-terminal region of A27L protein as the glycosaminoglycan-binding domain. J Virol **72**:8374–8379.

266. Hsiao JC, Chung CS, Chang W. 1999. Vaccinia virus envelope D8L protein binds to cell surface chondroitin sulfate and mediates the adsorption of intracellular mature virions to cells. J Virol **73**:8750–8761.

267. Hu K, Carroll J, Fedorovich S, Rickman C, Sukhodub A, Davletov B. 2002. Vesicular restriction of synaptobrevin suggests a role for calcium in membrane fusion. Nature **415**:646–650.

268. Huang H, Li Y, Sadaoka T, Tang H, Yamamoto T, Yamanishi K, Mori Y. 2006. Human herpesvirus 6 envelope cholesterol is required for virus entry. J Gen Virol **87**:277–285.

269. Huang IC, Bailey CC, Weyer JL, Radoshitzky SR, Becker MM, Chiang JJ, Brass AL, Ahmed AA, Chi X, Dong L, Longobardi LE, Boltz D, Kuhn JH, Elledge SJ, Bavari S, Denison MR, Choe H, Farzan M. 2011. Distinct patterns of IFITM-mediated restriction of filoviruses, SARS coronavirus, and influenza A virus. PLoS Pathog **7**:e1001258.

270. Huang K, Incognito L, Cheng X, Ulbrandt ND, Wu H. 2010. Respiratory syncytial virus-neutralizing monoclonal antibodies motavizumab and palivizumab inhibit fusion. J Virol **84**:8132–8140.

271. Hurtado C, Bustos MJ, Sabina P, Nogal ML, Granja AG, Gonzalez ME, Gonzalez-Porque P, Revilla Y, Carrascosa AL. 2008. Antiviral activity of lauryl gallate against animal viruses. Antivir Ther **13**:909–917.

272. Hutchinson L, Browne H, Wargent V, Davis-Poynter N, Primorac S, Goldsmith K, Minson AC, Johnson DC. 1992. A novel herpes simplex virus glycoprotein, gL, forms a complex with glycoprotein H (gH) and affects normal folding and surface expression of gH. J Virol **66**:2240–2250.

273. Iannello A, Debbeche O, Martin E, Attalah LH, Samarani S, Ahmad A. 2006. Viral strategies for evading antiviral cellular immune responses of the host. J Leukoc Biol **79**:16–35.

274. Ikeda M, Nozaki A, Sugiyama K, Tanaka T, Naganuma A, Tanaka K, Sekihara H, Shimotohno K, Saito M, Kato N. 2000. Characterization of antiviral activity of lactoferrin against hepatitis C virus infection in human cultured cells. Virus Res **66**:51–63.

275. Ikematsu H, Kawai N. 2011. Laninamivir octanoate: a new long-acting neuraminidase inhibitor for the treatment of influenza. Expert Rev Anti Infect Ther **9**:851–857.

276. Ingolfsson HI, Koeppe RE, Andersen OS. 2007. Curcumin is a modulator of bilayer material properties. Biochemistry **46**:10384–10391.

277. Isa P, Arias CF, Lopez S. 2006. Role of sialic acids in rotavirus infection. Glycoconj J **23**:27–37.

278. Isaacs CE, Wen GY, Xu W, Jia JH, Rohan L, Corbo C, Di Maggio V, Jenkins ECJ, Hillier S. 2008. Epigallocatechin gallate inactivates clinical isolates of herpes simplex virus. Antimicrob Agents Chemother **52**:962–970.

279. Isaacs CE, Xu W, Merz G, Hillier S, Rohan L, Wen GY. 2011. Digallate Dimers of (-)-Epigallocatechin Gallate Inactivate Herpes Simplex Virus. Antimicrob Agents Chemother **55**:5646-53.

280. Ison MG. 2011. Antivirals and resistance: influenza virus. Curr Opin Virol **1**:563–573.

281. Itoh M, Hetterich P, Isecke R, Brossmer R, Klenk HD. 1995. Suppression of influenza virus infection by an N-thioacetylneuraminic acid acrylamide copolymer resistant to neuraminidase. Virology **212**:340–347.

282. Jackson JO, Longnecker R. 2010. Reevaluating herpes simplex virus hemifusion. J Virol **84**:11814–11821.

283. Janssen HL, Reesink HW, Lawitz EJ, Zeuzem S, Rodriguez-Torres M, Patel K, van der Meer AJ, Patick AK, Chen A, Zhou Y, Persson R, King BD, Kauppinen S, Levin AA, Hodges MR. 2013. Treatment of HCV infection by targeting microRNA. N Engl J Med **368**:1685–1694.

284. Jia R, Xu F, Qian J, Yao Y, Miao C, Zheng YM, Liu SL, Guo F, Geng Y, Qiao W, Liang C. 2014. Identification of an endocytic signal essential for the antiviral action of IFITM3. Cell Microbiol **16**:1080–1093.

285. Jiang J, Cun W, Wu X, Shi Q, Tang H, Luo G. 2012. Hepatitis C virus attachment mediated by apolipoprotein E binding to cell surface heparan sulfate. J Virol **86**:7256–7267.

286. Joyce JG, Tung JS, Przysiecki CT, Cook JC, Lehman ED, Sands JA, Jansen KU, Keller PM. 1999. The L1 major capsid protein of human papillomavirus type 11 recombinant virus-like particles interacts with heparin and cell-surface glycosaminoglycans on human keratinocytes. J Biol Chem **274**:5810–5822.

287. Kane CJ, Menna JH, Sung CC, Yeh YC. 1988. Methyl gallate, methyl-3,4,5-trihydoxybenzoate, is a potent and highly specific inhibitor of herpes simplex virus in vitro. II. Antiviral activity of methyl gallate and its derivatives. Biosci Rep **8**:95–102.

288. Kapadia SB, Barth H, Baumert T, McKeating JA, Chisari FV. 2007. Initiation of hepatitis C virus infection is dependent on cholesterol and cooperativity between CD81 and scavenger receptor B type I. J Virol **81**:374–383.

289. Kaplan AS, Ben-Porat T. 1966. Mode of antiviral action of 5-iodouracil deoxyriboside. J Mol Biol **19**:320–332.

290. Katz DH, Marcelletti JF, Khalil MH, Pope LE, Katz LR. 1991. Antiviral activity of 1-docosanol, an inhibitor of lipid-enveloped viruses including herpes simplex. Proc Natl Acad Sci USA **88**:10825–10829.

291. Kawai K, Tsuno NH, Kitayama J, Okaji Y, Yazawa K, Asakage M, Hori N, Watanabe T, Takahashi K, Nagawa H. 2003. Epigallocatechin gallate, the main component of tea polyphenol, binds to CD4 and interferes with gp120 binding. J Allergy Clin Immunol **112**:951–957.

292. Khan AG, Whidby J, Miller MT, Scarborough H, Zatorski AV, Cygan A, Price AA, Yost SA, Bohannon CD, Jacob J, Grakoui A, Marcotrigiano J. 2014. Structure of the core ectodomain of the hepatitis C virus envelope glycoprotein 2. Nature **509**:361–364.

293. Kieff ED, Bachenheimer SL, Roizman B. 1971. Size, composition, and structure of the deoxyribonucleic acid of herpes simplex virus subtypes 1 and 2. J Virol **8**:125–132.

294. Kielian M, Chanel-Vos C, Liao M. 2010. Alphavirus Entry and Membrane Fusion. Viruses **2**:796–825.

295. Kielian M, Rey FA. 2006. Virus membrane-fusion proteins: more than one way to make a hairpin. Nat Rev Microbiol **4**:67–76.

296. Kilby JM, Hopkins S, Venetta TM, DiMassimo B, Cloud GA, Lee JY, Alldredge L, Hunter E, Lambert D, Bolognesi D, Matthews T, Johnson MR, Nowak MA, Shaw GM, Saag MS. 1998. Potent suppression of HIV-1 replication in humans by T-20, a peptide inhibitor of gp41-mediated virus entry. Nat Med **4**:1302–1307.

297. Kim K, Kim KH, Kim HY, Cho HK, Sakamoto N, Cheong J. 2010. Curcumin inhibits hepatitis C virus replication via suppressing the Akt-SREBP-1 pathway. FEBS Lett **584**:707–712.

298. Kim M, Kim SY, Lee HW, Shin JS, Kim P, Jung YS, Jeong HS, Hyun JK, Lee CK. 2013. Inhibition of influenza virus internalization by (-)-epigallocatechin-3-gallate. Antiviral Res **100**:460-72.

299. Kimberlin DW, Whitley RJ. 1996. Antiviral resistance: mechanisms, clinical significance, and future implications. J Antimicrob Chemother **37**:403–421.

300. Kirchner E, Guglielmi KM, Strauss HM, Dermody TS, Stehle T. 2008. Structure of reovirus sigma1 in complex with its receptor junctional adhesion molecule-A. PLoS Pathog **4**:e1000235.

301. Kirkham M, Parton RG. 2005. Clathrin-independent endocytosis: new insights into caveolae and non-caveolar lipid raft carriers. Biochim Biophys Acta **1746**:349–363.

302. Kiser JJ, Burton JRJ, Everson GT. 2013. Drug-drug interactions during antiviral therapy for chronic hepatitis C. Nat Rev Gastroenterol Hepatol **10**:596–606.

303. Kiss T, Fenyvesi F, Bacskay I, Varadi J, Fenyvesi E, Ivanyi R, Szente L, Tosaki A, Vecsernyes M. 2010. Evaluation of the cytotoxicity of beta-cyclodextrin derivatives: evidence for the role of cholesterol extraction. Eur J Pharm Sci **40**:376–380.

304. Klotman ME, Chang TL. 2006. Defensins in innate antiviral immunity. Nat Rev Immunol **6**:447–456.

305. Kohl NE, Emini EA, Schleif WA, Davis LJ, Heimbach JC, Dixon RA, Scolnick EM, Sigal IS. 1988. Active human immunodeficiency virus protease is required for viral infectivity. Proc Natl Acad Sci USA **85**:4686–4690.

306. Kong L, Giang E, Nieusma T, Kadam RU, Cogburn KE, Hua Y, Dai X, Stanfield RL, Burton DR, Ward AB, Wilson IA, Law M. 2013. Hepatitis C virus E2 envelope glycoprotein core structure. Science **342**:1090–1094.

307. Kota S, Sabbah A, Chang TH, Harnack R, Xiang Y, Meng X, Bose S. 2008. Role of human beta-defensin-2 during tumor necrosis factor-alpha/NF-kappaB-mediated innate antiviral response against human respiratory syncytial virus. J Biol Chem **283**:22417–22429.

308. Kratz JM, Andrighetti-Frohner CR, Kolling DJ, Leal PC, Cirne-Santos CC, Yunes RA, Nunes RJ, Trybala E, Bergstrom T, Frugulhetti IC, Barardi CR, Simoes CM. 2008a. Anti-HSV-1 and anti-HIV-1 activity of gallic acid and pentyl gallate. Mem Inst Oswaldo Cruz **103**:437–442.

309. Kratz JM, Andrighetti-Frohner CR, Leal PC, Nunes RJ, Yunes RA, Trybala E, Bergstrom T, Barardi CR, Simoes CM. 2008b. Evaluation of anti-HSV-2 activity of gallic acid and pentyl gallate. Biol Pharm Bull **31**:903–907.

310. Krey T, d'Alayer J, Kikuti CM, Saulnier A, Damier-Piolle L, Petitpas I, Johansson DX, Tawar RG, Baron B, Robert B, England P, Persson MA, Martin A, Rey FA. 2010. The disulfide bonds in glycoprotein E2 of hepatitis C virus reveal the tertiary organization of the molecule. PLoS Pathog **6**:e1000762.

311. Kroll DJ, Shaw HS, Oberlies NH. 2007. Milk thistle nomenclature: why it matters in cancer research and pharmacokinetic studies. Integr Cancer Ther **6**:110–119.

312. Krusat T, Streckert HJ. 1997. Heparin-dependent attachment of respiratory syncytial virus (RSV) to host cells. Arch Virol **142**:1247–1254.

313. Krystal M, Elliott RM, Benz EW, Young JF, Palese P. 1982. Evolution of influenza A and B viruses: conservation of structural features in the hemagglutinin genes. Proc Natl Acad Sci USA **79**:4800–4804.

314. Kupferschmidt K. 2014. Emerging diseases. Soaring MERS cases in Saudi Arabia raise alarms. Science **344**:457–458.

315. Kutluay SB, Doroghazi J, Roemer ME, Triezenberg SJ. 2008. Curcumin inhibits herpes simplex virus immediate-early gene expression by a mechanism independent of p300/CBP histone acetyltransferase activity. Virology **373**:239–247.

316. Lamb RA, Jardetzky TS. 2007. Structural basis of viral invasion: lessons from paramyxovirus F. Curr Opin Struct Biol **17**:427–436.

317. Lambert DM, Barney S, Lambert AL, Guthrie K, Medinas R, Davis DE, Bucy T, Erickson J, Merutka G, Petteway SRJ. 1996. Peptides from conserved regions of paramyxovirus fusion (F) proteins are potent inhibitors of viral fusion. Proc Natl Acad Sci USA **93**:2186–2191.

318. Lande MB, Donovan JM, Zeidel ML. 1995. The relationship between membrane fluidity and permeabilities to water, solutes, ammonia, and protons. J Gen Physiol **106**:67–84.

319. Lang J, Yang N, Deng J, Liu K, Yang P, Zhang G, Jiang C. 2011. Inhibition of SARS pseudovirus cell entry by lactoferrin binding to heparan sulfate proteoglycans. PLoS One **6**:e23710.

320. Lange Y, Ye J, Rigney M, Steck TL. 1999. Regulation of endoplasmic reticulum cholesterol by plasma membrane cholesterol. J Lipid Res **40**:2264–2270.

321. Lange Y, Ye J, Steck TL. 2004. How cholesterol homeostasis is regulated by plasma membrane cholesterol in excess of phospholipids. Proc Natl Acad Sci USA **101**:11664–11667.

322. Laquerre S, Argnani R, Anderson DB, Zucchini S, Manservigi R, Glorioso JC. 1998. Heparan sulfate proteoglycan binding by herpes simplex virus type 1 glycoproteins B and C, which differ in their contributions to virus attachment, penetration, and cell-to-cell spread. J Virol **72**:6119–6130.

323. Lauring AS, Andino R. 2010. Quasispecies theory and the behavior of RNA viruses. PLoS Pathog **6**:e1001005.

324. Lavillette D, Bartosch B, Nourrisson D, Verney G, Cosset FL, Penin F, Pecheur EI. 2006. Hepatitis C virus glycoproteins mediate low pH-dependent membrane fusion with liposomes. J Biol Chem **281**:3909–3917.

325. Law M, Carter GC, Roberts KL, Hollinshead M, Smith GL. 2006. Ligand-induced and nonfusogenic dissolution of a viral membrane. Proc Natl Acad Sci USA **103**:5989–5994.

326. Le Blanc I, Luyet PP, Pons V, Ferguson C, Emans N, Petiot A, Mayran N, Demaurex N, Faure J, Sadoul R, Parton RG, Gruenberg J. 2005. Endosome-to-cytosol transport of viral nucleocapsids. Nat Cell Biol **7**:653–664.

327. Lee AS-Y, Burdeinick-Kerr R, Whelan SPJ. 2014. A genome-wide siRNA screen identifies host factors required for vesicular stomatitis virus infection. J Virol **88:**8355-8360.

328. Lee E, Pavy M, Young N, Freeman C, Lobigs M. 2006a. Antiviral effect of the heparan sulfate mimetic, PI-88, against dengue and encephalitic flaviviruses. Antiviral Res **69**:31–38.

329. Lee JE, Fusco ML, Hessell AJ, Oswald WB, Burton DR, Saphire EO. 2008. Structure of the Ebola virus glycoprotein bound to an antibody from a human survivor. Nature **454**:177–182.

330. Lee MJ, Maliakal P, Chen L, Meng X, Bondoc FY, Prabhu S, Lambert G, Mohr S, Yang CS. 2002. Pharmacokinetics of Tea Catechins after Ingestion of Green Tea and (−)-Epigallocatechin-3-gallate by Humans. Cancer Epidemiol Biomarkers Prev **11**:1025–1032.

331. Lee PW, Hayes EC, Joklik WK. 1981. Protein sigma 1 is the reovirus cell attachment protein. Virology **108**:156–163.

332. Lee SJ, Lee HK, Jung MK, Mar W. 2006b. In vitro antiviral activity of 1,2,3,4,6-penta-O-galloyl-beta-D-glucose against hepatitis B virus. Biol Pharm Bull **29**:2131–2134.

333. Lees WJ, Spaltenstein A, Kingery-Wood JE, Whitesides GM. 1994. Polyacrylamides Bearing Pendant. alpha.-Sialoside Groups Strongly Inhibit Agglutination of Erythrocytes by Influenza A Virus: Multivalency and Steric Stabilization of Particulate Biological Systems. J Med Chem **37**:3419–3433.

334. Lehmann F, Tiralongo E, Tiralongo J. 2006. Sialic acid-specific lectins: occurrence, specificity and function. Cell Mol Life Sci **63**:1331–1354.

335. Leikina E, Delanoe-Ayari H, Melikov K, Cho MS, Chen A, Waring AJ, Wang W, Xie Y, Loo JA, Lehrer RI, Chernomordik LV. 2005. Carbohydrate-binding molecules inhibit viral fusion and entry by crosslinking membrane glycoproteins. Nat Immunol **6**:995–1001.

336. Leistner CM, Gruen-Bernhard S, Glebe D. 2008. Role of glycosaminoglycans for binding and infection of hepatitis B virus. Cell Microbiol **10**:122–133.

337. Leneva IA, Russell RJ, Boriskin YS, Hay AJ. 2009. Characteristics of arbidol-resistant mutants of influenza virus: implications for the mechanism of anti-influenza action of arbidol. Antiviral Res **81**:132–140.

338. Lentz BR. 1989. Membrane "fluidity" as detected by diphenylhexatriene probes. Chemistry and Physics of Lipids **50**:171–190.

339. Leopold PL, Crystal RG. 2007. Intracellular trafficking of adenovirus: many means to many ends. Adv Drug Deliv Rev **59**:810–821.

340. Lescar J, Roussel A, Wien MW, Navaza J, Fuller SD, Wengler G, Wengler G, Rey FA. 2001. The Fusion glycoprotein shell of Semliki Forest virus: an icosahedral assembly primed for fusogenic activation at endosomal pH. Cell **105**:137–148.

341. Levy S, Todd SC, Maecker HT. 1998. CD81 (TAPA-1): a molecule involved in signal transduction and cell adhesion in the immune system. Annu Rev Immunol **16**:89–109.

342. Li E, Stupack D, Bokoch GM, Nemerow GR. 1998a. Adenovirus endocytosis requires actin cytoskeleton reorganization mediated by Rho family GTPases. J Virol **72**:8806–8812.

343. Li E, Stupack D, Klemke R, Cheresh DA, Nemerow GR. 1998b. Adenovirus endocytosis via alpha(v) integrins requires phosphoinositide-3-OH kinase. J Virol **72**:2055–2061.

344. Li, K, Markosyan, RM, Zheng, YM, Golfetto, O, Bungart, B, Li, M, Ding, S, He, Y, Liang, C, Lee, JC, Gratton, E, Cohen, FS, Liu, SL. 2013a. IFITM proteins restrict viral membrane hemifusion. PLoS Pathog **9**:e1003124.

345. Li Y, Modis Y. 2014. A novel membrane fusion protein family in Flaviviridae? Trends Microbiol **22(4)**:176–182.

346. Li Y, Wang J, Kanai R, Modis Y. 2013b. Crystal structure of glycoprotein E2 from bovine viral diarrhea virus. Proc Natl Acad Sci USA **110**:6805–6810.

347. Liang TJ, Ghany MG. 2013. Current and future therapies for hepatitis C virus infection. New Eng J Med **368**:1907–1917.

348. Lieberman-Blum SS, Fung HB, Bandres JC. 2008. Maraviroc: a CCR5-receptor antagonist for the treatment of HIV-1 infection. Clin Ther **30**:1228–1250.

349. Ligeret H, Barthelemy S, Zini R, Tillement JP, Labidalle S, Morin D. 2004. Effects of curcumin and curcumin derivatives on mitochondrial permeability transition pore. Free Radic Biol Med **36**:919–929.

350. Lin CL, Chung CS, Heine HG, Chang W. 2000. Vaccinia virus envelope H3L protein binds to cell surface heparan sulfate and is important for intracellular mature virion morphogenesis and virus infection in vitro and in vivo. J Virol **74**:3353–3365.

351. Lin LT, Chen TY, Chung CY, Noyce RS, Grindley TB, McCormick C, Lin TC, Wang GH, Lin CC, Richardson CD. 2011. Hydrolyzable tannins (chebulagic acid and punicalagin) target viral glycoprotein-glycosaminoglycan interactions to inhibit herpes simplex virus 1 entry and cell-to-cell spread. J Virol **85**:4386–4398.

352. Lin LT, Chen TY, Lin SC, Chung CY, Lin TC, Wang GH, Anderson R, Lin CC, Richardson CD. 2013. Broad-spectrum antiviral activity of chebulagic acid and punicalagin against viruses that use glycosaminoglycans for entry. BMC Microbiol **13**:187.

353. Lin PF, Blair W, Wang T, Spicer T, Guo Q, Zhou N, Gong YF, Wang HG, Rose R, Yamanaka G, Robinson B, Li CB, Fridell R, Deminie C, Demers G, Yang Z, Zadjura L, Meanwell N, Colonno R. 2003. A small molecule HIV-1 inhibitor that targets the HIV-1 envelope and inhibits CD4 receptor binding. Proc Natl Acad Sci USA **100**:11013–11018.

354. Liu CK, Wei G, Atwood WJ. 1998. Infection of glial cells by the human polyomavirus JC is mediated by an N-linked glycoprotein containing terminal alpha(2-6)-linked sialic acids. J Virol **72**:4643–4649.

355. Liu G, Xiong S, Xiang YF, Guo CW, Ge F, Yang CR, Zhang YJ, Wang YF, Kitazato K. 2011. Antiviral activity and possible mechanisms of action of pentagalloylglucose (PGG) against influenza A virus. Arch Virol **156**:1359–1369.

356. Liu R, Paxton WA, Choe S, Ceradini D, Martin SR, Horuk R, MacDonald ME, Stuhlmann H, Koup RA, Landau NR. 1996. Homozygous defect in HIV-1 coreceptor accounts for resistance of some multiply-exposed individuals to HIV-1 infection. Cell **86**:367–377.

357. Liu R, Tewari M, Kong R, Zhang R, Ingravallo P, Ralston R. 2010. A peptide derived from hepatitis C virus E2 envelope protein inhibits a post-binding step in HCV entry. Antiviral Res **86**:172–179.

358. Liu S, Lu H, Zhao Q, He Y, Niu J, Debnath AK, Wu S, Jiang S. 2005. Theaflavin derivatives in black tea and catechin derivatives in green tea inhibit HIV-1 entry by targeting gp41. Biochim Biophys Acta **1723**:270–281.

359. Liu SY, Aliyari R, Chikere K, Li G, Marsden MD, Smith JK, Pernet O, Guo H, Nusbaum R, Zack JA, Freiberg AN, Su L, Lee B, Cheng G. 2013. Interferon-inducible cholesterol-25-hydroxylase broadly inhibits viral entry by production of 25-hydroxycholesterol. Immunity **38**:92–105.

360. Lorentsen KJ, Hendrix CW, Collins JM, Kornhauser DM, Petty BG, Klecker RW, Flexner C, Eckel RH, Lietman PS. 1989. Dextran sulfate is poorly absorbed after oral administration. Ann Intern Med **111**:561–566.

361. Lu J, Pan Q, Rong L, He W, Liu SL, Liang C. 2011. The IFITM proteins inhibit HIV-1 infection. J Virol **85**:2126–2137.

362. Lu L, Liu Q, Zhu Y, Chan KH, Qin L, Li Y, Wang Q, Chan JF, Du L, Yu F, Ma C, Ye S, Yuen KY, Zhang R, Jiang S. 2014. Structure-based discovery of Middle East respiratory syndrome coronavirus fusion inhibitor. Nat Commun **5**:3067.

363. Lu Y, Liu DX, Tam JP. 2008. Lipid rafts are involved in SARS-CoV entry into Vero E6 cells. Biochem Biophys Res Commun **369**:344–349.

364. Luo G, Torri A, Harte WE, Danetz S, Cianci C, Tiley L, Day S, Mullaney D, Yu KL, Ouellet C, Dextraze P, Meanwell N, Colonno R, Krystal M. 1997. Molecular mechanism underlying the action of a novel fusion inhibitor of influenza A virus. J Virol **71**:4062–4070.

365. Luo M. 2012. The nucleocapsid of vesicular stomatitis virus. Sci China Life Sci **55**:291–300.

366. Lupberger J, Zeisel MB, Xiao F, Thumann C, Fofana I, Zona L, Davis C, Mee CJ, Turek M, Gorke S, Royer C, Fischer B, Zahid MN, Lavillette D, Fresquet J, Cosset FL, Rothenberg SM, Pietschmann T, Patel AH, Pessaux P, Doffoel M, Raffelsberger W, Poch O, McKeating JA, Brino L, Baumert TF. 2011. EGFR and EphA2 are host factors for hepatitis C virus entry and possible targets for antiviral therapy. Nat Med **17**:589–595.

367. Ma Y, Xu L, Rodriguez-Agudo D, Li X, Heuman DM, Hylemon PB, Pandak WM, Ren S. 2008. 25-Hydroxycholesterol-3-sulfate regulates macrophage lipid metabolism via the LXR/SREBP-1 signaling pathway. American Journal of Physiology-Endocrinology and Metabolism **295**:E1369–E1379.

368. Mackenzie JM, Khromykh AA, Parton RG. 2007. Cholesterol manipulation by West Nile virus perturbs the cellular immune response. Cell Host Microbe **2**:229–239.

369. Mackewicz CE, Yuan J, Tran P, Diaz L, Mack E, Selsted ME, Levy JA. 2003. α-Defensins can have anti-HIV activity but are not CD8 cell anti-HIV factors. Aids **17**:F23–F32.

370. Macovei A, Radulescu C, Lazar C, Petrescu S, Durantel D, Dwek RA, Zitzmann N, Nichita NB. 2010. Hepatitis B virus requires intact caveolin-1 function for productive infection in HepaRG cells. J Virol **84**:243–253.

371. Maginnis MS, Forrest JC, Kopecky-Bromberg SA, Dickeson SK, Santoro SA, Zutter MM, Nemerow GR, Bergelson JM, Dermody TS. 2006. Beta1 integrin mediates internalization of mammalian reovirus. J Virol **80**:2760–2770.

372. Malakhov MP, Aschenbrenner LM, Smee DF, Wandersee MK, Sidwell RW, Gubareva LV, Mishin VP, Hayden FG, Kim DH, Ing A, Campbell ER, Yu M, Fang F. 2006. Sialidase fusion protein as a novel broad-spectrum inhibitor of influenza virus infection. Antimicrob Agents Chemother **50**:1470–1479.

373. Malkovsky M, Newell A, Dalgleish AG. 1988. Inactivation of HIV by nonoxynol-9. Lancet **1**:645.

374. Mammano F, Petit C, Clavel F. 1998. Resistance-associated loss of viral fitness in human immunodeficiency virus type 1: phenotypic analysis of protease and gag coevolution in protease inhibitor-treated patients. J Virol **72**:7632–7637.

375. Mammen M, Dahmann G, Whitesides GM. 1995. Effective inhibitors of hemagglutination by influenza virus synthesized from polymers having active ester groups. Insight into mechanism of inhibition. J Med Chem **38**:4179–4190.

376. Manie SN, de Breyne S, Vincent S, Gerlier D. 2000. Measles virus structural components are enriched into lipid raft microdomains: a potential cellular location for virus assembly. J Virol **74**:305–311.

377. Marcellin P, Chang T-T, Lim SG, Tong MJ, Sievert W, Shiffman ML, Jeffers L, Goodman Z, Wulfsohn MS, Xiong S. 2003. Adefovir dipivoxil for the treatment of hepatitis B e antigen–positive chronic hepatitis B. New Eng J Med **348**:808–816.

378. Marchetti M, Longhi C, Conte MP, Pisani S, Valenti P, Seganti L. 1996. Lactoferrin inhibits herpes simplex virus type 1 adsorption to Vero cells. Antiviral Res **29**:221–231.

379. Marchetti M, Superti F, Ammendolia MG, Rossi P, Valenti P, Seganti L. 1999. Inhibition of poliovirus type 1 infection by iron-, manganese- and zinc-saturated lactoferrin. Med Microbiol Immunol **187**:199–204.

380. Mardberg K, Trybala E, Glorioso JC, Bergstrom T. 2001. Mutational analysis of the major heparan sulfate-binding domain of herpes simplex virus type 1 glycoprotein C. J Gen Virol **82**:1941–1950.

381. Marjomaki V, Pietiainen V, Matilainen H, Upla P, Ivaska J, Nissinen L, Reunanen H, Huttunen P, Hyypia T, Heino J. 2002. Internalization of echovirus 1 in caveolae. J Virol **76**:1856–1865.

382. Martin DN, Uprichard SL. 2013. Identification of transferrin receptor 1 as a hepatitis C virus entry factor. Proc Natl Acad Sci USA **110**:10777–10782.

383. Martinez I, Melero JA. 2000. Binding of human respiratory syncytial virus to cells: implication of sulfated cell surface proteoglycans. J Gen Virol **81**:2715–2722.

384. Matlin KS, Reggio H, Helenius A, Simons K. 1981. Infectious entry pathway of influenza virus in a canine kidney cell line. J Cell Biol **91**:601–613.

385. Matrosovich M, Herrler G, Klenk HD. 2013. Sialic Acid Receptors of Viruses. Top Curr Chem doi:10.1007/128_2013_466.

386. Matrosovich M, Klenk HD. 2003. Natural and synthetic sialic acid-containing inhibitors of influenza virus receptor binding. Rev Med Virol **13**:85–97.

387. Matrosovich MN. 1989. Towards the development of antimicrobial drugs acting by inhibition of pathogen attachment to host cells: a need for polyvalency. FEBS Lett **252**:1–4.

388. Matsubara T, Onishi A, Saito T, Shimada A, Inoue H, Taki T, Nagata K, Okahata Y, Sato T. 2010. Sialic acid-mimic peptides as hemagglutinin inhibitors for anti-influenza therapy. J Med Chem **53**:4441–4449.

389. Matsumoto Y, Matsuura T, Aoyagi H, Matsuda M, Hmwe SS, Date T, Watanabe N, Watashi K, Suzuki R, Ichinose S, Wake K, Suzuki T, Miyamura T, Wakita T, Aizaki H. 2013. Antiviral activity of glycyrrhizin against hepatitis C virus in vitro. PLoS One **8**:e68992.

390. Matsumura T, Kato T, Sugiyama N, Tasaka-Fujita M, Murayama A, Masaki T, Wakita T, Imawari M. 2012. 25-Hydroxyvitamin D3 suppresses hepatitis C virus production. Hepatology **56**:1231–1239.

391. Mayor S, Pagano RE. 2007. Pathways of clathrin-independent endocytosis. Nat Rev Mol Cell Biol **8**:603–612.

392. Mazumder A, Raghavan K, Weinstein J, Kohn KW, Pommier Y. 1995. Inhibition of human immunodeficiency virus type-1 integrase by curcumin. Biochem Pharmacol **49**:1165–1170.

393. McColl DJ, Chen X. 2010. Strand transfer inhibitors of HIV-1 integrase: bringing IN a new era of antiretroviral therapy. Antiviral research **85**:101–118.

394. McLeish NJ, Williams CH, Kaloudas D, Roivainen MM, Stanway G. 2012. Symmetry-related clustering of positive charges is a common mechanism for heparan sulfate binding in enteroviruses. J Virol **86**:11163–11170.

395. Meerbach A, Neyts J, Balzarini J, Helbig B, De Clercq E, Wutzler P. 2001. In vitro activity of polyhydroxycarboxylates against herpesviruses and HIV. Antivir Chem Chemother **12**:337–345.

396. Meertens L, Bertaux C, Dragic T. 2006. Hepatitis C virus entry requires a critical postinternalization step and delivery to early endosomes via clathrin-coated vesicles. J Virol **80**:11571–11578.

397. Meier O, Boucke K, Hammer SV, Keller S, Stidwill RP, Hemmi S, Greber UF. 2002. Adenovirus triggers macropinocytosis and endosomal leakage together with its clathrin-mediated uptake. J Cell Biol **158**:1119–1131.

398. Meindl P, Bodo G, Palese P, Schulman J, Tuppy H. 1974. Inhibition of neuraminidase activity by derivatives of 2-deoxy-2,3-dehydro-N-acetylneuraminic acid. Virology **58**:457–463.

399. Mercer J, Helenius A. 2008. Vaccinia virus uses macropinocytosis and apoptotic mimicry to enter host cells. Science **320**:531–535.

400. Mercer J, Helenius A. 2009. Virus entry by macropinocytosis. Nat Cell Biol **11**:510–520.

401. Meuleman P, Albecka A, Belouzard S, Vercauteren K, Verhoye L, Wychowski C, Leroux-Roels G, Palmer KE, Dubuisson J. 2011. Griffithsin has antiviral activity against hepatitis C virus. Antimicrob Agents Chemother **55**:5159–5167.

402. Miyanari Y, Atsuzawa K, Usuda N, Watashi K, Hishiki T, Zayas M, Bartenschlager R, Wakita T, Hijikata M, Shimotohno K. 2007. The lipid droplet is an important organelle for hepatitis C virus production. Nat Cell Biol **9**:1089–1097.

403. Modis Y, Ogata S, Clements D, Harrison SC. 2004. Structure of the dengue virus envelope protein after membrane fusion. Nature **427**:313–319.

404. Mohan P, Schols D, Baba M, De Clercq E. 1992. Sulfonic acid polymers as a new class of human immunodeficiency virus inhibitors. Antiviral Res **18**:139–150.

405. Mohd Hanafiah K, Groeger J, Flaxman AD, Wiersma ST. 2013. Global epidemiology of hepatitis C virus infection: new estimates of age-specific antibody to HCV seroprevalence. Hepatology **57**:1333–1342.

406. Molina S, Castet V, Fournier-Wirth C, Pichard-Garcia L, Avner R, Harats D, Roitelman J, Barbaras R, Graber P, Ghersa P, Smolarsky M, Funaro A, Malavasi F, Larrey D, Coste J, Fabre JM, Sa-Cunha A, Maurel P. 2007. The low-density lipoprotein receptor plays a role in the infection of primary human hepatocytes by hepatitis C virus. J Hepatol **46**:411–419.

407. Monazahian M, Bohme I, Bonk S, Koch A, Scholz C, Grethe S, Thomssen R. 1999. Low density lipoprotein receptor as a candidate receptor for hepatitis C virus. J Med Virol **57**:223–229.

408. Moon HS, Lee HG, Choi YJ, Kim TG, Cho CS. 2007. Proposed mechanisms of (-)-epigallocatechin-3-gallate for anti-obesity. Chem Biol Interact **167**:85–98.

409. Moore JP, McKeating JA, Weiss RA, Sattentau QJ. 1990. Dissociation of gp120 from HIV-1 virions induced by soluble CD4. Science **250**:1139–1142.

410. Moore NF, Patzer EJ, Shaw JM, Thompson TE, Wagner RR. 1978. Interaction of vesicular stomatitis virus with lipid vesicles: depletion of cholesterol and effect on virion membrane fluidity and infectivity. J Virol **27**:320–329.

411. Morens DM, Fauci AS. 2013. Emerging infectious diseases: threats to human health and global stability. PLoS Pathog **9**:e1003467.

412. Mori S, Miyake S, Kobe T, Nakaya T, Fuller SD, Kato N, Kaihatsu K. 2008. Enhanced anti-influenza A virus activity of (-)-epigallocatechin-3-O-gallate fatty acid monoester derivatives: effect of alkyl chain length. Bioorg Med Chem Lett **18**:4249–4252.

413. Mori T, O'Keefe BR, Sowder RC, Bringans S, Gardella R, Berg S, Cochran P, Turpin JA, Buckheit RWJ, McMahon JB, Boyd MR. 2005. Isolation and characterization of griffithsin, a novel HIV-inactivating protein, from the red alga Griffithsia sp. J Biol Chem **280**:9345–9353.

414. Morikawa K, Zhao Z, Date T, Miyamoto M, Murayama A, Akazawa D, Tanabe J, Sone S, Wakita T. 2007. The roles of CD81 and glycosaminoglycans in the adsorption and uptake of infectious HCV particles. J Med Virol **79**:714–723.

415. Morin D, Barthelemy S, Zini R, Labidalle S, Tillement JP. 2001. Curcumin induces the mitochondrial permeability transition pore mediated by membrane protein thiol oxidation. FEBS Lett **495**:131–136.

416. Moss RB, Hansen C, Sanders RL, Hawley S, Li T, Steigbigel RT. 2012. A phase II study of DAS181, a novel host directed antiviral for the treatment of influenza infection. J Infect Dis **206**:1844–1851.

417. Moulard M, Lortat-Jacob H, Mondor I, Roca G, Wyatt R, Sodroski J, Zhao L, Olson W, Kwong PD, Sattentau QJ. 2000. Selective interactions of polyanions with basic surfaces on human immunodeficiency virus type 1 gp120. J Virol **74**:1948–1960.

418. Mousavi S, Malerd L, Berg T, Kjeken R. 2004. Clathrin-dependent endocytosis. Biochem J **377**:1–16.

419. Mudhasani R, Tran JP, Retterer C, Radoshitzky SR, Kota KP, Altamura LA, Smith JM, Packard BZ, Kuhn JH, Costantino J. 2013. IFITM-2 and IFITM-3 but not IFITM-1 restrict Rift Valley fever virus. J Virol **87**:8451–8464.

420. Mukoyama A, Ushijima H, Nishimura S, Koike H, Toda M, Hara Y, Shimamura T. 1991. Inhibition of rotavirus and enterovirus infections by tea extracts. Jpn J Med Sci Biol **44**:181–186.

421. Mulliner D, Wondrousch D, Schuurmann G. 2011. Predicting Michael-acceptor reactivity and toxicity through quantum chemical transition-state calculations. Org Biomol Chem **9**:8400–8412.

422. Munch J, Standker L, Adermann K, Schulz A, Schindler M, Chinnadurai R, Pohlmann S, Chaipan C, Biet T, Peters T, Meyer B, Wilhelm D, Lu H, Jing W, Jiang S, Forssmann WG, Kirchhoff F. 2007. Discovery and optimization of a natural HIV-1 entry inhibitor targeting the gp41 fusion peptide. Cell **129**:263–275.

423. Nakayama M, Suzuki K, Toda M, Okubo S, Hara Y, Shimamura T. 1993. Inhibition of the infectivity of influenza virus by tea polyphenols. Antiviral Res **21**:289–299.

424. Nanbo A, Imai M, Watanabe S, Noda T, Takahashi K, Neumann G, Halfmann P, Kawaoka Y. 2010. Ebolavirus is internalized into host cells via macropinocytosis in a viral glycoprotein-dependent manner. PLoS Pathog **6**:e1001121.

425. Nance CL, Siwak EB, Shearer WT. 2009. Preclinical development of the green tea catechin, epigallocatechin gallate, as an HIV-1 therapy. J Allergy Clin Immunol **123**:459–465.

426. Narayanan A, Kehn-Hall K, Senina S, Lundberg L, Van Duyne R, Guendel I, Das R, Baer A, Bethel L, Turell M, Hartman AL, Das B, Bailey C, Kashanchi F. 2012. Curcumin inhibits Rift Valley fever virus replication in human cells. J Biol Chem **287**:33198–33214.

427. Neu U, Bauer J, Stehle T. 2011. Viruses and sialic acids: rules of engagement. Curr Opin Struct Biol **21**:610–618.

428. Neyts J, Snoeck R, Wutzler P, Cushman M, Klöcking R, Helbig B, Wang P, De Clercq E. 1992. Poly (hydroxy) carboxylates as selective inhibitors of cytomegalovirus and herpes simplex virus replication. Antiviral Chem Chemother **3**:215–222.

429. Nguyen DH, Hildreth JE. 2000. Evidence for budding of human immunodeficiency virus type 1 selectively from glycolipid-enriched membrane lipid rafts. J Virol **74**:3264–3272.

430. Nicholls JM, Moss RB, Haslam SM. 2013. The use of sialidase therapy for respiratory viral infections. Antiviral Res **98**:401–409.

431. Nicola AV, McEvoy AM, Straus SE. 2003. Roles for endocytosis and low pH in herpes simplex virus entry into HeLa and Chinese hamster ovary cells. J Virol **77**:5324–5332.

432. Nijhuis M, Schuurman R, de Jong D, Erickson J, Gustchina E, Albert J, Schipper P, Gulnik S, Boucher CA. 1999. Increased fitness of drug resistant HIV-1 protease as a result of acquisition of compensatory mutations during suboptimal therapy. AIDS **13**:2349–2359.

433. Nilsson EC, Jamshidi F, Johansson SM, Oberste MS, Arnberg N. 2008. Sialic acid is a cellular receptor for coxsackievirus A24 variant, an emerging virus with pandemic potential. J Virol **82**:3061–3068.

434. Nimmerjahn F, Dudziak D, Dirmeier U, Hobom G, Riedel A, Schlee M, Staudt LM, Rosenwald A, Behrends U, Bornkamm GW, Mautner J. 2004. Active NF-kappaB signalling is a prerequisite for influenza virus infection. J Gen Virol **85**:2347–2356.

435. Nokhbeh MR, Hazra S, Alexander DA, Khan A, McAllister M, Suuronen EJ, Griffith M, Dimock K. 2005. Enterovirus 70 binds to different glycoconjugates containing alpha2,3-linked sialic acid on different cell lines. J Virol **79**:7087–7094.

436. Nowicka-Sans B, Gong YF, McAuliffe B, Dicker I, Ho HT, Zhou N, Eggers B, Lin PF, Ray N, Wind-Rotolo M, Zhu L, Majumdar A, Stock D, Lataillade M, Hanna GJ, Matiskella JD, Ueda Y, Wang T, Kadow JF, Meanwell NA, Krystal M. 2012. In vitro antiviral characteristics of HIV-1 attachment inhibitor BMS-626529, the active component of the prodrug BMS-663068. Antimicrob Agents Chemother **56**:3498–3507.

437. Nunes-Correia I, Eulalio A, Nir S, Pedroso de Lima MC. 2004. Caveolae as an additional route for influenza virus endocytosis in MDCK cells. Cell Mol Biol Lett **9**:47–60.

438. O'Donnell CD, Kovacs M, Akhtar J, Valyi-Nagy T, Shukla D. 2010. Expanding the role of 3-O sulfated heparan sulfate in herpes simplex virus type-1 entry. Virology **397**:389–398.

439. O'Keefe BR, Giomarelli B, Barnard DL, Shenoy SR, Chan PK, McMahon JB, Palmer KE, Barnett BW, Meyerholz DK, Wohlford-Lenane CL, McCray PBJ. 2010. Broad-spectrum in vitro activity and in vivo efficacy of the antiviral protein griffithsin against emerging viruses of the family Coronaviridae. J Virol **84**:2511–2521.

440. O'Keefe BR, Smee DF, Turpin JA, Saucedo CJ, Gustafson KR, Mori T, Blakeslee D, Buckheit R, Boyd MR. 2003. Potent anti-influenza activity of cyanovirin-N and interactions with viral hemagglutinin. Antimicrob Agents Chemother **47**:2518–2525.

441. O'Neill RE, Jaskunas R, Blobel G, Palese P, Moroianu J. 1995. Nuclear import of influenza virus RNA can be mediated by viral nucleoprotein and transport factors required for protein import. J Biol Chem **270**:22701–22704.

442. Oberg B. 1982. Antiviral effects of phosphonoformate (PFA, foscarnet sodium). Pharmacol Ther **19**:387–415.

443. Ochiai H, Sakai S, Hirabayashi T, Shimizu Y, Terasawa K. 1995. Inhibitory effect of bafilomycin A1, a specific inhibitor of vacuolar-type proton pump, on the growth of influenza A and B viruses in MDCK cells. Antiviral Res **27**:425–430.

444. Ohvo-Rekila H, Ramstedt B, Leppimaki P, Slotte JP. 2002. Cholesterol interactions with phospholipids in membranes. Prog Lipid Res **41**:66–97.

445. Okimasu E, Moromizato Y, Watanabe S, Sasaki J, Shiraishi N, Morimoto YM, Miyahara M, Utsumi K. 1983. Inhibition of phospholipase A2 and platelet aggregation by glycyrrhizin, an antiinflammation drug. Acta Med Okayama **37**:385–391.

446. Oldstone MB, Teijaro JR, Walsh KB, Rosen H. 2013. Dissecting influenza virus pathogenesis uncovers a novel chemical approach to combat the infection. Virology **435**:92–101.

447. Olsen BN, Schlesinger PH, Baker NA. 2009. Perturbations of membrane structure by cholesterol and cholesterol derivatives are determined by sterol orientation. J Am Chem Soc **131**:4854–4865.

448. Olsen BN, Schlesinger PH, Ory DS, Baker NA. 2011. 25-Hydroxycholesterol increases the availability of cholesterol in phospholipid membranes. Biophys J **100**:948–956.

449. Olsen BN, Schlesinger PH, Ory DS, Baker NA. 2012. Side-chain oxysterols: from cells to membranes to molecules. Biochim Biophys Acta **1818**:330–336.

450. Owen DM, Huang H, Ye J, Gale MJ. 2009. Apolipoprotein E on hepatitis C virion facilitates infection through interaction with low-density lipoprotein receptor. Virology **394**:99–108.

451. Padilla-S L, Rodriguez A, Gonzales MM, Gallego-G JC, Castano-O JC. 2014. Inhibitory effects of curcumin on dengue virus type 2-infected cells in vitro. Arch Virol **159**:573–579.

452. Palese P, Tobita K, Ueda M, Compans RW. 1974. Characterization of temperature sensitive influenza virus mutants defective in neuraminidase. Virology **61**:397–410.

453. Panda D, Das A, Dinh PX, Subramaniam S, Nayak D, Barrows NJ, Pearson JL, Thompson J, Kelly DL, Ladunga I, Pattnaik AK. 2011. RNAi screening reveals requirement for host cell secretory pathway in infection by diverse families of negative-strand RNA viruses. Proc Natl Acad Sci USA **108**:19036–19041.

454. Park K, Scott AL. 2010. Cholesterol 25-hydroxylase production by dendritic cells and macrophages is regulated by type I interferons. J Leukoc Biol **88**:1081–1087.

455. Parton RG, Joggerst B, Simons K. 1994. Regulated internalization of caveolae. J Cell Biol **127**:1199–1215.

456. Patel J, Patel AH, McLauchlan J. 2001. The transmembrane domain of the hepatitis C virus E2 glycoprotein is required for correct folding of the E1 glycoprotein and native complex formation. Virology **279**:58–68.

457. Patel M, Yanagishita M, Roderiquez G, Bou-Habib DC, Oravecz T, Hascall VC, Norcross MA. 1993. Cell-surface heparan sulfate proteoglycan mediates HIV-1 infection of T-cell lines. AIDS Res Hum Retroviruses **9**:167–174.

458. Patton JT, Davis NL, Wertz GW. 1984. N protein alone satisfies the requirement for protein synthesis during RNA replication of vesicular stomatitis virus. J Virol **49**:303–309.

459. Paul RW, Choi AH, Lee PW. 1989. The alpha-anomeric form of sialic acid is the minimal receptor determinant recognized by reovirus. Virology **172**:382–385.

460. Pawlotsky JM. 2013. NS5A inhibitors in the treatment of hepatitis C. J Hepatol **59**:375–382.

461. Pawlotsky JM. 2014. New Hepatitis C Therapies: The Toolbox, Strategies, and Challenges. Gastroenterology **146(5)**:1176–1192.

462. Pecheur EI. 2012. Lipoprotein receptors and lipid enzymes in hepatitis C virus entry and early steps of infection. Scientifica (Cairo) **2012**:709853.

463. Pecheur EI, Lavillette D, Alcaras F, Molle J, Boriskin YS, Roberts M, Cosset FL, Polyak SJ. 2007. Biochemical mechanism of hepatitis C virus inhibition by the broad-spectrum antiviral arbidol. Biochemistry **46**:6050–6059.

464. Pelkmans L, Helenius A. 2003. Insider information: what viruses tell us about endocytosis. Curr Opin Cell Biol **15**:414–422.

465. Penin F, Combet C, Germanidis G, Frainais PO, Deleage G, Pawlotsky JM. 2001. Conservation of the conformation and positive charges of hepatitis C virus E2 envelope glycoprotein hypervariable region 1 points to a role in cell attachment. J Virol **75**:5703–5710.

466. Perez L, Carrasco L. 1994. Involvement of the vacuolar H(+)-ATPase in animal virus entry. J Gen Virol **75**:2595–2606.

467. Pessin JE, Glaser M. 1980. Budding of Rous sarcoma virus and vesicular stomatitis virus from localized lipid regions in the plasma membrane of chicken embryo fibroblasts. J Biol Chem **255**:9044–9050.

468. Pezacki JP, Sagan SM, Tonary AM, Rouleau Y, Belanger S, Supekova L, Su AI. 2009. Transcriptional profiling of the effects of 25-hydroxycholesterol on human hepatocyte metabolism and the antiviral state it conveys against the hepatitis C virus. BMC Chem Biol **9**:2.

469. Pileri P, Uematsu Y, Campagnoli S, Galli G, Falugi F, Petracca R, Weiner AJ, Houghton M, Rosa D, Grandi G, Abrignani S. 1998. Binding of hepatitis C virus to CD81. Science **282**:938–941.

470. Pinto LH, Holsinger LJ, Lamb RA. 1992. Influenza virus M2 protein has ion channel activity. Cell **69**:517–528.

471. Pinto LH, Lamb RA. 2006. The M2 proton channels of influenza A and B viruses. J Biol Chem **281**:8997–9000.

472. Ploss A, Evans MJ, Gaysinskaya VA, Panis M, You H, de Jong YP, Rice CM. 2009. Human occludin is a hepatitis C virus entry factor required for infection of mouse cells. Nature **457**:882–886.

473. Plotch SJ, O'Hara B, Morin J, Palant O, LaRocque J, Bloom JD, Lang SAJ, DiGrandi MJ, Bradley M, Nilakantan R, Gluzman Y. 1999. Inhibition of influenza A virus replication by compounds interfering with the fusogenic function of the viral hemagglutinin. J Virol **73**:140–151.

474. Polozov IV, Bezrukov L, Gawrisch K, Zimmerberg J. 2008. Progressive ordering with decreasing temperature of the phospholipids of influenza virus. Nat Chem Biol **4**:248–255.

475. Pombo A, Ferreira J, Bridge E, Carmo-Fonseca M. 1994. Adenovirus replication and transcription sites are spatially separated in the nucleus of infected cells. EMBO J **13**:5075–5085.

476. Pompei R, Flore O, Marccialis MA, Pani A, Loddo B. 1979. Glycyrrhizic acid inhibits virus growth and inactivates virus particles. Nature **281**:689–690.

477. Pope LE, Marcelletti JF, Katz LR, Lin JY, Katz DH, Parish ML, Spear PG. 1998. The anti-herpes simplex virus activity of n-docosanol includes inhibition of the viral entry process. Antiviral Res **40**:85–94.

478. Pritchett TJ, Paulson JC. 1989. Basis for the potent inhibition of influenza virus infection by equine and guinea pig alpha 2-macroglobulin. J Biol Chem **264**:9850–9858.

479. Prusoff WH. 1959. Synthesis and biological activities of iododeoxyuridine, an analog of thymidine. Biochim Biophys Acta **32**:295–296.

480. Prusoff WH, Mancini WR, Lin TS, Lee JJ, Siegel SA, Otto MJ. 1984. Physical and biological consequences of incorporation of antiviral agents into virus DNA. Antiviral Res **4**:303–315.

481. Qian Z, Dominguez SR, Holmes KV. 2013. Role of the spike glycoprotein of human Middle East respiratory syndrome coronavirus (MERS-CoV) in virus entry and syncytia formation. PLoS One **8**:e76469.

482. Quigley JP, Rifkin DB, Reich E. 1971. Phospholipid composition of Rous sarcoma virus, host cell membranes and other enveloped RNA viruses. Virology **46**:106–116.

483. Racaniello VR. 1996. Early events in poliovirus infection: virus-receptor interactions. Proc Natl Acad Sci USA **93**:11378–11381.

484. Raghu H, Sharma-Walia N, Veettil MV, Sadagopan S, Chandran B. 2009. Kaposi's sarcoma-associated herpesvirus utilizes an actin polymerization-dependent macropinocytic pathway to enter human dermal microvascular endothelial and human umbilical vein endothelial cells. J Virol **83**:4895–4911.

485. Raman R, Sasisekharan V, Sasisekharan R. 2005. Structural insights into biological roles of protein-glycosaminoglycan interactions. Chem Biol **12**:267–277.

486. Rapaport D, Ovadia M, Shai Y. 1995. A synthetic peptide corresponding to a conserved heptad repeat domain is a potent inhibitor of Sendai virus-cell fusion: an emerging similarity with functional domains of other viruses. EMBO J **14**:5524–5531.

487. Ratcliff AN, Shi W, Arts EJ. 2013. HIV-1 resistance to maraviroc conferred by a CD4 binding site mutation in the envelope glycoprotein gp120. J Virol **87**:923–934.

488. Ray N, Blackburn LA, Doms RW. 2009. HR-2 mutations in human immunodeficiency virus type 1 gp41 restore fusion kinetics delayed by HR-1 mutations that cause clinical resistance to enfuvirtide. J Virol **83**:2989–2995.

489. Rechtman MM, Har-Noy O, Bar-Yishay I, Fishman S, Adamovich Y, Shaul Y, Halpern Z, Shlomai A. 2010. Curcumin inhibits hepatitis B virus via down-regulation of the metabolic coactivator PGC-1alpha. FEBS Lett **584**:2485–2490.

490. Reis Jr J, Mead D, Rodriguez L, Brown C. 2009. Transmission and pathogenesis of vesicular stomatitis viruses. Braz J Vet Pathol **2**:49–58.

491. Reiter DM, Frierson JM, Halvorson EE, Kobayashi T, Dermody TS, Stehle T. 2011. Crystal structure of reovirus attachment protein sigma1 in complex with sialylated oligosaccharides. PLoS Pathog **7**:e1002166.

492. Reuter JD, Myc A, Hayes MM, Gan Z, Roy R, Qin D, Yin R, Piehler LT, Esfand R, Tomalia DA, Baker JRJ. 1999. Inhibition of viral adhesion and infection by sialic-acid-conjugated dendritic polymers. Bioconjug Chem **10**:271–278.

493. Rey FA, Heinz FX, Mandl C, Kunz C, Harrison SC. 1995. The envelope glycoprotein from tick-borne encephalitis virus at 2A resolution. Nature **375**:291–298.

494. Roberts PC, Compans RW. 1998. Host cell dependence of viral morphology. Proc Natl Acad Sci USA **95**:5746–5751.

495. Roche S, Gaudin Y. 2002. Characterization of the equilibrium between the native and fusion-inactive conformation of rabies virus glycoprotein indicates that the fusion complex is made of several trimers. Virology **297**:128–135.

496. Roche S, Bressanelli S, Rey FA, Gaudin Y. 2006. Crystal structure of the low-pH form of the vesicular stomatitis virus glycoprotein G. Science **313**:187–191.

497. Roche S, Rey FA, Gaudin Y, Bressanelli S. 2007. Structure of the prefusion form of the vesicular stomatitis virus glycoprotein G. Science **315**:843–848.

498. Rogers GN, Herrler G, Paulson JC, Klenk HD. 1986. Influenza C virus uses 9-O-acetyl-N-acetylneuraminic acid as a high affinity receptor determinant for attachment to cells. J Biol Chem **261**:5947–5951.

499. Ronecker S, Zimmer G, Herrler G, Greiser-Wilke I, Grummer B. 2008. Formation of bovine viral diarrhea virus E1-E2 heterodimers is essential for virus entry and depends on charged residues in the transmembrane domains. J Gen Virol **89**:2114–2121.

500. Rosenberg RD. 1978. Heparin, antithrombin, and abnormal clotting. Annu Rev Med **29**:367–378.

501. Rosenquist A, Samuelsson B, Johansson PO, Cummings MD, Lenz O, Raboisson P, Simmen K, Vendeville S, de Kock H, Nilsson M, Horvath A, Kalmeijer R, de la Rosa G, Beumont-Mauviel M. 2014. Discovery and development of simeprevir (TMC435), a HCV NS3/4A protease inhibitor. J Med Chem **57**:1673–1693.

502. Rossman JS, Leser GP, Lamb RA. 2012. Filamentous influenza virus enters cells via macropinocytosis. J Virol **86**:10950–10960.

503. Roy AM, Parker JS, Parrish CR, Whittaker GR. 2000. Early stages of influenza virus entry into Mv-1 lung cells: involvement of dynamin. Virology **267**:17–28.v

504. Ruiz-Sancho A, Sheldon J, Soriano V. 2007. Telbivudine: a new option for the treatment of chronic hepatitis B. Expert Opin Biol Ther **7**:751–761.

505. Russell RJ, Kerry PS, Stevens DJ, Steinhauer DA, Martin SR, Gamblin SJ, Skehel JJ. 2008. Structure of influenza hemagglutinin in complex with an inhibitor of membrane fusion. Proc Natl Acad Sci USA **105**:17736–17741.

506. Rust MJ, Lakadamyali M, Zhang F, Zhuang X. 2004. Assembly of endocytic machinery around individual influenza viruses during viral entry. Nat Struct Mol Biol **11**:567–573.

507. Rydell GE, Nilsson J, Rodriguez-Diaz J, Ruvoën-Clouet N, Svensson L, Le Pendu J, Larson G. 2009. Human noroviruses recognize sialyl Lewis x neoglycoprotein. Glycobiology **19**:309–320.

508. Sagan SM, Rouleau Y, Leggiadro C, Supekova L, Schultz PG, Su AI, Pezacki JP. 2006. The influence of cholesterol and lipid metabolism on host cell structure and hepatitis C virus replication. Biochem Cell Biol **84**:67–79.

509. Sainz BJ, Barretto N, Martin DN, Hiraga N, Imamura M, Hussain S, Marsh KA, Yu X, Chayama K, Alrefai WA, Uprichard SL. 2012. Identification of the Niemann-Pick C1-like 1 cholesterol absorption receptor as a new hepatitis C virus entry factor. Nat Med **18**:281–285.

510. Sainz BJ, Mossel EC, Gallaher WR, Wimley WC, Peters CJ, Wilson RB, Garry RF. 2006. Inhibition of severe acute respiratory syndrome-associated coronavirus (SARS-CoV) infectivity by peptides analogous to the viral spike protein. Virus Res **120**:146–155.

511. Salvador B, Sexton NR, Carrion RJ, Nunneley J, Patterson JL, Steffen I, Lu K, Muench MO, Lembo D, Simmons G. 2013. Filoviruses utilize glycosaminoglycans for their attachment to target cells. J Virol **87**:3295–3304.

512. Santer DM, Ma MM, Hockman D, Landi A, Tyrrell DL, Houghton M. 2013. Enhanced activation of memory, but not naive, B cells in chronic hepatitis C virus-infected patients with cryoglobulinemia and advanced liver fibrosis. PLoS One **8**:e68308.

513. Sattentau QJ, Moore JP. 1991. Conformational changes induced in the human immunodeficiency virus envelope glycoprotein by soluble CD4 binding. J Exp Med **174**:407–415.

514. Sazuka M, Murakami S, Isemura M, Satoh K, Nukiwa T. 1995. Inhibitory effects of green tea infusion on in vitro invasion and in vivo metastasis of mouse lung carcinoma cells. Cancer Lett **98**:27–31.

515. Scarselli E, Ansuini H, Cerino R, Roccasecca RM, Acali S, Filocamo G, Traboni C, Nicosia A, Cortese R, Vitelli A. 2002. The human scavenger receptor class B type I is a novel candidate receptor for the hepatitis C virus. EMBO J **21**:5017–5025.

516. Schaap IA, Eghiaian F, des Georges A, Veigel C. 2012. Effect of envelope proteins on the mechanical properties of influenza virus. J Biol Chem **287**:41078–41088.

517. Scheiffele P, Rietveld A, Wilk T, Simons K. 1999. Influenza viruses select ordered lipid domains during budding from the plasma membrane. J Biol Chem **274**:2038–2044.

518. Schlegel R, Tralka TS, Willingham MC, Pastan I. 1983. Inhibition of VSV binding and infectivity by phosphatidylserine: is phosphatidylserine a VSV-binding site? Cell **32**:639–646.

519. Schloemer RH, Wagner RR. 1975. Cellular adsorption function of the sialoglycoprotein of vesicular stomatitis virus and its neuraminic acid. J Virol **15**:882–893.

520. Schmidt A, Wolde M, Thiele C, Fest W, Kratzin H, Podtelejnikov AV, Witke W, Huttner WB, Soling HD. 1999. Endophilin I mediates synaptic vesicle formation by transfer of arachidonate to lysophosphatidic acid. Nature **401**:133–141.

521. Schmidt AG, Lee K, Yang PL, Harrison SC. 2012. Small-molecule inhibitors of dengue-virus entry. PLoS Pathog **8**:e1002627.

522. Schmidt AG, Yang PL, Harrison SC. 2010. Peptide inhibitors of dengue-virus entry target a late-stage fusion intermediate. PLoS Pathog **6**:e1000851.

523. Schols D, Baba M, Pauwels R, Desmyter J, De Clercq E. 1989. Specific interaction of aurintricarboxylic acid with the human immunodeficiency virus/CD4 cell receptor. Proc Natl Acad Sci USA **86**:3322–3326.

524. Schols D, Wutzler P, Klocking R, Helbig B, De Clercq E. 1991. Selective inhibitory activity of polyhydroxycarboxylates derived from phenolic compounds against human immunodeficiency virus replication. J Acquir Immune Defic Syndr **4**:677–685.

525. Schowalter RM, Pastrana DV, Buck CB. 2011. Glycosaminoglycans and sialylated glycans sequentially facilitate Merkel cell polyomavirus infectious entry. PLoS Pathog **7**:e1002161.

526. Schroeder C. 2010. Cholesterol-binding viral proteins in virus entry and morphogenesis. Subcell Biochem **51**:77–108.

527. Schulz WL, Haj AK, Schiff LA. 2012. Reovirus uses multiple endocytic pathways for cell entry. J Virol **86**:12665–12675.

528. Scott SA, Holloway G, Coulson BS, Szyczew AJ, Kiefel MJ, von Itzstein M, Blanchard H. 2005. Crystallization and preliminary X-ray diffraction analysis of the sialic acid-binding domain (VP8*) of porcine rotavirus strain CRW-8. Acta Crystallogr Sect F Struct Biol Cryst Commun **61**:617–620.

529. Seifer M, Hamatake RK, Colonno RJ, Standring DN. 1998. In vitro inhibition of hepadnavirus polymerases by the triphosphates of BMS-200475 and lobucavir. Antimicrob Agents Chemother **42**:3200–3208.

530. Severini A, Liu XY, Wilson JS, Tyrrell DL. 1995. Mechanism of inhibition of duck hepatitis B virus polymerase by (-)-beta-L-2',3'-dideoxy-3'-thiacytidine. Antimicrob Agents Chemother **39**:1430–1435.

531. Shafer RW, Vuitton DA. 1999. Highly active antiretroviral therapy (HAART) for the treatment of infection with human immunodeficiency virus type 1. Biomedicine & pharmacotherapy **53**:73–86.

532. Sharma NR, Mateu G, Dreux M, Grakoui A, Cosset FL, Melikyan GB. 2011. Hepatitis C virus is primed by CD81 protein for low pH-dependent fusion. J Biol Chem **286**:30361–30376.

533. Sharma RA, Gescher AJ, Steward WP. 2005. Curcumin: the story so far. Eur J Cancer **41**:1955–1968.

534. Shetty AK, Peek LA. 2012. Peramivir for the treatment of influenza. Expert Rev Anti Infect Ther **10**:123–143.

535. Shieh MT, WuDunn D, Montgomery RI, Esko JD, Spear PG. 1992. Cell surface receptors for herpes simplex virus are heparan sulfate proteoglycans. J Cell Biol **116**:1273–1281.

536. Shih PC, Yang MS, Lin SC, Ho Y, Hsiao JC, Wang DR, Yu SS, Chang W, Tzou DL. 2009. A turn-like structure "KKPE" segment mediates the specific binding of viral protein A27 to heparin and heparan sulfate on cell surfaces. J Biol Chem **284**:36535–36546.

537. Shinitzky M, Inbar M. 1976. Microviscosity parameters and protein mobility in biological membranes. Biochim Biophys Acta **433**:133–149.

538. Short JJ, Pereboev AV, Kawakami Y, Vasu C, Holterman MJ, Curiel,DT. 2004. Adenovirus serotype 3 utilizes CD80 (B7.1) and CD86 (B7.2) as cellular attachment receptors. Virology **322**:349–359.

539. Shukla D, Spear PG. 2001. Herpesviruses and heparan sulfate: an intimate relationship in aid of viral entry. J Clin Invest **108**:503–510.

540. Si X, Wang Y, Wong J, Zhang J, McManus BM, Luo H. 2007. Dysregulation of the ubiquitin-proteasome system by curcumin suppresses coxsackievirus B3 replication. J Virol **81**:3142–3150.

541. Sieczkarski SB, Whittaker GR. 2002. Influenza virus can enter and infect cells in the absence of clathrin-mediated endocytosis. J Virol **76**:10455–10464.

542. Skehel JJ, Wiley DC. 2000. Receptor binding and membrane fusion in virus entry: the influenza hemagglutinin. Annu Rev Biochem **69**:531–569.

543. Sluis-Cremer N, Tachedjian G. 2008. Mechanisms of inhibition of HIV replication by non-nucleoside reverse transcriptase inhibitors. Virus Res **134**:147–156.

544. Smirnov Y, Kuznetsova MA, Kaverin NV. 1991. The genetic aspects of influenza virus filamentous particle formation. Arch Virol **118**:279–284.

545. Smit JM, Bittman R, Wilschut J. 1999. Low-pH-dependent fusion of Sindbis virus with receptor-free cholesterol- and sphingolipid-containing liposomes. J Virol **73**:8476–8484.

546. Smith GL, Vanderplasschen A, Law M. 2002. The formation and function of extracellular enveloped vaccinia virus. J Gen Virol **83**:2915–2931.

547. Smith JG, Nemerow GR. 2008. Mechanism of adenovirus neutralization by Human alpha-defensins. Cell Host Microbe **3**:11–19.

548. Smith JS, Robinson NJ. 2002. Age-specific prevalence of infection with herpes simplex virus types 2 and 1: a global review. J Infect Dis **186 Suppl 1**:S3–28.

549. Smith S, Weston S, Kellam P, Marsh M. 2014. IFITM proteins-cellular inhibitors of viral entry. Curr Opin Virol **4C**:71–77.

550. Smith TJ. 2011. Green Tea Polyphenols in drug discovery - a success or failure? Expert Opin Drug Discov **6**:589–595.

551. Sofia MJ, Bao D, Chang W, Du J, Nagarathnam D, Rachakonda S, Reddy PG, Ross BS, Wang P, Zhang HR, Bansal S, Espiritu C, Keilman M, Lam AM, Steuer HM, Niu C, Otto MJ, Furman PA. 2010. Discovery of a beta-d-2'-deoxy-2'-alpha-fluoro-2'-beta-C-methyluridine nucleotide prodrug (PSI-7977) for the treatment of hepatitis C virus. J Med Chem **53**:7202–7218.

552. Sollner T, Whiteheart SW, Brunner M, Erdjument-Bromage H, Geromanos S, Tempst P, Rothman JE. 1993. SNAP receptors implicated in vesicle targeting and fusion. Nature **362**:318–324.

553. Song JM, Lee KH, Seong BL. 2005. Antiviral effect of catechins in green tea on influenza virus. Antiviral Res **68**:66–74.

554. Sparks MA, Williams KW, Whitesides GM. 1993. Neuraminidase-resistant hemagglutination inhibitors: acrylamide copolymers containing a C-glycoside of N-acetylneuraminic acid. J Med Chem **36**:778–783.

555. Spoden G, Freitag K, Husmann M, Boller K, Sapp M, Lambert C, Florin L. 2008. Clathrin- and caveolin-independent entry of human papillomavirus type 16--involvement of tetraspanin-enriched microdomains (TEMs). PLoS One **3**:e3313.

556. Squires MS, Hudson EA, Howells L, Sale S, Houghton CE, Jones JL, Fox LH, Dickens M, Prigent SA, Manson MM. 2003. Relevance of mitogen activated protein kinase (MAPK) and phosphotidylinositol-3-kinase/protein kinase B (PI3K/PKB) pathways to induction of apoptosis by curcumin in breast cells. Biochem Pharmacol **65**:361–376.

557. St Vincent MR, Colpitts CC, Ustinov AV, Muqadas M, Joyce MA, Barsby NL, Epand RF, Epand RM, Khramyshev SA, Valueva OA, Korshun VA, Tyrrell DL, Schang LM. 2010. Rigid amphipathic fusion inhibitors, small molecule antiviral compounds against enveloped viruses. Proc Natl Acad Sci USA **107**:17339–17344.

558. Steinmann J, Buer J, Pietschmann T, Steinmann E. 2013. Anti-infective properties of epigallocatechin-3-gallate (EGCG), a component of green tea. Br J Pharmacol **168**:1059–1073.

559. Stiasny K, Heinz FX. 2004. Effect of membrane curvature-modifying lipids on membrane fusion by tick-borne encephalitis virus. J Virol **78**:8536–8542.

560. Sturzenbecker LJ, Nibert M, Furlong D, Fields BN. 1987. Intracellular digestion of reovirus particles requires a low pH and is an essential step in the viral infectious cycle. J Virol **61**:2351–2361.

561. Su AI, Pezacki JP, Wodicka L, Brideau AD, Supekova L, Thimme R, Wieland S, Bukh J, Purcell RH, Schultz PG, Chisari FV. 2002. Genomic analysis of the host response to hepatitis C virus infection. Proc Natl Acad Sci USA **99**:15669–15674.

562. Su PY, Liu YT, Chang HY, Huang SW, Wang YF, Yu CK, Wang JR, Chang CF. 2012. Cell surface sialylation affects binding of enterovirus 71 to rhabdomyosarcoma and neuroblastoma cells. BMC Microbiol **12**:162.

563. Subtil A, Gaidarov I, Kobylarz K, Lampson MA, Keen JH, McGraw TE. 1999. Acute cholesterol depletion inhibits clathrin-coated pit budding. Proc Natl Acad Sci USA **96**:6775–6780.

564. Summa V, Ludmerer SW, McCauley JA, Fandozzi C, Burlein C, Claudio G, Coleman PJ, Dimuzio JM, Ferrara M, Di Filippo M, Gates AT, Graham DJ, Harper S, Hazuda DJ, McHale C, Monteagudo E, Pucci V, Rowley M, Rudd MT, Soriano A, Stahlhut MW, Vacca JP, Olsen DB, Liverton NJ, Carroll SS. 2012. MK-5172, a selective inhibitor of hepatitis C virus NS3/4a protease with broad activity across genotypes and resistant variants. Antimicrob Agents Chemother **56**:4161–4167.

565. Summers J, Mason WS. 1982. Replication of the genome of a hepatitis B--like virus by reverse transcription of an RNA intermediate. Cell **29**:403–415.

566. Sun X, Whittaker GR. 2003. Role for influenza virus envelope cholesterol in virus entry and infection. J Virol **77**:12543–12551.

567. Sun X, Yau VK, Briggs BJ, Whittaker GR. 2005. Role of clathrin-mediated endocytosis during vesicular stomatitis virus entry into host cells. Virology **338**:53–60.

568. Sun XL. 2007. Recent anti-influenza strategies in multivalent sialyloligosaccharides and sialylmimetics approaches. Curr Med Chem **14**:2304–2313.

569. Suo Z, Johnson KA. 1998. Selective inhibition of HIV-1 reverse transcriptase by an antiviral inhibitor, (R)-9-(2-Phosphonylmethoxypropyl)adenine. J Biol Chem **273**:27250–27258.

570. Superti F, Girmenta C, Seganti L, Orsi N. 1986. Role of sialic acid in cell receptors for vesicular stomatitis virus. Acta Virol **30**:10–18.

571. Suzuki S, Lee B, Luo W, Tovell D, Robins MJ, Tyrrell DL. 1988. Inhibition of duck hepatitis B virus replication by purine 2',3'-dideoxynucleosides. Biochem Biophys Res Commun **156**:1144–1151.

572. Suzuki Y, Hirabayashi Y, Suzuki T, Matsumoto M. 1985. Occurrence of O-glycosidically peptide-linked oligosaccharides of poly-N-acetyllactosamine type (erythroglycan II) in the I-antigenically active Sendai virus receptor sialoglycoprotein GP-2. J Biochem **98**:1653–1659.

573. Sy T, Jamal MM. 2006. Epidemiology of hepatitis C virus (HCV) infection. Int J Med Sci **3**:41–46.

574. Tambuyzer L, Azijn H, Rimsky LT, Vingerhoets J, Lecocq P, Kraus G, Picchio G, de Bethune MP. 2009. Compilation and prevalence of mutations associated with resistance to non-nucleoside reverse transcriptase inhibitors. Antivir Ther **14**:103–109.

575. Tamura M, Natori K, Kobayashi M, Miyamura T, Takeda N. 2004. Genogroup II noroviruses efficiently bind to heparan sulfate proteoglycan associated with the cellular membrane. J Virol **78**:3817–3826.

576. Tan CW, Poh CL, Sam IC, Chan YF. 2013. Enterovirus 71 uses cell surface heparan sulfate glycosaminoglycan as an attachment receptor. J Virol **87**:611–620.

577. Tatti S, Stockfleth E, Beutner KR, Tawfik H, Elsasser U, Weyrauch P, Mescheder A. 2010. Polyphenon E: a new treatment for external anogenital warts. Br J Dermatol **162**:176–184.

578. Taubenberger JK, Kash JC. 2010. Influenza virus evolution, host adaptation, and pandemic formation. Cell Host Microbe **7**:440–451.

579. Taylor FR, Kandutsch AA. 1989. Metabolism of 25-hydroxycholesterol in mammalian cell cultures. Side-chain scission to pregnenolone in mouse L929 fibroblasts. J Lipid Res **30**:899–905.

580. Teissier E, Pecheur EI. 2007. Lipids as modulators of membrane fusion mediated by viral fusion proteins. Eur Biophys J **36**:887–899.

581. Teissier E, Penin F, Pecheur EI. 2011a. Targeting cell entry of enveloped viruses as an antiviral strategy. Molecules **16**:221–250.

582. Teissier E, Zandomeneghi G, Loquet A, Lavillette D, Lavergne JP, Montserret R, Cosset FL, Bockmann A, Meier BH, Penin F, Pecheur EI. 2011b. Mechanism of inhibition of enveloped virus membrane fusion by the antiviral drug arbidol. PLoS One **6**:e15874.

583. Temesgen Z, Talwani R, Rizza SA. 2014. Dolutegravir, an HIV integrase inhibitor for the treatment of HIV infection. Drugs Today (Barc) **50**:7–14.

584. Terao-Muto Y, Yoneda M, Seki T, Watanabe A, Tsukiyama-Kohara K, Fujita K, Kai C. 2008. Heparin-like glycosaminoglycans prevent the infection of measles virus in SLAM-negative cell lines. Antiviral Res **80**:370–376.

585. Townsley AC, Weisberg AS, Wagenaar TR, Moss B. 2006. Vaccinia virus entry into cells via a low-pH-dependent endosomal pathway. J Virol **80**:8899–8908.

586. Trybala E, Bergstrom T, Svennerholm B, Jeansson S, Glorioso JC, Olofsson S. 1994. Localization of a functional site on herpes simplex virus type 1 glycoprotein C involved in binding to cell surface heparan sulphate. J Gen Virol **75**:743–752.

587. Tsai HH, Juang WF, Chang CM, Hou TY, Lee JB. 2013. Molecular mechanism of Ca(2+)-catalyzed fusion of phospholipid micelles. Biochim Biophys Acta **1828**:2729–2738.

588. Tsamis F, Gavrilov S, Kajumo F, Seibert C, Kuhmann S, Ketas T, Trkola A, Palani A, Clader JW, Tagat JR, McCombie S, Baroudy B, Moore JP, Sakmar TP, Dragic T. 2003. Analysis of the mechanism by which the small-molecule CCR5 antagonists SCH-351125 and SCH-350581 inhibit human immunodeficiency virus type 1 entry. J Virol **77**:5201–5208.

589. Turner SR, Strohbach JW, Tommasi RA, Aristoff PA, Johnson PD, Skulnick HI, Dolak LA, Seest EP, Tomich PK, Bohanon MJ, Horng MM, Lynn JC, Chong KT, Hinshaw RR, Watenpaugh KD, Janakiraman MN, Thaisrivongs S. 1998. Tipranavir (PNU-140690): a potent, orally bioavailable nonpeptidic HIV protease inhibitor of the 5,6-dihydro-4-hydroxy-2-pyrone sulfonamide class. J Med Chem **41**:3467–3476.

590. Uncapher CR, DeWitt CM, Colonno RJ. 1991. The major and minor group receptor families contain all but one human rhinovirus serotype. Virology **180**:814–817.

591. Uozaki M, Yamasaki H, Katsuyama Y, Higuchi M, Higuti T, Koyama AH. 2007. Antiviral effect of octyl gallate against DNA and RNA viruses. Antiviral Res **73**:85–91.

592. Vajragupta O, Boonchoong P, Morris GM, Olson AJ. 2005. Active site binding modes of curcumin in HIV-1 protease and integrase. Bioorg Med Chem Lett **15**:3364–3368.

593. Van Damme L, Ramjee G, Alary M, Vuylsteke B, Chandeying V, Rees H, Sirivongrangson P, Mukenge-Tshibaka L, Ettiegne-Traore V, Uaheowitchai C, Karim SS, Masse B, Perriens J, Laga M. 2002. Effectiveness of COL-1492, a nonoxynol-9 vaginal gel, on HIV-1 transmission in female sex workers: a randomised controlled trial. Lancet **360**:971–977.

594. van der Strate BW, Beljaars L, Molema G, Harmsen MC, Meijer DK. 2001. Antiviral activities of lactoferrin. Antiviral Res **52**:225–239.

595. Vanderlinden E, Goktas F, Cesur Z, Froeyen M, Reed ML, Russell CJ, Cesur N, Naesens L. 2010. Novel inhibitors of influenza virus fusion: structure-activity relationship and interaction with the viral hemagglutinin. J Virol **84**:4277–4288.

596. Vanderplasschen A, Hollinshead M, Smith GL. 1998. Intracellular and extracellular vaccinia virions enter cells by different mechanisms. J Gen Virol **79**:877–887.

597. Varki A. 1994. Selectin ligands. Proc Natl Acad Sci USA **91**:7390–7397.

598. Venkataraman N, Cole AL, Ruchala P, Waring AJ, Lehrer RI, Stuchlik O, Pohl J, Cole AM. 2009. Reawakening retrocyclins: ancestral human defensins active against HIV-1. PLoS Biol **7**:e95.

599. Vicenzi E, Canducci F, Pinna D, Mancini N, Carletti S, Lazzarin A, Bordignon C, Poli G, Clementi M. 2004. Coronaviridae and SARS-associated coronavirus strain HSR1. Emerg Infect Dis **10**:413–418.

600. Vigant F, Hollmann A, Lee J, Santos NC, Jung ME, Lee B. 2014. The rigid amphipathic fusion inhibitor dUY11 acts through photosensitization of viruses. J Virol **88**:1849–1853.

601. Vigant F, Lee J, Hollmann A, Tanner LB, Akyol Ataman Z, Yun T, Shui G, Aguilar HC, Zhang D, Meriwether D, Roman-Sosa G, Robinson LR, Juelich TL, Buczkowski H, Chou S, Castanho MA, Wolf MC, Smith JK, Banyard A, Kielian M, Reddy S, Wenk MR, Selke M, Santos NC, Freiberg AN, Jung ME, Lee B. 2013. A mechanistic paradigm for broad-spectrum antivirals that target virus-cell fusion. PLoS Pathog **9**:e1003297.

602. Villalain J. 2010. Membranotropic effects of arbidol, a broad anti-viral molecule, on phospholipid model membranes. J Phys Chem B **114**:8544–8554.

603. Villar E, Barroso IM. 2006. Role of sialic acid-containing molecules in paramyxovirus entry into the host cell: a minireview. Glycoconj J **23**:5–17.

604. Vives RR, Imberty A, Sattentau QJ, Lortat-Jacob H. 2005. Heparan sulfate targets the HIV-1 envelope glycoprotein gp120 coreceptor binding site. J Biol Chem **280**:21353–21357.

605. Vlasak R, Luytjes W, Spaan W, Palese P. 1988. Human and bovine coronaviruses recognize sialic acid-containing receptors similar to those of influenza C viruses. Proc Natl Acad Sci USA **85**:4526–4529.

606. Vlieghe P, Lisowski V, Martinez J, Khrestchatisky M. 2010. Synthetic therapeutic peptides: science and market. Drug Discov Today **15**:40–56.

607. Vogel SS, Leikina EA, Chernomordik LV. 1993. Lysophosphatidylcholine reversibly arrests exocytosis and viral fusion at a stage between triggering and membrane merger. J Biol Chem **268**:25764–25768.

608. von Itzstein M, Wu WY, Kok GB, Pegg MS, Dyason JC, Jin B, Van Phan T, Smythe ML, White HF, Oliver SW, Colman PM, Varghese JN, Ryan DM, Woods JM, Bethell RC, Hotham VJ, Cameron JM, Penn CR. 1993. Rational design of potent sialidase-based inhibitors of influenza virus replication. Nature **363**:418–423.

609. Wagoner J, Negash A, Kane OJ, Martinez LE, Nahmias Y, Bourne N, Owen DM, Grove J, Brimacombe C, McKeating JA, Pecheur EI, Graf TN, Oberlies NH, Lohmann V, Cao F, Tavis JE, Polyak SJ. 2010. Multiple effects of silymarin on the hepatitis C virus lifecycle. Hepatology **51**:1912–1921.

610. Waheed AA, Freed EO. 2009. Lipids and membrane microdomains in HIV-1 replication. Virus Res **143**:162–176.

611. Waldmann M, Jirmann R, Hoelscher K, Wienke M, Niemeyer FC, Rehders D, Meyer B. 2014. A nanomolar multivalent ligand as entry inhibitor of the hemagglutinin of avian influenza. J Am Chem Soc **136**:783–788.

612. Wang D, Veena MS, Stevenson K, Tang C, Ho B, Suh JD, Duarte VM, Faull KF, Mehta K, Srivatsan ES, Wang MB. 2008a. Liposome-encapsulated curcumin suppresses growth of head and neck squamous cell carcinoma in vitro and in xenografts through the inhibition of nuclear factor kappaB by an AKT-independent pathway. Clin Cancer Res **14**:6228–6236.

613. Wang H, Yang P, Liu K, Guo F, Zhang Y, Zhang G, Jiang C. 2008b. SARS coronavirus entry into host cells through a novel clathrin- and caveolae-independent endocytic pathway. Cell Res **18**:290–301.

614. Wang K, Huang S, Kapoor-Munshi A, Nemerow G. 1998. Adenovirus internalization and infection require dynamin. J Virol **72**:3455–3458.

615. Wang KS, Kuhn RJ, Strauss EG, Ou S, Strauss JH. 1992. High-affinity laminin receptor is a receptor for Sindbis virus in mammalian cells. J Virol **66**:4992–5001.

616. Wang Q, Tian X, Chen X, Ma J. 2007. Structural basis for receptor specificity of influenza B virus hemagglutinin. Proc Natl Acad Sci USA **104**:16874–16879.

617. Warren CJ, Griffin LM, Little AS, Huang I-C, Farzan M, Pyeon D. 2014. The antiviral restriction factors IFITM1, 2 and 3 do not inhibit infection of human papillomavirus, cytomegalovirus and adenovirus. PloS one **9**:e96579.

618. Weber JM, Ruzindana-Umunyana A, Imbeault L, Sircar S. 2003. Inhibition of adenovirus infection and adenain by green tea catechins. Antiviral Res **58**:167–173.

619. Wei X, Decker JM, Liu H, Zhang Z, Arani RB, Kilby JM, Saag MS, Wu X, Shaw GM, Kappes JC. 2002. Emergence of resistant human immunodeficiency virus type 1 in patients receiving fusion inhibitor (T-20) monotherapy. Antimicrob Agents Chemother **46**:1896–1905.

620. Weidner JM, Jiang D, Pan XB, Chang J, Block TM, Guo JT. 2010. Interferon-induced cell membrane proteins, IFITM3 and tetherin, inhibit vesicular stomatitis virus infection via distinct mechanisms. J Virol **84**:12646–12657.

621. Weis W, Brown JH, Cusack S, Paulson JC, Skehel JJ, Wiley DC. 1988. Structure of the influenza virus haemagglutinin complexed with its receptor, sialic acid. Nature **333**:426–431.

622. Weissenhorn W, Calder LJ, Wharton SA, Skehel JJ, Wiley DC. 1998a. The central structural feature of the membrane fusion protein subunit from the Ebola virus glycoprotein is a long triple-stranded coiled coil. Proc Natl Acad Sci USA **95**:6032–6036.

623. Weissenhorn W, Carfi A, Lee KH, Skehel JJ, Wiley DC. 1998b. Crystal structure of the Ebola virus membrane fusion subunit, GP2, from the envelope glycoprotein ectodomain. Mol Cell **2**:605–616.

624. Weissenhorn W, Dessen A, Harrison SC, Skehel JJ, Wiley DC. 1997. Atomic structure of the ectodomain from HIV-1 gp41. Nature **387**:426–430.

625. Wensing AM, van Maarseveen NM, Nijhuis M. 2010. Fifteen years of HIV Protease Inhibitors: raising the barrier to resistance. Antiviral Res **85**:59–74.

626. Westby M, Lewis M, Whitcomb J, Youle M, Pozniak AL, James IT, Jenkins TM, Perros M, van der Ryst E. 2006. Emergence of CXCR4-using human immunodeficiency virus type 1 (HIV-1) variants in a minority of HIV-1-infected patients following treatment with the CCR5 antagonist maraviroc is from a pretreatment CXCR4-using virus reservoir. J Virol **80**:4909–4920.

627. Westby M, Smith-Burchnell C, Mori J, Lewis M, Mosley M, Stockdale M, Dorr P, Ciaramella G, Perros M. 2007. Reduced maximal inhibition in phenotypic susceptibility assays indicates that viral strains resistant to the CCR5 antagonist maraviroc utilize inhibitor-bound receptor for entry. J Virol **81**:2359–2371.

628. Whitbeck JC, Peng C, Lou H, Xu R, Willis SH, Ponce de Leon M, Peng T, Nicola AV, Montgomery RI, Warner MS, Soulika AM, Spruce LA, Moore WT, Lambris JD, Spear PG, Cohen GH, Eisenberg RJ. 1997. Glycoprotein D of herpes simplex virus (HSV) binds directly to HVEM, a member of the tumor necrosis factor receptor superfamily and a mediator of HSV entry. J Virol **71**:6083–6093.

629. Whitley RJ. 2006. Herpes simplex encephalitis: adolescents and adults. Antiviral Res **71**:141–148.

630. Wickham TJ, Mathias P, Cheresh DA, Nemerow GR. 1993. Integrins alpha v beta 3 and alpha v beta 5 promote adenovirus internalization but not virus attachment. Cell **73**:309–319.

631. Wickham TJ, Filardo EJ, Cheresh DA, Nemerow GR. 1994. Integrin alpha v beta 5 selectively promotes adenovirus mediated cell membrane permeabilization. J Cell Biol **127**:257–264.

632. Wild CT, Shugars DC, Greenwell TK, McDanal CB, Matthews TJ. 1994. Peptides corresponding to a predictive alpha-helical domain of human immunodeficiency virus type 1 gp41 are potent inhibitors of virus infection. Proc Natl Acad Sci USA **91**:9770–9774.

633. Wiley DC, Skehel JJ. 1987. The structure and function of the hemagglutinin membrane glycoprotein of influenza virus. Annu Rev Biochem **56**:365–394.

634. Wilkins C, Woodward J, Lau DT, Barnes A, Joyce M, McFarlane N, McKeating JA, Tyrrell DL, Gale MJ. 2013. IFITM1 is a tight junction protein that inhibits hepatitis C virus entry. Hepatology **57**:461–469.

635. Wills T, Vega V. 2012. Elvitegravir: a once-daily inhibitor of HIV-1 integrase. Expert Opin Investig Drugs **21**:395–401.

636. Wilson IA, Skehel JJ, Wiley DC. 1981. Structure of the haemagglutinin membrane glycoprotein of influenza virus at 3A resolution. Nature **289**:366–373.

637. Wilson SS, Wiens ME, Smith JG. 2013. Antiviral mechanisms of human defensins. J Mol Biol **425**:4965–4980.

638. Wittels M, Spear PG. 1991. Penetration of cells by herpes simplex virus does not require a low pH-dependent endocytic pathway. Virus Res **18**:271–290.

639. Witvrouw M, De Clercq E. 1997. Sulfated polysaccharides extracted from sea algae as potential antiviral drugs. Gen Pharmacol **29**:497–511.

640. Wolf MC, Freiberg AN, Zhang T, Akyol-Ataman Z, Grock A, Hong PW, Li J, Watson NF, Fang AQ, Aguilar HC, Porotto M, Honko AN, Damoiseaux R, Miller JP, Woodson SE, Chantasirivisal S, Fontanes V, Negrete OA, Krogstad P, Dasgupta A, Moscona A, Hensley LE, Whelan SP, Faull KF, Holbrook MR, Jung ME, Lee B. 2010. A broad-spectrum antiviral targeting entry of enveloped viruses. Proc Natl Acad Sci USA **107**:3157–3162.

641. Wolfram S, Raederstorff D, Preller M, Wang Y, Teixeira SR, Riegger C, Weber P. 2006. Epigallocatechin gallate supplementation alleviates diabetes in rodents. J Nutr **136**:2512–2518.

642. Wolkerstorfer A, Kurz H, Bachhofner N, Szolar OH. 2009. Glycyrrhizin inhibits influenza A virus uptake into the cell. Antiviral Res **83**:171–178.

643. Woo JH, Kim YH, Choi YJ, Kim DG, Lee KS, Bae JH, Min DS, Chang JS, Jeong YJ, Lee YH, Park JW, Kwon TK. 2003. Molecular mechanisms of curcumin-induced cytotoxicity: induction of apoptosis through generation of reactive oxygen species, down-regulation of Bcl-XL and IAP, the release of cytochrome c and inhibition of Akt. Carcinogenesis **24**:1199–1208.

644. Wu HF, Monroe DM, Church FC. 1995. Characterization of the glycosaminoglycan-binding region of lactoferrin. Arch Biochem Biophys **317**:85–92.

645. Wu X, Lee EM, Hammack C, Robotham JM, Basu M, Lang J, Brinton MA, Tang H. 2014. Cell Death-Inducing DFFA-Like Effector b Is Required for Hepatitis C Virus Entry into Hepatocytes. J Virol **88**:8433–8444.

646. WuDunn D, Spear PG. 1989. Initial interaction of herpes simplex virus with cells is binding to heparan sulfate. J Virol **63**:52–58.

647. Xiao F, Fofana I, Thumann C, Mailly L, Alles R, Robinet E, Meyer N, Schaeffer M, Habersetzer F, Doffoel M, Leyssen P, Neyts J, Zeisel MB, Baumert TF. 2014. Synergy of entry inhibitors with direct-acting antivirals uncovers novel combinations for prevention and treatment of hepatitis C. Gut: doi: 10.1136/gutjnl-2013-306155.

648. Xu J, Wang J, Deng F, Hu Z, Wang H. 2008. Green tea extract and its major component epigallocatechin gallate inhibits hepatitis B virus in vitro. Antiviral Res **78**:242–249.

649. Xu Y, Lou Z, Liu Y, Pang H, Tien P, Gao GF, Rao Z. 2004. Crystal structure of severe acute respiratory syndrome coronavirus spike protein fusion core. J Biol Chem **279**:49414–49419.

650. Yamada S, Ohnishi S. 1986. Vesicular stomatitis virus binds and fuses with phospholipid domain in target cell membranes. Biochemistry **25**:3703–3708.

651. Yamaguchi K, Honda M, Ikigai H, Hara Y, Shimamura T. 2002. Inhibitory effects of (-)-epigallocatechin gallate on the life cycle of human immunodeficiency virus type 1 (HIV-1). Antiviral Res **53**:19–34.

652. Yamamoto M, Aizaki H, Fukasawa M, Teraoka T, Miyamura T, Wakita T, Suzuki T. 2011. Structural requirements of virion-associated cholesterol for infectivity, buoyant density and apolipoprotein association of hepatitis C virus. J Gen Virol **92**:2082–2087.

653. Yamasaki H, Uozaki M, Katsuyama Y, Utsunomiya H, Arakawa T, Higuchi M, Higuti T, Koyama AH. 2007. Antiviral effect of octyl gallate against influenza and other RNA viruses. Int J Mol Med **19**:685–688.

654. Yang B, Chuang H, Yang KD. 2009. Sialylated glycans as receptor and inhibitor of enterovirus 71 infection to DLD-1 intestinal cells. Virol J **6**:141.

655. Yasin B, Wang W, Pang M, Cheshenko N, Hong T, Waring AJ, Herold BC, Wagar EA, Lehrer RI. 2004. Theta defensins protect cells from infection by herpes simplex virus by inhibiting viral adhesion and entry. J Virol **78**:5147–5156.

656. Yeagle PL, Smith FT, Young JE, Flanagan TD. 1994. Inhibition of membrane fusion by lysophosphatidylcholine. Biochemistry **33**:1820–1827.

657. Zandi K, Ramedani E, Mohammadi K, Tajbakhsh S, Deilami I, Rastian Z, Fouladvand M, Yousefi F, Farshadpour F. 2010. Evaluation of antiviral activities of curcumin derivatives against HSV-1 in Vero cell line. Nat Prod Commun **5**:1935–1938.

658. Zeisel MB, Koutsoudakis G, Schnober EK, Haberstroh A, Blum HE, Cosset FL, Wakita T, Jaeck D, Doffoel M, Royer C, Soulier E, Schvoerer E, Schuster C, Stoll-Keller F, Bartenschlager R, Pietschmann T, Barth H, Baumert TF. 2007. Scavenger receptor class B type I is a key host factor for hepatitis C virus infection required for an entry step closely linked to CD81. Hepatology **46**:1722–1731.

659. Zhang J, Randall G, Higginbottom A, Monk P, Rice CM, McKeating JA. 2004. CD81 is required for hepatitis C virus glycoprotein-mediated viral infection. J Virol **78**:1448–1455.

660. Zhang Y, Bergelson JM. 2005. Adenovirus receptors. J Virol **79**:12125–12131.

661. Zhang Y, Whittaker GR. 2014. Influenza entry pathways in polarized MDCK cells. Biochem Biophys Res Commun doi: 10.1016/j.bbrc.2014.05.095.

662. Zhu Z, Gershon MD, Ambron R, Gabel C, Gershon AA. 1995. Infection of cells by varicella zoster virus: inhibition of viral entry by mannose 6-phosphate and heparin. Proc Natl Acad Sci USA **92**:3546–3550.

663. Zimmerberg J, Kozlov MM. 2006. How proteins produce cellular membrane curvature. Nat Rev Mol Cell Biol **7**:9–19.

664. Zona L, Lupberger J, Sidahmed-Adrar N, Thumann C, Harris HJ, Barnes A, Florentin J, Tawar RG, Xiao F, Turek M, Durand SC, Duong FH, Heim MH, Cosset FL, Hirsch I, Samuel D, Brino L, Zeisel MB, Le Naour F, McKeating JA, Baumert TF. 2013. HRas signal transduction promotes hepatitis C virus cell entry by triggering assembly of the host tetraspanin receptor complex. Cell Host Microbe **13**:302–313.